Methyl ester functionalised poly(2-oxazoline)s

Proefschrift

ter verkrijging van de graad van doctor
aan de Radboud Universiteit Nijmegen
op gezag van de rector magnificus,
volgens besluit van het college van decanen

en
ter verkrijging van de graad van doctor in de wetenschappen: chemie
aan de Universiteit Gent
op gezag van de rector prof. dr. Anne De Paepe,

in het openbaar te verdedigen op dinsdag 19 april 2016
om 12.30 uur precies

door
Petra Johanna Maria Bouten
geboren op 5 oktober 1986
te Eindhoven

Promotoren:

Prof. dr. ir. J.C.M. van Hest

Prof. dr. R. Hoogenboom (Universiteit Gent, België)

Manuscriptcommissie:

Prof. dr. A.E. Rowan

Prof. dr. R.J.M. Nolte

Prof. dr. S. Van Vlierberghe (Universiteit Gent, België)

Prof. dr. ir. B. de Geest (Universiteit Gent, België)

Dr. D.W.P.M. Löwik

Dr. ir. J.P.A. Heuts (Technische Universiteit Eindhoven)

Dr. G. Volet (Université Paris-Est, Frankrijk)

Paranimfen

Rosa Félix Lanao

Maarten Vergaelen

Cover design

Jos der Kinderen

Cover foto's

Piet Bouten

Petra Bouten

Hiel veul renners an de start
Nog mier kenners langs de kant
En inens dan giet ’t hard
Trekt ’t circus dor ’t land

De longe vol met frisse lucht
En de oege zeen vol veur
Elke bocht is heer berucht
Hande trekke an ’t steur

Na boave, nar boave
Umhoeg, zo snel ’t giet
Nar boave, nar boave
’t moeiste oetzicht dat bestiet

De veut vast op ’t pedaal
En de spiere die stoan strak
Elke berg het zien verhaal
Genne meater din is vlak

Nar boave, nar boave
Dor de zomerwind umermd
Heer boave, als enne oave
Din te lang is veurverwermd

Oaver afgeslete stien
Doffe klappe op de maag
Fietste met owelf alien
De latste meaters van vandaag

Nar boave, nar boave, nar boave

Nar boave, nar boave
An de kant, ik lig op stoem
Nar boave, nar boave
Onderweg nar miene droem
Want doarboave loert de kans
Winnaar van de Tour de France

Nar boave, nar boave, nar boave
’t podium dat keumt in zicht
Nar boave, nar boave, nar boave
Oet de schaduw van ‘t licht

Nar boave, nar boave, nar boave
In de allerlatste sprint
Nar boave, nar boave
Dreit ’t felgekleurde lint

Nar boave, nar boave, nar boave
Waterdruppels in de zon
Nar boave, nar boave, nar boave
De moeiste platst op ’t balkon

Nar boave, nar boave, nar boave

Jack Poels [2008]
Nar Boave

Inhoudsopgave

List of abbreviations

1PrOH	1-propanol
2PrOH	2-propanol
A	Frequency factor
BCN	bicyclo[6.1.0]nonyne
C3MestOx	2-methoxycarbonylpropyl-2-oxazoline
CE	Conformité Eruopéene (European Conformity)
CROP	Cationic ring opening polymerisation
CSF	Cerebrospinal fluid
CPP	Cell penetrating peptide
*c*PropOx	2-cyclopropyl-2-oxazoline
CuAAC	Copper(I)-catalysed azide-alkyne cycloaddition
Đ	Dispersity
DABAL-Me_3	1,4-diazobicyclo[2.2.2]octane
DCM	Dichloromethane
DHMPA	2,2-Bis(hydroxymethyl)-propionic acid
DIC	Diisopropyl carbodiimide
DMA	*N,N*-dimethylacetamide
DP	Degree of polymerisation
DSC	Differential scanning calorimetry
E_A	Activation energy
EDC	1-Ethyl-3-(3-dimethylaminopropyl)carbodiimide
EtOH	Ethanol
EtOx	2-ethyl-2-oxazoline
FDA	U.S. Food and Drug Administration
FTIR	Fourier transform infrared spectroscopy
GC	Gas chromatography
GRTs	Guanidinium-rich transporters
HA	Hyaluronic acid
HA-MA	Methacrylated hyaluronic acid
HDI	Hexamethylene diisocyanate
IEMA	2-Isocyanatoethyl methacrylate
IPD	Isophorone diisocyanate
*i*PropOx	2-isopropyl-2-oxazoline
K3	Trilysine
k_p	polymerisation rate constant
LCSC	Lower critical solution concentration
LCST	Lower critical solution temperature
MeOH	Methanol
MeOx	2-methyl-2-oxazoline
MeOTs	methyl p-toluenesulfonate
MestOx	2-methoxycarbonylethyl-2-oxazoline
MMA	Methyl methacrylate
M_n	Number average molecular weight
MDI	Diphenyl methane diisocyanate
MoTrs	Molecular transporters
NHS	*N*-Hydroxysuccinimide
NMR	Nuclear magnetic resonance
nPropOx	2-*n*-propyl-2-oxazoline
PAOX	poly(2-alkyl/ary-2-oxazoline)

PC3MestOx	poly(2-methoxycarbonylpropyl-2-oxazoline)
PCL	Poly(ε-caprolactone)
P*c*PropOx	poly(2-cyclopropyl-2-oxazoline)
PDMS	Poly(dimethyl siloxane)
PEG	Poly(ethylene glycol)
PEI	Poly(ethylene imine)
PEtOx	poly(2-ethyl-2-oxazoline)
PFP	Pentafluorophenyl
PGA	Poly(glycolic acid)
PGLSA	Poly(glycerol succinic acid)
PGSA	Poly(glycerol sebacate acrylate)
P*i*PropOx	poly(2-isopropyl-2-oxazoline)
PLA	Poly(lactic acid)
PLC	Poly(L-lactide-*co*-caprolactone)
PLGA	Poly(lactic-*co*-glycolic acid)
PMeOx	poly(2-methyl-2-oxazoline)
PMestOx	poly(2-methoxycarbonylethyl-2-oxazoline)
PMMA	polymethylmethacrylate
P*n*BuOx	poly(2-*n*-butyl-2-oxazoline
PNIPAAm	poly(*N*-isopropyl acrylamide)
P*n*PropOx	poly(2-*n*-propyl-2-oxazoline)
PPhOx	poly(2-phenyl-2-oxazoline)
PPropOx	poly(2-propyl-2-oxazoline)
Plu	Pluronic (PEG-PPO-PEG)
Plu-SH	Thiol functionalized Pluronic
PPO	Poly(propylene oxide)
PropOx	2-propyl-2-oxazoline
PTMEG	Poly(tetramethylene ether glycol)
PTMC	Poly(trimethylene carbonate)
R8	Octa-arginine
r^{app}	Apparent reactivity ratio
SEC	Size exclusion chromatography
T_{CP}	Cloud point temperature
TEA	Triethylamine
T_g	Glass transition temperature
TGA	Thermogravimetric analysis
THF	Tetrahydrofuran
T_m	melting temperature

Chapter 1

Introduction

Part of this work has been published:

Petra J.M. Bouten, Marleen Zonjee, Johan Bender, Simon T.K. Yauw, Harry van Goor, Jan C.M. van Hest, Richard Hoogenboom, *The chemistry of tissue adhesive materials*, **Progress in Polymer Science**, 2014, 39, 7, 1375-1405

1.1 The chemistry of tissue adhesive materials

Each year millions of people suffer from wounds that do not heal spontaneously, but which require closure via a medical procedure. These wounds not only include skin wounds but are also caused by any surgical or traumatic disruption of solid and hollow organs, connective tissue, muscles, tendons and membranes. Suturing is the most common method to achieve tissue approximation and wound healing. For many purposes suturing has proven to be very suitable. Sutures can provide great tensile strength and show relatively low failure rate.[1] Suture materials can be grossly divided in biologic or synthetic and in absorbable or non-absorbable materials. Nylon was the first synthetic suture applied and is still the most widely used non-absorbable suture. Disadvantages are the need to remove the suture, provoking high stress concentrations at the suture point and granuloma formation when it resides for prolonged periods of time in the body. Absorbable sutures are made of catgut, poly(lactic-*co*-glycolic acid) (PLGA), poly(glycolic acid), polydioxanone or poly(trimethylene carbonate) (PTMC), and degrade between 7 to 120 days depending on the material, which is long after they have lost tensile strength.[2] Absorbable sutures, however, frequently evoke inflammatory reactions and are relatively expensive. A common feature of suturing is the inevitable penetration of surrounding tissue, nerve damage and post-surgical adhesion which can occur, and ischemia and necrosis of entrapped tissue caused by damaged capillaries. Needle holes and necrotic spaces might provide a passage for fluids or air to leak out. Such compromised tissue anastomosis may result in severe complications depending on the leaking material (e.g. blood, bowel content, bile, cerebrospinal fluid or air). Gastro-intestinal anastomoses, for example, have a 3-15% risk of leakage which can cause intra-abdominal abscesses, fistula, peritonitis and mortality.[3, 4] Other disadvantages of suturing are that it is time-consuming, not always technically possible, anaesthesia is needed and it induces undesirable scar formation.[5]

Staples are a frequently used alternative to sutures. The application is faster compared to sutures and both absorbable and non-absorbable staples are available. Like sutures, however, staples tend to damage surrounding tissue, evoke an inflammatory response and cause scar tissue formation including intra-abdominal adhesions. Most importantly, the use of staples also harbours a significant failure rate.[1, 2]

In the past decades, a wide variety of chemical and mechanical closure materials has been developed with the intention of providing more reliable, more practical and faster methods of tissue closure or connection without compromising tissue vascularisation. They can be categorised in haemostatic agents, sealants and adhesives. A haemostatic agent initiates the formation of a blood clot, resulting in fibrin networks binding or covering tissues. Sealants are used to provide a watertight (e.g. for cerebrospinal fluid (CSF)) or airtight (e.g. after lung surgery) seal. Tissue adhesives are glues or patches that bind various tissues together in order to allow for the natural healing process to occur. Tissue adhesives are applied to a variety of tissues, such as skin, muscle and intestine.[6, 7]

Any material used as a haemostatic agent, sealant, adhesive or a combination of these should meet extensive requirements. Spotnitz and Burke in 2008[6] listed five main requirements: safety, efficacy, usability, cost and approval from the US Food and Drug Administration (FDA) for use in the US and CE mark approval for use in the EU.[7] Some more specific requirements are biocompatibility, biodegradability, mechanical compliance with underlying tissue, an acceptable swelling index and shelf stability. Depending on the desired application a requirement can also be water tightness, tuneable adhesion and even the ability to enhance the healing process by delivery of drugs or growth factors.

Biocompatibility means that the components and their degradation products should be non-toxic and non-haemolytic and cause minimal inflammatory or immune reactions. Also, the risk of microbial transmission or contamination and the risk of carcinogenic activity should be negligible. The material or its adhesive reaction must not have irritating effects and should not jeopardise normal wound healing. Degradation should occur via hydrolysis or enzymatic breakdown and the time frame in which this occurs must be sufficiently long for the wound to heal, ideally degradation should start after 3 weeks and the tissue adhesive material should be completely degraded after 3 months. For complete clearance, all degradation products have to be metabolised by the body or excreted via the kidneys or liver.

Regarding quality and functionality, tissue adhesives must not only have sufficient adhesive and cohesive strength, but also the flexibility to comply with underlying tissue and the ability to retain these properties in moist or wet conditions. The swelling index should be low to prevent compression of nerves and blood vessels. Ideally, the adhesive product is easy to produce, store and apply.

This chapter will describe the state of the art of the different polymeric materials available in the surgical toolbox for wound closure and discuss their advantages and drawbacks. This includes both the materials already on the market and new adhesives reported in recent scientific literature. These materials will be addressed from a polymer chemistry viewpoint, with a focus on synthetic polymers and biomimetic tissue adhesives. Materials based on polysaccharides and proteins are not included in this chapter, more information can be found in recent review articles.[5-11] Even though we try to compare the different materials as quantitatively as possible, the majority of papers unfortunately only provide qualitative data. Even when quantitative data are available it is hard to compare different studies, because the used tests and test conditions differ a lot, which has a major influence on the quantitative evaluation. In the second part of this chapter, poly(2-oxazoline)s are described as potentially interesting polymers for the preparation of tissue adhesive materials.

1.1.2 Polycyanoacrylates

In 1949 cyanoacrylates were first reported by Ardis,[12, 13] although their relevance for adhesive purposes was only recognised by Coover et al. in 1959.[14] Since then cyanoacrylates have found application as superglues in households, in the automotive and construction industries. In the 1960s the potential of cyanoacrylates for the use of wound closure was discovered.[15] Their popularity for this application can be ascribed to a variety of favourable properties. The liquid monomers show a high reactivity and polymerise in seconds at room temperature without addition of a catalyst, heat or pressure. Due to the electron-withdrawing nitrile group, the acrylate bond is polarised and therefore susceptible to nucleophilic attack by weak bases such as water or amines. After initiation by water the monomers rapidly react via anionic polymerisation. The reaction rate is inversely proportional to the length of the alkyl side chain. Adhesion between the glue and the tissue is accomplished via covalent bonds between the cyanoacrylate and functional groups in the tissue proteins, for example the primary amines of the lysine side chains. When applied on tissue, the monomers flow into the cracks and channels of the tissue surface, giving a strong bonding between the tissue and the glue. Also important for the strength is the mechanical interlocking of the polycyanoacrylates with the underlying tissue.

Different cyanoacrylate monomers have been reported to be interesting as tissue adhesives (Figure 1).[16] The strength of the adhesive is determined by the length of the alkyl chain, where shorter chains (butyl cyanoacrylates) give stronger polymerised networks than longer

chains (2-octyl cyanoacrylate); the longer alkyl chains on the other hand give more flexible bonds resulting in a higher breaking strength.[9, 17]

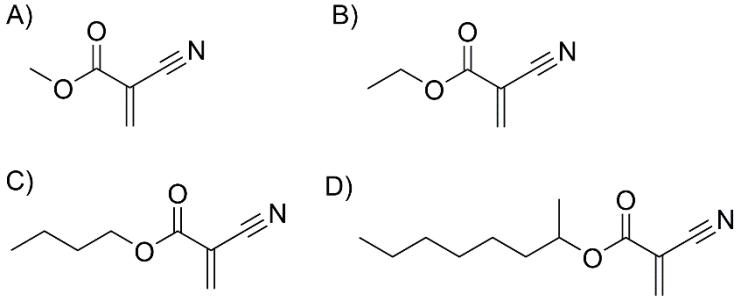

Figure 1: Structures of cyanoacrylates used as tissue adhesives with A) methyl-cyanoacrylate, B) ethyl-cyanoacrylate, C) n-butyl cyanoacrylate and D) 2-octyl cyanoacrylate.

The first cyanoacrylates applied in clinical settings were methyl-2-cyanoacrylate (Figure 1A) and ethyl-2-cyanoacrylate (Figure 1B) for wound closing purposes varying from abdominal to eye surgery. However, the fast degradation of the resulting polymers leads to accumulation of the degradation products in tissue and causes a histotoxic reaction, i.e. an inflammatory response. Degradation of the polymer occurs via hydrolysis leading to release of cyanoacetate and formaldehyde, a histotoxic component.[9, 18] This is much less of a problem for polymers with longer alkyl chains, since they degrade more slowly, due to steric hindrance and higher hydrophobicity (Figure 1C-D).[9] Due to the histotoxic reaction, the use of the short side chain, methyl- and ethyl-cyanoacrylates is nowadays mostly abandoned.[18-20] Besides cytotoxic limitations, cyanoacrylates also have poor mechanical properties. After polymerisation the adhesives become brittle, especially for ethyl- and butyl-cyanoacrylates, so they can fracture when applied in long incisions or skin creases.[16] Some cases are reported where a foreign body reaction occurs after the use of 2-octyl cyanoacrylate.[21]

Despite these drawbacks, cyanoacrylate tissue adhesive have been available since the 1980s in Canada and Europe, and several products that are commercially available are summarised in Table 1. These are all medical cyanoacrylate formulations with longer alkyl chains, used for suture-less closure of wounds and surgical incisions. In 1998 the FDA approved the use of 2-octyl cyanoacrylate from Dermabond® for the closure of topical skin incisions. Poly(2-octyl cyanoacrylate) degrades slowly, usually after 7 till 10 days the strip sloughs off the skin before the histotoxic degradation products are formed.[16] Indermil® consisting of n-butyl-cyanoacrylate, and Dermabond® also have an approved claim for usage as a barrier against microbial penetration.[9] n-Butyl cyanoacrylates are found to be cytotoxic in undiluted form; however, when diluted ten times with culture medium the cytotoxicity is acceptable, because in vitro studies showed that L929 cells were quite unaffected by the glue with a viability score above 70%.[22] Different studies have been performed comparing polycyanoacrylates with the use of sutures for wound closure, providing, however, no conclusive answer on which methodology is better regarding the cosmetic outcome, wound dehiscence (rupture along a suture) or prevention of infection.[16, 17, 23, 24] Internal application of cyanoacrylate adhesives remains troublesome: inflammatory responses that inhibit collagen remodelling and thus wound healing, and even pancreatic tumour development have been reported.[9]

Table 1: Commercially available cyanoacrylate tissue adhesives

Commercial product	Manufacturer	Approved indications	Constituents
Histoacryl® and Histoacryl® Blue[9]	B. Braun	Closure of topical skin incisions and trauma-induced skin lacerations	n-butyl-2-cyanoacrylate
Dermabond®[9, 21]	Ethicon	Closure of topical skin incisions and trauma-induced skin lacerations Barrier to microbial penetrations	2-octyl-2-cyanoacrylate
Indermil®[9]	Henkel	Closure of topical skin incisions and trauma-induced skin lacerations Barrier to microbial penetrations	n-butyl-2-cyanoacrylate
Omnex®[9]	Ethicon	blocking the passage of blood, body fluids or air	n-octyl-2-cyanoacrylate / butyl lactoyl-2-cyano acrylate
Glubran® and Glubran2®[22]	GEM Italy	synthetic surgical glue, CE certified for internal and external use, with haemostatic, adhesive, sealer and bacteriostatic properties	n-butyl-2-cyanoacrylate / methacryloxysulpholane
IFABond®	IFA medical	Class III implantable device designed to offer an alternative to staples and sutures (mesh)	N-hexyl-2-cyanoacrylate

1.1.3 Poly(ethylene glycol)-based tissue adhesives

Another important class of tissue adhesives is based on poly(ethylene glycol) (PEG). PEG has properties favourable for the use in medical sciences: the polymer is water-soluble, biocompatible, and shows a stealth-like behaviour in vivo, i.e. it is not readily recognised by the immune system.[25-27] Three major classes of PEG-based tissue adhesives can be distinguished: photopolymerisable adhesives (FocalSeal®, successor of AdvaSeal), PEG-trilysine adhesives (DuraSeal™) and adhesives based on two differently functionalised PEG polymers (CoSeal®, SprayGel).[6, 9]

The first photopolymerisable and biodegradable PEG-based adhesive dates back to 1993 and consists of a triblock copolymer with a PEG middle block and poly(dl-lactic acid) (PLA) or poly(glycolic acid) (PGA) outer blocks.[28] These ABA-triblock copolymers are prepared by using PEG as bifunctional macroinitiator for the ring-opening polymerisation of lactide or glycolide, followed by end-functionalisation of the terminal hydroxyl groups with photopolymerisable acrylate moieties (Figure 2A). In an aqueous environment these triblock

copolymers form micellar gels in which the hydrophobic outer blocks aggregate and the PEG acts as hydrophilic linker between these hydrophobic domains. This self-assembly process enables fast polymerisation due to high local acrylate concentration in the hydrophobic micellar core. The acquired gel itself is non-adhesive to tissue after polymerisation, whereas direct polymerisation in contact with tissue gives an adhered complex, which is ascribed to the formation of an interpenetrating network with the extracellular proteins in the tissue.[28]

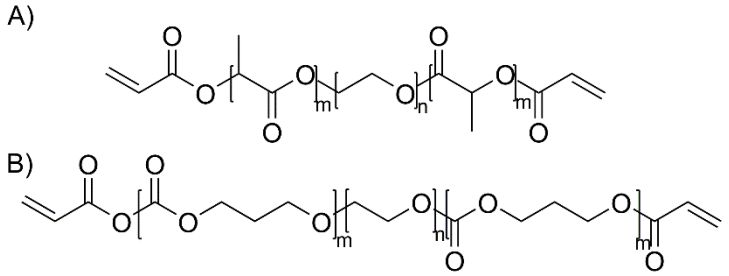

Figure 2: Two different photopolymerisable block copolymer building blocks for hydrogel tissue adhesives with A) PLA_m-PEG_n-PLA_m diacrylate and B) $PTMC_m$-PEG_n-$PTMC_m$ diacrylate.

FocalSeal® is a sealant based on this self-assembly principle[29] and is approved by the FDA since 2000 for sealing air leaks after lung surgery.[29] To obtain a hydrogel with mechanical properties appropriate for the use as tissue adhesive, a second ABA triblock copolymer is added containing poly(trimethylene carbonate) (PTMC) instead of the PLA blocks (Figure 2B). The PEG-PLA polymer is used as primer solution and is brushed onto the tissue and, due to its low viscosity, allowed to flow into the cracks to obtain good adhesion, after which the sealant solution of the PTMC-PEG polymer is added, providing better mechanical properties. After polymerisation using irradiation with light of 470-520 nm in the presence of a photo-initiator, usually eosin Y, the hydrogel is formed due to formation of crosslinks between the acrylate groups of the polymers.[9, 29-31] The resulting sealant consists for more than 80 wt% of water. Over time the sealant degrades by hydrolysis of the poly(ester) blocks, releasing biocompatible degradation products, namely lactic acid and PEG, that can be metabolised or cleared by the kidneys.[31] Other photopolymerisable PEG sealants have also been reported, which work via the same principle. These triblock copolymers consist of PEG as middle block and poly(propylene fumarate)[32, 33] or poly(succinic acid) as outer blocks.[34]

Besides sealants for lung surgery, PEG photopolymerisable tissue adhesives have also been applied for repair of the ventricular wall.[35] The use of these photopolymerisable tissue adhesives is, however, not widespread due to the limitation that irradiation is needed for the polymerisation reaction, which is not applicable to all places in the body. Furthermore, the generated free radicals during the polymerisation process may cause damage to healthy tissue.

A second tissue adhesive based on PEG is known as DuraSeal™ Dural Sealant device. First reports of DuraSeal™ date from 2003[36] when this sealant was used in combination with sutures for dural closure (the outermost membrane around the brain) to prevent leakage of cerebrospinal fluid (CSF), which is one of the potentially dangerous complications of cranial surgery.[37] DuraSeal is a two-component system, which spontaneously forms a crosslinked gel when the components are mixed. The first solution contains trilysine (Figure 3A), a tetra-amine crosslinker, dissolved in sodium borate buffer (pH 10.2) and the second solution consists of an aqueous solution (sodium phosphate buffer, pH 4.0) of a four-armed star-PEG end-capped with *N*-hydroxysuccinimide-esters (NHS) (Figure 3B). The PEG mixture also contains a dye, FD&C Blue No. 1, for easy visualisation.[36, 38, 39] This DuraSeal tissue adhesive can be applied by simultaneously spraying the two components onto the tissue, whereby the amines of trilysine react with the NHS-esters, resulting in the formation of amide bonds,

giving a crosslinked network in seconds (Figure 4). Furthermore, upon application on the tissue the aqueous solution will fill the cavities of the tissue surface and the amine and thiol groups of proteins present in the tissue also react with the NHS-functionalised polymer gel providing covalent adhesion to the tissue.[36, 40]

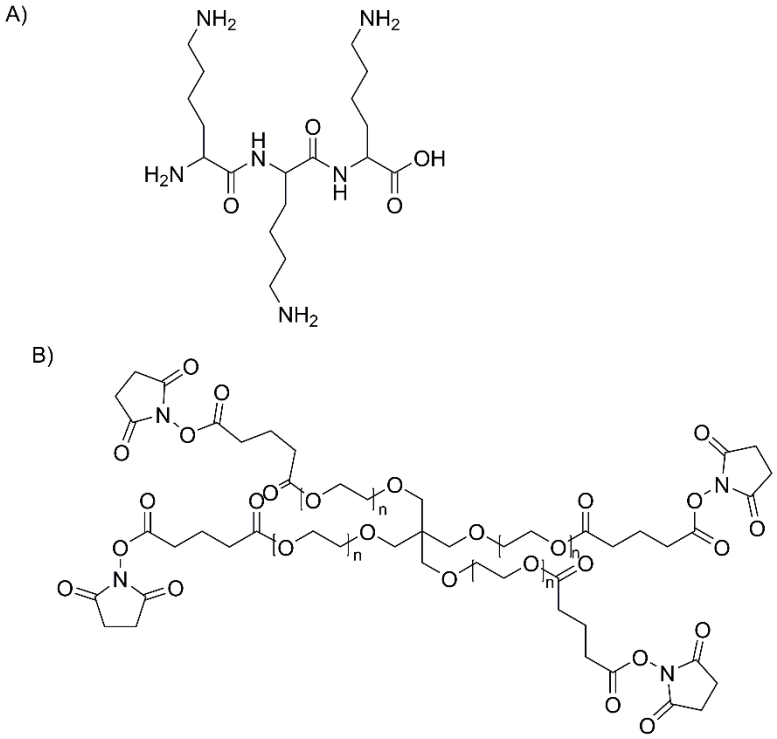

Figure 3: Structures of A) trilysine and B) pentaerythritol poly(ethylene glycol) ether tetrasuccinimidyl glutarate.

The resulting crosslinked gel is a seal giving close to 100% efficacy in watertight closure after brain surgery in human patients.[37, 40] Hydrolysis of this tissue adhesive starts to take place after 4-8 weeks, mostly by hydrolysis of the ester linkages and enzymatic degradation of the lysine units, giving degradation products that are readily cleared from the body by renal clearance.[41] A possible downside of the DuraSeal™ is the uptake of water and, therefore, the swelling of the hydrogel (about 50%) after application. This limits the use of DuraSeal™ in, e.g., bone structures due to the possible oppression of nerves.[6, 42, 43] A modified two compound adhesive DuraSeal™ Xact Adhesion Barrier and Sealant System (DSX) claims to suppress this swelling by introducing more crosslinks between the PEG linker and trilysine. Therefore, this sealant can possibly be used in other applications.[39, 44, 45] Since the chemical composition of the components and the resulting hydrogel are identical to DuraSeal™,[39] it is most likely that lower swelling is achieved by changing the ratio of PEG versus trilysine to get a higher crosslinking density. A final drawback of DuraSeal is the two-component design that can lead to clogging of the syringes, during mixing of the components in the syringe, when not used completely or if the adhesive is not applied quickly enough.

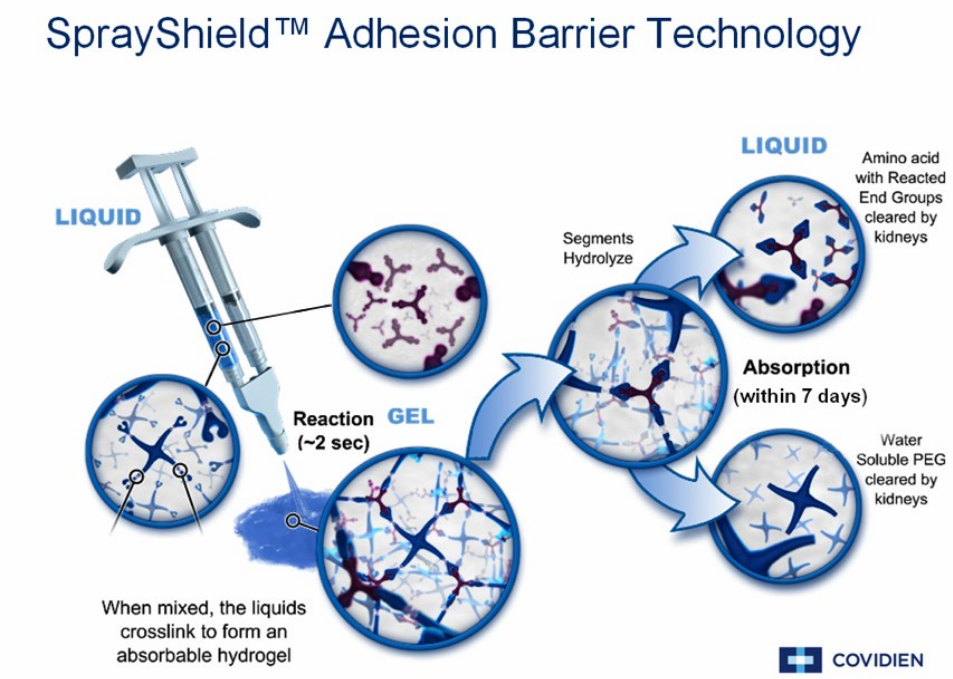

Figure 4: A schematic overview of the process of applying DuraSeal™ using a two component system with a solution of PEG and a solution of trilysine41 Copyright© 2013 Covidien. All rights reserved. Used with Permission of Covidien.

The third important class of PEG-based tissue adhesives are the so called PEG-PEG adhesives, like CoSeal® Surgical Sealant. This two-component tissue sealant contains a 20% (w/v) solution of a four-armed star-PEG polymer of 10 kDa molecular weight end-capped with thiol end groups (Figure 5) in a sodium phosphate/sodium carbonate buffer (pH 9.6) and a second component comprising a 20% (w/v) solution of a 10 kDa four-armed star-PEG end-functionalised with NHS-ester groups, the same as in the DuraSeal Sealant (Figure 3B), in sodium phosphate buffer (pH 6.0).[46, 47] Upon mixing these functional PEG solutions, the thiol reacts with the NHS-ester resulting in the formation of a thioester linkage between the two PEG polymers, giving a crosslinked network within 3 seconds. A small amount of disulfide bridges is also formed. Covalent bonding to the tissue takes place via an amidation reaction between amines present in the tissue and the thioesters in the PEG network.[9, 46, 47] However, even when CoSeal® is applied on non-reactive surfaces, like poly(tetrafluorethene), adhesion to the material is observed, indicating mechanical bonding when the liquid solution flows into the cracks of the material. Hydrolysis of the thioesters and the glutarate esters (present in the star-PEG with NHS groups) leads to degradation of the hydrogel within several weeks.[46] This faster degradation compared to DuraSeal results from the lower stability of the thioester groups in comparison to the amide bonds in DuraSeal.

The main disadvantage of this PEG-PEG hydrogel is its high degree of swelling after application (about 4 times its original size). Furthermore, adhesion to the surrounding tissue is relatively weak.[6, 9, 48] The mechanical strength of DuraSeal™ was compared with CoSeal® In a 2005 study, revealing a higher mechanical strength of the DuraSeal™ adhesive.[49]

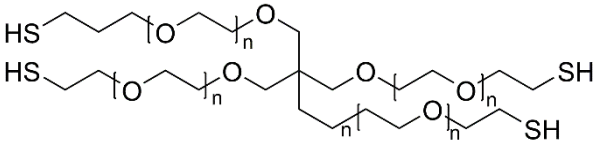

Figure 5: Structure of pentaerythritol poly(ethylene glycol) ether tetra thiol, used in CoSeal®.

Another example of a PEG-PEG sealant is the SprayGel adhesion barrier system, which consists of two reactive PEG solutions. One solution contains NHS-functionalised star-PEG and the other amine-functionalised star-PEG and methylene blue for visualisation. Upon mixing an adhesive hydrogel is formed, which remains intact for 5 to 7 days after which the degradation products are excreted by renal clearance.[50] The system was reported to prevent adhesion after genealogical and colorectal surgery. [50-53] Although early preliminary clinical trials showed the effectiveness of this PEG-PEG sealant, a larger-scale study was stopped owing to a lack of efficacy.[54]

The synthetic hydrogels described above, typically based on PEG, are commonly applied as a surgical tissue tape. They offer the benefit of not containing any human/animal material, are safe and well tolerated, bind strongly and covalently to wet tissue surfaces (adhesion), have a good elasticity and ductility, and are biodegradable. They do have some weaknesses as well, preventing more widespread applications. First of all, they are relatively difficult to handle. The hydrogel is produced in situ out of two components, which are individually stored as freeze-dried products. Before use, they have to be dissolved, and are then applied through a dual syringe spray. Once applied, the hydrogel shows a fast crosslinking, resulting in a short handling time. Moreover, as the hydrogels have a rather weak cohesion (internal strength), they behave more like a gel than a film. This is related to the poor mechanical properties of PEG, due to its low glass transition temperature (T_g < -40 °C)[55] and the tendency to crystallise in a brittle material. The crosslink density of the hydrogel is furthermore relatively low, since it is limited by the number of end-groups in PEG. The large swelling of these hydrogels is another important downside. Therefore, these PEG-based adhesives are regarded as a valuable add-on to sutures, but are inappropriate to function as a strong tissue adhesive that can fully replace them. Apart from this, these PEG-based hydrogel tissue adhesives are rather costly, albeit this has not limited its use in the clinic so far.

Table 2 provides an overview of the polymer-based tissue adhesive products that are currently on the market.

Table 2: Overview of commercially available tissue adhesive materials based on synthetic polymers

Commercial product	Approved indications	Constituents
FocalSeal-L (Focal Inc.), replaced AdvaSeal [28, 29]	Sealing lung air leaks	Photopolymerisable PEG-co-poly(lactic acid)/poly(trimethylene carbonate)
DuraSeal (Covidien), DuraSeal Xact [37-39, 44]	Adjunct to sutures for dural repair Anti-adhesion (SprayShield) Retina reattachment Nerve sciatic anastomosis Vascular closure	Tetra-NHS-derivatised PEG and trilysine
CoSeal (Cohesion Technologies)[46, 47]	Adjunct haemostasis in vascular surgery; inhibiting suture line bleeding	Tetra-NHS-derivatised PEG and tetra-thiol-derivatised PEG
SprayGel (Covidien)[50-52]	Adhesion barrier in gynaecological and colorectal procedures	Tetra-NHS-derivatised PEG and tetra-amine-derivatised PEG
TissuGlu®[56-58]	Prevention of seroma formation	Lysine di/tri isocyanate-PEG

	under skin flaps	prepolymers
TissuePatch (TissueMed)[59-63]	Air leakage in thoracic surgery Sealing and reinforcing soft tissues adjunct to sutures Dural repair in cranial surgery, adjunct to sutures	poly-((*N*-vinylpyrrolidone)$_{50}$-*co*-(acrylic acid)$_{25}$-*co*- (acrylic acid *N*-hydroxysuccinimide ester)$_{25}$)
OcuSeal (Hyperbranch Medical Technology)[64-68]	dressing for corneal lacerations and bandage for corneal transplants	poly(glycerol succinic acid) and PEG-aldehyde
Adherus (Hyperbranch)[69, 70]	Surgical sealant for dural repair, hernia mesh fixation, spinal and cardiovascular applications	Activated PEG and branched poly(ethylene imine)

1.1.4 Polyurethanes

A wide variety of polyurethanes is used for different tissue adhesive or sealant purposes, because of the excellent thermal stability at physiological temperature and absence of haemolytic behaviour of this class of synthetic polymers.[71] The most prominent commercial example is TissuGlu® Surgical Adhesive, which is used for abdominal tissue bonding.

A frequently observed side effect after abdominal or breast surgery is fluid accumulation under the skin, resulting in a so-called seroma. This leads to discomfort by patients and regularly requires drainage to remove the fluid. After surgery, the abdominal skin tissue has to reconnect to the underlying layers of the abdominal wall. However, imperfect connections lead to a void between the skin and the underlying tissue. Fluid accumulation after surgery might be due to the occurrence of this void. Therefore, this tissue adhesive TissuGlu® Surgical Adhesive has been developed to reduce the dead space by forming a bond between the tissue layers.[56]

TissuGlu® is a polyurethane-based adhesive of Cohera Medical Inc. and it is a one-component glue consisting of a hyperbranched polymer with isocyanate end groups containing about 50 wt% of lysine. [56, 57] This polyurethane prepolymer is made by reacting a combination of lysine diisocyanate and lysine triisocyanate with diols and polyols such as PEG and glycerol.[58] When this pre-polymer comes in contact with the water present in tissue it further crosslinks to form a solid network by hydrolysis of some of the isocyanate groups into amines, which react with the remaining isocyanate groups to form the network via urea linkages. Crosslinking takes place within 25 minutes, which gives surgeons enough time to close the abdominal skin. [56, 57] The obtained adhesive is biodegradable due to hydrolysis and enzymatic degradation of the lysine-based linkages, giving a variety of water-soluble degradation products like polyols (e.g. glycerol), lysine (57%), ethanol and carbon dioxide (7%), which can all be readily cleared from the body.[56, 57] Results of TissuGlu® after abdominoplasty surgery in dogs showed little evidence of fluid accumulation after five days, whereas the control group, not treated with the adhesive, revealed significant fluid accumulation. [56] Trials with human patients show that TissuGlu® is safe to use and, indeed, may decrease the extent of fluid accumulation.[72] A CE Mark approval in 2011 has led to commercialisation of TissuGlu® in Europe.[5]

Cohera Medical Inc. also developed a single component Sylys® Surgical Sealant, which is based on the combination of triethoxysilane chemistry and the same urethane chemistry as TissueGlu®. The alkoxysilane in the mixture also reacts with diols and polyols, thereby

providing enhanced crosslinking density. This tissue adhesive can be used to provide support after anastomosis in combination with prevention of leakage.[58, 73]

Polyurethanes are also being used for bone fixation, haemostasis and sealing of vascular grafts in several surgery procedures.[74-76] Vascular grafts are slightly permeable for blood, causing leakage of blood into the body. Therefore sealants are needed to water-tighten these grafts and polyurethanes can be used for this purpose. A suitable polyurethane has been synthesised via the reaction of 4,4-diphenylmethane diisocyanate (MDI) with a poly(tetramethylene ether glycol) (PTMEG) of 1000 Da; subsequently 2,2-bis(hydroxymethyl)-propionic acid (DHMPA) was added to this pre-polymer giving the final poly(urethane) (Figure 6).[5, 75] Besides water-tightening the artificial blood vessel, the sealant must also be able to bind proteins present in the bloodstream, which is important for the blood/biomaterial interaction. For this purpose DHMPA is introduced as this leads to the functionalisation of the product with carboxylic acid groups to which proteins can be bound using EDC chemistry (1-ethyl-3-(3-dimethylaminopropyl)carbodiimide). [5, 75] No in vivo studies are yet reported. It should be noted that the rather hydrophobic and stable character of PTMEG might cause problems due to accumulation.

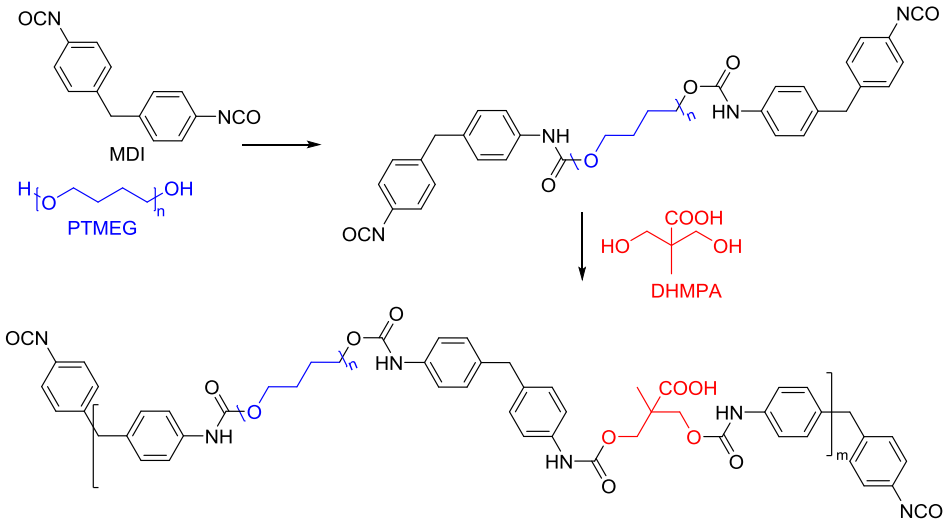

Figure 6: A polyurethane consisting of MDI (black), PTMEG (blue) and DHMPA (red) where the carboxyl groups can covalently bind to tissue.

1.1.5 Polyesters

Aliphatic polyesters such as poly(ε-caprolactone) (PCL) and poly(lactic-co-glycolic acid) (PLGA), which have been widely used in biomedical applications, have also been applied as tissue adhesives. Ferreira et al[77] end-functionalised PCL (Figure 7A) with different isocyanate groups, namely isophorone diisocyanate (IPD, Figure 7B) and hexamethylene diisocyanate (HDI, Figure 7C), to obtain tissue-reactive polymers. This tissue-reactive isocyanate group and its crosslinking mechanism are already explained in section 1.1.4 The adhesive properties were tested by placing the polymers between two pieces of gelatin, followed by pulling apart the gelatin sheets. IPD-modified PCL was able to efficiently bind the gelatin parts together, since mechanical failure occurred in the gelatin matrix without compromising the glued section. The HDI-modified PCL on the other hand was less effective, as pulling led to separation of the two pieces, probably due to a lower NCO concentration in this polymer.[77] A potential limitation of these systems is the absence of crosslinks, i.e. the system fully relies on chain entanglements of linear chains.

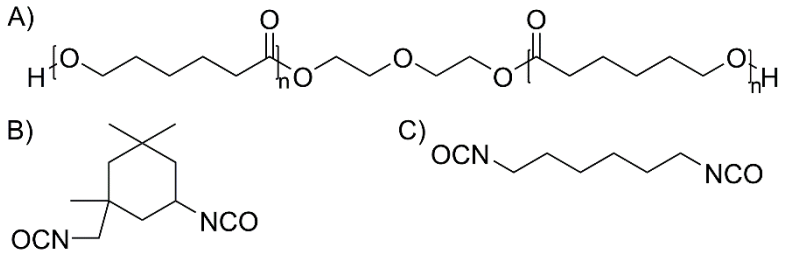

Figure 7: Chemical structures of A) poly(ε-caprolactone) (PCL), B)isophorone diisocyanate (IPD) and C) hexamethylene diisocyanate (HDI).

Instead of using amines present in tissue to react with the isocyanates in the polymer material also faster curing radical crosslinking systems can be applied. Therefore, the biodegradable PCL was modified with 2-isocyanatoethylmethacrylate (IEMA) to form a macromonomer (Figure 8A). Photoinitiator Irgacure 2959 (Figure 8B) was used to start the radical polymerisation of PCL-IEMA and a crosslinked network was formed within 60 seconds and showed a low swelling ratio up to 3%. The crosslinked polymers are biodegradable by hydrolysis of the ester bonds in PCL and after 6 weeks about 10 weight % loss was found. The adhesive strength of this material was tested in the same manner as described above. The polymer and photoinitiator were placed between two pieces of gelatin followed by 60 seconds of irradiation to start the polymerisation. The resulting PCL network was able to hold the gelatin pieces together, similar to the IPD-modified PCL, which is based on interpenetration of the polymer network and the tissue.[78] No in vivo studies are reported yet.

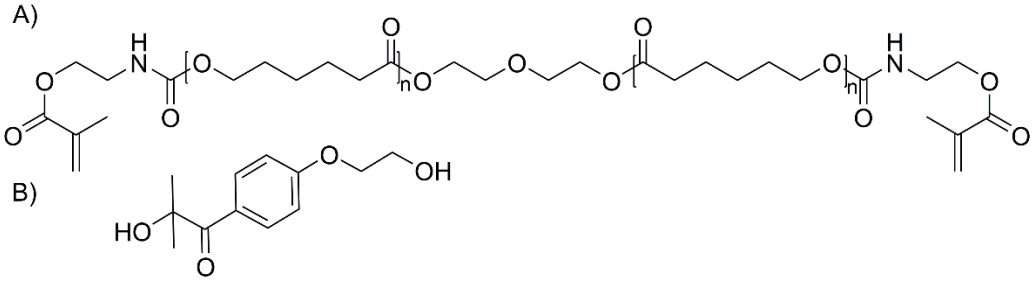

Figure 8: A) Photocrosslinkable poly(ester) consisting of PCL and IEMA and B) photoinitiator Irgacure 2959.

A recently commercialised example of a tissue adhesive based on PLGA is TissuePatch™. This tissue adhesive and sealant is used in the prevention of air leakage after lung surgery or prevention of fluid leakage after surgery on soft tissue.[59] A related sealant is TissuePatchDural™, which is used for watertight closure of the dura to prevent leakage of CSF in patients after brain surgery.[61, 62] Both adhesives are patches based on multiple layers consisting of two different polymers, namely PLGA (Figure 9B) accounting for 23% of the mass of the TissuePatch™ and poly((*N*-vinylpyrrolidone)$_{50}$-*co*-(acrylic acid)$_{25}$-*co*- (acrylic acid NHS-ester)$_{25}$) (Figure 9A). TissuePatch™ is composed of four layers (Figure 9C), where layers 2 and 3 represent the adhesive NHS-functionalised polymer and layers 1 and 4 consist of PLGA interspersed with the NHS-functionalised polymer.[63] For easy visualisation methylene blue is added.[60] When the patch is applied on tissue it covalently binds to the amine groups present in proteins on the tissue surface that attack the NHS-moieties of the TissuePatch™ creating amide bonds between the patch and the tissue.[59] Adhesion to the tissue occurs within a minute. The tape degrades due to hydrolysis of the amide bonds and the PLGA in the body within 50 days.[79] The major advantage of the tape in comparison to the previously discussed sprays is that it is ready to use, so no costly and cumbersome preparation time in the operating theatre is needed.

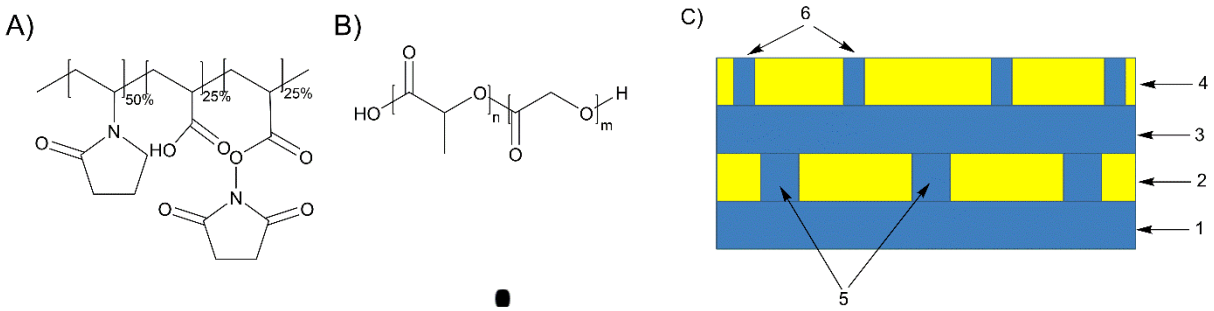

Figure 9: The two polymers present in TissuePatch™: A) poly((*N*-vinylpyrrolidone)$_{50}$-*co*-(acrylic acid)$_{25}$-*co*- (acrylic acid *N*-hydroxysuccinimide ester)$_{25}$) B) poly(lactic-*co*-glycolic acid), C) a schematic overview of the patch where blue layers 1 and 3 represent the NHS-polymer, yellow layers 2 and 4 represent the PLGA layers with openings where the NHS-polymer is present (5 and 6).

1.1.6 Dendrimers and hyperbranched polymers

Dendrimers are perfectly branched polymers grown from a central core. The addition of a branching layer, or generation [G_n], leads to an exponential increase in the number of peripheral groups. Due to their large number of functional groups at their periphery, dendrimers are attractive crosslinkable building blocks for tissue adhesives.[80] In 2002 the use of dendritic tissue adhesives for ophthalmology was reported.[81] These dendritic structures were copolymers consisting of a linear polymer PEG and a dendrimer of poly(glycerol succinic acid) (PGLSA). Different dendrimer generations were made and functionalised with methyl methacrylate (MMA) end groups, giving a series of ([G_n]-PGLSA-MMA)$_2$-PEG dendrimers (Figure 10). An aqueous solution of this dendrimer and photoinitiator, namely ethyl eosin, was added to an animal eye in which a laceration was made and the solution was radically polymerised to form a hydrogel. Binding to the tissue was ascribed to the formation of an interpenetrating network between the crosslinked polymer and the tissue,[81] in which the polymers and tissue were intertwined but not covalently bound.[82] The hydrogels with different dendritic generations were compared in terms of polymerisation time, gel formation and water solubility of the initial components. It turned out that the first generation dendrimer [G_1]-PGLSA-MMA)$_2$-PEG$_n$ (Figure 10) was the optimal hydrogel for this application.[81]

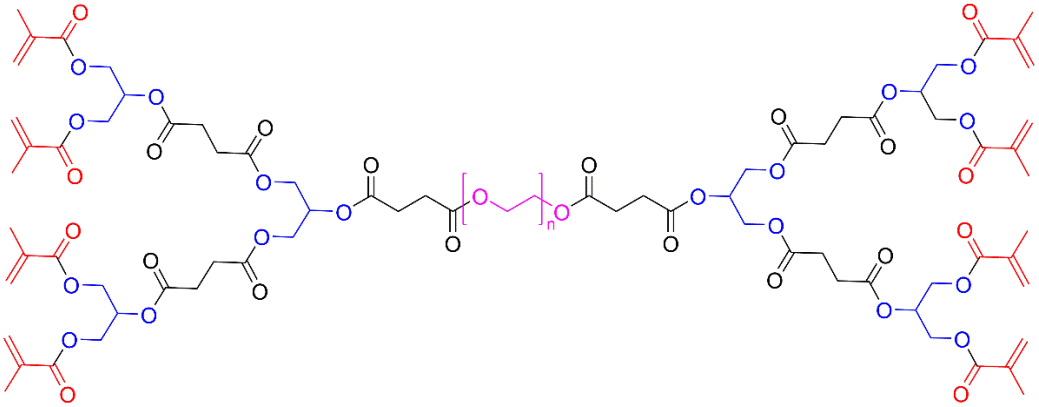

Figure 10: The structure of ([G_1]-PGLSA-MMA)$_2$-PEG$_n$ with PEG in pink, the succinic acid moieties in black, glycerol in blue and the methacrylate groups in red.

Dendrimers containing different PEG building blocks with a molecular weight of either 3.4, 10 or 20 kDa were also compared and concentrations of the polymers were varied between 10% w/v, 20% w/v and 40% w/v. Tissue adhesives are generally tested by making an incision in tissue and gluing this together with the tissue adhesive. The space under the laceration is filled with liquid until leakage is observed. The pressure at which this happens is the leaking pressure. Leaking pressures of a 4.1 mm laceration on the eye were measured using the [G_1]-

PGLSA-MMA)$_2$-PEG$_n$ adhesive, showing that the 10% [G$_1$]-PGLSA-MMA)$_2$-PEG$_{220}$ hydrogel best withstood pressure.[83] No in vivo degradation time or mechanism were reported in literature, although the ester bonds should be susceptible to hydrolysis.

These dendritic tissue adhesives are as effective as traditional sutures in closing a corneal incision in in vitro studies. Both methods have however their downsides. Sutures inflict trauma on the tissue, bring unnecessary strain on the cornea and may give an inflammation reaction. The major downside of using these photocrosslinkable dendrimers is the need of an argon laser to start the polymerisation as well as the radical polymerisation process itself. Therefore, research is focused on finding spontaneous dendritic crosslinking adhesives.[67, 84]

A spontaneous crosslinking system was developed based on the reaction between a lysine-based dendrimer with cysteine end groups ([G$_2$]-(Lys)$_3$-(Cys)$_4$) (Figure 11A) and a range of linear PEG$_{75}$ chains end-functionalised with aldehydes (Figure 11B-D). The 1,2-thiolamine moiety present in cysteine readily reacts with aldehydes, forming a thiazolidine linkage (Figure 11E). Crosslinking between the two components occurred within three minutes at room temperature and pH 3-9, and was successfully used to seal a corneal incision in vitro.[64] The ester aldehyde PEG-2-oxoethyl succinate (Figure 11D) furthermore showed a rearrangement reaction of the thiazolidine linkage into a pseudoproline, which is more stable (Figure 11F).[65] Due to hydrolysis of the thiazolidine or the pseudoproline linker the hydrogels degraded into biocompatible compounds. The degradation time of the gels with either PEG$_{75}$-propionic aldehyde, PEG$_{75}$-butyric aldehyde or PEG$_{75}$-ester aldehyde were 3h, 1.5 weeks or 24 weeks respectively due to the formation of more stable pseudoproline linkages. The short degradation time of the PEG$_{75}$-propionic aldehyde makes it unsuitable as tissue adhesive. The polymers showed no cytotoxicity in rabbit eyes[66] and this sealant is expected to soon become commercially available as OcuSeal and CE mark trials have been started.[68]

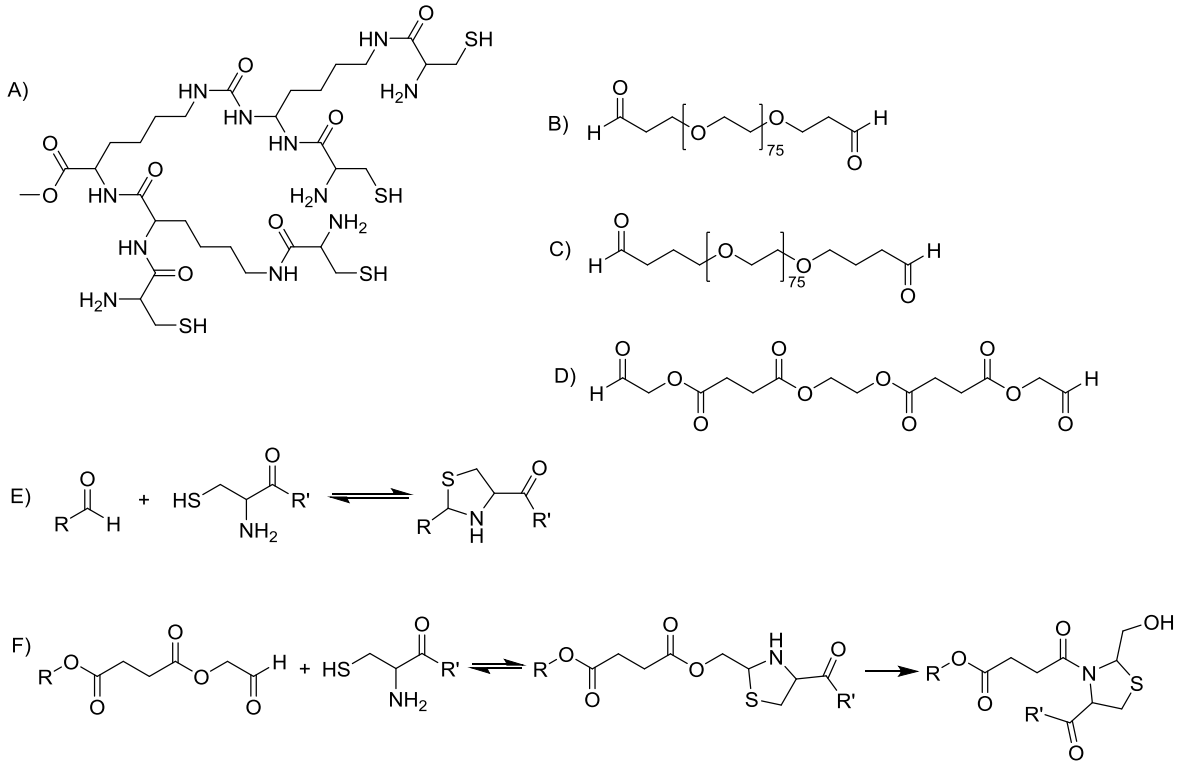

Figure 11: Different components of a hydrogel based on a peptide dendrimer and a PEG-aldehyde with a) [G$_2$]-(Lys)$_3$-Cys$_4$, b) PEG$_{75}$-propionic aldehyde, c) PEG$_{75}$-butyric aldehyde, d) PEG$_{75}$-ester

aldehyde and the reaction between the peptide dendrimer and the PEG-aldehyde to form a e) thiazolidine linkage or f) a thiazolidine linkage that rearranges to a pseudoproline.

PEG lysine-based dendrons bearing four terminal thiols (Figure 12) can be crosslinked with poly(ethylene glycol) disuccinimidyl valerate to obtain a biocompatible adhesive hydrogel, which is formed within seconds by the formation of thioester bonds. This hydrogel can seal a 2.5 mm hole in a vein surface and withstands 250 mmHg pressure. The gel can be disassembled by addition of an excess thiol-containing solution leading to thiol-thiolester exchange and disruption of the crosslinks. By addition of an amine-containing solution, the gel is not degraded. In contrast, a hydrogel of PEG lysine dendron bearing amine groups cannot be degraded by addition of thiols.[85] This recently reported hydrogel is the first example of a tissue adhesive, which can be degraded on demand. This specific feature might be very useful to temporarily close a wound, allowing easy opening for definitive surgical care.

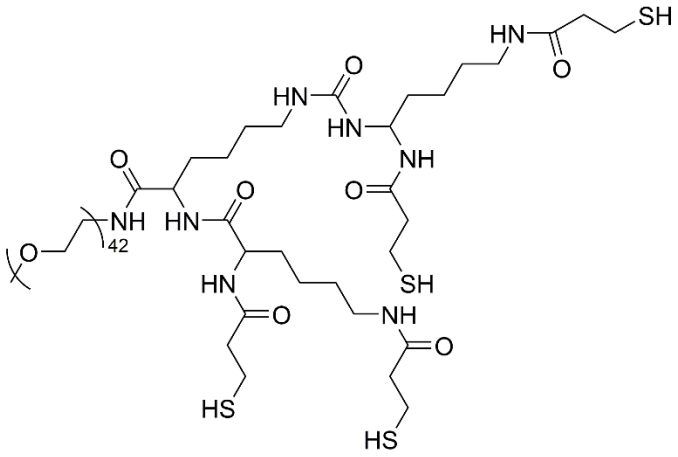

Figure 12: PEG lysine dendron bearing four terminal thiol groups

Hyperbranch Medical Technology Inc. developed sealants (Adherus) based on hyperbranched poly(ethylene imine) (PEI) and an NHS-activated poly(ethylene glycol).[69, 70] PEI (Figure 13) is mostly investigated as non-viral vector system for gene delivery. One of the main concerns of this polymer is its cytotoxicity due to strong electrostatic interactions with the extracellular matrix and cell membranes. Chemical modifications can however reduce the cytotoxicity. Linear PEI (l-PEI) (Figure 13A) only contains secondary amines and also has lower toxicity than hyperbranched PEI (Figure 13B) that contains primary, secondary and tertiary amines.[86] The Adherus Sealant consists of a dual syringe where one syringe contains the NHS-activated PEG solution and the other the PEI solution. The reaction mechanism is the same as for other NHS containing tissue adhesive materials as described in section 1.1.3 and 1.1.5. Upon mixing, a crosslinked hydrogel was quickly formed.[70] The maximum swelling was 25% and the hydrogel was fully resorbed in 90 days.[69]

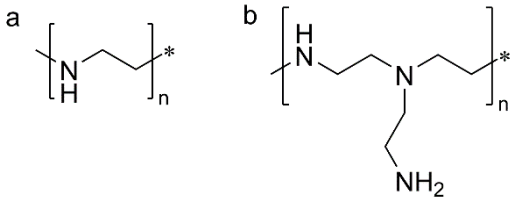

Figure 13: Structures of a) linear and b) hyperbranched poly(ethylene imine).

l-PEI can be prepared by acidic hydrolysis of poly(2-methyl-2-oxazoline) or poly(2-ethyl-2-oxazoline),[86] which are biocompatible and show similar stealth behaviour as PEG (see also section 1.2).[26, 87] Therefore, partial hydrolysis of poly(2-oxazoline)s leading to a copolymer of

poly(2-oxazoline) and l-PEI yields a material with lower toxicity than pure l-PEI (Figure 14).[88] Furthermore, the secondary amino groups present in such a copolymer can be crosslinked with diglycidyl ether to form a hydrogel.[89] Even though the reported hydrogel was not shown to exhibit adhesive properties, this methodology has the potential to be used for tissue adhesive materials as the utilised diglycidyl ether crosslinker can also react with the amines present in tissue.

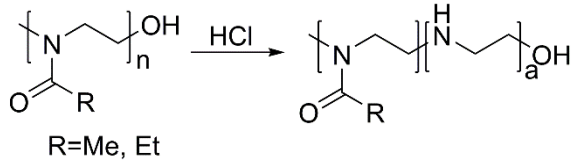

Figure 14: Partial hydrolysis of poly(2-oxazolline) to poly(2-oxazoline-co-ethylene imine).

1.1.7 Mussel adhesive protein-based polymers

A relatively recent development are tissue adhesives inspired by naturally occurring adhesive proteins. One of the main classes investigated are the protein glues produced by mussels. Mussels strongly adhere to natural or man-made underwater structures. They are mechanically robust and operate under saline conditions. These properties have inspired materials scientists to investigate how synthetic mimics of these protein glues can be made and applied in a biomedical setting. The mussel proteins responsible for the adhesive behaviour are well adapted for metal complexation, π-π or π–cation interactions, coulombic interactions and hydrogen bonding. They contain as key elements the amino acids lysine and tyrosine, of which the latter is post-translationally modified to L-3,4-dihydroxyphenylalanine (DOPA). Subsequent oxidation of DOPA leads to quinone formation (Figure 15).[90-93] Although the exact mechanism of crosslinking is still unclear, it is demonstrated that oxidation of DOPA by metal ions or enzymes is necessary to adhere to surfaces or tissue. It is therefore proposed that during maturation of the adhesive plaque of the mussel, the quinone moieties crosslink with other quinones (radical mechanism), amines and/or thiols (Michael addition).[92-94] In addition, crosslinking by metal complexation of three catechol groups to an iron(III) ion might play a role in crosslinking.[95, 96]

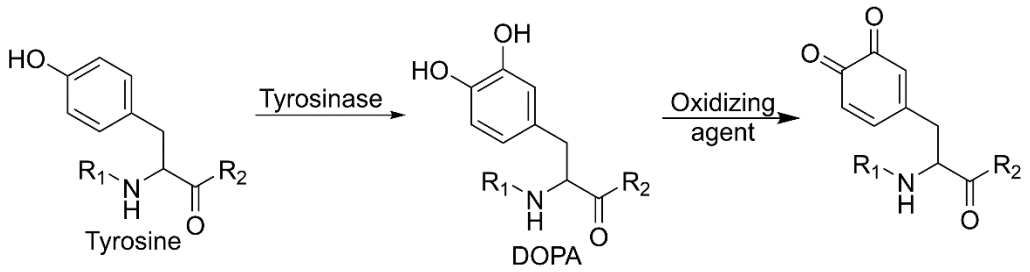

Figure 15: Tyrosine residues are post-translationally modified by the enzyme tyrosinase giving DOPA in mussel adhesive proteins.

Adhesive proteins were extracted and tested for adhesive strengths, which were comparable to fibrin glue. Application was limited for patient use because long curing times, 12-24 h, were needed.[97] Adding oxidizing agents resulted in adhesive strengths which were greater than octyl and butyl cyanoacrylate after only one hour of curing time.[98] Because protein extraction[97, 98] and genetically engineered proteins[92] resulted in low yields[99], biomimetic synthetic polymers have been developed comprising DOPA moieties. To obtain adhesive material with tuneable properties 3,4-dihydroxystyrene, which mimics the catechol side chain of DOPA, was copolymerised with styrene yielding a variety of poly[$(3,4\text{-dihydroxystyrene})_x$-co-$\text{styrene}_y$] copolymers (Figure 16).[93, 100] The copolymer was crosslinked using various crosslinking agents. Dichromate ($Cr_2O_7^{2-}$) showed the fastest crosslinking, while Fe(III) and

periodate (IO_4^-) promoted hardening to the largest extent.[100] The hydrogel with optimal adhesive properties was composed of poly[$(3,4\text{-dihydroxystyrene})_{33\%}$-co-$\text{styrene}_{67\%}$]. When increasing the catechol content, too much crosslinking was obtained, biasing the system toward extra cohesion and thus lowering surface attachment, a copolymer containing 5% catechol groups already showed increased adhesive properties. The adhesion strength of the polymer on aluminium plates was compared with other adhesive glues such as ethyl cyanoacrylate and showed similar results. The polymer has improved adhesion properties compared to mussel adhesive protein obtained via an extraction process. However, the curing time for these biomimetic polymers still amounted to 1h and no adhesive studies on tissues are reported yet.[93]

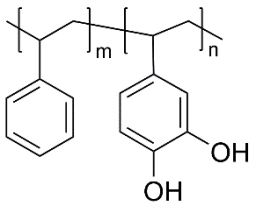

Figure 16: The structure of a poly[$(3,4\text{-dihydroxystyrene})_x$-co-styreney] a biomimetic of the mussel adhesive protein.

DOPA-functionalised poly(ethylene glycol) was first reported in 2002.[101] The triblock copolymer of PEG-poly(propylene oxide) (PPO)-PEG (PEG-PPO-PEG, Pluronics) was functionalised with DOPA and DOPA methyl ester. [101] Pluronics show temperature dependant sol-gel transition behavior at a lower critical solution temperature (LCST), primarily due to micelle formation.[102] The DOPA modified PEG-PPO-PEG demonstrated higher micellisation transition temperatures and were more muco-adhesive than the unmodified Pluronics.[101]
In follow-up research PEG-DOPA hydrogels were published.[94] Linear and branched PEG were modified with DOPA endgroups (Figure 17). When the polymer contained two or more catechol units, upon oxidative crosslinking a hydrogel was formed within 1 minute, whereby the gelation time could be controlled by the type and concentration of polymer and oxidising agent. [94]

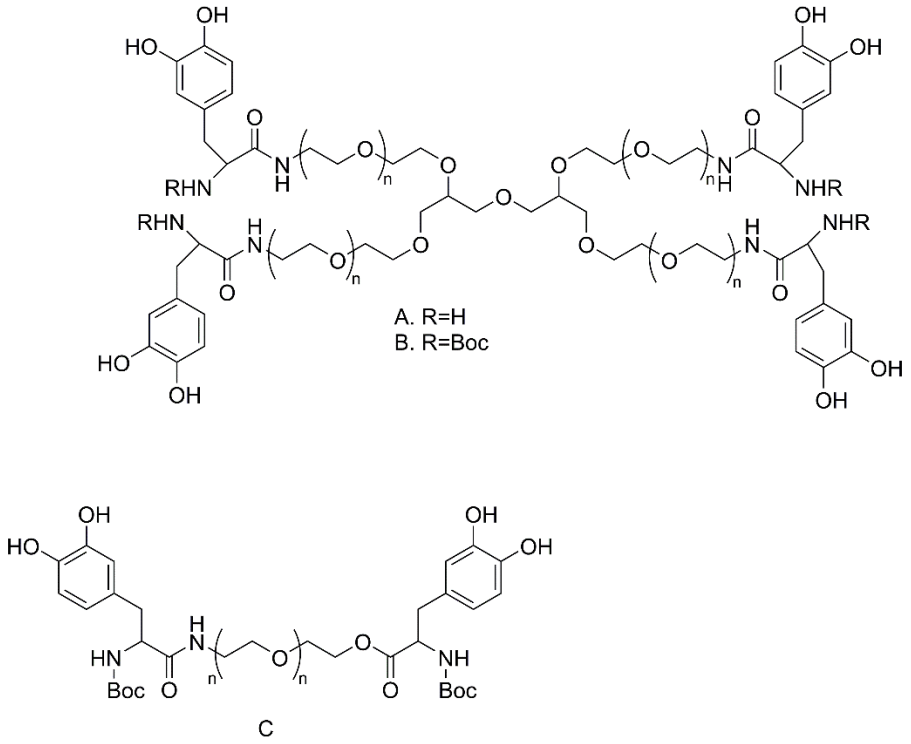

Figure 17: Chemical structures of DOPA-PEG

The four-armed star-PEG functionalised with four DOPA molecules (Figure 17A and B) was mixed with thermally responsive $NaIO_4$-filled liposomes. The liposomes are stable at room temperature and disassemble upon heating, thereby releasing the $NaIO_4$. When the two solutions were mixed and brought to 37 ˚C $NaIO_4$ was released from the liposomes and used to oxidise the catechol groups, resulting in rapid hydrogel formation. The strength of the hydrogel was tested on porcine skin and showed better mechanical properties than fibrin glue. The hydrogel was allowed to cure for 24h in this study before the mechanical properties were tested. A disadvantage of this glue is the need for $NaIO_4$, which is toxic.[103] Nonetheless, this adhesive was tested in mice to immobilise transplanted islets at external liver surfaces and an epididymal fat pad. The tissue showed minimal acute or chronic inflammatory response. The hydrogel maintained an intact interface with the tissue for up to one year.[104] This adhesive was compared with other sealants, namely Dermabond (2-octyl cyanoacrylate), Histoacryl (n-butyl-2-cyanoacrylate), SprayGel (4 arm PEG-NHS and 4 arm PEG-NH_2), photopolymerised PEG sealant and fibrin glue, for sealing foetal membranes in vitro. Only the PEG-DOPA sealant met the requirements of membrane bonding and non-toxicity.[105] To overcome the problem of long degradation times, a dipeptide of alanine-alanine was incorporated between the PEG polymer and the DOPA moiety. Even though this dipeptide is susceptible to enzymatic degradation, in vitro studies showed no degradation and only slow degradation was found in vivo.[106]

Murphy et al[107] developed PEG-polycaprolactone (PCL) copolymers with DOPA end-groups. This tissue adhesive was solvent cast onto surgical meshes used for hernia repair to provide adhesive coated meshes. The films were cured by addition of sodium periodate and up to 30 wt% of PCL-triol. These constructs had significantly higher adhesive strengths than fibrin glue. The degradation, mechanical and physical properties were tuned by varying polymer composition, PCL-triol content, coating density and oxidant concentration. This adhesive can eliminate the need for mechanical fixation of meshes and probably be used as reinforcement for soft tissue and surgical repair.[107] The PEG-PCL-DOPA polymer was tested for tendon

repair. Its adhesive strength was significantly higher compared to Tisseel fibrin glue and reached 60% of the Dermabond strength. The adhesive was coated onto a biological scaffold and this was placed over a transected tendon improving the biomechanical properties compared to suture repair.[108]

Citric acid, PEG and dopamine have also been combined to form catechol-containing prepolymers (Figure 18). This adhesive was applied in a dual syringe system with the prepolymer in one syringe and a sodium periodate (initiator) solution in the other, resulting in an injectable citrate-based mussel-inspired bioadhesive (iCMBA). After mixing, gel times varied from 18 seconds to just over 5 minutes, depending on the structure of the prepolymer, the amount of initiator and the amount of dopamine present. In vivo studies in rats showed only minor acute inflammation. Bleeding wounds in these rats were closed with the iCMBA within 2 minutes, without the use of sutures. iCMBAs showed 2.5 to 8 times greater strength than fibrin glue. Due to the ester linkages, the tissue adhesive formulation is biodegradable.[109]

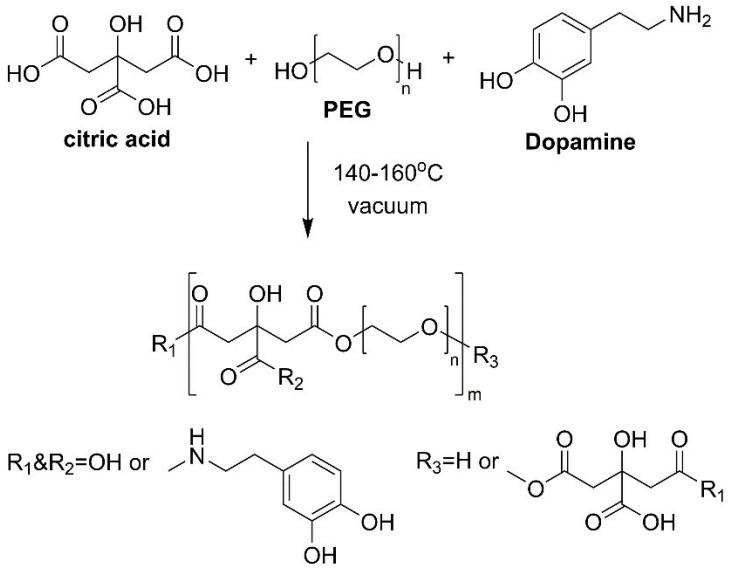

Figure 18: Schematic representation of iCMBA pre-polymer synthesis.

Another possible wound dressing hydrogel consists of thiol-functionalised poly(ethylene glycol)-poly(propylene oxide)-poly(ethylene glycol) (PEG-PPO-PEG) (Plu-SH, Figure 19B) and catechol-functionalised hyaluronic acid (HA) (Figure 19A). The crosslinking between the thiol and quinone groups, obtained by oxidation of the catechol groups, led to the formation of a hydrogel upon mixing (Figure 20) whereas reaction with amine groups present in the tissue proteins gave adhesion to the tissue. This mixture is thermosensitive; at room temperature the two polymers were barely crosslinked, leading to a low viscous reaction mixture. However, at the body temperature of 37 °C, above the LCST of Plu-SH, the mixture became highly crosslinked giving a robust hydrogel. For in vivo studies a premixed solution of 16 wt% was injected subcutaneously into mice where the hydrogel was allowed to form. After 21 days 78 wt% of the hydrogel was still present, showing slow degradation. The hydrogel was adhered to the surrounding tissue, although both HA and Plu by themselves are normally used as anti-adhesive materials in surgery. The adhesion was therefore due to the reaction between the lysine residues in tissue with the remaining catechol moieties.[110] Instead of hyaluronic acid, chitosan can also be functionalised with DOPA groups resulting in a hydrogel with similar properties. After 25 days in vivo, this gel maintained 97% of its original weight, so it degrades even slower.[111] Since chitosan shows haemostatic behavior, a possible additional use of the latter gel could be to stop excessive bleeding.

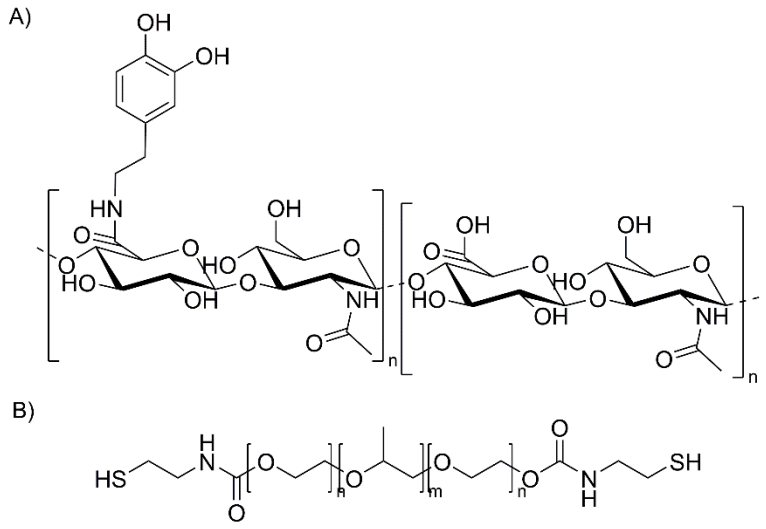

Figure 19: Structures of A) catechol-functionalized hyaluronic acid and B) thiol-functionalized poly(ethylene glycol)-poly(propylene oxide)-poly(ethylene glycol) (Plu-SH).

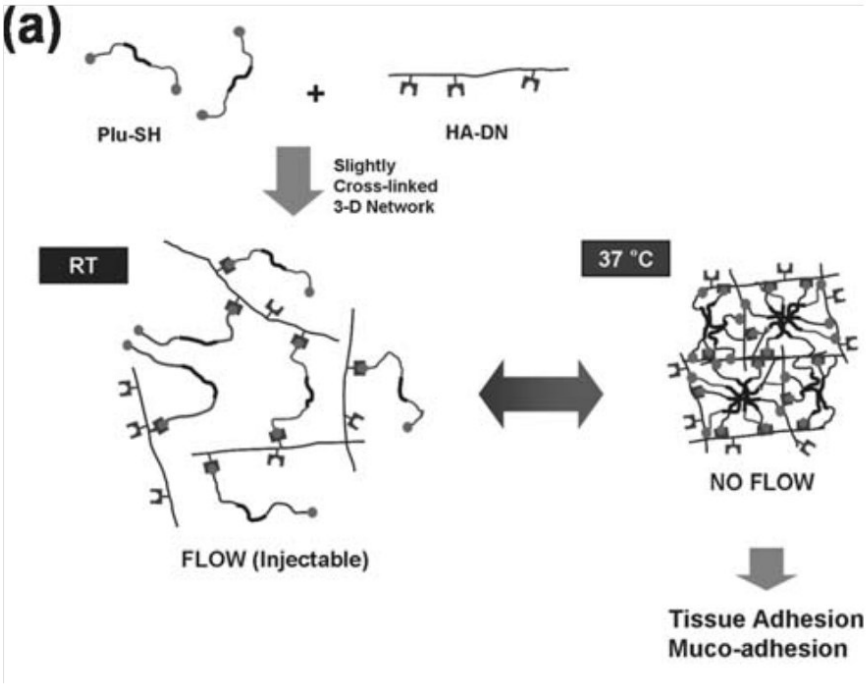

Figure 20: A schematic representation of HA/Pluronic hydrogels. Slightly cross-linked 3-D network formation of HA/Pluronic hydrogels and their sol–gel transition behavior. Reproduced from ref[110] with permission of The Royal Society of Chemistry

Swelling is one of the main issues of PEG-based materials leading to adhesion failure of the gel and, therefore, polymeric branched gels based on PPO-PEG were developed. The 4 arm PPO-PEG block copolymer (tetronic polymer) is end-functionalised with DOPA moieties and exhibits LCST behavior based on collapse of the PPO block. When crosslinking is performed at room temperature a hydrogel is formed that contracts upon heating to physiological temperatures due to collapse of the PPO. By varying the gel formation temperature and polymer concentration, swelling can be controlled between 0 and -25%. The tissue adhesion of this PPO-PEG material was better than PEG based adhesives.[112]

Catechol oxidation requires cytotoxic oxidising agents or high pH values (>8). To avoid these conditions, a water-soluble biocatalyst was developed. This catalyst consists of hematin, an iron-containing heme group which has been studied as an oxidative catalyst, grafted onto chitosan to improve solubility. However, hydrogen peroxide is needed for the oxidation of the catechols, which raises concerns about cytotoxicity of the formulation, even though cytotoxicity studies showed 95% cell viability. Hydrogels were prepared using this catalyst and these showed enhanced tissue adhesion compared to hydrogels formed by a pH trigger.[113] If hydrogen peroxide can be produced in situ, the cytotoxicity concerns will be avoided.

The main concerns of using mussel adhesive protein mimics are the long degradation times and the use of toxic oxidising agents like periodate and iron (III). Since most of these systems are PEG based, all previously mentioned drawbacks (section 1.1.3) associated with the use of this polymer also account here. Nonetheless, DOPA-functionalised polymers show high potential as tissue adhesives, although no clinical studies have been performed to date.

1.1.8 General discussion on polymer-based tissue adhesives

The use of sutures or staples for closure of incisions has certain drawbacks, especially when delicate and vulnerable tissues, prone to leakage of fluids or gas, have to be closed or connected. Tissue adhesives seem a good alternative for these purposes. Additionally, tissue adhesives can be used in combination with sutures to yield a water tight seal. Many different synthetic polymers, polysaccharide- and protein-based adhesives have already entered the market.[8] They, however, have several drawbacks as well. When comparing these three types of adhesives, general problems arise for each of the different classes.

A main class of synthetic adhesives are the cyanoacrylates, which are suitable for closure of skin incisions. However, due to their toxic degradation products (formaldehyde) other applications are difficult to realize. PEG-based hydrogels don't have this problem, but significantly swell in vivo and thereby limit applications close to nerves. The PEG gels often also lack good mechanical strength, which greatly limits their applicability. The general challenge regarding synthetic adhesives is to find polymers which are non-toxic and which display good gel strength. The variety of polymers used at the moment is therefore small and most adhesives are based on either PEG, polyurethanes or PLGA. Clearly there is a need for new synthetic polymers which satisfy better the criteria for an optimal tissue adhesive. Biomimetic adhesives are a rapidly expanding research field. Especially the introduction of the dihydroxyphenyl moiety (DOPA), responsible for the adhesive behavior of mussel adhesive proteins, into synthetic polymers, such as polystyrene or PEG, is being explored. This research area shows a lot of perspective in adhesion strength, but long degradation times and the use of toxic oxidizing agents are major concerns. The long degradation problems can be solved by using biodegradable polymers or by introducing dipeptides which are susceptible to enzymatic degradation.

A limited number of reactive groups are frequently used for tissue adhesive materials. The most popular functional moieties are methacrylates for photopolymerisation and NHS-esters or aldehydes for spontaneous crosslinking with amines. The large downside of using methacrylate functionalisation is the absence of a direct linkage to tissue and the use of external irradiation to start the polymerization. NHS-ester chemistry is very popular in the search for new adhesives due to its reactivity towards amines which are widely present in tissue. It is used in various synthetic polymer-based adhesives and in chondroitin sulphate adhesives.[8] It also does not have the problems associated with toxicity as is the case with glutaraldehyde or formaldehyde-based crosslinkers. Functional groups which are less

frequently used are isocyanates and DOPA. Isocyanates can react with all sorts of nucleophiles, including water, which as a side reaction diminishes the possibility of the isocyanates to bind to tissue. DOPA is already discussed before.

The list of functional moieties used in tissue adhesives is much more extended when the patent literature is taken into account.[8] It will however be difficult to promote one of these alternative chemistries into real applications, as the abovementioned existing coupling routes are at the moment still sufficient and reliable.

Looking at the general direction that the research on adhesives is taking and the demands of the market, a future tissue adhesive should ideally fulfil all following requirements:

- The adhesive and its metabolites are biocompatible, biodegradable and non-toxic, giving no allergic or histotoxic reaction;
- Tuneable adhesion time for different applications;
- Cohesion strength matches the application
- Short or no preparation time, be readily usable for surgeons;
- Swelling index is acceptable;
- The tissue adhesive is shelf-stable;
- Tuneable degradation time;
- Coloured for easy visualization;
- No device or extra reagents are needed for application.

Despite the large amount of research on tissue adhesives, there is no product on the market that complies with all of these requirements, leaving opportunity for further improvement in the (near) future. However, when trying to bring a new tissue adhesive to the market, the largest challenge will probably be to find a unique quality that stands out from the rest, by incorporating special properties (anti-microbial activity or haemostatic behavior for example) or to significantly outperform all current products. It is to be expected that more advanced adhesives will soon enter the market, especially those that are easier applicable for surgeons, have better adhesive and mechanical properties, as well as more switchable adhesives allowing on demand removal. One class of polymers that is regarded to be potentially very interesting for biomedical applications are the poly(2-oxazoline)s which are described in the second part of this chapter.

1.2 Poly(2-oxazoline)s

Poly(2-alkyl/aryl-2-oxazoline)s (PAOx) are an interesting class of polymers because of their tuneable properties, biocompatibility, stealth behavior and thermosensitivity.[87, 114-116] The living cationic ring opening polymerisation (CROP) of 2-oxazoline monomers (Figure 21) was first reported by four independent research groups in the 1960s,[117-120] which provides easy access to well-defined polymers with controlled end group functionalities, incorporated by the use of functional initiating and terminating agents.

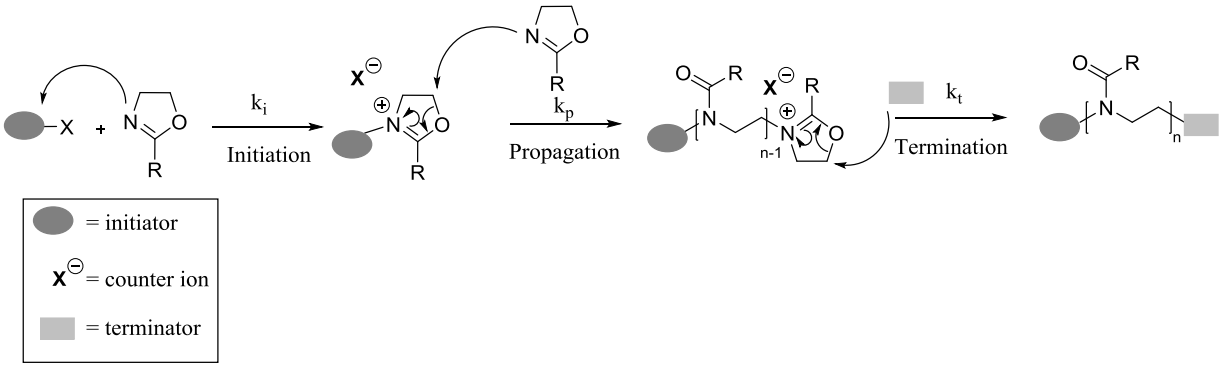

Figure 21: Polymerisation mechanism of 2-oxazoline monomers to yield poly(2-alkyl/aryl-2-oxazoline)s

1.2.1 Monomer synthesis

2-Oxazoline monomers can be prepared via different routes, of which the Witte-Seeliger synthesis, modified Wenker method and the α-deprotonation route are mostly used.[114, 121, 122]

The Witte-Seeliger synthesis[123] is the most commonly used method to synthesize a 2-oxazoline monomer. In a one-step synthesis a nitrile and 2-aminoalcohol are reacted in the presence of a Lewis acid catalyst, e.g. zinc acetate, to activate the nitrile function (Figure 22). During this synthesis ammonia is released, which is the biggest drawback of this synthesis because it can act as terminating agent preventing the polymerisation. This reaction is performed at high temperatures, typically 130 °C, which limits the choice of reagents; furthermore, the release of ammonia can cause problems when functional groups are incorporated.

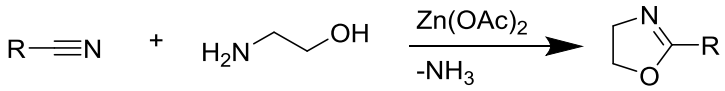

Figure 22: The Witte-Seeliger procedure for the preparation of 2-oxazolines

The modified Wenker method[122, 124-126] provides milder reaction conditions. In this multistep process (Figure 23) an activated carboxylic acid, usually an acid chloride commercially available or home-made, is reacted with 2-chloroethylamine hydrochloride to form a secondary amide. This intermediate compound is subsequently ring-closed under basic conditions to yield the monomer.

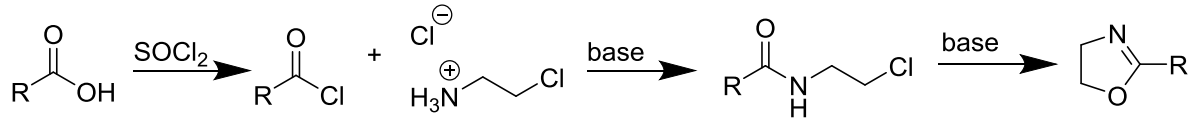

Figure 23: Modified Wenker synthesis of oxazoline monomers

A more recent route for monomer synthesis is the α-deprotonation of 2-methyl-2-oxazoline (MeOx),[127, 128] followed by a nucleophilic substitution with an alkylbromide (Figure 24). The deprotonation is performed with n-butyllithium/tetramethylethylenediamine (n-BuLi/TMEDA) or lithium diisopropyl amide (LDA).

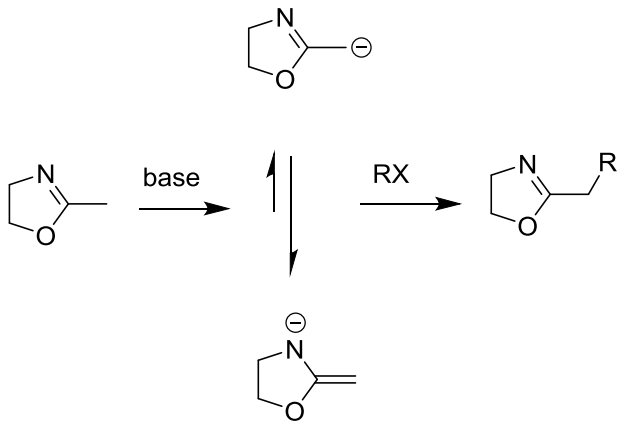

Figure 24: α-deprotonation of MeOx followed by nucleophilic substitution with an alkylbromide.

1.2.2 Polymerisation mechanism

During initiation the nitrogen of the first monomer attacks the electrophilic initiator, such as tosylates, triflates, methyl iodides or alkyl halides, resulting in the formation of an oxazolinium cation. A fast initiation is needed to avoid slow or incomplete initiation which will lead to a deviation of the desired first order kinetics yielding broader molecular mass distributions and higher dispersities.[114, 115] The nucleophilicity of the counterion influences the equilibrium between the cyclic ionic active species and the covalent species.[114, 115, 129, 130] Functional initiators can be used to introduce groups which can be used for later post polymerisation modification, to e.g. alkyne,[131, 132] anthracene[122, 133, 134] methacrylate[135] or other unsaturated substituents.[122, 136, 137]

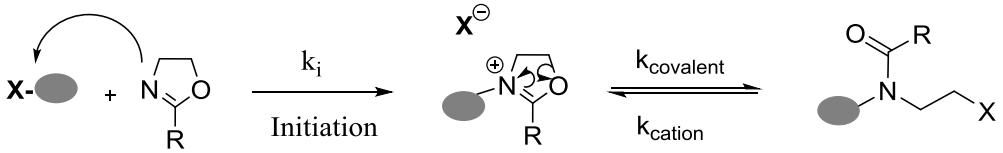

Figure 25: Imitation mechanism of CROP of 2-oxazolines and the equilibrium between covalent and ionic species

The next monomer subsequently attacks this cation, leading to the formation of the ring-opened poly(2-oxazoline) which still has the active propagating cationic chain end. The addition of the first monomer to the cation formed during initiation ($k_{p,1}$) is the rate-determining step. After this the propagation rate (k_p) dramatically increases due to the interaction of the carbonyl of the penultimate unit with the oxazolinium ring, (Figure 26) resulting in the stabilisation of the transition state and shift towards the more reactive species.[129, 130] Also during polymerisation covalent or ionic species can be present depending on the counterion and the nucleophilicity of the monomer, the more oxazolinium species present the faster the polymerisation proceeds. Chloride counterions result in covalent propagating species while tosylate and triflate counterions yield ionic oxazolinium species.[115, 122, 129, 130]

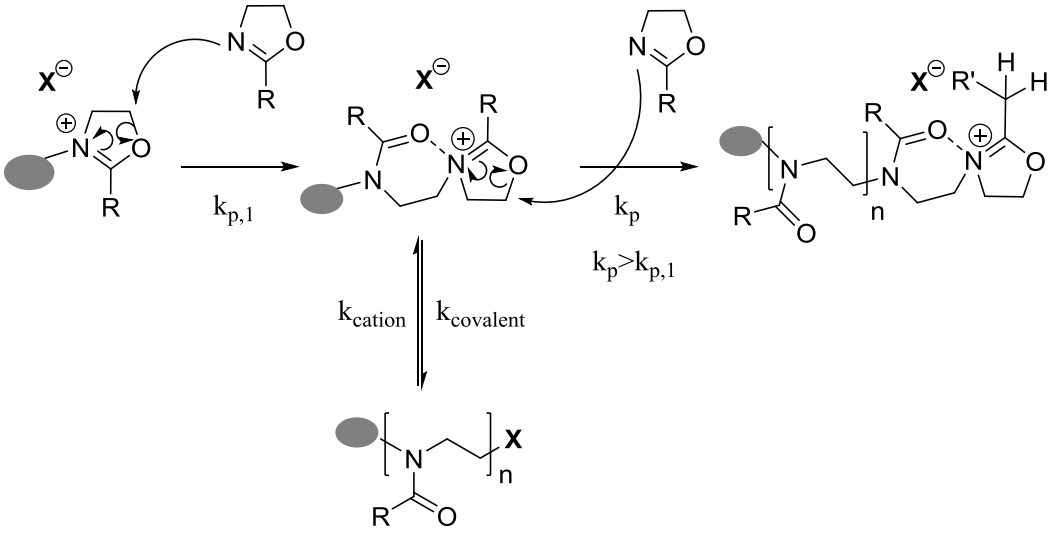

Figure 26: Propagation mechanism of CROP of 2-oxazolines

A living polymerisation is characterised by fast initiation and the absence of undesired transfer and termination reactions and the overall rate will thus follow first-order kinetics:

$$-\frac{d[M]}{dt} = k_p[P^+][M]$$

where [M] is the monomer concentration, t is the reaction time and $[P^+]$ is the concentration of growing chains. Because the polymerisation is living, $[P^+]$ is constant and equal to the initiator concentration $[I_0]$, so the equation can be rewritten and integrated:

$$ln\left(\frac{[M]_0}{[M]_t}\right) = k_p[I]_0 t$$

The propagation rate constant (k_p) can be determined by measuring monomer concentrations at different time intervals and subsequently calculated from the linear first order kinetic plot. True living polymerisations also have a linear correlation between conversion and number averaged molecular weights because all polymers grow at the same time.

The k_p of 2-oxazolines is dependent on temperature and monomer structure. Conditions for polymerisation were optimised revealing a reaction temperature of 140 °C in a microwave reactor as ideal conditions due to the minimum side reactions. Because the boiling point of acetonitrile, the most common solvent for oxazoline polymerisation, is 82 °C, an overpressure is created in a closed reaction vessel. Similar kinetics were obtained by microwave synthesis and conventional heating in pressure tubes, demonstrating that no specific microwave effect occurs.[138] The polymerisation can be performed over a wide range of temperatures without the occurrence of significant chain-transfer reactions.[114, 115]

Side chain functionalisation can be obtain by (co)polymerisation of a functional monomer. Nucleophilic groups which can interfere with the polymerisation should be protected. The simplest monomers bear linear alkyl side chains varying in length (Figure 27 **1**-**4**),[139] more complex monomers bear chains which contain protected carboxylic acids[126, 140, 141] (Figure 27 **5**), protected alcohols[140] (Figure 27 **6**), alkynes[142] for performing copper(I)-catalysed azide-alkyne cycloaddition (CuAAC) click chemistry (Figure 27 **7**), azides[143, 144] for CuAAC (Figure 27 **8**), protected amines[145] (Figure 27 **9**), protected aldehydes,[127] branched or cyclic alkyl chains,[120, 128, 146] inert perfluorinated chains,[120, 147] aromatic chains,[120, 148-150] fatty acids[151, 152] or terminal alkyl chains for thiol-ene or thiol-yne chemistry.[125, 142]

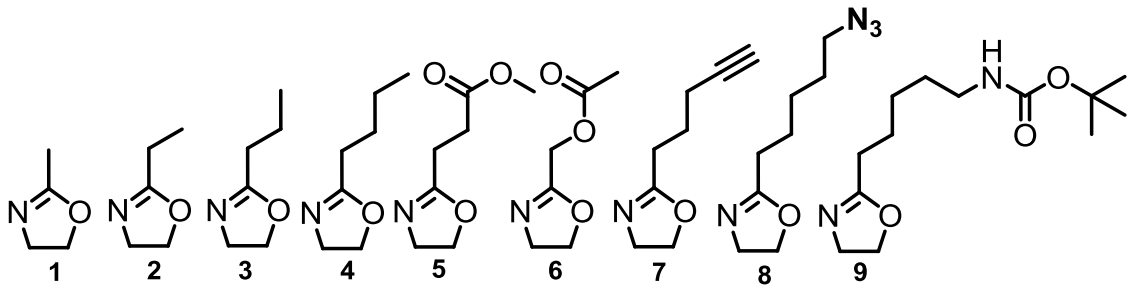

Figure 27: Different monomer structures. From left to right **1**: 2-methyl-2-oxazoline (MeOx), **2**: 2-ethyl-2-oxazoline (EtOx), **3**: 2-*n*-propyl-2-oxazoline (*n*PropOx), **4**: 2-n-butyl-2-oxazoline, **5**: protected acid oxazoline, **6**: protected alcohol oxazoline, **7**: alkyne functionalized oxazoline, **8**: azide functionalized oxazoline, **9**: protected amine oxazoline

After the polymerisation is finished a terminating agent can be added; in literature piperidine[136, 153] or a methanolic sodium or potassium hydroxide[122, 154] are mostly used.[114, 136] The latter one results in a hydroxyl terminus which can be functionalised. All nucleophilic reagents can be used as terminating agent. Some bear functional groups for post modification, e.g. azide,[133, 155] piperazine[142, 156, 157] or polymerisable groups.[158-160]

The synthetic versatility of poly(2-oxazoline)s allows the copolymerisation of different monomers to tune properties, gives easy access to a wide diversity of polymer structures, like block copolymers and non-linear architectures.[87, 114, 115, 121, 122, 161, 162]

1.2.3 Polymer properties

The poly(2-oxazoline) polymer properties can be tuned by variation of the side chain of the oxazoline monomer and copolymerisation of monomers with diverse properties.[87, 114, 115, 163] In this section the solution and thermal properties and biocompatibility are discussed.

1.2.3.1 Aqueous solution behaviour

Poly(2-methyl-2-oxazoline) (PMeOx) is water soluble in the entire temperature range under atmospheric pressure. Poly(2-ethyl-2-oxazoline) (PEtOx) and poly(2-propyl-2-oxazoline) (PPropOx) show lower critical solution temperature (LCST) behaviour. At low temperatures the polymer is completely water soluble, but upon heating it undergoes an entropy-driven dehydration which results in the collapse of the polymer chain (Figure 28). This phase separation of high polymer concentration droplets results in a turbid or cloudy solution, which occurs at the cloud point temperature (T_{CP}). The incorporation of more hydrophilic monomers will favour the water solubility, so the hydrophobic-hydrophilic balance in the polymer will determine the T_{CP}. The LCST is defined as the temperature minimum of the phase diagram (Figure 29), the corresponding concentration is the lower critical solution concentration (LCSC).[163, 164]

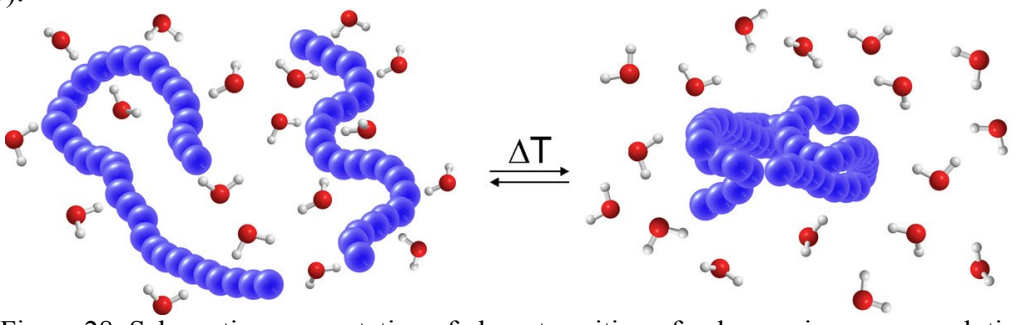

Figure 28: Schematic representation of phase transition of polymers in aqueous solution.

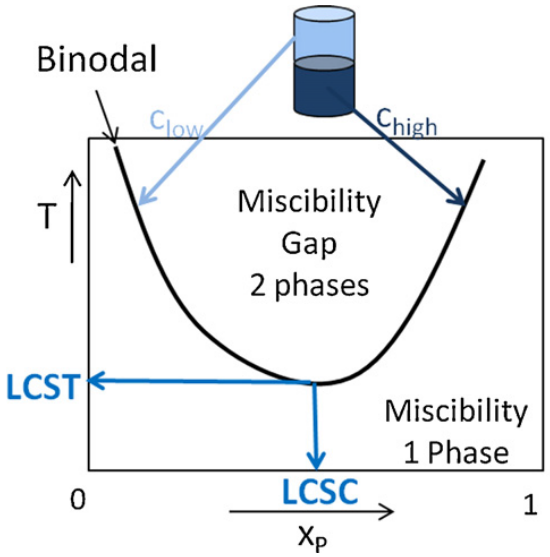

Figure 29: Temperature composition phase diagram for polymers exhibiting LCST behaviour

PEtOx has an LCST of 60 °C, but depending on molecular weight, concentration and end groups, soluble polymers up to 100 °C can be obtained.[87, 114, 163, 165] Increasing the side chain with one carbon atom to obtain PPropOx leads to a dramatic decrease of the LCST. Poly(2-*n*-propyl-2-oxazoline) (P*n*PropOx) has a transition temperature of 25 °C, poly(2-cyclopropyl-2-oxazoline) (P*c*PropOx) of 30 °C and poly(2-isopropyl-2-oxazoline) (P*i*PropOx) of 35 °C, while side chains with four or more carbon atoms are fully water insoluble. [114, 166, 167]

T_{CP}s can be tuned from 9 °C to 100 °C by varying the molecular weight and composition of the polymer by incorporation of more hydrophobic or hydrophilic monomeric units, either by copolymerisation or post-modification.[153, 154, 163, 168-171] The addition of salts to the polymer solutions can also influence the cloud points. Sodium chloride will lead to salting out, decreasing the T_{CP}, while tetrabutylammonium bromide causes salting in, increasing the T_{CP}.[172, 173]

1.2.3.2 Thermal properties

PAOx is a highly thermally stable polymer which only starts to degrade above 300 °C.[88, 114] PMeOx and PEtOx are amorphous polymers with glass transition temperatures (T_g) of 80 and 60 °C respectively. Nonetheless, melting transitions have been reported: PMeOx fibres are semicrystalline with a melting transition of 200 °C,[120] and PEtOx can crystallize when isothermally heated above its LCST, resulting in a melting temperature (T_m) of 201 °C.[174] PnPropOx is an amorphous polymer, while PiPropOx can be crystallised upon isothermal heating above LCST.[175, 176] Polymers with longer side chains show lower T_gs, correlated inversely with chain length, poly(2-hexyl-2-oxazoline) has a T_g of -10 °C. Polymers with longer side chains only exhibit melting temperatures.[152] T_gs of aromatic PAOx polymers are higher compared to poly(2-alkyl-2-oxazolines) due to the higher rigidity.[177] The thermal properties can also be tuned by copolymerisation.[120, 170, 178]

1.2.3.3 Biocompatibility and stealth behaviour

PEG is regarded as the gold standard biocompatible polymer for biomedical applications,[55] but still has some drawbacks like oxidative degradation and, upon prolonged exposure in the human body, the occurrence of an immune response as indicated by the presence of PEG antibodies.

The biocompatibility of PMeOx was already proven in 1989; by injection of ^{125}I-labeled polymers into mice, no accumulation was found in organs. However, a small, probably high molecular weight fraction was found in the muscles and skin.[179] More recent work showed that well-defined PMeOx and PEtOx do not accumulate in tissue and show rapid blood clearance.[180] Stealth behaviour was proven by coating of liposomes with PMeOx or PEtOx, resulting in enhanced circulation times in rats and mice. PMeOx and PEG-decorated liposomes had similar circulation times, while PEtOx was cleared slightly faster.[181, 182] Rathna showed that PEtOx improved the biocompatibility of hydrogels.[183]

Polymer-drug/protein conjugation is a well-known method to improve circulation time, solubility and immunogenicity.[87, 116] Many proteins, e.g. catalase, trypsin, BSA, insulin, have been coupled with PMeOx or PEtOx showing similar performances as PEG conjugates.[116, 184, 185] Only a few PAOx-drug conjugates are known in literature.[116] Serina Therapeutics developed the most promising one; a ritigotine-PAOx conjugate which provides an increased circulation time of this drug, enabling once-a-week injection of the conjugate to Parkinson's disease patients.[186]

PAOx-based micellar or aggregated drug systems are more studied than the conjugates, these systems can be formed by the self-assembly of amphiphilic block copolymers. Multiple drugs can be loaded at the same time into the micelle/polymersome, enhancing solubility of hydrophobic drugs in the hydrophobic core and circulation times and reducing side effects.[187] Aggregates based on poly(2-phenyl-2-oxazoline) (PPhOx)-PMeOx gradient or block copolymers and di- and triblock copolymers of poly(2-*n*-butyl-2-oxazoline) (P*n*BuOx) have been used for drug loading.[188-190] Assemblies of other ABA triblock copolymers, consisting of PMeOx-PDMS-PMeOx (PDMS=polydimethylsiloxane), have been loaded with various proteins or DNA.[191-194]

1.3 Outline of thesis

Today a wide variety of tissue adhesive materials are available on the market, but unfortunately none of them fulfils all requirements needed for an optimal material. New polymeric materials are needed for this application; poly(2-oxazoline)s might be an interesting class of materials, based on their biocompatibility, stealth behaviour and tuneable properties. In particular, poly(2-oxazoline)s have the advantage compared to PEG that side-chain functionalities can be introduced, which increases the density of reactive groups considerably. In order to be useful for tissue tape applications, the reactive moieties are preferably NHS esters, which can be used for crosslinking with multi-amine compounds and which can adhere to tissue. In this thesis a new series of poly(2-oxazoline)s is described which can be used for the development of a tissue tape. The first chapters focus on the synthesis and physical properties of poly(2-oxazoline) copolymers, which can be modified into the desired NHS ester- functional polymers. In the final chapter application of the obtained polymers in the development of a tissue tape is reported.

Chapter 2 describes the preparation of methyl ester functionalised poly(2-oxazoline)s. Synthetic strategies for the synthesis of two monomers with different chain lengths (ethyl or propyl spacer between the oxazoline and ester moiety) were optimised and homo- and copolymerisation kinetics studies were performed. In this way the distribution of these functional monomers along the polymer chain was determined, which is important for functionalisation later on.

In **chapter 3** four series of methyl ester-containing copolymers were prepared by copolymerisation of the two methyl ester monomers in different ratios with either EtOx or *n*PropOx. Also the homopolymers of the two methyl ester-containing monomer were synthesised. The physical properties of these side chain functionalised polymers, such as cloud point temperatures, glass transition temperatures and thermal stability were determined in relation to their composition.

In **chapter 4** the amidation of a methyl ester oxazoline homopolymer with a series of primary and secondary amines was investigated in order to introduce new properties. In particular cloud point- and glass transition temperatures and thermal stability were determined.

In **chapter 5** the side-chain functionalisation of poly(2-oxazoline) copolymers was used to synthesise polymeric mimics of cell penetrating peptides. Therefore copolymers with methyl ester and ethyl side chains were modified in an efficient three-step process into guanidines. Polymers of different degree of functionalisation and with a random or blocky structure were prepared. These guanidine-functionalised polymers were tested for toxicity and cell uptake as a function of their composition.

In **chapter 6** a first approach to a poly-(2-oxazoline) based tissue tape was developed. Methyl ester functional poly(2-oxazoline)s were modified into either NHS esters or amines. The NHS polymers were combined with the amine-functional polymers in ratios that ensured sufficient crosslinking, while leaving NHS groups available for conjugation with tissue. NHS:NH_2 ratios ranging from 1:1 to 10:1 were tested. The crosslinked films were placed on a biodegradable backing material to improve the mechanical stability of the adhesive tape. The adhesion on tissue and cohesion of the tapes was finally tested, demonstrating the feasibility of the approach.

1.4 References

1. Lloyd, J. D.; Marque, M. J.; Kacprowicz, R. F. *Emerg. Med. Clin. North Am.* **2007,** 25, (1), 73-81.
2. Tajirian, A. L.; Goldberg, D. J. *J. Cosmet. Laser Ther.* **2010,** 12, (6), 296-302.
3. Bruce, J.; Krukowski, Z. H.; Al-Khairy, G.; Russell, E. M.; Park, K. G. *Br. J. Surg.* **2001,** 88, (9), 1157-68.
4. Pickleman, J.; Watson, W.; Cunningham, J.; Fisher, S. G.; Gamelli, R. *Journal of the American College of Surgeons* **1999,** 188, (5), 473-82.
5. Duarte, A. P.; Coelho, J. F.; Bordado, J. C.; Cidade, M. T.; Gil, M. H. *Prog. Polym. Sci.* **2012,** 37, (8), 1031-1050.
6. Spotnitz, W. D.; Burks, S. *Transfusion* **2008,** 48, (7), 1502-16.
7. Spotnitz, W. D.; Burks, S. *Clinical and applied thrombosis/hemostasis* **2010,** 16, (5), 497-514.
8. Bouten, P. J. M.; Zonjee, M.; Bender, J.; Yauw, S. T. K.; van Goor, H.; van Hest, J. C. M.; Hoogenboom, R. *Prog. Polym. Sci.* **2014,** 39, (7), 1375-1405.
9. Bhatia, S., Traumatic Injuries Chapter 10 Traumatic Injuries. In *Biomaterials for Clinical Applications*, Springer New York: 2010; pp 213-258.
10. Mehdizadeh, M.; Yang, J. *Macromol. Biosci.* **2013,** 13, (3), 271-88.
11. Jayakumar, R.; Prabaharan, M.; Sudheesh Kumar, P. T.; Nair, S. V.; Tamura, H. *Biotechnol. Adv.* **2011,** 29, (3), 322-337.

12. Ardis, A. E. Preparation of monomeric alkyl alpha-cyano-acrylates, US pat 2,467,926. 1947.
13. Ardis, A. E. Preparation of monomeric alkyl alpha-cyano-acrylates, US pat 2,467,927. 1947.
14. Coover, H. W.; Joyner, F. B.; Shearer, N. H.; Wicker, T. H. *Society of Plastic Engineers* **1959,** 15, 413-417.
15. Leonard, F. *Ann. N.Y. Acad. Sci.* **1968,** 146, (1), 203-13.
16. Singer, A. J.; Quinn, J. V.; Hollander, J. E. *Am. J. Emerg. Med.* **2008,** 26, (4), 490-6.
17. Chow, A.; Marshall, H.; Zacharakis, E.; Paraskeva, P.; Purkayastha, S. *J. Am. Coll. Surg.* **2010,** 211, (1), 114-125.
18. Trott, A. T. *Jama* **1997,** 277, (19), 1559-60.
19. Ronis, M. L.; Harwick, J. D.; Fung, R.; Dellavecchia, M. *The Laryngoscope* **1984,** 94, (2 Pt 1), 210-3.
20. Leggat, P. A.; Smith, D. R.; Kedjarune, U. *ANZ J. Surg.* **2007,** 77, (4), 209-13.
21. Dragu, A.; Unglaub, F.; Schwarz, S.; Beier, J. P.; Kneser, U.; Bach, A. D.; Horch, R. E. *Archives of orthopaedic and trauma surgery* **2009,** 129, (2), 167-9.
22. Montanaro, L.; Arciola, C. R.; Cenni, E.; Ciapetti, G.; Savioli, F.; Filippini, F.; Barsanti, L. A. *Biomaterials* **2001,** 22, (1), 59-66.
23. Zempsky, W. T.; Parrotti, D.; Grem, C.; Nichols, J. *Pediatr. Emerg. Care* **2004,** 20, (8), 519-24.
24. Liebelt, E. L. *Curr. Opin. Pediatr.* **1997,** 9, (5), 459-64.
25. Klibanov, A. L.; Maruyama, K.; Torchilin, V. P.; Huang, L. *FEBS Lett.* **1990,** 268, (1), 235-7.
26. Knop, K.; Hoogenboom, R.; Fischer, D.; Schubert, U. S. *Angew. Chem. Int. Ed.* **2010,** 49, (36), 6288-308.
27. Caliceti, P.; Veronese, F. M. *Adv. Drug Delivery Rev.* **2003,** 55, (10), 1261-77.
28. Sawhney, A. S.; Pathak, C. P.; Hubbell, J. A. *Macromolecules* **1993,** 26, (4), 581-587.
29. Focal Inc, Summary of safety and effectiveness data FocalSeal. http://www.accessdata.fda.gov/cdrh_docs/pdf/P990028b.pdf (last accessed 2015-04-23),
30. Quinn, J. V., *Tissue Adhesives in Clinical Medicine*. BC Decker, Incorporated: 2005.
31. Macchiarini, P.; Wain, J.; Almy, S.; Dartevelle, P. *The Journal of thoracic and cardiovascular surgery* **1999,** 117, (4), 751-8.
32. Suggs, L. J.; Kao, E. Y.; Palombo, L. L.; Krishnan, R. S.; Widmer, M. S.; Mikos, A. G. *Journal of biomaterials science. Polymer edition* **1998,** 9, (7), 653-66.
33. Suggs, L. J.; Krishnan, R. S.; Garcia, C. A.; Peter, S. J.; Anderson, J. M.; Mikos, A. G. *Journal of biomedical materials research* **1998,** 42, (2), 312-20.
34. Nivasu, V. M.; Reddy, T. T.; Tammishetti, S. *Biomaterials* **2004,** 25, (16), 3283-91.
35. Tanaka, K.; Takamoto, S.; Ohtsuka, T.; Kotsuka, Y.; Kawauchi, M. *Ann. Thorac. Surg.* **1999,** 68, (4), 1308-12; discussion 1312-3.
36. Preul, M. C.; Bichard, W. D.; Spetzler, R. F. *Neurosurgery* **2003,** 53, (5), 1189-98; discussion 1198-9.
37. Cosgrove, G. R.; Delashaw, J. B.; Grotenhuis, J. A.; Tew, J. M.; Van Loveren, H.; Spetzler, R. F.; Payner, T.; Rosseau, G.; Shaffrey, M. E.; Hopkins, L. N.; Byrne, R.; Norbash, A. *J. Neurosurg.* **2007,** 106, (1), 52-8.
38. Confluent Surgical Inc, FDA Executive Summary DuraSeal Dural Sealant System. http://www.fda.gov/ohrms/dockets/ac/04/briefing/2004-4083b1_02_executive%20summary.pdf (last accessed 2015-04-23),
39. Confluent Surgical Inc, FDA Executive Summary for DuraSeal Xact Sealant System. http://www.fda.gov/ohrms/dockets/ac/09/briefing/2009-4437b1-01%20FDA%20Executive%20Summary.pdf (last accessed 2015-04-23),

40. Boogaarts, J. D.; Grotenhuis, J. A.; Bartels, R. H.; Beems, T. *Neurosurgery* **2005,** 57, (1 Suppl), 146-51; discussion 146-51.
41. Covidien DuraSeal information. http://www.durasealinfo.com/durasealcranial/pages.aspx?page=WhatIsDuraSealCranial/Technology (last accessed 2015-04-23),
42. Lee, G.; Lee, C. K.; Bynevelt, M. *Spine* **2010,** 35, (25), E1522-4.
43. Thavarajah, D.; De Lacy, P.; Hussain, R.; Redfern, R. M. *Spine* **2010,** 35, (1), E25-6.
44. Preul, M. C.; Campbell, P. K.; Garlick, D. S.; Spetzler, R. F. *Journal of neurosurgery. Spine* **2010,** 12, (4), 381-90.
45. Fransen, P. *Spine Journal* **2010,** 10, (9), 751-61.
46. Goode, J. L.; Harvey, E.; Chandeysson, P.; Zhou, S.; Das, S.; Durfor, C.; Elespuru, R.; Herrera, H.; Kennell, L.; Langone, J.; Merrit, K.; Nimmagada, R.; Weiss, R.; Fitzgerald, M. A.; Brown, L. Review Memorandum: Cohesion Technologies: CoSeal Surgical Sealant: P010022. http://www.fda.gov/ohrms/dockets/ac/01/briefing/3790b2_05_FDA_cohesion.doc (last accessed 2015-04-23),
47. Wallace, D. G.; Cruise, G. M.; Rhee, W. M.; Schroeder, J. A.; Prior, J. J.; Ju, J.; Maroney, M.; Duronio, J.; Ngo, M. H.; Estridge, T.; Coker, G. C. *Journal of biomedical materials research* **2001,** 58, (5), 545-55.
48. Saunders, M. M.; Baxter, Z. C.; Abou-Elella, A.; Kunselman, A. R.; Trussell, J. C. *Fertil. Steril.*. **2009,** 91, (2), 560-5.
49. Campbell, P. K.; Bennet, S. L.; Driscoll, A.; Sawhney, A. S. Evaluation of Absorbable Surgical Sealants : In vitro Testing. http://www.durasealinfo.com/imageServer.aspx/doc179399.pdf?contentID=14109&contenttype=application/pdf (last accessed 2014-01-10),
50. Johns, D. A.; Ferland, R.; Dunn, R. *J. Am. Assoc. Gynecol. Laparosc.* **2003,** 10, (3), 334-8.
51. Dunn, R.; Lyman, M. D.; Edelman, P. G.; Campbell, P. K. *Fertil. Steril.* **2001,** 75, (2), 411-6.
52. Ferland, R.; Mulani, D.; Campbell, P. K. *Human Reproduction* **2001,** 16, (12), 2718-23.
53. Tjandra, J. J.; Chan, M. K. *Dis. Colon Rectum* **2008,** 51, (6), 956-60.
54. Schnuriger, B.; Barmparas, G.; Branco, B. C.; Lustenberger, T.; Inaba, K.; Demetriades, D. *Am. J. Surg.* **2011,** 201, (1), 111-21.
55. Harris, J. M., *Poly(Ethylene Glycol) Chemistry. Biotechnical and Biomedical Applications*. Springer US: 1992.
56. Gilbert, T. W.; Badylak, S. F.; Gusenoff, J.; Beckman, E. J.; Clower, D. M.; Daly, P.; Rubin, J. P. *Plast. Reconstr. Surg.* **2008,** 122, (1), 95-102.
57. Cohera Medical Inc, Presentation: Development of a single component, high strength, biocompatible surgical adhesive MKT-0021. http://www.coheramedical.com/products/tissuglu/the_science (last accessed 2015-04-23),
58. Beckman, E. J. One-part moisture-curable tissue sealant, WO 2011/150199 A2. 2011.
59. Ltd, T. Tissuemed Ltd, TissuePatch 3 the synthetic self-adhesive surgical sealant film. http://www.marlog.net/Tissuepatch3.brochure.pdf (last accessed 2015-04-23),
60. Thompson, I. Adhesive sealant biomaterials. http://www.tissuemed.com/wp-content/uploads/TB2101.pdf (last accessed 2015-04-23),
61. von der Brelie, C.; Soehle, M.; Clusmann, H. R. *Br. J. Neurosurg.* **2012,** 26, (2), 231-5.
62. Ferroli, P.; Acerbi, F.; Broggi, M.; Schiariti, M.; Albanese, E.; Tringali, G.; Franzini, A.; Broggi, G. *World Neurosurg.* **2013,** 79, (3-4), 551-7.

63. Fortune, D. H.; Kettlewell, G.; Mandley, D. J.; Morris, D.; Thompson, I. Tissue-adhesive formulations, WO 2007/099370 A2. 2007.
64. Wathier, M.; Jung, P. J.; Carnahan, M. A.; Kim, T.; Grinstaff, M. W. *J. Am. Chem. Soc.* **2004,** 126, (40), 12744-5.
65. Wathier, M.; Johnson, C. S.; Kim, T.; Grinstaff, M. W. *Bioconjugate Chem.* **2006,** 17, (4), 873-6.
66. Oelker, A. M.; Berlin, J. A.; Wathier, M.; Grinstaff, M. W. *Biomacromolecules* **2011,** 12, (5), 1658-65.
67. Velazquez, A. J.; Carnahan, M. A.; Kristinsson, J.; Stinnett, S.; Grinstaff, M. W.; Kim, T. *Arch. Ophthalmol.* **2004,** 122, (6), 867-70.
68. Larkin, H. Liquid bandage for ocular use set to enter CE mark trials. http://www.bd.com/resource.aspx?IDX=15027 (last accessed 2015-04-23),
69. HyperBranch Medical Technology Inc, Adherus dural sealant. http://www.spiegelberg.de/documents/adherus_dural_sealant_brochure_2013_en.pdf (last accessed 2013-12-18),
70. Stockman, K. E.; Carnahan, M. A.; D'Alessio, K. R.; Grinstaff, M. W. Crosslinked gels comprising polyalkyleneimines and their uses as medical devices, WO 2007/082061 A2. 2007.
71. Ferreira, P.; Pereira, R.; Coelho, J. F.; Silva, A. F.; Gil, M. H. *Int. J. Biol. Macromol.* **2007,** 40, (2), 144-52.
72. Walgenbach, K. J.; Bannasch, H.; Kalthoff, S.; Rubin, J. P. *Aesthetic Plast. Surg.* **2012,** 36, (3), 491-6.
73. Cohera Medical Inc, The science behind Sylys surgical sealant. http://www.coheramedical.com/products/sylys_science (last accessed 2015-04-23),
74. Lipatova, T. E., Medical polymer adhesives. In *Biopolymers/Non-Exclusion HPLC*, Springer Berlin Heidelberg: 1986; Vol. 79, pp 65-93.
75. Phaneuf, M. D.; Dempsey, D. J.; Bide, M. J.; Quist, W. C.; LoGerfo, F. W. *Biomaterials* **2001,** 22, (5), 463-9.
76. Heiss, C.; Kraus, R.; Schluckebier, D.; Stiller, A.-C.; Wenisch, S.; Schnettler, R. *Eur. J. Trauma* **2006,** 32, (2), 141-148.
77. Ferreira, P.; Silva, A. F.; Pinto, M. I.; Gil, M. H. *Journal of materials science. Materials in medicine* **2008,** 19, (1), 111-20.
78. Ferreira, P.; Coelho, J. F.; Gil, M. H. *Int. J. Pharm.* **2008,** 352, (1-2), 172-81.
79. Della Puppa, A.; Rossetto, M.; Scienza, R. *Br. J. Neurosurg.* **2010,** 24, (5), 609-11.
80. Grinstaff, M. W. *J. Polym. Sci., Part A: Polym. Chem.* **2008,** 46, (2), 383-400.
81. Carnahan, M. A.; Middleton, C.; Kim, J.; Kim, T.; Grinstaff, M. W. *J. Am. Chem. Soc.* **2002,** 124, (19), 5291-3.
82. Nic, M.; Jirat, J.; Kosata, B., Interpenetrating Polymer Network. In *IUPAC. Compendium of Chemical Terminology*, McNaught, A. D.; WIlkinson, A., Eds. Blackwell Scientific Publications: Oxford, 1997; Vol. 2nd ed. (the "Gold book").
83. Degoricija, L.; Johnson, C. S.; Wathier, M.; Kim, T.; Grinstaff, M. W. *Invest. Ophthalmol. Vis. Sci.* **2007,** 48, (5), 2037-42.
84. Berdahl, J. P.; Johnson, C. S.; Proia, A. D.; Grinstaff, M. W.; Kim, T. *Arch. Ophthalmol.* **2009,** 127, (4), 442-7.
85. Ghobril, C.; Charoen, K.; Rodriguez, E. K.; Nazarian, A.; Grinstaff, M. W. *Angew. Chem. Int. Ed.* **2013,** 52, (52), 14070-4.
86. Jager, M.; Schubert, S.; Ochrimenko, S.; Fischer, D.; Schubert, U. S. *Chem. Soc. Rev.* **2012,** 41, (13), 4755-67.
87. Hoogenboom, R. *Angew. Chem. Int. Ed.* **2009,** 48, 7978-7994.

88. Van Kuringen, H. P.; Lenoir, J.; Adriaens, E.; Bender, J.; De Geest, B. G.; Hoogenboom, R. *Macromol. Biosci.* **2012,** 12, (8), 1114-23.
89. Legros, C.; De Pauw-Gillet, M.-C.; Tam, K. C.; Lecommmandoux, S.; Taton, D. *Polym. Chem.* **2013,** 4, (17), 4801-4808.
90. Strausberg, R. L.; Link, R. P. *Trends Biotechnol.* **1990,** 8, (2), 53-7.
91. Waite, J. H. *Int. J. Adhes. Adhes.* **1987,** 7, (1), 9-14.
92. Vreeland, V.; Waite, J. H.; Epstein, L. *J. Phycol.* **1998,** 34, (1), 1-8.
93. Matos-Perez, C. R.; White, J. D.; Wilker, J. J. *J. Am. Chem. Soc.* **2012,** 134, (22), 9498-505.
94. Lee, B. P.; Dalsin, J. L.; Messersmith, P. B. *Biomacromolecules* **2002,** 3, (5), 1038-47.
95. Faure, E.; Falentin-Daudré, C.; Jérôme, C.; Lyskawa, J.; Fournier, D.; Woisel, P.; Detrembleur, C. *Prog. Polym. Sci.* **2013,** 38, (1), 236-270.
96. Barrett, D. G.; Fullenkamp, D. E.; He, L.; Holten-Andersen, N.; Lee, K. Y.; Messersmith, P. B. *Adv. Funct. Mater.* **2013,** 23, (9), 1111-1119.
97. Ninan, L.; Monahan, J.; Stroshine, R. L.; Wilker, J. J.; Shi, R. *Biomaterials* **2003,** 24, (22), 4091-9.
98. Ninan, L.; Stroshine, R. L.; Wilker, J. J.; Shi, R. *Acta Biomater.* **2007,** 3, (5), 687-94.
99. Wang, J.; Liu, C.; Lu, X.; Yin, M. *Biomaterials* **2007,** 28, (23), 3456-68.
100. Westwood, G.; Horton, T. N.; Wilker, J. J. *Macromolecules* **2007,** 40, (11), 3960-3964.
101. Huang, K.; Lee, B. P.; Ingram, D. R.; Messersmith, P. B. *Biomacromolecules* **2002,** 3, (2), 397-406.
102. Lee, Y. M.; Kim, S. S.; Park, M. H.; Song, K. W.; Sung, Y. K.; Kang, I. K. *Journal of materials science. Materials in medicine* **2000,** 11, (12), 817-23.
103. Burke, S. A.; Ritter-Jones, M.; Lee, B. P.; Messersmith, P. B. *Biomedical Materials* **2007,** 2, (4), 203-10.
104. Brubaker, C. E.; Kissler, H.; Wang, L. J.; Kaufman, D. B.; Messersmith, P. B. *Biomaterials* **2010,** 31, (3), 420-7.
105. Bilic, G.; Brubaker, C.; Messersmith, P. B.; Mallik, A. S.; Quinn, T. M.; Haller, C.; Done, E.; Gucciardo, L.; Zeisberger, S. M.; Zimmermann, R.; Deprest, J.; Zisch, A. H. *Am. J. Obstet. Gynecol.* **2010,** 202, (1), 85.e1-9.
106. Brubaker, C. E.; Messersmith, P. B. *Biomacromolecules* **2011,** 12, (12), 4326-34.
107. Murphy, J. L.; Vollenweider, L.; Xu, F.; Lee, B. P. *Biomacromolecules* **2010,** 11, (11), 2976-84.
108. Brodie, M.; Vollenweider, L.; Murphy, J. L.; Xu, F.; Lyman, A.; Lew, W. D.; Lee, B. P. *Biomedical Materials* **2011,** 6, (1), 015014.
109. Mehdizadeh, M.; Weng, H.; Gyawali, D.; Tang, L.; Yang, J. *Biomaterials* **2012,** 33, (32), 7972-83.
110. Lee, Y.; Chung, H. J.; Yeo, S.; Ahn, C.-H.; Lee, H.; Messersmith, P. B.; Park, T. G. *Soft Matter* **2010,** 6, (5), 977-983.
111. Ryu, J. H.; Lee, Y.; Kong, W. H.; Kim, T. G.; Park, T. G.; Lee, H. *Biomacromolecules* **2011,** 12, (7), 2653-9.
112. Barrett, D. G.; Bushnell, G. G.; Messersmith, P. B. *Adv. Healthcare Mater.* **2013,** 2, (5), 745-55.
113. Ryu, J. H.; Lee, Y.; Do, M. J.; Jo, S. D.; Kim, J. S.; Kim, B. S.; Im, G. I.; Park, T. G.; Lee, H. *Acta Biomater.* **2014,** 10, (1), 224-33.
114. Verbraeken, B.; Lava, K.; Hoogenboom, R., Poly(2-oxazoline)s. In *Encyclopedia of Polymer Science and Technology*, John Wiley & Sons, Inc.: 2014; pp 1-51.
115. Hoogenboom, R., Polyethers and Polyoxazolines. In *Handbook of Ring-Opening Polymerization*, Wiley-VCH Verlag GmbH & Co. KGaA: 2009; pp 141-164.

116. Luxenhofer, R.; Han, Y.; Schulz, A.; Tong, J.; He, Z.; Kabanov, A. V.; Jordan, R. *Macromol. Rapid Commun.* **2012,** 33, (19), 1613-1631.
117. Seeliger, W.; Aufderhaar, E.; Diepers, W.; Feinauer, R.; Nehring, R.; Thier, W.; Hellmann, H. *Angew. Chem. Int. Ed.* **1966,** 5, 875-888.
118. Tomalia, D. A.; Sheetz, D. P. *J. Polym. Sci., Part A: Polym. Chem.* **1966,** 4, 2253-2265.
119. Kagiya, T.; Narisawa, S.; Maeda, T.; Fukui, K. *J. Polym. Sci. Pol. Lett.* **1966,** 4, 441-445.
120. Bassiri, T. G.; Levy, A.; Litt, M. *J. Polym. Sci., Part B: Polym. Lett.* **1967,** 5, 871-879.
121. Kobayashi, S. *Prog. Polym. Sci.* **1990,** 15, (5), 751-823.
122. Aoi, K.; Okada, M. *Prog. Polym. Sci.* **1996,** 21, (1), 151-208.
123. Witte, H.; Seeliger, W. *Liebigs Ann.* **1974,** 1974, (6), 996-1009.
124. Wenker, H. *J. Am. Chem. Soc.* **1935,** 57, (6), 1079-1080.
125. Gress, A.; Volkel, A.; Schlaad, H. *Macromolecules* **2007,** 40, 7928-7933.
126. Zarka, M. T.; Nuyken, O.; Weberskirch, R. *Chem. Eur. J.* **2003,** 9, 3228-3234.
127. Taubmann, C.; Luxenhofer, R.; Cesana, S.; Jordan, R. *Macromol. Biosci.* **2005,** 5, 603-612.
128. Kempe, K.; Jacobs, S.; Lambermont-Thijs, H. M. L.; Fijten, M. M. W. M.; Hoogenboom, R.; Schubert, U. S. *Macromolecules* **2010,** 43, (9), 4098-4104.
129. Hoogenboom, R.; Paulus, R. M.; Fijten, M. W. M.; Schubert, U. S. *J. Polym. Sci., Part A: Polym. Chem.* **2005,** 43, (7), 1487-1497.
130. Saegusa, T.; Ikeda, H. *Macromolecules* **1973,** 6, (6), 808-811.
131. Fijten, M. W. M.; Haensch, C.; van Lankvelt, B. M.; Hoogenboom, R.; Schubert, U. S. *Macromol. Chem. Phys.* **2008,** 209, 1887-1895.
132. Chapman, R.; Bouten, P. J. M.; Hoogenboom, R.; Jolliffe, K. A.; Perrier, S. *Chem. Commun.* **2013,** 49, 6522-6524.
133. Kempe, K.; Hoogenboom, R.; Jaeger, M.; Schubert, U. S. *Macromolecules* **2011,** 44, (16), 6424-6432.
134. Bartz, T.; Klapper, M.; Müllen, K. *Macromol. Chem. Phys.* **1994,** 195, (3), 1097-1109.
135. Weber, C.; Becer, R. C.; Baumgaertel, A.; Hoogenboom, R.; Schubert, U. S. *Des. Monomers Polym.* **2009,** 12, (2), 149-165.
136. Guillerm, B.; Monge, S.; Lapinte, V.; Robin, J. J. *Macromol. Rapid Commun.* **2012,** 33, 1600-1612.
137. Kobayashi, S.; Uyama, H.; Mori, T.; Narita, Y. *Chem. Lett.* **1991,** 20, (10), 1771-1774.
138. Wiesbrock, F.; Hoogenboom, R.; Abeln, C. H.; Schubert, U. S. *Macromol. Rapid Commun.* **2004,** 25, 1895-1899.
139. Hoogenboom, R.; Fijten, M. W. M.; Thijs, H. M. L.; Van Lankvelt, B. M.; Schubert, U. S. *Des. Monomers Polym.* **2005,** 8, 659-671.
140. Levy, A.; Litt, M. *J. Polym. Sci., Part A: Polym. Chem.* **1968,** 6, 1883-1894.
141. Bouten, P. J. M.; Hertsen, D.; Vergaelen, M.; Monnery, B. D.; Boerman, M. A.; Goossens, H.; Catak, S.; van Hest, J. C. M.; Van Speybroeck, V.; Hoogenboom, R. *Polym. Chem.* **2015,** 6, (4), 514-518.
142. Luxenhofer, R.; Jordan, R. *Macromolecules* **2006,** 39, (10), 3509-3516.
143. Le Fer, G.; Amiel, C.; Volet, G. *European Polymer Journal* **2015,** 71, 523-533.
144. Lav, T.-X.; Lemechko, P.; Renard, E.; Amiel, C.; Langlois, V.; Volet, G. *Reactive and Functional Polymers* **2013,** 73, (8), 1001-1008.
145. Cesana, S.; Auernheimer, J.; Jordan, R.; Kessler, H.; Nuyken, O. *Macromol. Chem. Phys.* **2006,** 207, (2), 183-192.
146. Park, J.-S.; Akiyama, Y.; Winnik, F. M.; Kataoka, K. *Macromolecules* **2004,** 37, (18), 6786-6792.

147. Weberskirch, R.; Preuschen, J.; Spiess, H. W.; Nuyken, O. *Macromol. Chem. Phys.* **2000,** 201, (10), 995-1007.
148. Kempe, K.; Lobert, M.; Hoogenboom, R.; Schubert, U. S. *J. Polym. Sci., Part A: Polym. Chem.* **2009,** 47, (15), 3829-3838.
149. Persigehl, P.; Jordan, R.; Nuyken, O. *Macromolecules* **2000,** 33, (19), 6977-6981.
150. Lobert, M.; Thijs, H. M.; Erdmenger, T.; Eckardt, R.; Ulbricht, C.; Hoogenboom, R.; Schubert, U. S. *Chemistry (Weinheim an der Bergstrasse, Germany)* **2008,** 14, (33), 10396-407.
151. Hoogenboom, R.; Schubert, U. S. *Green Chem.* **2006,** 8, (10), 895-899.
152. Hoogenboom, R. *Eur. J. Lipid Sci. Technol.* **2011,** 113, (1), 59-71.
153. Huber, S.; Jordan, R. *Colloid. Polym. Sci.* **2008,** 286, (4), 395-402.
154. Park, J.-S.; Kataoka, K. *Macromolecules* **2006,** 39, (19), 6622-6630.
155. Volet, G.; Lav, T. X.; Babinot, J.; Amiel, C. *Macromol. Chem. Phys.* **2011,** 212, 118-124.
156. Rueda, J. C.; Komber, H.; Cedrón, J. C.; Voit, B.; Shevtsova, G. *Macromol. Chem. Phys.* **2003,** 204, (7), 947-953.
157. Meyer, M.; Schlaad, H. *Macromolecules* **2006,** 39, (11), 3967-3970.
158. Weber, C.; Czaplewska, J. A.; Baumgaertel, A.; Altuntas, E.; Gottschaldt, M.; Hoogenboom, R.; Schubert, U. S. *Macromolecules* **2011,** 45, (1), 46-55.
159. Christova, D.; Velichkova, R.; Goethals, E. J. *Macromol. Rapid Commun.* **1997,** 18, (12), 1067-1073.
160. Groß, A.; Maier, G.; Nuyken, O. *Macromol. Chem. Phys.* **1996,** 197, (9), 2811-2826.
161. Kobayashi, S.; Igarashi, T.; Moriuchi, Y.; Saegusa, T. *Macromolecules* **1986,** 19, (3), 535-541.
162. Kobayashi, S.; Uyama, H. *J. Polym. Sci., Part A: Polym. Chem.* **2002,** 40, (2), 192-209.
163. Weber, C.; Hoogenboom, R.; Schubert, U. S. *Prog. Polym. Sci.* **2012,** 37, (5), 686-714.
164. Vancoillie, G.; Frank, D.; Hoogenboom, R. *Prog. Polym. Sci.* **2014,** 39, (6), 1074-1095.
165. Roy, D.; Brooks, W. L. A.; Sumerlin, B. S. *Chem. Soc. Rev.* **2013,** 42, (17), 7214-7243.
166. Bloksma, M. M.; Weber, C.; Perevyazko, I. Y.; Kuse, A.; Baumgärtel, A.; Vollrath, A.; Hoogenboom, R.; Schubert, U. S. *Macromolecules* **2011,** 44, (11), 4057-4064.
167. Park, J.-S.; Kataoka, K. *Macromolecules* **2007,** 40, (10), 3599-3609.
168. Diehl, C.; Schlaad, H. *Macromol. Biosci.* **2009,** 9, (2), 157-161.
169. Glassner, M.; Lava, K.; de la Rosa, V. R.; Hoogenboom, R. *J. Polym. Sci., Part A: Polym. Chem.* **2014,** 52, (21), 3118-3122.
170. Hoogenboom, R.; Thijs, H. M. L.; Jochems, M. J. H. C.; van Lankvelt, B. M.; Fijten, M. W. M.; Schubert, U. S. *Chem. Commun.* **2008,** 44, 5758-5760.
171. Lambermont-Thijs, H. M. L.; Hoogenboom, R.; Fustin, C.-A.; Bomal-D'Haese, C.; Gohy, J.-F.; Schubert, U. S. *J. Polym. Sci., Part A: Polym. Chem.* **2009,** 47, (2), 515-522.
172. Lin, P.; Clash, C.; Pearce, E. M.; Kwei, T. K.; Aponte, M. A. *J. Polym. Sci., Part B: Polym. Phys.* **1988,** 26, (3), 603-619.
173. Lambermont-Thijs, H. M. L.; Fijten, M. W. M.; van der Linden, A. J.; van Lankvelt, B. M.; Bloksma, M. M.; Schubert, U. S.; Hoogenboom, R. *Macromolecules* **2011,** 44, (11), 4320-4325.
174. Guner, P. T.; Miko, A.; Schweinberger, F. F.; Demirel, A. L. *Polym. Chem.* **2012,** 3, (2), 322-324.
175. Meyer, M.; Antonietti, M.; Schlaad, H. *Soft Matter* **2007,** 3, (4), 430-431.

176. Katsumoto, Y.; Tsuchiizu, A.; Qiu, X.; Winnik, F. M. *Macromolecules* **2012,** 45, (8), 3531-3541.
177. Wiesbrock, F.; Hoogenboom, R.; Leenen, M. A. M.; Meier, M. A. R.; Schubert, U. S. *Macromolecules* **2005,** 38, 5025-5034.
178. Fijten, M. W. M.; Kranenburg, J. M.; Thijs, H. M. L.; Paulus, R. M.; van Lankvelt, B. M.; de Hullu, J.; Springintveld, M.; Thielen, D. J. G.; Tweedie, C. A.; Hoogenboom, R.; Van Vliet, K. J.; Schubert, U. S. *Macromolecules* **2007,** 40, (16), 5879-5886.
179. Goddard, P.; Hutchinson, L. E.; Brown, J.; Brookman, L. J. *J. Controlled Release* **1989,** 10, (1), 5-16.
180. Gaertner, F. C.; Luxenhofer, R.; Blechert, B.; Jordan, R.; Essler, M. *J Control Release* **2007,** 119, (3), 291-300.
181. Woodle, M. C.; Engbers, C. M.; Zalipsky, S. *Bioconjugate Chem.* **1994,** 5, (6), 493-496.
182. Zalipsky, S.; Hansen, C. B.; Oaks, J. M.; Allen, T. M. *J Pharm Sci* **1996,** 85, 133-137.
183. Rathna, G. V. *Journal of materials science. Materials in medicine* **2008,** 19, (6), 2351-8.
184. Mero, A.; Pasut, G.; Via, L. D.; Fijten, M. W. M.; Schubert, U. S.; Hoogenboom, R.; Veronese, F. M. *J. Controlled Release* **2008,** 125, 87-95.
185. de la Rosa, V. R. *Journal of materials science. Materials in medicine* **2014,** 25, (5), 1211-25.
186. Eskow Jaunarajs, K. L.; Standaert, D. G.; Viegas, T. X.; Bentley, M. D.; Fang, Z.; Dizman, B.; Yoon, K.; Weimer, R.; Ravenscroft, P.; Johnston, T. H.; Hill, M. P.; Brotchie, J. M.; Moreadith, R. W. *Movement Disorders* **2013,** 28, (12), 1675-82.
187. Tyrrell, Z. L.; Shen, Y.; Radosz, M. *Prog. Polym. Sci.* **2010,** 35, (9), 1128-1143.
188. Krumm, C.; Fik, C. P.; Meuris, M.; Dropalla, G. J.; Geltenpoth, H.; Sickmann, A.; Tiller, J. C. *Macromol. Rapid Commun.* **2012,** 33, (19), 1677-1682.
189. Luxenhofer, R.; Schulz, A.; Roques, C.; Li, S.; Bronich, T. K.; Batrakova, E. V.; Jordan, R.; Kabanov, A. V. *Biomaterials* **2010,** 31, (18), 4972-4979.
190. Milonaki, Y.; Kaditi, E.; Pispas, S.; Demetzos, C. *J. Polym. Sci., Part A: Polym. Chem.* **2012,** 50, (6), 1226-1237.
191. Graff, A.; Sauer, M.; Van Gelder, P.; Meier, W. *Proc. Natl. Acad. Sci. U.S.A.* **2002,** 99, (8), 5064-5068.
192. Ranquin, A.; Versées, W.; Meier, W.; Steyaert, J.; Van Gelder, P. *Nano Lett.* **2005,** 5, (11), 2220-2224.
193. Ben-Haim, N.; Broz, P.; Marsch, S.; Meier, W.; Hunziker, P. *Nano Lett.* **2008,** 8, (5), 1368-1373.
194. Broz, P.; Ben-Haim, N.; Grzelakowski, M.; Marsch, S.; Meier, W.; Hunziker, P. *J. Cardiovasc. Pharmacol.* **2008,** 51, (3), 246-52.

Chapter 2

Polymerisation kinetics of methyl ester-containing 2-oxazoline monomers

Parts of this work have been published:

Petra J.M. Bouten, Dietmar Hertsen, Maarten Vergaelen, Bryn D. Monnery, Marcel A. Boerman, Hannelore Goossens, Saron Catak, Jan C.M. van Hest, Veronique Van Speybroeck, Richard Hoogenboom, *Accelerated living cationic ring-opening polymerization of a methyl ester functionalized 2-oxazoline monomer*, **Polymer Chemistry**, 2015, 6, 514-518

Petra J.M. Bouten, Dietmar Hertsen, Maarten Vergaelen, Bryn D. Monnery, Saron Catak, Jan C.M. van Hest, Veronique Van Speybroeck, Richard Hoogenboom, *Synthesis of poly(2-oxazoline)s with side chain methyl ester functionalities: Detailed understanding of living copolymerisation behavior of methyl ester containing monomers with 2-alkyl-2-oxazolines*, **Journal of Polymer Science Part A: Polymer Chemistry**, 2015, 53, 2649-2661

Abstract

Poly(2-oxazoline)s with methyl ester-functionalised side chains are interesting as they can undergo a direct amidation reaction or can be hydrolysed to the carboxylic acid, making them versatile functional polymers for conjugation. Here we present detailed studies on the homo- and copolymerisation kinetics of two methyl ester-functionalised 2-oxazoline monomers with 2-methyl-2-oxazoline, 2-ethyl-2-oxazoline and 2-*n*-propyl-2-oxazoline. The homopolymerisation of the methyl ester-functionalised monomers is found to be faster compared with the alkyl monomers, while copolymerisation unexpectedly reveals that the order of monomer incorporation is reversed. The methyl ester-containing monomers are found to significantly accelerate the polymerisation of all present monomers due to extra stabilisation of the oxazolinium cation by the carbonyl of the methyl ester side chain.

Introduction

The living cationic ring-opening polymerisation (CROP) of 2-oxazoline monomers (Scheme 1) was first reported in the 1960s,[1-4] providing easy access to a wide variety of well-defined poly(2-alkyl/aryl-2-oxazoline)s (PAOx) with controlled end-group functionality during initiation and termination.[5-9] PAOx are an interesting class of polymers because of their highly tuneable and diverse properties.[6, 10-12] Poly(2-methyl-2-oxazoline) (PMeOx) and poly(2-ethyl-2-oxazoline) (PEtOx) are of special interest for biomedical applications because of their water solubility, biocompatibility and stealth behaviour, similar to poly(ethylene glycol) (PEG).[6, 10, 11, 13] PEtOx and poly(2- propyl-2-oxazoline) (PPropOx) show lower critical solution (LCST) behaviour with better reversibility compared to the gold standard poly(*N*-isopropylacrylamide).[14-16] The properties of PAOx can be easily tuned by variation of the side chain substituents, also enabling the incorporation of (protected) side-chain functionalities.[17-29]

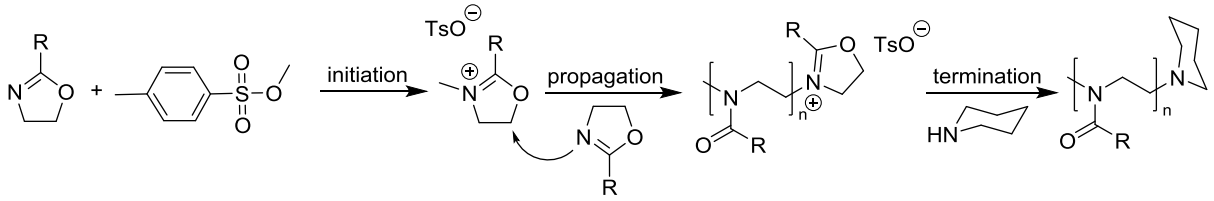

Scheme 1: Cationic ring-opening polymerisation of 2-oxazolines with methyl p-toluenesulfonate as initiator and piperidine as terminating agent.

PAOx with methyl ester-functionalised side chains are especially interesting as the methyl ester can be hydrolysed to the carboxylic acid, a versatile functionality for conjugation of peptides and proteins, as well as the introduction of pH-responsive behaviour. Moreover, PAOx with side chain methyl ester groups can undergo direct amidation with a variety of functional amines to easily introduce functional moieties, such as amine, alcohol or hydrazide units.[30, 31] Even though the synthesis and polymerisation of 2-methoxycarbonyl-ethyl-2-oxazoline, a methyl ester-containing oxazoline monomer (MestOx; Scheme 2), was already first reported by Levy and Litt in 1968[17] and this monomer has also been used more recently by the groups of Nuyken and Voit,[17-20, 22, 23] the (co)polymerisation kinetics of MestOx are yet unknown.

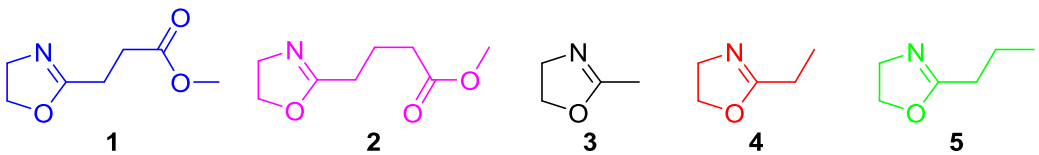

Scheme 2: Monomer structures of MestOx (**1**), C3MestOx (**2**), MeOx (**3**), EtOx (**4**), and *n*PropOx (**5**).

In this chapter we describe an improved synthesis for MestOx (**1**) and the synthesis of a new methyl ester-containing monomer with a C3-spacer between the oxazoline ring and the methyl ester, namely 2-methoxycarboxypropyl-2-oxazoline (C3MestOx, **2**). Detailed studies on the homo- and copolymerisation kinetics of these two methyl ester-functionalised 2-oxazoline monomers, MestOx and C3MestOx, with MeOx (**3**), EtOx (**4**) and 2-*n*-propyl-2-oxazoline (*n*PropOx, **5**) are reported. To better understand the observed copolymerisation rate constants, the Arrhenius parameters of the MestOx and C3MestOx homopolymerisations as well as the MestOx-MeOx copolymerisation were also determined by studying the (co)polymerisation at different temperatures.

Results and discussion

Monomer synthesis

The 2-methyl ester-functionalised-2-oxazoline monomers, MestOx and C3MestOx, were prepared from commercially available acid chlorides **1a** and **2a** through a reaction with 2-chloroethylamine hydrochloride in the presence of triethylamine yielding intermediate compounds **1b** and **2b**. The monomers (**1** and **2**) were obtained by ring-closure of these intermediate compounds with a strong non-nucleophilic base (sodium carbonate) to avoid saponification of the ester. This latter reaction was performed on a rotary evaporator under reduced pressure to allow good mixing of the precursor oil and the solid base and to ease the release of carbon dioxide. The monomers were obtained pure after distilling them twice over barium oxide. It should be noted that the synthesis of C3MestOx was easier due to the lower viscosity of the amide precursor **2b** in comparison to **1b**. As a result, the ring-closing reaction that involves release of CO_2 proceeded significantly faster.

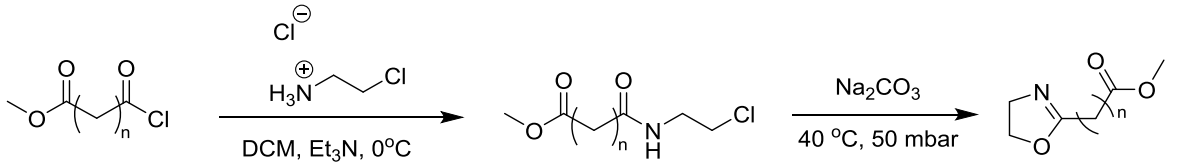

Scheme 3: Synthesis of methyl ester-containing 2-oxazoline monomers

Homopolymerisation kinetics

All monomers (MestOx, C3MestOx, MeOx, EtOx and nPropOx) were polymerised with methyl p-toluenesulfonate (MeOTs) as initiator,[32] acetonitrile as solvent under microwave irradiation at both 80 and 140 °C and 3 M monomer concentration with a [M]/[I] ratio of 100.[33] The corresponding first order kinetic plots obtained at 140 °C are shown in Figure 30A revealing linear first order kinetics for all monomers, indicating a constant concentration of propagating species in time and, thus, the absence of termination reactions. Each data point represents a separate polymerisation and, thus, the linearity proves the good reproducibility. The livingness of these homopolymerisations was confirmed by a linear increase of the number average molecular weight (M_n) with conversion as well as the low dispersities of the resulting polymers (Đ < 1.17, Figure 30B). Similar results were obtained at 80 °C, also revealing living polymerisation of all monomers (Figure 30 C and D).

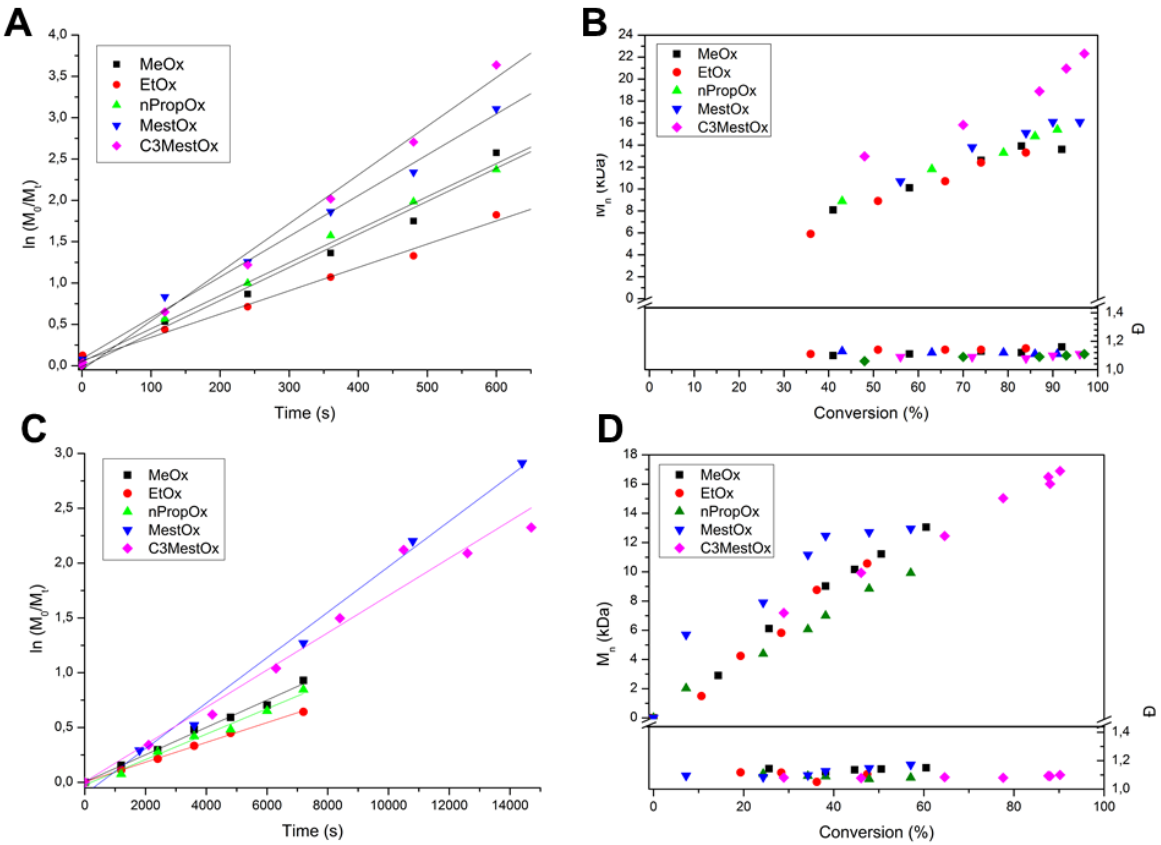

Figure 30: A) First order kinetic plot for homopolymerisation of MeOx, EtOx, nPropOx, MestOx and C3MestOx at 140 °C and B) corresponding number average molecular weight (M_n) and dispersity (Đ) plotted against conversion, C) First order kinetic plot for homopolymerisation of MeOx, EtOx, *n*PropOx, MestOx and C3MestOx at 80 °C and D) corresponding number average molecular weight (M_n) and dispersity (Đ) plotted against conversion.

The polymerisation rate constants (k_p) were calculated from the slope of the kinetic plots in Figure 30 and Figure 32, which are summarized in Table 3. The rates obtained for MeOx and EtOx were in good agreement with previously reported values,[34] but the k_p of nPropOx at 140 °C was slightly higher, possibly due to a small overshoot in temperature to 150 °C during the heating of the reaction mixture.

(C3)MestOx, however, revealed a significantly faster polymerisation with k_ps of 0.171 and 0.193 L mol^{-1} s^{-1} for **1** and **2** respectively. This fast propagation might be related to the activation of the chain ends and/or stabilization of the transition state by nearby MestOx residues. This mechanism is also indirectly supported by literature[35] as it has been shown that the first monomer addition to the oxazolinium cation formed during initiation ($k_{p,1}$) is the rate determining step. After this, the propagation rate (k_p) dramatically increases proposedly due to the interaction of the carbonyl of the penultimate unit with the oxazolinium ring, resulting in the stabilization of the transition state and shift towards the more reactive species. The (C3)MestOx monomers have an additional carbonyl group that could enhance this effect (Figure 31), leading to stabilization of the transition state and higher electrophilicity of the 5 position and thus enhancing the reactivity of the living chain end.[36, 37] A similar intramolecular activation occurs between the amide carbonyl of the last monomer before the oxazolinium chain leading to a higher k_p compared to $k_{p,1}$ for the first monomer addition during CROP.[35]

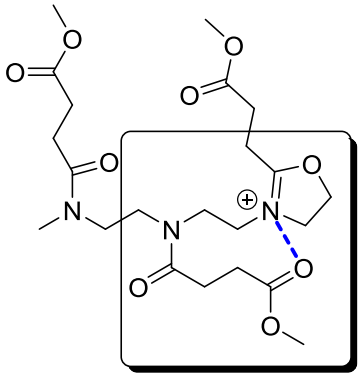

Figure 31: Proposed stabilisation mechanism of the oxazolinium transition state by the side chain ester group

Table 3:Homopolymerisation rate constants

Monomer 1	**T (°C)**	**k_p (10^{-3} L $mol^{-1}s^{-1}$)**	**T (°C)**	**k_p (10^{-3} L $mol^{-1}s^{-1}$)**	**T (°C)**	**k_p (10^{-3} L $mol^{-1}s^{-1}$)**	**T (°C)**	**k_p (10^{-3} L $mol^{-1}s^{-1}$)**
MeOx	140	133 ± 4					80	4.1 ± 0.2
EtOx	140	99 ± 3					80	3.0 ± 0.1
nPropOx	140	133 ± 3					80	3.9 ± 0.3
MestOx	140	171 ± 4	120	59 ± 2	100	28 ± 2	80	6.9 ± 0.3
C3MestOx	140	193 ± 4	120	49 ± 1	100	17 ± 1	80	5.3 ± 0.4

At 140 °C MestOx polymerised faster than C3MestOx, while at 80 °C the order was reversed, but both of them were still faster than MeOx, EtOx and nPropOx (Table 3). Similar results were obtained for the intermediate temperatures 120 and 100 °C, also revealing linear living polymerisation kinetics (Figure 32). At these intermediate temperatures MestOx also polymerised faster than C3MestOx. The livingness of these homopolymerisations was confirmed by a linear increase of the number average molecular weight (M_n) with conversion as well as the low dispersities of the resulting polymers (Đ < 1.17, Figure S 1).

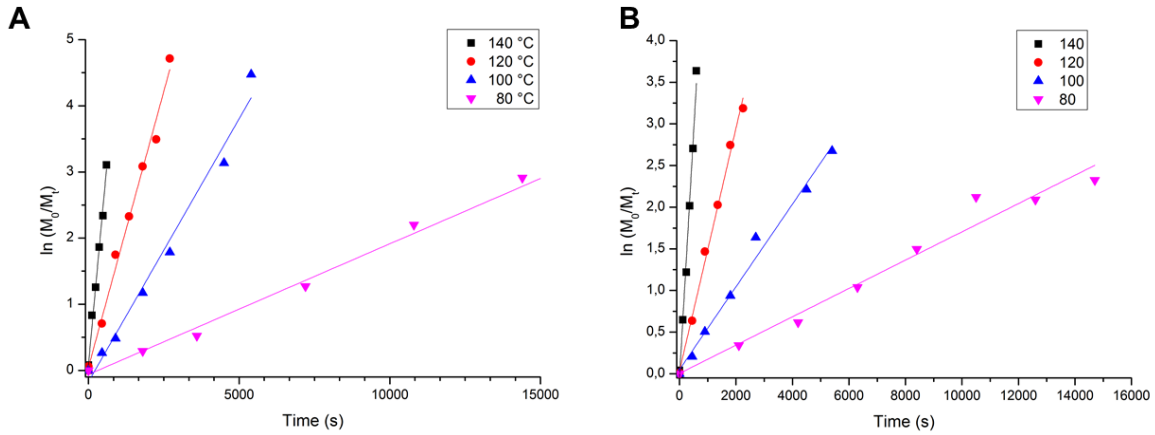

Figure 32:First order kinetic plots for homopolymerisation of A) MestOx and B) C3MestOx at different temperatures

The logarithms of the k_ps of MestOx and C3MestOx showed a linear relationship with the inverse temperature as expected based on the Arrhenius equation (eq 1).

$$k_p = Ae^{\frac{-E_A}{RT}} \qquad (1)$$

The Arrhenius plots for the MestOx and C3MestOx homopolymerisations are shown in Figure 33. From these plots the activation energy ($E_{A,\ MestOx}$= 63.0 ± 4.3 kJ mol^{-1}, $E_{A,C3MestOx}$ =

71.7 ± 4.9 kJ mol^{-1}) and the frequency factor (A_{MestOx} = 1.54 ± 0.13 * 10^{7} L mol^{-1} s^{-1}, $A_{C3MestOx}$ = 1.92 ± 0.15 *10^{8} L mol^{-1} s^{-1}) were calculated. These activation energies are lower than for MeOx (E_A = 75.4 ± 0.5 kJ mol^{-1})[38] and EtOx (E_A = 73.4 ± 0.5 kJ mol^{-1}),[39] thereby indicating that the methyl ester groups indeed lower the activation barrier for monomer addition, especially for MestOx.

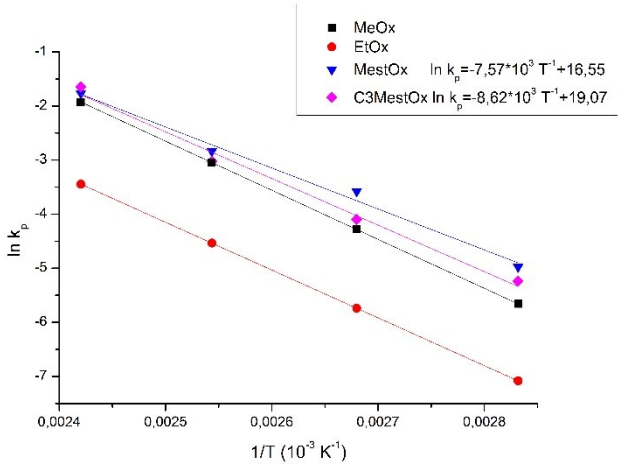

Figure 33: Arrhenius plot of MestOx and C3MestOx. The data from literature of MeOx[38] and EtOx[39] are included for comparison.

Copolymerisations

To further examine this intriguing polymerisation behaviour of (C3)MestOx, copolymerisations were studied with MeOx, EtOx and nPropOx, with a monomer to monomer ratio of 50:50 using the same conditions as for the homopolymerisations. For MeOx-C3MestOx copolymerisations at 140 °C, the monomer ratios of 75:25 and 25:75 were also included, but not further discussed. Commonly, the copolymerisation of different 2-oxazoline monomers follows the same relative order of monomer incorporation as the corresponding homopolymerisations of the individual monomers,[40-43] the only reported exception being the copolymerisation of 2-butyl-4-ethyl-2-oxazoline with 2-phenyl-2-oxazoline ascribed to steric constraints.[44] Remarkably, here the first order kinetic plots revealed that MeOx, EtOx and nPropOx were incorporated faster than MestOx and C3MestOx, which is the reversed order compared to the homopolymerisations (Figure 34, Figure 35 and Figure S 4).

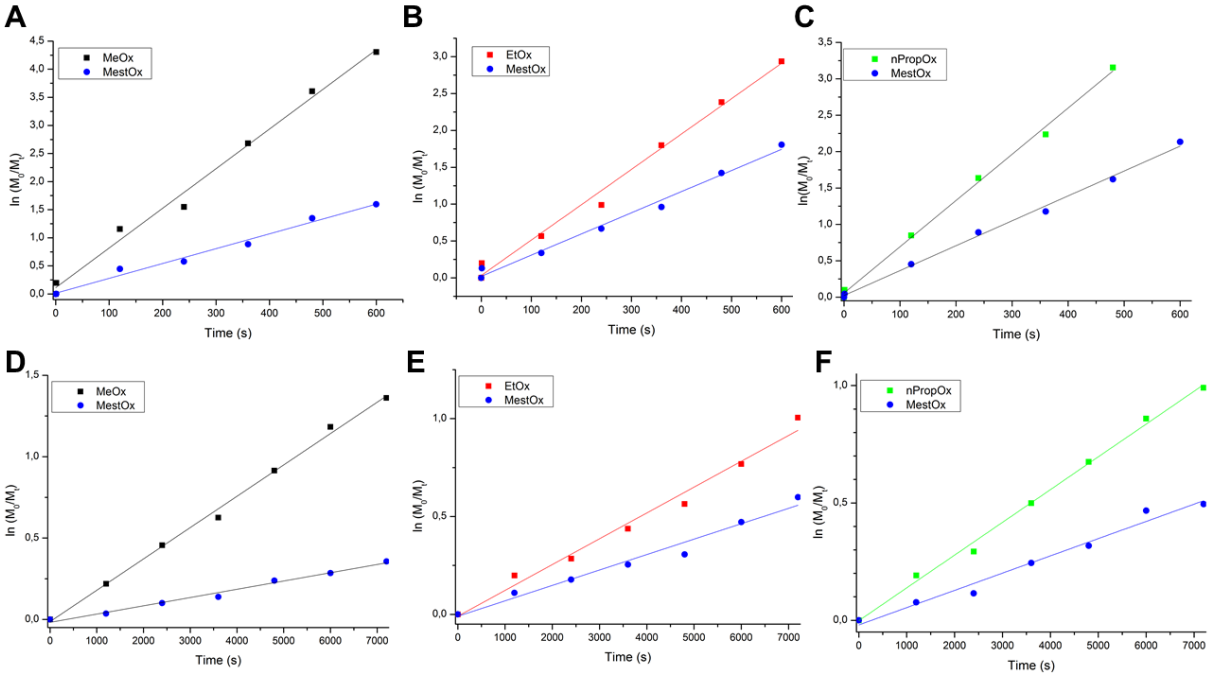

Figure 34: First order kinetic plots for copolymerisation of MestOx with A) MeOx at 140 °C, B) EtOx at 140 °C, C) nPropOx at 140 °C, D) MeOx at 80 °C, E) EtOx at 80°C and F) nPropOx at 80°C.

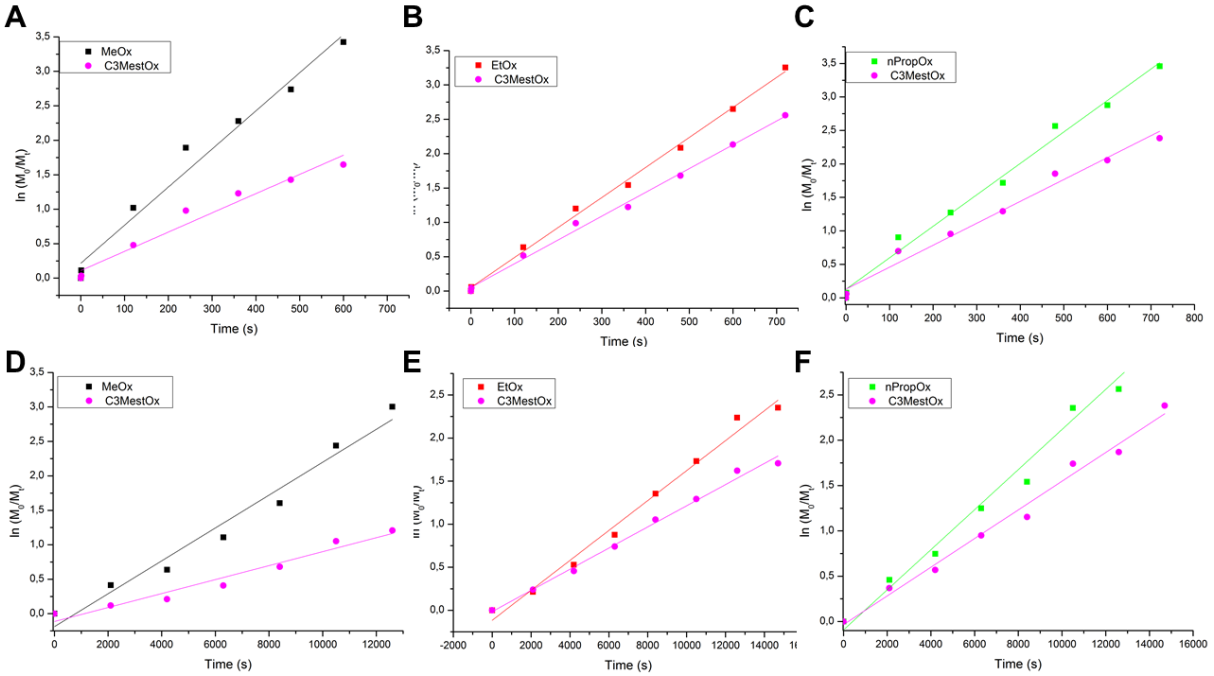

Figure 35: First order kinetic plots for copolymerisation of C3MestOx with A) MeOx at 140 °C, B) EtOx at 140 °C, C) nPropOx at 140 °C, D) MeOx at 80 °C, E) EtOx at 80°C and F) nPropOx at 80°C.

All first order kinetic plots furthermore revealed a linear increase, indicating a constant concentration of propagating species in time and, thus, the absence of termination reactions. Each data point represents a separate polymerisation and the linearity, thus, also proves the good reproducibility. The livingness of the polymerisation was confirmed by the linearly increasing M_n with conversion as well as low Đ values (Đ<1.17, Figure S 2 - Figure S 4).

The k_ps were calculated from the slope of the kinetic plots and are summarized in Table 4. Compared to the k_ps of the homopolymerisations, the incorporation of 2-alkyl-2-oxazoline monomers was accelerated while the incorporation of MestOx and C3MestOx was slowed

down. This can be explained by the activation of the alkyl monomer by the interaction of the incoming alkyl monomer with the methyl ester side chain of the growing polymer chain. This theory is supported by modelling experiments.[36, 37]

By dividing both k_ps the apparent reactivity ratios (r^{app}) for both monomers were calculated (Table 4).[45] For copolymerisations of MestOx and C3MestOx with EtOx and *n*PropOx, the different reaction temperatures (140 and 80 °C) did not influence the apparent reactivity ratios and thus the monomer distribution of the resulting polymer is independent of the temperature. In fact, for these copolymerisations r_1^{app} is smaller than 1.9 while r_2^{app} is larger than 0.5, so there is only a minor deviation from an ideal random monomer distribution. This was indeed confirmed by a visualisation of the average monomer distributions along the polymer chain using a calculation based on the first order kinetic plots (Figure 36B and Figure 37).

Table 4: Copolymerisation rates and apparent reactivity ratios

Monomer 1	**Monomer 2**	**T (°C)**	**$k_{p,1}$ (10^{-3} L mol^{-1}s^{-1})**	**$k_{p,2}$(10^{-3} L mol^{-1}s^{-1})**	**r_1^{app} (k_1/k_2)**	**r_2^{app} (k_2/k_1)**
MeOx	MestOx	140	244 ± 6	89 ± 3	2.74	0.37
EtOx	MestOx	140	162 ± 4	97 ± 3	1.67	0.60
nPropOx	MestOx	140	212 ± 6	114 ± 3	1.86	0.54
MeOx	C3MestOx	140	184 ± 12	93 ± 8	1.98	0.50
EtOx	C3MestOx	140	144 ± 3	113 ± 3	1.26	0.79
nPropOx	C3MestOx	140	157 ± 7	109 ± 6	1.44	0.70
MeOx	MestOx	120	73 ± 6	27 ± 2	2.71	0.37
MeOx	MestOx	100	29 ± 1	8.9 ± 0.4	3.29	0.30
MeOx	MestOx	80	5.1 ± 0.1	1.3 ± 0.1	3.79	0.26
EtOx	MestOx	80	4.5 ± 0.3	2.7 ± 0.2	1.68	0.60
nPropOx	MestOx	80	4.7± 0.1	2.5 ± 0.2	1.90	0.53
MeOx	C3MestOx	80	7.9 ± 0.6	3.4 ± 0.03	2.36	0.42
EtOx	C3MestOx	80	5.8 ± 0.3	4.1 ± 0.1	1.41	0.71
nPropOx	C3MestOx	80	7.4 ±0.4	5.3 ± 0.2	1.40	0.72
MeOx(75 mol%)	C3MestOx(25 mol%)	140	181 ± 3	92 ± 5	1.96	0.51
MeOx(25 mol%)	C3MestOx(75 mol%)	140	278 ± 8	120 ± 8	2.32	0.43

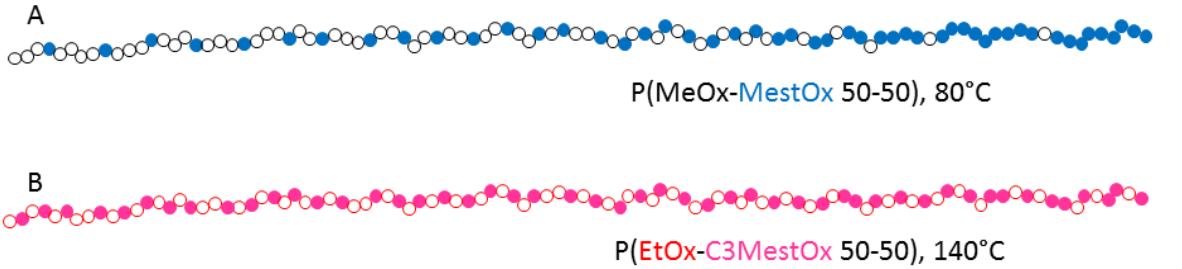

Figure 36: Monomer distribution of A) MeOx (black, open) and MestOx (blue) after 80 °C and B) EtOx (red, open) and C3MestOx (pink) after copolymerisation at 140 °C copolymerisation along the polymer chain, calculated from kinetics plots

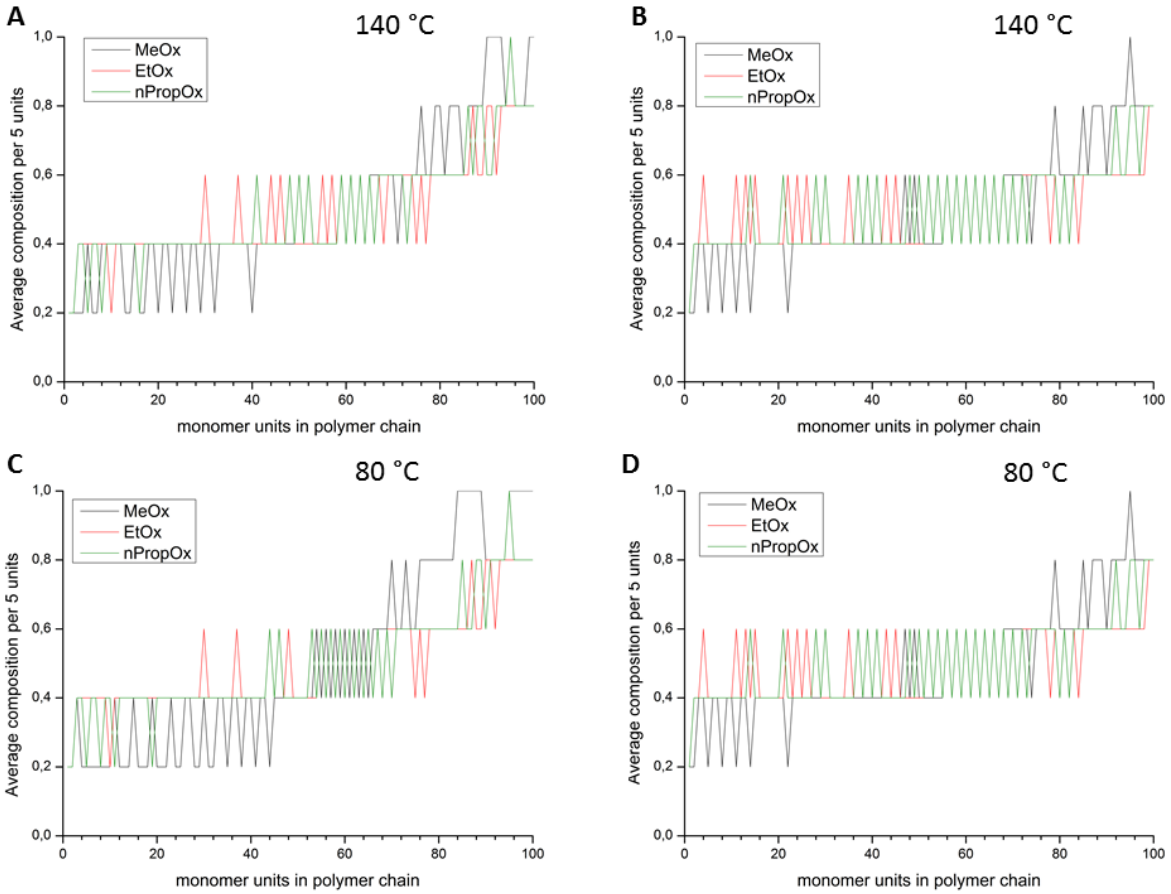

Figure 37: Gradient plots of the instantaneous copolymer composition along the polymer chains for A) MestOx copolymers at 140 °C, B) C3MestOx copolymers at 140 °C, C)MestOx copolymers at 80 °C and D)C3MestOx copolymers at 80 °C. On the y-axis 0 refers to no MestOx, 1 refers to fully MestOx and 0.5 to an equimolar mixture of both monomers, the average composition of 5 consecutive monomers is plotted.

The copolymerisations of the more reactive MeOx with MestOx and C3MestOx exhibited an r_1^{app} which was larger than 1.9 and an r_2^{app} which was smaller than 0.5, so the monomer distribution significantly deviated from an ideal random distribution, and consequently, a gradient copolymer was formed. The strength of the gradient was determined by polymerisation temperature, with a lower temperature leading to a more pronounced gradient, and type of monomer, with MestOx resulting in a stronger gradient than C3MestOx.

In Figure 36A the most extreme gradient is shown, obtained from MeOx and MestOx copolymerized at 80 °C An overview of all the different gradients is plotted in Figure 37; a (C3)MestOx monomeric unit was given a value of 1 and an alkyl monomer a value of 0, the average per 5 units was calculated and plotted.

As the MeOx-MestOx copolymerisation showed the strongest gradient formation as well as a temperature dependence of r^{app}, MeOx-MestOx kinetic studies were also performed at two intermediate temperatures (100 and 120 °C). Both temperatures also revealed linear first order kinetics (Figure 38), indicating a constant concentration of propagating species in time and, thus, absence of termination reactions. The livingness was again confirmed by a linear increase of the M_n with conversion as well as low dispersities of the resulting polymer ($Đ < 1.13$, Figure S 5). The k_ps and r^{app} values are listed in Table 4. The r^{app} values are plotted versus temperature in Figure 39A; upon raising temperature up to 120 °C the difference in

reaction rates became smaller, while there was no further decrease noticeable when the temperature was further increased to 140 °C. The gradient plots of MeOx-MestOx copolymerisations at different temperatures are depicted in Figure 39B, showing slightly stronger gradient formation at lower temperatures.

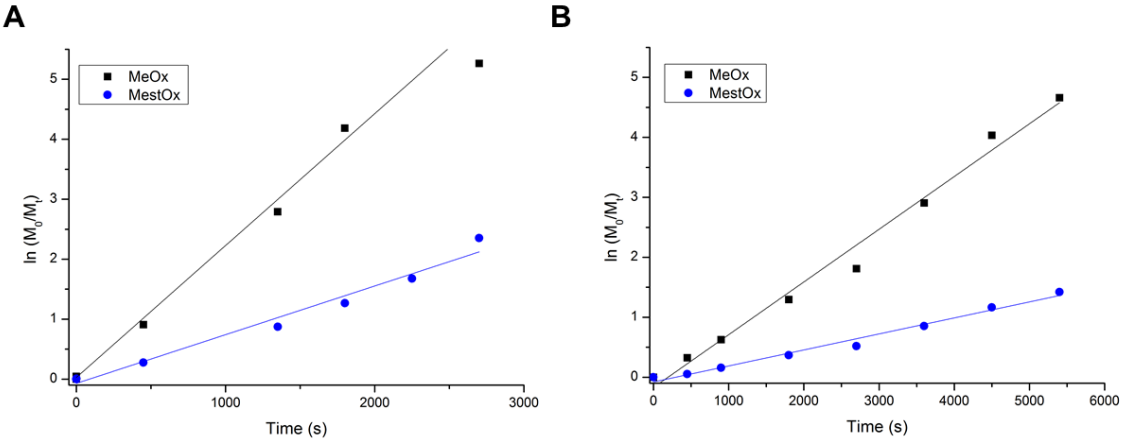

Figure 38: First order kinetic plots of copolymerisation of MeOx and MestOx at A) 120 °C and B) 100 °C

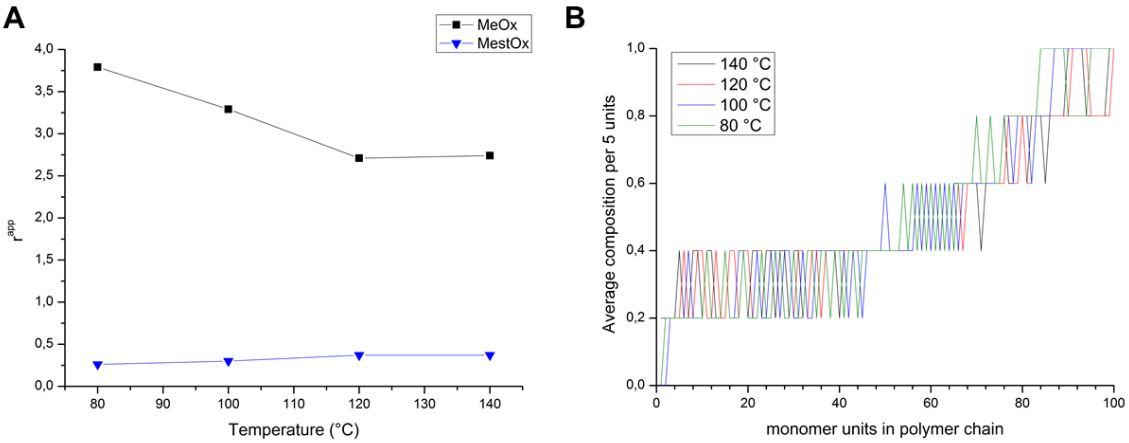

Figure 39: A) Temperature dependence of the apparent reactivity ratios of MeOx-MestOx copolymerisation and B) Gradient plots of MeOx-MestOx copolymerisation at different temperatures.

Because the k_ps were determined at different temperatures an Arrhenius plot could be made (Figure 40) and from this the activation energy ($E_{A,\ MeOx}$= 76.1 ± 5.8 kJ mol^{-1}, $E_{A,MestOx}$ = 83.4 ± 5.6 kJ mol^{-1}) and the frequency factor (A_{MeOx} = 1.04 ± 0.09* 10^7 L mol^{-1} s^{-1}, A_{MestOx} = 3.27 ± 0.27 *10^9 L mol^{-1} s^{-1}) were calculated. The activation energy of MeOx in the copolymerization is comparable to the activation energy of MeOx in homopolymerisation ($E_{A,MeOx}$ = 75.4 kJ mol^{-1}), while the activation energy of MestOx was raised in comparison with homopolymerisation ($E_{A,\ MestOx}$= 63.0 ± 4.3 kJ mol^{-1}), because the MestOx itself is probably less nucleophilic towards MeOx-oxazolinium chain ends.

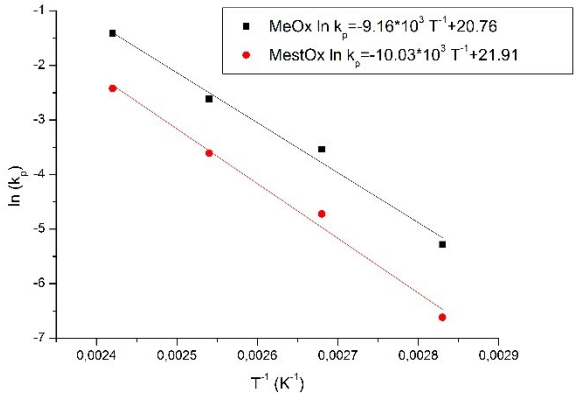

Figure 40: Arrhenius plot of MeOx-MestOx copolymerisation

Conclusions

The methyl ester-containing 2-oxazoline monomers, MestOx and C3MestOx were successfully synthesized via the reaction of an acid chloride with 2-chloroethylamine and subsequent ring closure with powderous sodium carbonate. Homopolymerisation kinetic studies revealed a faster propagation of MestOx and C3MestOx compared to the alkyl monomers, MeOx, EtOx and nPropOx, while in copolymerisation a reversal of monomer incorporation rate was found. In case of EtOx and *n*PropOx copolymerisations this led to a minor deviation from ideal random monomer distribution, whereas copolymerisation of MeOx with either MestOx or C3MestOx led to gradient polymers. The large difference in reaction rates between homo- and copolymerisation of MeOx with the ester-containing oxazolines was further corroborated by the determination of the activation energy of MeOx during copolymerisation, which was comparable to homopolymerisation, while the activation energy of MestOx was increased.

Acknowledgements

Maarten Vergaelen and Bryn Monnery are acknowledged for their help in performing monomer synthesis and (co)polymerisation studies. Dietmar Hertsen, Hannelore Goossens, Saron Catak and Veronique van Spey are thanked for performing DFT calculations on the (co)polymerisations. Yentl Verleysen, Willem Uyttendaele and Wouter Vandeplassche are acknowledged for the MeOx-C3MestOx kinetics at 140 °C.

Experimental section

Materials 2-Chloroethylamine hydrochloride, methyl p-toluenesulfonate (MeOTs) and sodium carbonate powder were purchased from Acros Organics. All other reagents were purchased from Sigma Aldrich and used as received, except 2-methyl-2-oxazoline (MeOx), 2-ethyl-2-oxazoline (EtOx) and methyl p-toluenesulfonate (MeOTs). These were purified by distillation over barium oxide and stored under argon. Dry solvents were obtained from a solvent purification system from J.C. Meyer, with aluminium oxide drying system and a nitrogen flow.

Instrumentation Nuclear magnetic resonance (NMR) spectra were recorded on a Bruker DMC300 (300 MHz for ^{1}H, 75 MHz for 13C) or a Bruker DMX 500 (500 MHz for ^{1}H, 125 MHz for 13C).

Electro spray ionisation mass (ESI MS) spectra were recorded on a Thermo Finnigan LCQ Advantage Max.

Polymerisation reaction mixtures were prepared in a VIGOR Sci-Lab SG 1200/750 Glovebox system, with less than 1 ppm of O_2 and H_2O.

Polymerisations were carried out in a Biotage Initiator Microwave System with Robot Sixty utilizing capped reaction vials. These vials were heated to 120 °C overnight, allowed to cool to room temperature and filled with nitrogen prior to use. All microwave polymerisations were performed with temperature control (IR sensor).

Size exclusion chromatography (SEC) was performed on an Agilent 1260 - series HPLC system equipped with a 1260 online degasser, a 1260 ISO-pump, a 1260 automatic liquid sampler, a thermostatted column compartment, a 1260 diode array detector (DAD) and a 1260 refractive index detector (RID). Analyses were performed on a PSS Gram30 column in series with a PSS Gram1000 column at 50 °C. *N,N*-dimethylacetamide (DMA), containing 50 mM of LiCl, was used as an eluent, at a flow rate of 0.593 ml min^{-1}. The SEC traces were analysed using the Agilent Chemstation software with the GPC add on. Number average molecular weights (M_n) and dispersity (Đ) values were calculated against polymethylmethacrylate (PMMA) standards.

Gas chromatography (GC) was performed on a 7890A from Agilent Technologies with an Agilent J&W Advanced Capillary GC column (30 m, 0.320 mm, and 0.25 μm). Injections were performed with an Agilent Technologies 7693 auto sampler. Detection was done with a Flame ionization detector (FID) detector. Injector and detector temperatures were kept constant at 250 and 280 °C, respectively. The column was initially set at 50 °C, followed by two heating stages: from 50 °C to 100 °C with a rate of 20 °C /min and from 100 °C to 300 °C with a rate of 40 °C /min, and then held at this temperature for 0.5 minutes. Conversion was determined based on the integration of monomer peaks using acetonitrile (CH_3CN) as an internal standard.

Monomer synthesis

Synthesis of methyl 4-(2-chloroethyl)amino-4-oxobutanoate (1b, MestOx-precursor) Methyl succinyl chloride (**1a**, 50 g, 332.1 mmol, 40.88 mL) and 2-chloroethylamine hydrochloride (38.52 g, 332.1 mmol) were suspended in dry dichloromethane (375 mL) under an argon atmosphere. The reaction mixture was cooled continuously to 0°C while triethylamine (TEA) (72.25 g, 714 mmol, 99.2 mL) was added dropwise within 2 hours. The reaction was allowed to warm to room temperature overnight, after full addition of the TEA. The mixture was washed with water (2x50 mL) and brine (1x 50 mL). The organic phase was dried over Na_2SO_4 and the solvent was removed under reduced pressure. The resulting product was purified by filtration column chromatography (neutral Al_2O_3, DCM:MeOH 99:1) yielding product **1b** as a yellow oil (107 g, 664.2 mmol, 83%).

^{1}H NMR ($CDCl_3$,500 MHz): δ 6.1 (br, 1H, NH), 3.68 (t, 2.1 Hz, 2H, CH_2Cl), 3.61 (m, 5H, OCH_3 & $C\underline{H}_2CH_2Cl$), 2.68 (t, 7.0 Hz, 2 H, $NC{=}OC\underline{H}_2$), 2.52 (t, 7.0 Hz, 2H, $C\underline{H}_2COOCH_3$)
^{13}C NMR (75 MHz, $CDCl_3$): δ 172.9 (C=ONH), 171.1 ($\underline{C}{=}OOCH_3$), 51.4 (OCH_3), 43.5 ($\underline{C}H_2CH_2Cl$), 40.8 (CH_2Cl), 30.5 ($CH_3C{=}O\underline{C}H_2$), 28.8 ($CH_3C{=}OCH_2\underline{C}H_2$)
ESI MS: m/z: calculated 193.05, found 194.1&196.1 [$M+H^+$], 216.1&218.1 [$M+Na^+$]

Synthesis of 2-methoxycarbonylethyl-2-oxazoline (1, MestOx) The precursor (**1b**, 107 g, 552.6 mmol) and anhydrous sodium carbonate (52.7 g, 497.3 mmol) were mixed. The reaction was performed for 48 hours by mounting the flask on a rotary evaporator (40 °C, 50 mbar) to allow good mixing of the salt in the viscous mixture and providing a larger surface area for evaporation of the released CO_2. Subsequently dichloromethane (DCM) was added, the reaction mixture was filtered and the solvent was removed under reduced pressure. The oil was distilled twice over barium oxide, under reduced pressure yielding a colourless liquid that crystallized in time into a white solid (60 g, 381.8 mmol, 69%).

^{1}H NMR ($CDCl_3$, 500 MHz,): δ 4.3 (t, 2H, 9.4 Hz, CH_2O), 3. 8 (t, 9.4 Hz, 2H, CH_2N=), 3.7 (s, 3H, $COOCH_3$), 2.7 (t, 2H, 7.3 Hz, CH_2COO), 2.6 (t, 2H, 7.3 Hz, CH_2C(=N)O)
^{13}C NMR ($CDCl_3$, 75 MHz): δ 172.9 ($\underline{C}OOCH_3$), 169.2 (C(=N)O), 67.6 (CH_2O), 54.3 (CH_2N), 51.9 (OCH_3), 30.2 ($\underline{C}H_2COO$), 23.2 (CH_2N)
ESI MS: m/z: calculated 157.07, found 158.1 [M+H$^+$]

Synthesis of methyl 5-((2-chloroethyl)amino)-5-oxopentanoate (2b, C3MestOx precursor) Glutaric acid monomethyl ester chloride (**2a**, 50 g, 303.8 mmol, 41.98 mL) and 2-chloroethylamine hydrochloride (35.24 g, 303.8 mmol) were suspended in dry dichloromethane (375 mL) under an argon atmosphere. The reaction mixture was cooled continuously to 0°C while triethylamine (TEA) (66.09 g, 653 mmol, 90.8 mL) was added dropwise within 2 hours. The reaction was allowed to warm to room temperature overnight, after full addition of the TEA. The mixture was washed with water (2x50 mL) and brine (1x 50 mL). The organic phase was dried over Na_2SO_4 and the solvent was removed under reduced pressure. A yellow liquid (60 g, 289 mmol, 95%) was obtained.

1H NMR (CDCl3, 300 MHz): δ 6.0 (br, 1H, NH), 3.67 (s, 3H, OCH_3), 3.61 (m, 4H, CH_2Cl & $C\underline{H}_2CH_2Cl$), 2.39 (t, 7.3 Hz, 2 H, NHC=O$C\underline{H}_2$), 2.27 (t, 7.3 Hz, 2H, $C\underline{H}_2COOCH_3$), 1.97 (qt, 7.3 Hz, 2H, $CH_2C\underline{H}_2CH_2$)
13C NMR ($CDCl_3$, 125 MHz): δ 173.4 (C=ONH), 172.4 ($\underline{C}$=OOCH_3), 51.8 (OCH_3), 44.2 (CH_2Cl), 41.3 ($NHCH_2$), 35.5 (NHC=O$\underline{C}H_2$), 33.1 (CH_3C=O$\underline{C}H_2$), 20.9 ($CH_2\underline{C}H_2CH_2$)
ESI MS: m/z: calculated 207.07, found 208.0&210.0 [M+H$^+$]

Synthesis of 2-methoxycarbonylpropyl-2-oxazoline (2, C3MestOx) The precursor (**2b**, 60 g, 289 mmol) and anhydrous sodium carbonate (27.6 g, 260 mmol) were mixed. The reaction was performed overnight by mounting the flask on the rotary evaporator (40 °C, 50 mbar) to allow good mixing of the salt in the viscous mixture and providing a larger surface area for evaporation of the released CO_2. Subsequently, DCM was added, the reaction mixture was filtered and the solvent was removed under reduced pressure. The oil was distilled twice over barium oxide, under reduced pressure, yielding a colourless liquid (24.8 g, 145 mmol, 50%).

^{1}H NMR ($CDCl_3$, 500 MHz): δ 4.3 (t, 2H, 9.5 Hz, CH_2O), 3. 8 (t, 9.5 Hz, 2H, CH_2N=), 3.7 (s, 3H, $COOCH_3$), 2.7 (t, 2H, 7.3 Hz, CH_2COO), 2.6 (t, 2H, 7.3 Hz, CH_2C(=N)O)), 1.97 (quint, 7.3 Hz, 2H, $CH_2C\underline{H}_2CH_2$)
^{13}C NMR ($CDCl_3$, 75 MHz): δ 173.6 ($\underline{C}OOCH_3$), 167.8 (C(=N)O), 67.3 (CH_2O), 54.5 (CH_2N), 51.7 (OCH_3), 32.9 ($\underline{C}H_2COOCH_3$), 27.2 ($\underline{C}H_2C$(=N)O), 21.3 ($CH_2\underline{C}H_2CH_2$)
ESI MS: m/z: calculated 171.09, found 172.1[M+H$^+$]

Synthesis of 2-*n*-propyl-2-oxazoline (5, *n*PropOx) *n*PropOx was synthesized according to literature.[34] In brief, butyronitrile (32.78 mL, 26.02 g, 377 mmol)), amino ethanol (25 mL, 25.30 g, 414 mmol) and zinc acetate dihydrate (1.382 g, 7.53 mmol) were refluxed at 130 °C

overnight. The reaction mixture was cooled to room temperature, and dichloromethane was added. The organic phase was washed 3 times with water and once with brine. The combined organic phases were dried over sodium sulphate. After removing the dichloromethane under reduced pressure, the monomer was purified by fractional distillation over barium oxide.

^{1}H NMR ($CDCl_3$, 500 MHz): δ 4.2 (t, 2H, 9.5 Hz, CH_2O), 3. 8 (t, 9.5 Hz, 2H, CH_2N=), 2.2 (t, 2H, 7.3 Hz, CH_2C(=N)O), 1.7 (quint, 2H, 7.3 Hz, $CH_2C\underline{H}_2CH_2$), 1.0 (t, 7.3 Hz, 2H, $CH_2CH_2C\underline{H}_3$).

Polymerisation kinetics Stock solutions (7 mL) for polymerisation kinetics were prepared in the glovebox. Total monomer concentration $[M_{tot}] = [M_1] + [M_2] = 3$ M, monomer (M_1 + M_2):initiator ratio $\frac{(M]}{[I]} = 100$, MeOTs was used as an initiator, acetonitrile (CH_3CN) was used as solvent. For most copolymerisations the ratio of both monomers was 50:50, only for MeOx-C3MestOx copolymerisation at 140 °C ratios of 75:25 and 25:75 were used. The stock solution was divided in 0.7 mL portions in separate 0.5-2 mL Biotage reaction vials. The polymerisation times used are listed in Table 5. After heating, 0.1 mL polymerisation mixture was diluted with 0.9 mL of chloroform for GC measurement. Conversion was determined based on the integral of monomer peaks using acetonitrile as an internal standard. A second sample of 0.1 mL was diluted with 0.9 mL of DMA containing 50 mM of LiCl for SEC measurement to determine M_n and Đ.

Table 5: Overview of different reaction times at different temperatures

Sample	140 °C	120 °C	100 °C	80 °C, MestOx homo	80 °C, MestOx co	80 °C, C3MestOx
1	1 s	1 s	7 min 30 s	30 min	20 min	35 min
2	2 min	7 min 30 s	15 min	1 h	40 min	1 h 10 min
3	4 min	15 min	30 min	2 h	1 h	1 h 45 min
4	6 min	22 min 30 s	45 min	3 h	1h 20 min	2 h 20 min
5	8 min	30 min	1 h	4 h	1 h 40 min	2 h 55 min
6	10 min	37 min 30 s	1 h 15 min	5 h	2 h	3 h 30 min
7	12 min	45 min	1 h 30 min	6 h		4 h 05 min

Supporting information

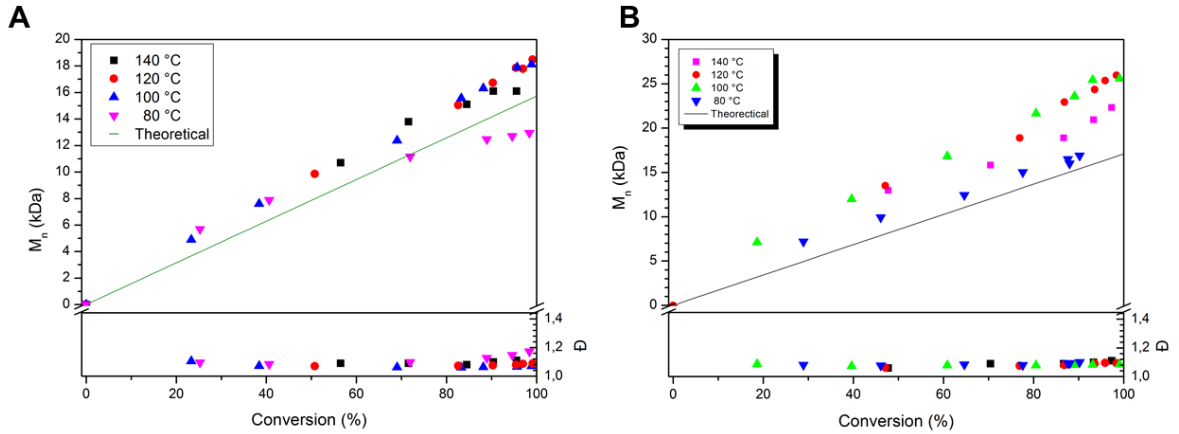

Figure S 1: M_n against conversion plot, including Đ of A) $PMestOx_{100}$ and B) $PC3MestOx_{100}$, polymerisation at different temperatures. The discrepancies with the theoretical M_n values are caused by the PMMA standards used for the SEC calibration.

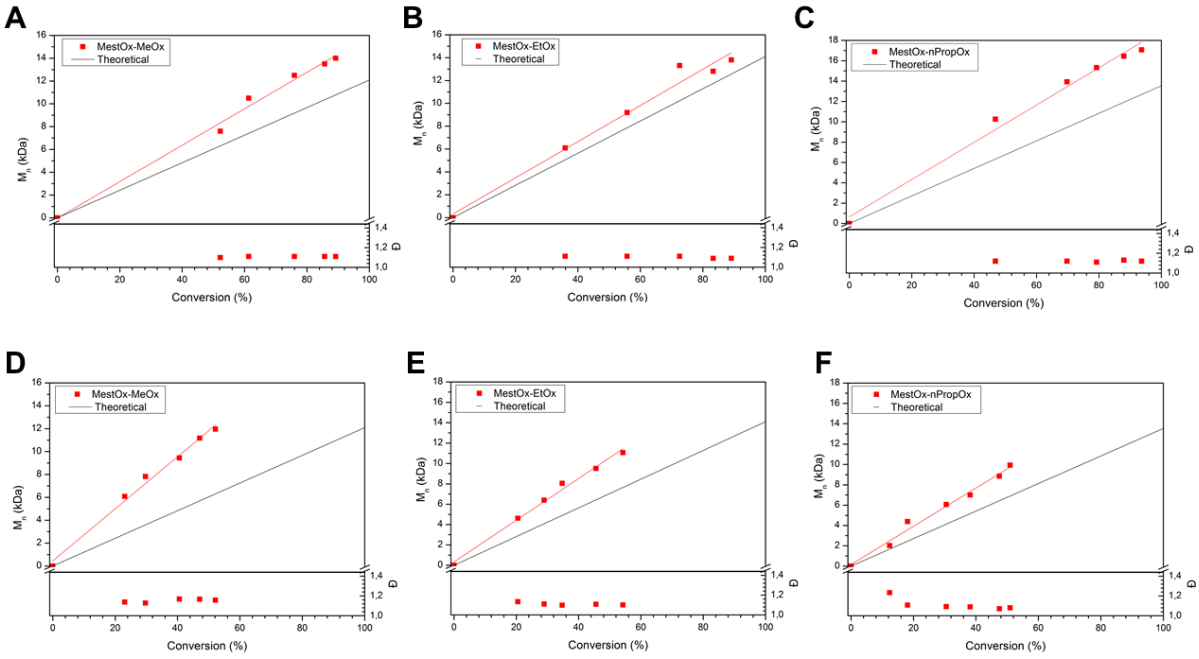

Figure S 2: M_n against conversion plot, including Đ of A) $P(MeOx_{50}\text{-}MestOx_{50})$ copolymer, polymerisation at 140 °C, B) $P(EtOx_{50}\text{-}MestOx_{50})$ copolymer, polymerisation at 140 °C,.C) $P(n PropOx_{50}\text{-}MestOx_{50})$ copolymer, polymerisation at 140 °C, D) $P(MeOx_{50}\text{-}MestOx_{50})$ copolymer, polymerisation at 80 °C, E) $P(EtOx_{50}\text{-}MestOx_{50})$ copolymer, polymerisation at 80 °C, F) $P(n PropOx_{50}\text{-}MestOx_{50})$ copolymer, polymerisation at 80 °C. The discrepancy with the theoretical M_n values is caused by the PMMA standards used for the SEC calibration.

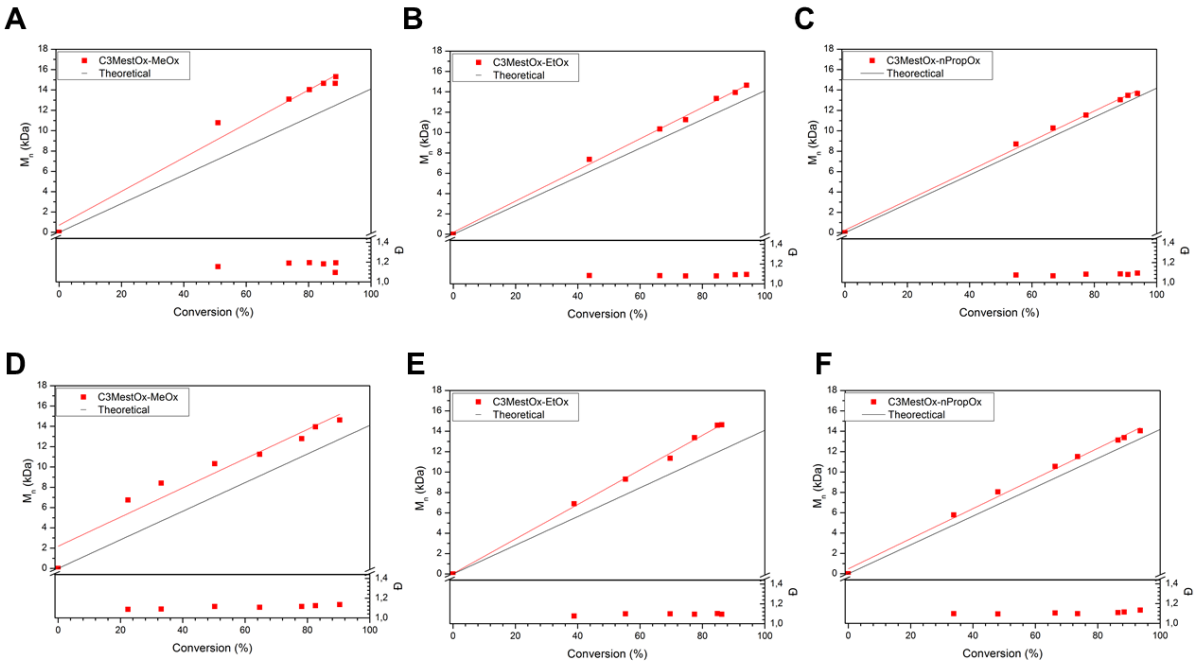

Figure S 3: M_n against conversion plot, including Đ of A) P($MeOx_{50}$-C3MestOx_{50}) copolymer, polymerisation at 140 °C, B) P($EtOx_{50}$-C3MestOx_{50}) copolymer, polymerisation at 140 °C, C) P(*n*PropOx_{50}-C3MestOx_{50}) copolymer, polymerisation at 140 °C, D) P($MeOx_{50}$-C3MestOx_{50}) copolymer, polymerisation at 80 °C, E) P($EtOx_{50}$-C3MestOx_{50}) copolymer, polymerisation at 80 °C, F) P(*n*PropOx_{50}-C3MestOx_{50}) copolymer, polymerisation at 80 °C. The discrepancy with the theoretical M_n values is caused by the PMMA standards used for the SEC calibration.

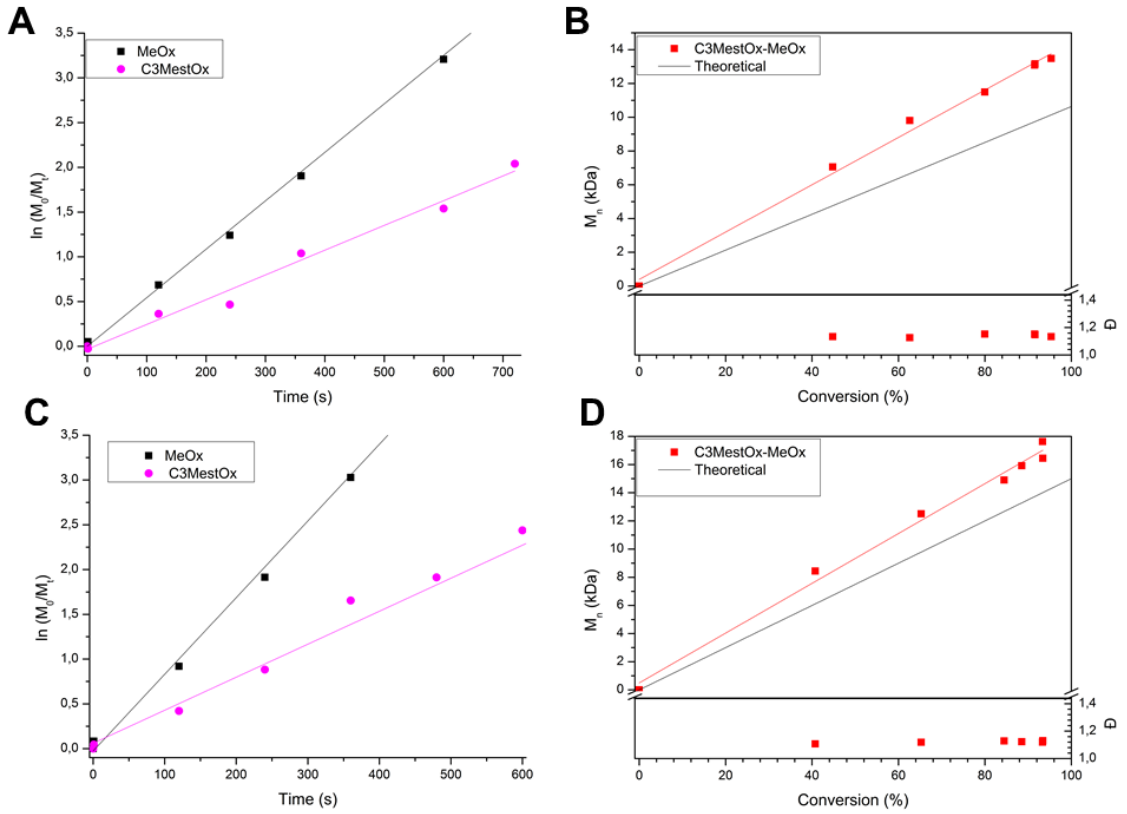

Figure S 4: A) First order kinetic plots for copolymerisation of C3MestOx (25 mol%) with MeOx (75 mol%) at 140 °C, B) M_n against conversion plot, including Đ of P(MeO_{75}-C3MestOx_{25}) copolymer, polymerisation at 140 °C, C) First order kinetic plots for copolymerisation of C3MestOx (75 mol%)

with MeOx (25 mol%) at 140 °C, B) M_n against conversion plot, including Đ of P(MeO_{25}-C3MestOx_{75}) copolymer, polymerisation at 140 °C.

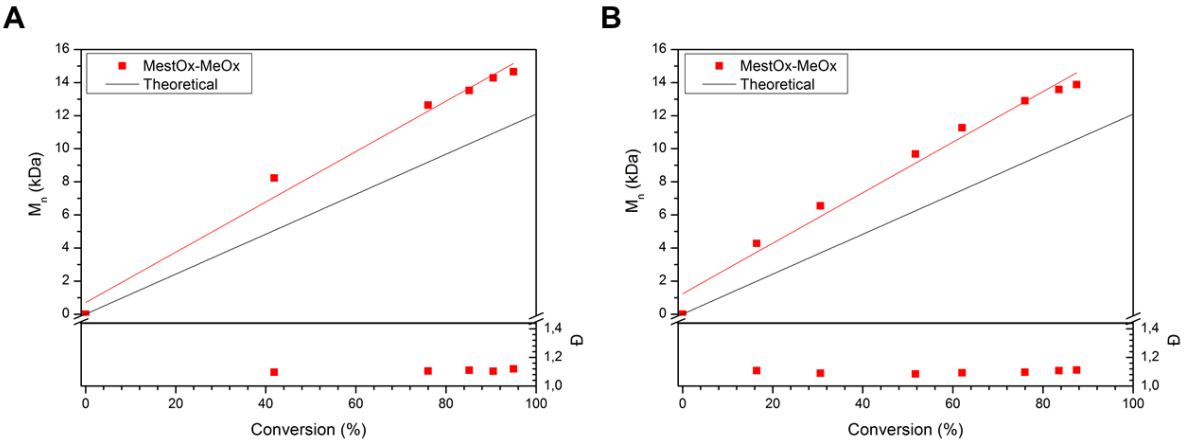

Figure S 5: M_n against conversion plot, including Đ of A) P($MeOx_{50}$-MestOx_{50}) copolymer, polymerisation at 120 °C and B) P($MeOx_{50}$-MestOx_{50}) copolymer, polymerisation at 100 °C. The discrepancy with the theoretical M_n values is caused by the PMMA standards used for the SEC calibration.

References

1. Seeliger, W.; Aufderhaar, E.; Diepers, W.; Feinauer, R.; Nehring, R.; Thier, W.; Hellmann, H. *Angew. Chem. Int. Ed.* **1966,** 5, 875-888.
2. Tomalia, D. A.; Sheetz, D. P. *J. Polym. Sci., Part A: Polym. Chem.* **1966,** 4, 2253-2265.
3. Kagiya, T.; Narisawa, S.; Maeda, T.; Fukui, K. *J. Polym. Sci. Pol. Lett.* **1966,** 4, 441-445.
4. Bassiri, T. G.; Levy, A.; Litt, M. *J. Polym. Sci., Part B: Polym. Lett.* **1967,** 5, 871-879.
5. Fijten, M. W. M.; Haensch, C.; van Lankvelt, B. M.; Hoogenboom, R.; Schubert, U. S. *Macromol. Chem. Phys.* **2008,** 209, 1887-1895.
6. Hoogenboom, R. *Angew. Chem. Int. Ed.* **2009,** 48, 7978-7994.
7. Volet, G.; Lav, T. X.; Babinot, J.; Amiel, C. *Macromol. Chem. Phys.* **2011,** 212, 118-124.
8. Guillerm, B.; Monge, S.; Lapinte, V.; Robin, J. J. *Macromol. Rapid Commun.* **2012,** 33, 1600-1612.
9. Schenk, V.; Rossegger, E.; Ebner, C.; Bangerl, F.; Reichmann, K.; Hoffmann, B.; Höpfner, M.; Wiesbrock, F. *Polymers* **2014,** 6, (2), 264-279.
10. Zalipsky, S.; Hansen, C. B.; Oaks, J. M.; Allen, T. M. *J Pharm Sci* **1996,** 85, 133-137.
11. Mero, A.; Pasut, G.; Via, L. D.; Fijten, M. W. M.; Schubert, U. S.; Hoogenboom, R.; Veronese, F. M. *J. Controlled Release* **2008,** 125, 87-95.
12. Luxenhofer, R.; Han, Y.; Schulz, A.; Tong, J.; He, Z.; Kabanov, A. V.; Jordan, R. *Macromol. Rapid Commun.* **2012,** 33, (19), 1613-1631.
13. Luxenhofer, R.; Sahay, G.; Schulz, A.; Alakhova, D.; Bronich, T. K.; Jordan, R.; Kabanov, A. V. *J. Controlled Release* **2011,** 153, (1), 73-82.
14. Diehl, C.; Schlaad, H. *Macromol. Biosci.* **2009,** 9, (2), 157-161.
15. Weber, C.; Hoogenboom, R.; Schubert, U. S. *Prog. Polym. Sci.* **2012,** 37, (5), 686-714.
16. Hoogenboom, R.; Thijs, H. M. L.; Jochems, M. J. H. C.; van Lankvelt, B. M.; Fijten, M. W. M.; Schubert, U. S. *Chem. Commun.* **2008**, (44), 5758-5760.

17. Levy, A.; Litt, M. *J. Polym. Sci., Part A: Polym. Chem.* **1968,** 6, 1883-1894.
18. Zarka, M. T.; Nuyken, O.; Weberskirch, R. *Chem. Eur. J.* **2003,** 9, 3228-3234.
19. Kotre, T.; Zarka, M. T.; Krause, J. O.; Buchmeiser, M. R.; Weberskirch, R.; Nuyken, O. *Macromol. Symp.* **2004,** 217, 203-214.
20. Rueda, J. C.; Zschoche, S.; Komber, H.; Krahl, F.; Arndt, K. F.; Voit, B. *Macromol. Chem. Phys.* **2010,** 211, 706-716.
21. Liu, Y.; Wang, Y.; Wang, Y. F.; Lu, J.; Pinon, V.; Weck, M. *J. Am. Chem. Soc.* **2011,** 133, 14260-14263.
22. Zschoche, S.; Rueda, J. C.; Binner, M.; Komber, H.; Janke, A.; Arndt, K. F.; Lehmann, S.; Voit, B. *Macromol. Chem. Phys.* **2012,** 213, 215-226.
23. Rueda, J. C.; Campos, E.; Komber, H.; Zschoche, S.; Haussler, L.; Voit, B. *Des. Monomers Polym.* **2014,** 17, 208-216.
24. Taubmann, C.; Luxenhofer, R.; Cesana, S.; Jordan, R. *Macromol. Biosci.* **2005,** 5, 603-612.
25. Gress, A.; Volkel, A.; Schlaad, H. *Macromolecules* **2007,** 40, 7928-7933.
26. Zschoche, S.; Rueda, J.; Boyko, V.; Krahl, F.; Arndt, K. F.; Voit, B. *Macromol. Chem. Phys.* **2010,** 211, 1035-1042.
27. Kelly, A. M.; Hecke, A.; Wirnsberger, B.; Wiesbrock, F. *Macromol. Rapid Commun.* **2011,** 32, 1815-1819.
28. Legros, C.; Pauw-Gillet, M.-C. D.; Tam, K. C.; Lecommandoux, S.; Taton, D. *Eur. Polym. J.* **2015,** 62, 322-330.
29. Lava, K.; Verbraeken, B.; Hoogenboom, R. *Eur. Polym. J.* **2015,** 65, 98-111.
30. Hoogenboom, R., Polyoxazoline polymers and methods for their preparation, conjugates of these polymers and medical uses thereof. WO2013103297A1: 2013.
31. Mees, M.; Hoogenboom, R. *Macromolecules* **2015,** 48, (11), 3531-3538.
32. Glassner, M.; D'hooge, D. R.; Young Park, J.; Van Steenberge, P. H. M.; Monnery, B. D.; Reyniers, M.-F.; Hoogenboom, R. *Eur. Polym. J.* **2015,** 65, 298-304.
33. Wiesbrock, F.; Hoogenboom, R.; Abeln, C. H.; Schubert, U. S. *Macromol. Rapid Commun.* **2004,** 25, (22), 1895-1899.
34. Hoogenboom, R.; Fijten, M. W. M.; Thijs, H. M. L.; Van Lankvelt, B. M.; Schubert, U. S. *Des. Monomers Polym.* **2005,** 8, 659-671.
35. Saegusa, T.; Ikeda, H. *Macromolecules* **1973,** 6, (6), 808-811.
36. Bouten, P. J. M.; Hertsen, D.; Vergaelen, M.; Monnery, B. D.; Boerman, M. A.; Goossens, H.; Catak, S.; van Hest, J. C. M.; Van Speybroeck, V.; Hoogenboom, R. *Polym. Chem.* **2015,** 6, (4), 514-518.
37. Bouten, P. J. M.; Hertsen, D.; Vergaelen, M.; Monnery, B. M.; Catak, S.; van Hest, J. C. M.; Van Speybroeck, V.; Hoogenboom, R. *J. Polym. Sci., Part A: Polym. Chem.* **2015,** accepted.
38. Wiesbrock, F.; Hoogenboom, R.; Leenen, M. A. M.; Meier, M. A. R.; Schubert, U. S. *Macromolecules* **2005,** 38, 5025-5034.
39. Wiesbrock, F.; Hoogenboom, R.; Abeln, C. H.; Schubert, U. S. *Macromol. Rapid Commun.* **2004,** 25, 1895-1899.
40. Hoogenboom, R.; Thijs, H. M. L.; Fijten, M. W. M.; van Lankvelt, B. M.; Schubert, U. S. *J. Polym. Sci., Part A: Polym. Chem.* **2007,** 45, (3), 416-422.
41. Hoogenboom, R.; Wiesbrock, F.; Leenen, M. A. M.; van der Loop, M.; van Nispen, S. F. G. M.; Schubert, U. S. *Aust. J. Chem.* **2007,** 60, (9), 656-661.
42. Huber, S.; Jordan, R. *Colloid. Polym. Sci.* **2008,** 286, (4), 395-402.
43. Park, J.-S.; Kataoka, K. *Macromolecules* **2006,** 39, (19), 6622-6630.

44. Lambermont-Thijs, H. M. L.; Fijten, M. W. M.; van der Linden, A. J.; van Lankvelt, B. M.; Bloksma, M. M.; Schubert, U. S.; Hoogenboom, R. *Macromolecules* **2011,** 44, (11), 4320-4325.
45. Puskas, J. E.; McAuley, K. B.; Chan, S. W. P. *Macromol. Symp.* **2006,** 243, (1), 46-52.

Chapter 3:

Thermal properties of methyl ester-containing poly(2-oxazoline)s

Part of this work has been published:

Petra J.M. Bouten, Kathleen Lava, Jan C.M. van Hest, Richard Hoogenboom, *Thermal Properties of Methyl Ester-Containing Poly(2-oxazoline)s*, **Polymers**, 2016, 7, 10, 1998-2008

Abstract
This chapter describes the synthesis and thermal properties in solution and bulk of poly(2-alkyl-oxazoline)s (PAOx) containing a methyl ester side chain. Homopolymers of 2-methoxycarbonylethyl-2-oxazoline (MestOx) and 2-methoxycarbonylpropyl-2-oxazoline (C3MestOx) as well as copolymers with 2-ethyl-2-oxazoline (EtOx) and 2-*n*-propyl-2-oxazoline (*n*PropOx) were prepared with systematic variations in composition. Investigation of the solution properties of these polymers revealed that the cloud point temperatures (T_{CP}s) could be tuned between 24 and 108 °C depending on the PAOx composition. To the best of our knowledge, the T_{CP}s of PMestOx and PC3MestOx are reported for the first time and they closely resemble the T_{CP}s of PEtOx and PnPropOx, respectively, indicating similar hydrophilicity of the methyl ester and alkyl side chains. Furthermore, the thermal transitions and thermal stability of these polymers were investigated by DSC and TGA measurements, respectively, revealing amorphous polymers with glass transition temperatures between -2 °C and 54 °C that are thermally stable up to > 300 °C.

Introduction
Smart polymeric materials can change their physical properties in response to external stimuli, such as temperature, ionic strength, pH, chemical and biological stimuli, light or electromagnetic radiation.[1-3] Thermoresponsive polymeric behaviour has most extensively been studied, in particular how polymer solubility is affected by temperature changes. One of the best characterized thermoresponsive polymers is poly(*N*-isopropyl acrylamide) (PNIPAAm), which displays a lower critical solution temperature (LCST) of 32 °C, just below body temperature.[2-5] Other classes of thermoresponsive polymers that have emerged in recent years are for example poly(oligo ethylene glycol acrylate)s,[2, 6] polyisocyanopeptides grafted with oligo(ethylene glycol) side chains,[7-9] poly(2-oxazine)s[10] and poly(2-oxazoline)s.[3, 5, 11-17] These types of polymers can be applied in temperature sensors,[18] protein chromatography[19] and various biomedical applications such as drug delivery and tissue engineering.[1] For these latter applications thermoresponsive polymers are needed that are biocompatible and that can be conveniently functionalized.

A polymer class which fulfils these requirements is the class of poly(2-alkyl/aryl-2-oxazoline)s (PAOx) as they are biocompatible, thermoresponsive and have tuneable properties.[15, 20, 21] Poly(2-methyl-2-oxazoline) (PMeOx) and poly(2-ethyl-2-oxazoline) (PEtOx) are interesting for biomedical applications because they show stealth behaviour similar to poly(ethylene glycol) (PEG).[15, 20-24] Furthermore, PEtOx and poly(2-propyl-2-oxazoline)s (PPropOx) show thermoresponsive properties. PEtOx has an LCST of 60 °C, poly(2-*n*-propyl-2-oxazoline) (P*n*PropOx) of 25 °C, poly(2-cyclopropyl-2-oxazoline) (P*c*PropOx) of 30 °C and poly(2-isopropyl-2-oxazoline) (P*i*PropOx) of 38 °C.[3, 5, 15, 25] Cloud points can be tuned from 9 °C to 100 °C by varying the molecular weight and composition of the polymer by incorporation of more hydrophobic or hydrophilic monomeric units, either by copolymerisation or post-polymerisation modification.[5, 11-13, 26, 27]

Functional groups, often protected, can be introduced into PAOx by making use of a functional monomer or initiator during the living cationic ring opening polymerisation (CROP, Scheme 1) of 2-oxazoline monomers or by using a functional terminating agent, yielding well-defined PAOx with control over number and type of functionalities.[15, 28-37] Methyl esters are especially interesting, because they can undergo a direct amidation with a variety of amines to easily introduce other functional groups such as alcohols, hydrazide and amines.[38-41] Moreover, the ester can be hydrolysed to the corresponding carboxylic acid

providing a versatile handle for conjugation as well as a means to introduce pH responsiveness. Although the potential of side-chain methyl ester-containing PAOx copolymers is well established, there is remarkably little known about their thermal features and thermoresponsive behaviour.[32, 42-46]

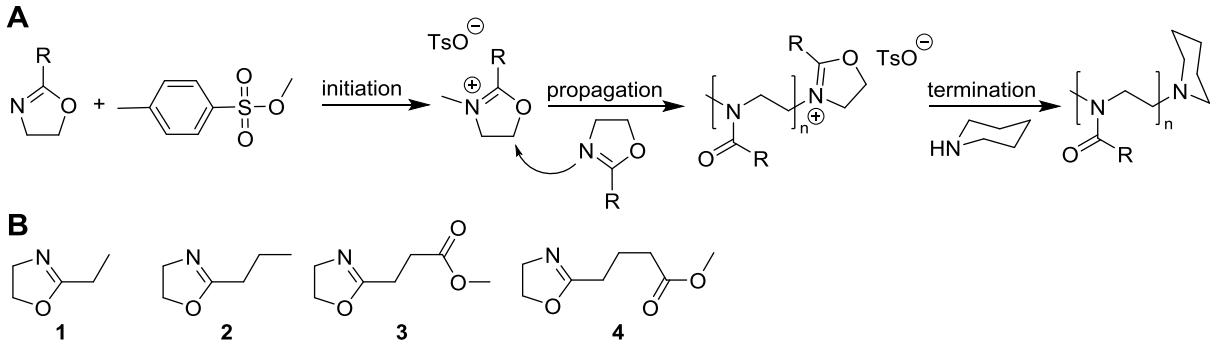

Scheme 4: A) Cationic ring-opening polymerisation of 2-oxazolines with methyl p-toluenesulfonate as initiator and piperidine as terminating agent and B) Monomer structures of EtOx (**1**), *n*PropOx (**2**), MestOx (**3**) and C3MestOx (**4**)

In this chapter we describe the synthesis and thermal properties of methyl ester-containing PAOx. Homopolymers and copolymers of 2-ethyl-2-oxazoline (EtOx, **1**) and 2-*n*-propyl-2-oxazoline (*n*PropOx, **2**) with 2-methoxycarbonylethyl-2-oxazoline (MestOx, **3**) and 2-methoxycarbonylpropyl-2-oxazoline (C3MestOx, **4**) were prepared with 10, 20, 30, 50 and 70 mol% methyl ester content. The thermal solution and bulk properties of these polymers were determined by turbidimetry, differential scanning calorimetry (DSC) and thermal gravimetric analysis (TGA), respectively.

Results and discussion

Series of homopolymers and copolymers of EtOx and nPropOx with MestOx and C3MestOx were prepared[36, 37] with varying feed ratio of 10, 20, 30 50 and 70 mol% MestOx or C3MestOx and a constant monomer to initiator ratio of [M]/[I] = 100, yielding four sets of copolymers. Also random and block copolymers of 2-methyl-2-oxazoline and C3MestOx were prepared with feed ratios of 50:50 and 25:75. All polymers were terminated with piperidine instead of the widely used methanolic sodium hydroxide to avoid saponification of the methyl ester. All polymers were characterised by ^{1}H NMR spectroscopy and SEC and were obtained with the desired composition and a narrow dispersity (Đ < 1.21, Table 6).

Table 6: Overview of synthesis and characterisation data of studied (co)polymers

Monomer 1	**Monomer 2**	**Feed ratio (M1:M2)**	**Composition[a] (M1:M2)**	**SEC[b]**		**T_{CP} (°C)[c]**		**T_g[d] (°C)**	**TGA (°C)[e]**	
				M_n (kDa)	Đ	Heating	Cooling		5 %	50%
MestOx	-	100:0	100:0	19.4	1.10	101	102	39	258	353
C3MestOx	-	100:0	100:0	24.1	1.12	26	26	-1	325	360
EtOx*	-	100:0	100:0	14.0*	1.19*	91*	91*	54*		
nPropOx	-	100:0	100:0	16.6	1.10	27	23	35	312	406
EtOx	MestOx	90:10	91:9	18.9	1.14	93	96	53	322	403
EtOx	MestOx	80:20	82:18	16.9	1.14	99	102	45	293	389
EtOx	MestOx	70:30	70:30	17.4	1.13	103	106	44	310	376
EtOx	MestOx	50:50	49:51	19.3	1.14	#	#	39	306	365
EtOx	MestOx	30:70	29:71	22.8	1.16	102	104	38	296	359
nPropOx	MestOx	90:10	90:10	21.0	1.12	25	24	30	327	393
nPropOx	MestOx	80:20	79:21	15.5	1.12	27	30	30	306	385
nPropOx	MestOx	70:30	68:32	16.3	1.13	32	36	30	303	377

nPropOx	MestOx	50:50	48:52		20.6	1.15		40	40		32		310	367
nPropOx	MestOx	30:70	27:73		29.3	1.19		55	54		35.0		309	367
EtOx	C3MestOx	90:10	90:10		21.1	1.13		89	89		43		334	399
EtOx	C3MestOx	80:20	82:18		21.8	1.14		78	79		39		313	382
EtOx	C3MestOx	70:30	70:30		21.6	1.14		71	78		27		316	377
EtOx	C3MestOx	50:50	50:50		22.7	1.14		56	56		17		322	369
EtOx	C3MestOx	30:70	30:70		24.1	1.14		42	43		-2		320	363
nPropOx	C3MestOx	90:10	90:10		19.2	1.21		24	25		28		321	399
nPropOx	C3MestOx	80:20	79:21		20.7	1.15		25	32		18		328	385
nPropOx	C3MestOx	70:30	68:32		21.0	1.15		25	301		15		332	379
nPropOx	C3MestOx	50:50	48:52		16.7	1.21		26	27		12		311	368
nPropOx	C3MestOx	30:70	28:72		18.8	1.16		25	30		5		304	361

* Literature values [26]

no cloud point temperature observed up to 110 °C

a. determined by ^{1}H NMR spectroscopy
b. determined by SEC against PMMA standards
c. determined by turbidimetry measurements
d. determined by DSC measurements
e. 5%: loss of 5 wt% after loss of solvents; for some polymers it was difficult to determine the point where all solvents were removed and for these the start of the flatter area was used for calculation of the 5% weight loss temperature. 50%: loss of 50 w% from the total mass

Cloud point temperatures (T_{CP}s) of the homo- and copolymers were determined by turbidimetry of 5 mg mL^{-1} aqueous solutions. All polymers, except EtOx$_{49}$-MestOx$_{51}$, showed reversible LCST behaviour covering a broad temperature range (24-108 °C, Table 6) depending on the polymer composition with nearly no hysteresis between heating and cooling cycles (Figure 41 and Figure S 6-Figure S 11). In some cases the T_{CP} in the cooling cycles was slightly higher than in the heating cycles; this can be possibly explained by the fact that redissolution of these polymers was a rather slow process, leading to lower concentrations in solution during cooling and thus an increase of T_{CP}. However, the precipitates were fully dissolved when the solution cooled down completely.

Interestingly, the homopolymers of MestOx (PMestOx) and C3MestOx (PC3MestOx) also showed thermo-responsive properties. PMestOx displayed a shallow transition with a T_{CP} of 101 °C similar to PEtOx with a degree of polymerization of 100 (Figure 41A), whereas PC3MestOx exhibited a sharp transition at 26 °C (Figure 41B) comparable to PnPropOx. When the polymers were heated above 100 °C during turbidimetry measurements, the T_{CP} slightly increased during every run (Figure 41, Figure 43 and Figure S 6-Figure S 12), which is ascribed to partial hydrolysis of the methyl ester groups resulting in the corresponding carboxylic acid, as was confirmed by ^{1}H NMR spectroscopy (Figure S 14 and Figure S 14). The determined average T_{CP} of all heating and cooling cycles are reported in Table 6, except for the polymers that were heated above 100 °C for which the T_{CP} in the first heating and cooling runs are listed.

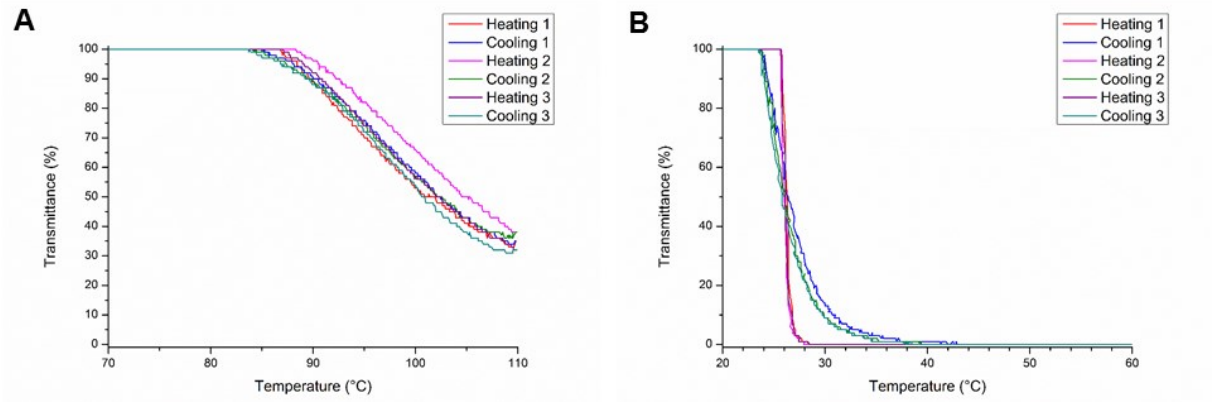

Figure 41: Turbidity measurements for A) PMestOx and B) PC3MestOx

The T_{CP}'s of the different copolymers (Table 6) are plotted as a function of the copolymer composition (Figure 42). The relationship between the T_{CP}s and EtOx content of the EtOx-C3MestOx copolymers is linear (Figure 42A), and thus with this monomer combination the T_{CP} can straightforwardly be tuned between the T_{CP}s of the corresponding homopolymers by varying the polymer composition. A linear relationship between copolymer composition and T_{CP} was previously also described for P(*i*PropOx-*n*PropOx), P(*i*PropOx-EtOx) and P(*c*PropOx-EtOx) copolymers.[13, 14, 26]

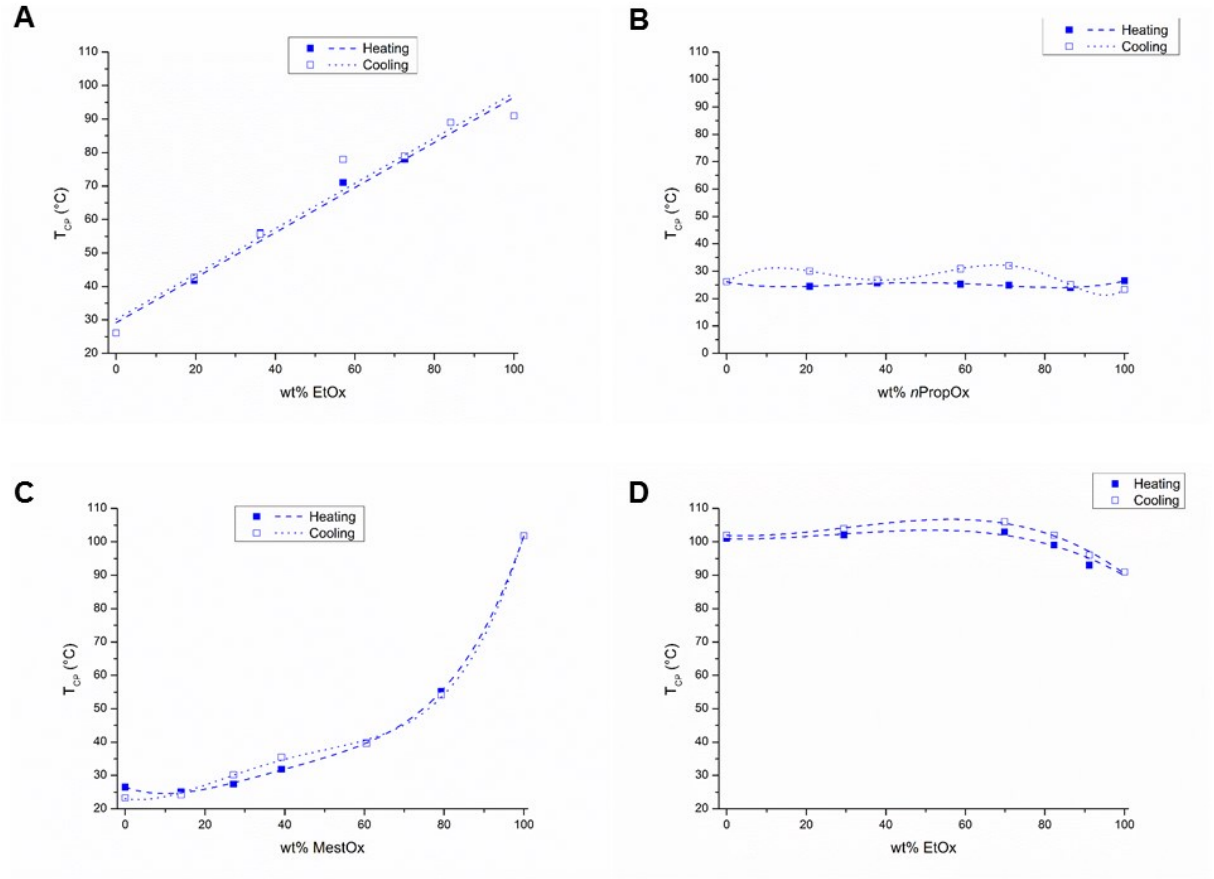

Figure 42: Cloud point temperatures (T_{CP}) as function of polymer composition of A) P(EtOx-C3MestOx), B) P(*n*PropOx-C3MestOx), C) P(*n*PropOx-MestOx and D) P(EtOx-MestOx), lines are added to guide the eye.

All T_{CP}s of *n*PropOx-C3MestOx copolymers were in between 24 and 26.5 °C (Figure 42B), revealing that varying the polymer composition hardly changed the thermo-responsive behaviour. This behaviour was expected as the hydrophobicity of both monomers and the T_{CP}'s of the homopolymers are comparable.
In the *n*PropOx-MestOx copolymer series, the T_{CP}s exponentially increased with increasing MestOx content (Figure 42C). A similar trend was also reported for EtOx-*n*PropOx copolymers.[14, 27] The hydrophobic nPropOx monomer seems to be more dominant in determining the overall polymer hydrophilicity and T_{CP} than the hydrophilic MestOx monomer.
Copolymers of EtOx and MestOx displayed T_{CP}s in between 93 °C and 103 °C at EtOx-MestOx comonomer ratios of 90-10, 80-20, 70-30 and 30-70 (Figure 42D, Table 6), whereas surprisingly the copolymer with a 50-50 comonomer ratio did not show a transition up to 110 °C. This observation indicates more efficient polymer hydration and/or decreased polymer-polymer interactions, which both may be related to near random placement of the smaller ethyl and larger methoxycarbonylethyl side chains.

Copolymers of MeOx and C3MestOx only showed thermoresponsive behaviour for the 25:75 feed ratio (Figure 43). Both 50:50 polymers did not show a transition up to 110 °C (Figure S 12). P(MeOx-C3MestOx 25-75) showed a similar transition as the EtOx and *n*PropOx copolymers described above (Figure 43A). The block copolymer, P(MeOx-b-C3MestOx 25-75), showed a different transmittance curve (Figure 43B). The transmittance goes down a bit with increasing temperature and subsequently goes back to 100%, this minimum indicates the

formation of particles and is already described in literature for PEtOx-block-(P(EtOx-stat-PropOx) polymers.[47] The increase in transmittance after the minimum is explained as fragmentation into smaller micelle like structures. Upon further heating all the present particles aggregate leading to a decrease of the transmittance.

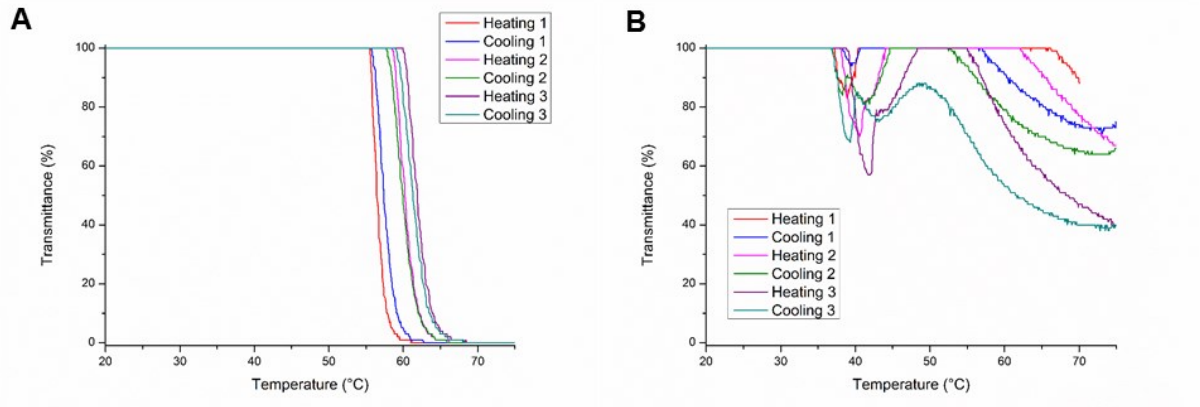

Figure 43: Turbidity measurements for A) P(MeOx-C3MestOx 25-75) and B) P(MeOx-b-C3MestOx 25-75).

The thermal bulk properties of the homo- and copolymers were investigated by differential scanning calorimetry (DSC) and thermogravimetric analysis (TGA). All polymers showed a clear glass transition (Figure 44, Figure S 15, Table 6), indicating that they are amorphous. The T_gs of the homopolymers PMestOx (T_g = 39 °C) and PnPropOx (T_g = 35 °C) are comparable, while PC3MestOx has a T_g of -1 °C and PEtOx has a T_g of 54°C. The rather low T_g of PC3MestOx indicates high chain mobility induced by the side chain.

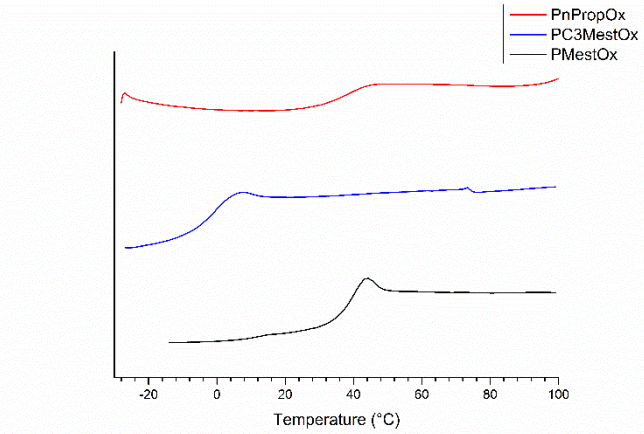

Figure 44: DSC traces of second heating run (10 K min-1) of PMestOx, PC3MestOx and P*n*PropOx homopolymers

The T_gs of the copolymers are plotted in Figure 45. In the P(EtOx-MestOx) copolymer series, the T_gs did not change much up to 40 wt% EtOx (Figure 45A) and from this point on it increased linearly towards the T_g of PEtOx. The T_g of the MestOx homopolymer is slightly higher than the T_g of P(EtOx-MestOx 30-70), indicating that the packing between the polymer chains is better, i.e. not distorted by other monomeric units, so there is more interaction between the polyamide backbones in the homopolymers. A very similar trend in T_g was observed for P(EtOx-C3MestOx) copolymers (Figure 45B), with the exception that after already 20 wt% incorporation of EtOx the glass transition temperature started to increase

linearly with increasing amount of EtOx, possibly due to the larger difference in T_g of the homopolymers.

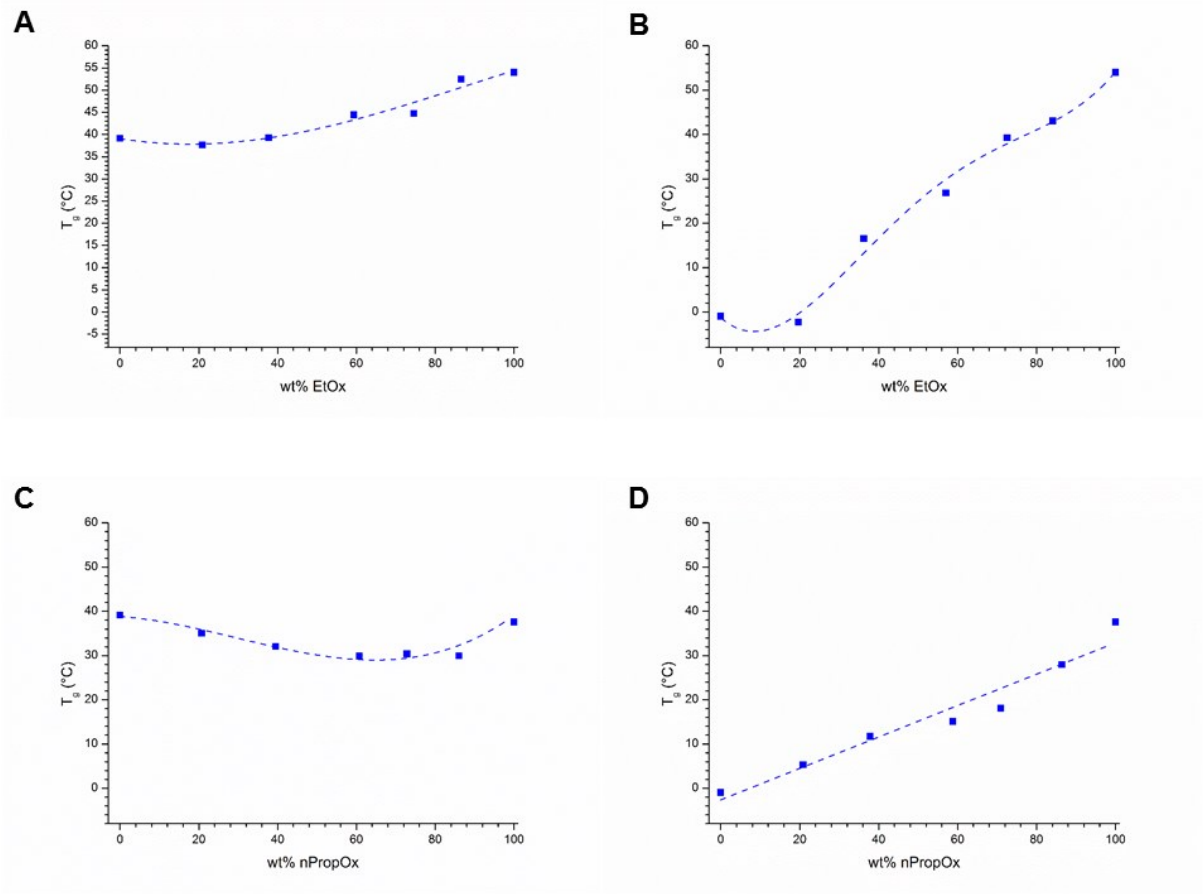

Figure 45: Glass transition temperatures as function of polymer composition of A) P(EtOx-MestOx), B) P(EtOx-C3MestOx), C) P(nPropOx-MestOx) and D) P(nPropOx-C3MestOx). Lines are added to guide the eye and empirical formulas are given to describe the correlation of Tg with the wt% of comonomer.

For the P(nPropOx-MestOx) copolymers all measured T_gs were lower than those of the homopolymers (Figure 45C) and the T_gs only vary 5 °C within the composition range. A similar trend was recently reported for copolymers of 2-cyclopropyl-2-oxazoline (cPropOx) and EtOx,[26] and this can be ascribed to suppression of interchain interactions. The T_g of nPropOx-C3MestOx copolymers increased linearly with increasing nPropOx content (Figure 45D), so with this combination of monomers the glass transition can be accurately tuned between the T_gs of the corresponding homopolymers by varying the monomer ratios.

TGA analysis revealed that the PMestOx homopolymer was thermally stable up to 250 °C (Figure 46A), while all other homo- and copolymers were stable at least up to 300 °C (Figure 46 and Figure S 16). The lower stability of PMestOx is rather surprising, especially compared to PC3MestOx and may indicate that the close proximity of the secondary amide to the ester group decreases the stability of the latter. In Table 6 the temperature for 5 % and 50% weight loss are listed, whereby the 5 wt% loss was determined after loss of solvents. However, not all polymers show a plateau after loss of solvent and for these the start of the flatter area was used for calculation of the 5% weight loss temperature. The 50% loss is reported as the 50% loss of the total weight. In general, when more (C3)MestOx was incorporated into the copolymers, the thermal stability slightly decreased, because the P(C3)MestOx

homopolymers are less stable than PEtOx or PnPropOx homopolymers, most likely due to decomposition of the methyl ester units.

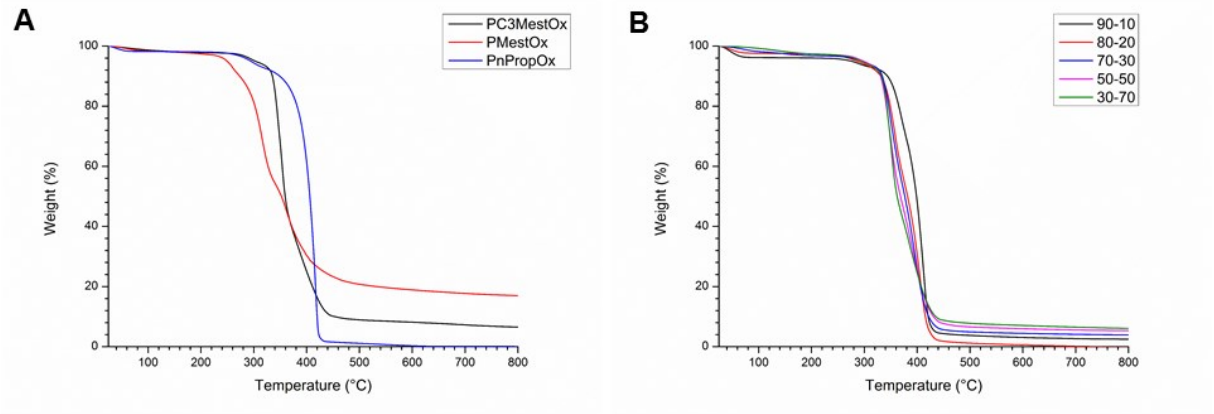

Figure 46: Thermogravimetric analysis of A) PMestOx, PC3MestOx and PnPropOx homopolymers and B) P(EtOx-C3MestOx) copolymers

Conclusions

Homo- and copolymers of MestOx and C3MestOx with EtOx and *n*PropOx were successfully synthesized. All polymers, except P(EtOx$_{49}$-MestOx$_{51}$), showed T_{CP}s that varied in between 24 °C and 108 °C depending on the composition, at a concentration of 5 mg/mL in water. Interestingly, PC3MestOx has a low T_{CP} of 26 °C making it interesting for biomedical applications. DSC measurements revealed that all polymers are amorphous with T_g's between -2 °C and 54 °C. For P(EtOx-MestOx), P(EtOx-C3MestOx) and P(*n*PropOx-C3MestOx) copolymers the glass transition temperature can be tuned in between the T_gs of the homopolymers. However, for P(*n*PropOx-MestOx) copolymers, the T_gs of all copolymers are lower than the ones of both homopolymers, indicating suppression of interchain interactions. All homo- and copolymers are thermally stable up to at least 250 °C, whereby copolymers with more (C3)MestOx were found to be less stable. Nonetheless, the stabilities will allow thermal processing, e.g. hot-melt extrusion, at temperatures well above room temperature.

Acknowledgements

Kathleen Lava is acknowledged for performing DSC and TGA measurements. Yentl Verleysen, Willem Uyttendaele and Wouter Vandeplassche are thanked for the preparation of P(MeOx-C3MestOx) copolymers.

Experimental section

Materials

2-Chloroethylamine hydrochloride, methyl p-toluenesulfonate (MeOTs) and sodium carbonate were purchased from Acros Organics. EtOx was kindly donated by Polymer Chemistry Innovations. All other reagents were purchased from Sigma Aldrich and used as received. EtOx and methyl *p*-toluenesulfonate (MeOTs) were purified by distillation over barium oxide and stored under argon. Dry solvents were obtained from a solvent purification system from J.C. Meyer, with aluminium oxide drying system and a nitrogen flow. MestOx,[36] C3MestOx[37] and *n*PropOx[48] were prepared according to literature procedures.

Instrumentation

Nuclear magnetic resonance (NMR) spectra were recorded on a Bruker DMC300 (300 MHz for ^{1}H, 75 MHz for ^{13}C).
Polymerisation reaction mixtures were prepared in a VIGOR Sci-Lab SG 1200/750 Glovebox system, with purity levels of less than 1 ppm for O_2 and H_2O.
Polymerisations were carried out in a Biotage Initiator Microwave System with Robot Sixty utilizing capped reaction vials. These vials were heated to 120 °C overnight, allowed to cool to room temperature and filled with nitrogen prior to use. All microwave polymerisations were performed with temperature control (IR sensor).
Size exclusion chromatography (SEC) was performed on an Agilent 1260 - series HPLC system equipped with a 1260 online degasser, a 1260 ISO-pump, a 1260 automatic liquid sampler, a thermostatted column compartment, a 1260 diode array detector (DAD) and a 1260 refractive index detector (RID). Analyses were performed on a PSS Gram30 column in series with a PSS Gram1000 column at 50 °C. N,N-dimethylacetamide (DMA), containing 50 mM of LiCl, was used as an eluent, at a flow rate of 0.593 ml min^{-1}. The SEC traces were analysed using the Agilent Chemstation software with the GPC add on. Number average molecular weights (M_n) and dispersity (Đ) values were calculated against poly(methyl methacrylate) PMMA standards.
Turbidity measurements were performed on an Avantium Crystal 16 platform. Solutions of the polymers were prepared in MilliQ water at 5 mg mL^{-1} and were stirred at room temperature until all polymer was dissolved. Three heating cycles were applied with a heating/cooling rate of 1 °C min^{-1}, temperature ranges of 5-45, 20-60, 20-75, 60-105 or 70-110 °C were used depending on the polymer, and with hold steps of 5 min at the extreme low temperatures, no hold time was applied when the samples were heated above 100 °C; all measurements were performed with a stirring rate of 700 rpm. The cloud points are given as the 50% transmittance point during heating. GC vials with open caps and septa were used for these measurements allowing heating until 110 °C with minor pressure build-up as noticed by slight expansion of the septum.
Differential scanning calorimetry (DSC) traces were recorded under nitrogen with a Mettler-Toledo DSC1 module. Glass transition temperatures were obtained from the second heating run with heating/cooling rates of 10 K min^{-1}. Indium was used as a standard for temperature and enthalpy calibrations.
Thermogravimetric analysis (TGA) was performed with a Mettler Toledo TGA/SDTA851e instrument under nitrogen atmosphere at a heating rate of 10 ° C min^{-1} between 25 °C and 800 °C.

Polymer Synthesis

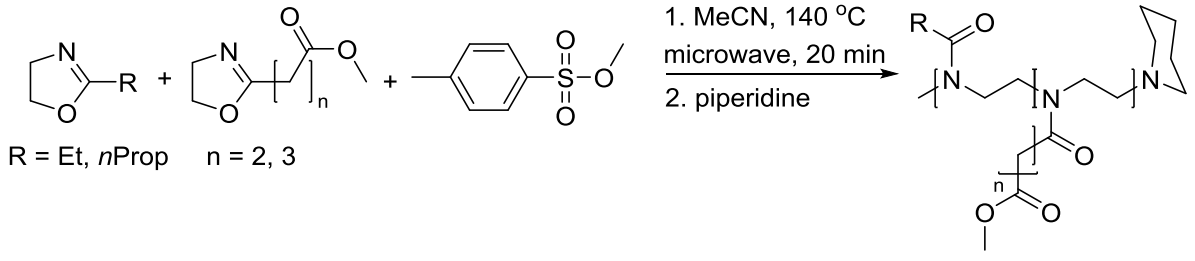

Scheme 5: Reaction conditions for the cationic ring opening copolymerisation of 2-oxazolines

Polymerisation mixtures with a total monomer concentration of 4 M in acetonitrile, an overall [M]/[I] ratio of 100 and MeOTs as initiator, were prepared in the glovebox under argon and the reactor vials were crimped air-tight inside the glovebox. Polymerisations were carried out under microwave irradiation at 140 °C for 20 minutes aiming for full conversion.[36, 37] After cooling to room temperature, the polymerisations were quenched by the addition of

piperidine. After removal of the solvents under reduced pressure, the polymers were redissolved in dichloromethane and precipitated in cold diethyl ether twice. The polymers were dried in the vacuum oven at 50 °C before further analysis.

^{1}H NMR data of the polymers synthesized

PMestOx
^{1}H NMR ($CDCl_3$, 300 MHz): δ 3.64 (br, $COOCH_3$, 297 H), 3.46 (br, NCH_2CH_2N, 396 H), 3.14 (br, CH_2NCH_2 piperidine, 4 H), 2.96 (s, NCH_3, 3 H), 2.63 (br, $COCH_2CH_2CO$, 396 H), 1.78 (s, $CH_2CH_2CH_2$ piperidine, 6 H)

PC3MestOx
^{1}H NMR ($CDCl_3$, 300 MHz): δ 3.64 (br, $COOCH_3$, 267 H), 3.46 (br, NCH_2CH_2N, 356 H), 3.14 (br, CH_2NCH_2 piperidine, 4 H), 2.96 (s, NCH_3, 3 H), 2.63 (br, $COCH_2CH_2CH_2CO$, 356 H), 1.90 (br, $COCH_2CH_2CH_2CO$, 178 H), 1.78 (s, $CH_2CH_2CH_2$ piperidine, 6 H)

PnPropOx
^{1}H NMR ($CDCl_3$, 300 MHz): δ 3.46 (br, NCH_2CH_2N, 380 H), 3.14 (b, CH_2NCH_2 piperidine, 4 H), 2.96 (s, NCH_3, 3 H), 2.27 (b, $COCH_2$, 190 H), 1.78 (s, $CH_2CH_2CH_2$ piperidine, 6 H), 1.63 (b, $COCH_2CH_2$, 190 H), 0.95 (br, CH_2CH_3, 285 H)

P(EtOx-MestOx 90-10)
^{1}H NMR ($CDCl_3$, 300 MHz): δ 3.64 (br, $COOCH_3$, 24 H), 3.46 (br, NCH_2CH_2N, 380 H), 3.14 (b, CH_2NCH_2 piperidine, 4 H), 2.96 (s, NCH_3, 3 H), 2.63 (b, $COCH_2CH_2CO$, 32 H), 2.27 (b, $COCH_2$, 174 H), 1.78 (s, $CH_2CH_2CH_2$ piperidine, 6 H), 1.12 (br, CH_2CH_3, 261 H)

P(EtOx-MestOx 80-20)
^{1}H NMR ($CDCl_3$, 300 MHz): δ 3.64 (br, $COOCH_3$, 57 H), 3.46 (br, NCH_2CH_2N, 388 H), 3.14 (b, CH_2NCH_2 piperidine, 4 H), 2.96 (s, NCH_3, 3 H), 2.63 (b, $COCH_2CH_2CO$, 76 H), 2.27 (b, $COCH_2$, 156 H), 1.78 (s, $CH_2CH_2CH_2$ piperidine, 6 H), 1.12 (br, CH_2CH_3, 234 H)

P(EtOx-MestOx 70-30)
^{1}H NMR ($CDCl_3$, 300 MHz): δ 3.64 (br, $COOCH_3$, 87 H), 3.46 (br, NCH_2CH_2N, 388 H), 3.14 (b, CH_2NCH_2 piperidine, 4 H), 2.96 (s, NCH_3, 3 H), 2.63 (b, $COCH_2CH_2CO$, 116 H), 2.27 (b, $COCH_2$, 136 H), 1.78 (s, $CH_2CH_2CH_2$ piperidine, 6 H), 1.12 (br, CH_2CH_3, 204 H)

P(EtOx-MestOx 50-50)
^{1}H NMR ($CDCl_3$, 300 MHz): δ 3.64 (br, $COOCH_3$, 147 H), 3.46 (br, NCH_2CH_2N, 384 H), 3.14 (b, CH_2NCH_2 piperidine, 4 H), 2.96 (s, NCH_3, 3 H), 2.63 (b, $COCH_2CH_2CO$, 196 H), 2.27 (b, $COCH_2$, 96 H), 1.78 (s, $CH_2CH_2CH_2$ piperidine, 6 H), 1.12 (br, CH_2CH_3, 144 H)

P(EtOx-MestOx 30-70)
^{1}H NMR ($CDCl_3$, 300 MHz): δ 3.64 (br, $COOCH_3$, 207 H), 3.46 (br, NCH_2CH_2N, 388 H), 3.14 (b, CH_2NCH_2 piperidine, 4 H), 2.96 (s, NCH_3, 3 H), 2.63 (b, $COCH_2CH_2CO$, 276 H), 2.27 (b, $COCH_2$, 56 H), 1.78 (s, $CH_2CH_2CH_2$ piperidine, 6 H), 1.12 (br, CH_2CH_3, 84 H)

P(EtOx-C3MestOx 90-10)
^{1}H NMR ($CDCl_3$, 300 MHz): δ 3.64 (br, $COOCH_3$, 30 H), 3.46 (br, NCH_2CH_2N, 392 H), 3.14 (b, CH_2NCH_2 piperidine, 4 H), 2.96 (s, NCH_3, 3 H), 2.63 (b, $COCH_2CH_2CH_2CO$, 40 H), 2.27 (b, $COCH_2$, 174 H), 1.90 (br, $COCH_2CH_2CH_2CO$, 20 H), 1.78 (s, $CH_2CH_2CH_2$ piperidine, 6 H), 1.12 (br, CH_2CH_3, 261 H)

P(EtOx-C3MestOx 80-20)
^{1}H NMR ($CDCl_3$, 300 MHz): δ 3.64 (br, $COOCH_3$, 57 H), 3.46 (br, NCH_2CH_2N, 392 H), 3.14 (b, CH_2NCH_2 piperidine, 4 H), 2.96 (s, NCH_3, 3 H), 2.63 (b, $COCH_2CH_2CH_2CO$, 76 H), 2.27 (b, $COCH_2$, 158 H), 1.90 (br, $COCH_2CH_2CH_2CO$, 38 H), 1.78 (s, $CH_2CH_2CH_2$ piperidine, 6 H), 1.12 (br, CH_2CH_3, 237 H)

P(EtOx-C3MestOx 70-30)
^{1}H NMR ($CDCl_3$, 300 MHz): δ 3.64 (br, $COOCH_3$, 57 H), 3.46 (br, NCH_2CH_2N, 388 H), 3.14 (b, CH_2NCH_2 piperidine, 4 H), 2.96 (s, NCH_3, 3 H), 2.63 (b, $COCH_2CH_2CH_2CO$, 116 H), 2.27 (b, $COCH_2$, 136 H), 1.90 (br, $COCH_2CH_2CH_2CO$, 58 H), 1.78 (s, $CH_2CH_2CH_2$ piperidine, 6 H), 1.12 (br, CH_2CH_3, 204 H)

P(EtOx-C3MestOx 50-50)
^{1}H NMR ($CDCl_3$, 300 MHz): δ 3.64 (br, $COOCH_3$, 147 H), 3.46 (br, NCH_2CH_2N, 388 H), 3.14 (b, CH_2NCH_2 piperidine, 4 H), 2.96 (s, NCH_3, 3 H), 2.63 (b, $COCH_2CH_2CH_2CO$, 196 H), 2.27 (b, $COCH_2$, 96 H), 1.90 (br, $COCH_2CH_2CH_2CO$, 98 H), 1.78 (s, $CH_2CH_2CH_2$ piperidine, 6 H), 1.12 (br, CH_2CH_3, 144 H)

P(EtOx-C3MestOx 30-70)
^{1}H NMR ($CDCl_3$, 300 MHz): δ 3.64 (br, $COOCH_3$, 204 H), 3.46 (br, NCH_2CH_2N, 384 H), 3.14 (b, CH_2NCH_2 piperidine, 4 H), 2.96 (s, NCH_3, 3 H), 2.63 (b, $COCH_2CH_2CH_2CO$, 204 H), 2.27 (b, $COCH_2$, 56 H), 1.90 (br, $COCH_2CH_2CH_2CO$, 136 H), 1.78 (s, $CH_2CH_2CH_2$ piperidine, 6 H), 1.12 (br, CH_2CH_3, 84 H)

P(nPropOx-MestOx 90-10)
^{1}H NMR ($CDCl_3$, 300 MHz): δ 3.64 (br, $COOCH_3$, 30 H), 3.46 (br, NCH_2CH_2N, 376 H), 3.14 (b, CH_2NCH_2 piperidine, 4 H), 2.96 (s, NCH_3, 3 H), 2.63 (b, $COCH_2CH_2CO$, 40 H), 2.27 (b, $COCH_2$, 168 H), 1.78 (s, $CH_2CH_2CH_2$ piperidine, 6 H), 1.63 (b, $COCH_2CH_2$, 168 H), 0.95 (br, CH_2CH_3, 252 H)

P(nPropOx-MestOx 80-20)
^{1}H NMR ($CDCl_3$, 300 MHz): δ 3.64 (br, $COOCH_3$, 57 H), 3.46 (br, NCH_2CH_2N, 396 H), 3.14 (b, CH_2NCH_2 piperidine, 4 H), 2.96 (s, NCH_3, 3 H), 2.63 (b, $COCH_2CH_2CO$, 76 H), 2.27 (b, $COCH_2$, 160 H), 1.78 (s, $CH_2CH_2CH_2$ piperidine, 6 H), 1.63 (b, $COCH_2CH_2$, 160 H), 0.95 (br, CH_2CH_3, 240 H)

P(nPropOx-MestOx 70-30)
^{1}H NMR ($CDCl_3$, 300 MHz): δ 3.64 (br, $COOCH_3$, 87 H), 3.46 (br, NCH_2CH_2N, 368 H), 3.14 (b, CH_2NCH_2 piperidine, 4 H), 2.96 (s, NCH_3, 3 H), 2.63 (b, $COCH_2CH_2CO$, 116 H), 2.27 (b, $COCH_2$, 126 H), 1.78 (s, $CH_2CH_2CH_2$ piperidine, 6 H), 1.63 (b, $COCH_2CH_2$, 126 H), 0.95 (br, CH_2CH_3, 189 H)

P(nPropOx-MestOx 50-50)
^{1}H NMR ($CDCl_3$, 300 MHz): δ 3.64 (br, $COOCH_3$, 150 H), 3.46 (br, NCH_2CH_2N, 380 H), 3.14 (b, CH_2NCH_2 piperidine, 4 H), 2.96 (s, NCH_3, 3 H), 2.63 (b, $COCH_2CH_2CO$, 200 H), 2.27 (b, $COCH_2$, 90 H), 1.78 (s, $CH_2CH_2CH_2$ piperidine, 6 H), 1.63 (b, $COCH_2CH_2$, 90 H), 0.95 (br, CH_2CH_3, 135 H)

P(nPropOx-MestOx 30-70)
^{1}H NMR ($CDCl_3$, 300 MHz): δ 3.64 (br, $COOCH_3$, 231 H), 3.46 (br, NCH_2CH_2N, 420 H), 3.14 (b, CH_2NCH_2 piperidine, 4 H), 2.96 (s, NCH_3, 3 H), 2.63 (b, $COCH_2CH_2CO$, 308 H), 2.27 (b, $COCH_2$, 56 H), 1.78 (s, $CH_2CH_2CH_2$ piperidine, 6 H), 1.63 (b, $COCH_2CH_2$, 56 H), 0.95 (br, CH_2CH_3, 118 H)

P(nPropOx-C3MestOx 90-10)
^{1}H NMR ($CDCl_3$, 300 MHz): δ 3.64 (br, $COOCH_3$, 30 H), 3.46 (br, NCH_2CH_2N, 416 H), 3.14 (b, CH_2NCH_2 piperidine, 4 H), 2.96 (s, NCH_3, 3 H), 2.63 (b, $COCH_2CH_2CH_2CO$, 40 H), 2.27 (b, $COCH_2$, 188 H), 1.90 (br, $COCH_2CH_2CH_2CO$, 20 H), 1.78 (s, $CH_2CH_2CH_2$ piperidine, 6 H), 1.63 (b, $COCH_2CH_2$, 188 H), 0.95 (br, CH_2CH_3, 282 H)

P(nPropOx-C3MestOx 80-20)
^{1}H NMR ($CDCl_3$, 300 MHz): δ 3.64 (br, $COOCH_3$, 57 H), 3.46 (br, NCH_2CH_2N, 368 H), 3.14 (b, CH_2NCH_2 piperidine, 4 H), 2.96 (s, NCH_3, 3 H), 2.63 (b, $COCH_2CH_2CH_2CO$, 76 H), 2.27 (b, $COCH_2$, 146 H), 1.90 (br, $COCH_2CH_2CH_2CO$, 38 H), 1.78 (s, $CH_2CH_2CH_2$ piperidine, 6 H), 1.63 (b, $COCH_2CH_2$, 146 H), 0.95 (br, CH_2CH_3, 292 H)

P(nPropOx-C3MestOx 70-30)
^{1}H NMR ($CDCl_3$, 300 MHz): δ 3.64 (br, $COOCH_3$, 87 H), 3.46 (br, NCH_2CH_2N, 372 H), 3.14 (b, CH_2NCH_2 piperidine, 4 H), 2.96 (s, NCH_3, 3 H), 2.63 (b, $COCH_2CH_2CH_2CO$, 116 H), 2.27 (b, $COCH_2$, 168 H), 1.90 (br, $COCH_2CH_2CH_2CO$, 58 H), 1.78 (s, $CH_2CH_2CH_2$ piperidine, 6 H), 1.63 (b, $COCH_2CH_2$, 168 H), 0.95 (br, CH_2CH_3, 192 H)

P(nPropOx-C3MestOx 50-50)
^{1}H NMR ($CDCl_3$, 300 MHz): δ 3.64 (br, $COOCH_3$, 147 H), 3.46 (br, NCH_2CH_2N, 376 H), 3.14 (b, CH_2NCH_2 piperidine, 4 H), 2.96 (s, NCH_3, 3 H), 2.63 (b, $COCH_2CH_2CH_2CO$, 196 H), 2.27 (b, $COCH_2$, 90 H), 1.90 (br, $COCH_2CH_2CH_2CO$, 98 H), 1.78 (s, $CH_2CH_2CH_2$ piperidine, 6 H), 1.63 (b, $COCH_2CH_2$, 90 H), 0.95 (br, CH_2CH_3, 175 H)

P(nPropOx-C3MestOx 30-70)
^{1}H NMR ($CDCl_3$, 300 MHz): δ 3.64 (br, $COOCH_3$, 204 H), 3.46 (br, NCH_2CH_2N, 380 H), 3.14 (b, CH_2NCH_2 piperidine, 4 H), 2.96 (s, NCH_3, 3 H), 2.63 (b, $COCH_2CH_2CH_2CO$, 272 H), 2.27 (b, $COCH_2$, 54 H), 1.90 (br, $COCH_2CH_2CH_2CO$, 136 H), 1.78 (s, $CH_2CH_2CH_2$ piperidine, 6 H), 1.63 (b, $COCH_2CH_2$, 54 H), 0.95 (br, CH_2CH_3, 81 H)

P(MeOx-C3MestOx 25-75)
^{1}H NMR ($CDCl_3$, 300 MHz): δ 3.64 (br, $COOCH_3$, 222 H), 3.46 (br, NCH_2CH_2N, 400 H), 3.14 (b, CH_2NCH_2 piperidine, 4 H), 2.96 (s, NCH_3, 3 H), 2.63 (b, $COCH_2CH_2CH_2CO$, 304 H), 2.14 (b, $COCH_3$, 78 H), 1.90 (br, $COCH_2CH_2CH_2CO$, 148 H), 1.78 (s, $CH_2CH_2CH_2$ piperidine, 6 H)

P(MeOx-C3MestOx 25-b-75)
^{1}H NMR ($CDCl_3$, 300 MHz): δ 3.64 (br, $COOCH_3$, 234 H), 3.46 (br, NCH_2CH_2N, 412 H), 3.14 (b, CH_2NCH_2 piperidine, 4 H), 2.96 (s, NCH_3, 3 H), 2.63 (b, $COCH_2CH_2CH_2CO$, 312 H), 2.14 (b, $COCH_3$, 75 H), 1.90 (br, $COCH_2CH_2CH_2CO$, 156 H), 1.78 (s, $CH_2CH_2CH_2$ piperidine, 6 H)

P(MeOx-C3MestOx 50-50)
^{1}H NMR ($CDCl_3$, 300 MHz): δ 3.64 (br, $COOCH_3$, 153 H), 3.46 (br, NCH_2CH_2N, 392 H), 3.14 (b, CH_2NCH_2 piperidine, 4 H), 2.96 (s, NCH_3, 3 H), 2.63 (b, $COCH_2CH_2CH_2CO$, 200 H), 2.14 (b, $COCH_3$, 144 H), 1.90 (br, $COCH_2CH_2CH_2CO$, 100 H), 1.78 (s, $CH_2CH_2CH_2$ piperidine, 6 H)

P(MeOx-C3MestOx 25-b-75)
^{1}H NMR ($CDCl_3$, 300 MHz): δ 3.64 (br, $COOCH_3$, 138 H), 3.46 (br, NCH_2CH_2N, 388 H), 3.14 (b, CH_2NCH_2 piperidine, 4 H), 2.96 (s, NCH_3, 3 H), 2.63 (b, $COCH_2CH_2CH_2CO$, 184 H), 2.14 (b, $COCH_3$, 153 H), 1.90 (br, $COCH_2CH_2CH_2CO$, 92 H), 1.78 (s, $CH_2CH_2CH_2$ piperidine, 6 H)

Supplementary information

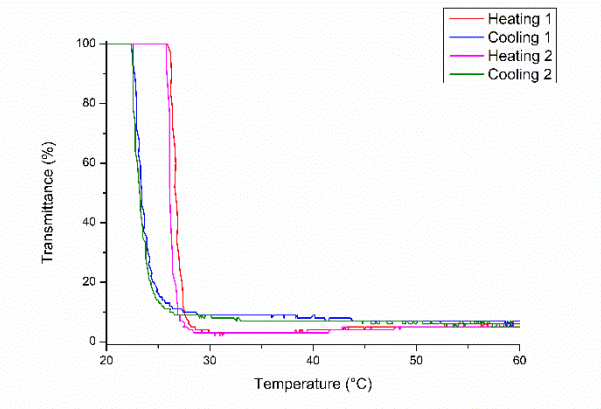

Figure S 6: Turbidity curves during heating and cooling of P(nPropOx) aqueous solutions (5 mg/mL) with a heating/cooling rate of 1 °C min^{-1}.

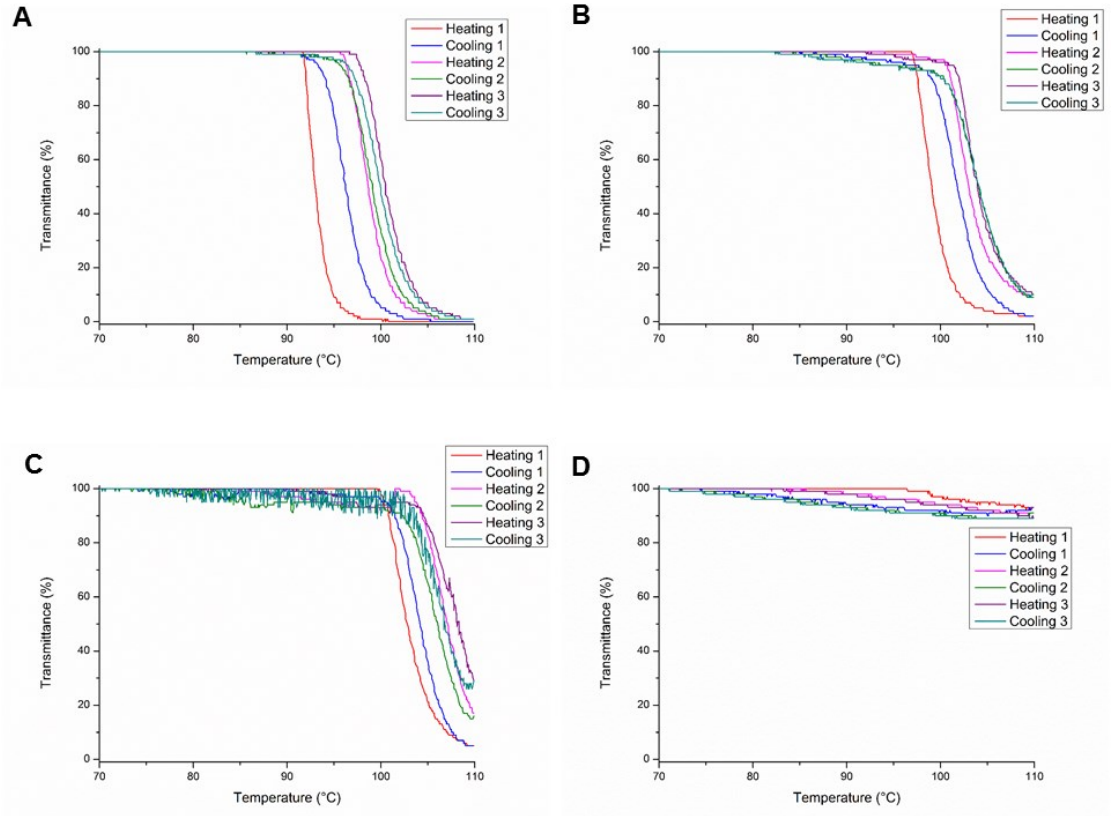

Figure S 7: Turbidity curves during heating and cooling of aqueous solutions (5 mg/mL) with a heating/cooling rate of 1 °C min^{-1} of A) P(EtOx-MestOx 90-10), B) P(EtOx-MestOx 80-20), C) P(EtOx-MestOx 70-30) and D) P(EtOx-MestOx 50-50)

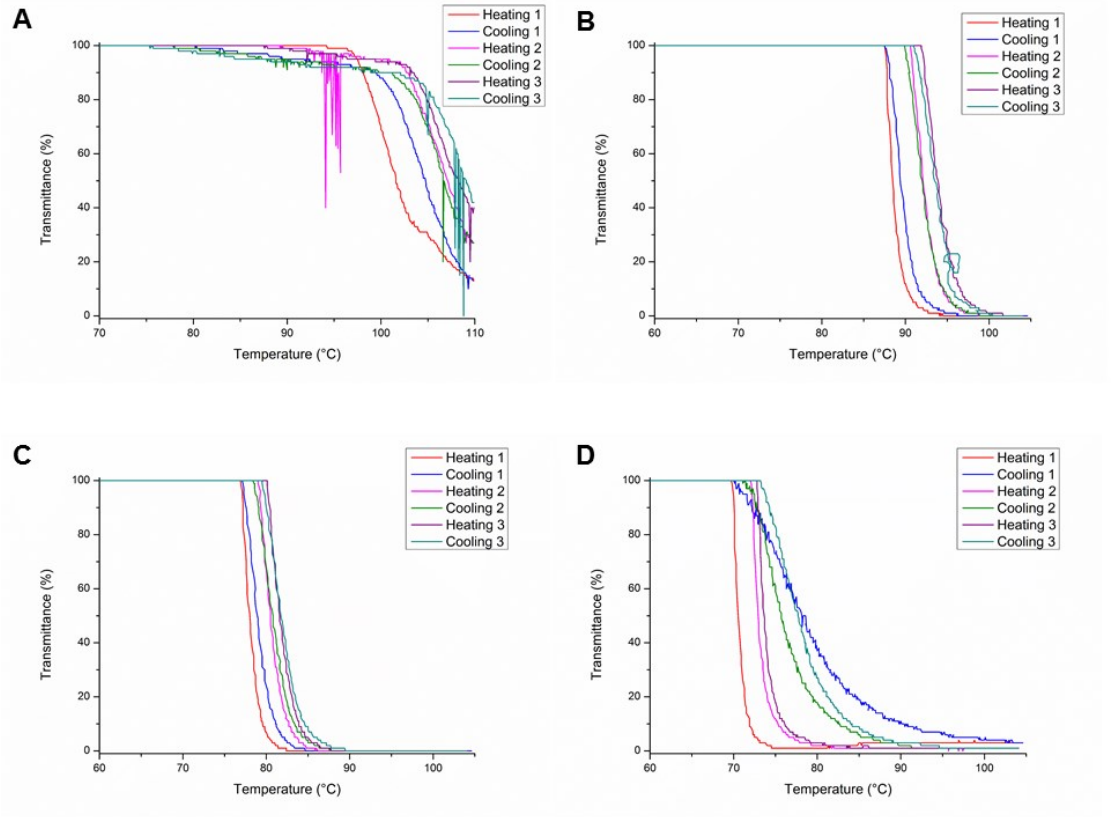

Figure S 8: Turbidity curves during heating and cooling of aqueous solutions (5 mg/mL) with a heating/cooling rate of 1 °C min^{-1} of A) P(EtOx-MestOx 30-70), B) P(EtOx-C3MestOx 90-10), C) P(EtOx-C3MestOx 80-20) and D) P(EtOx-C3MestOx 70-30)

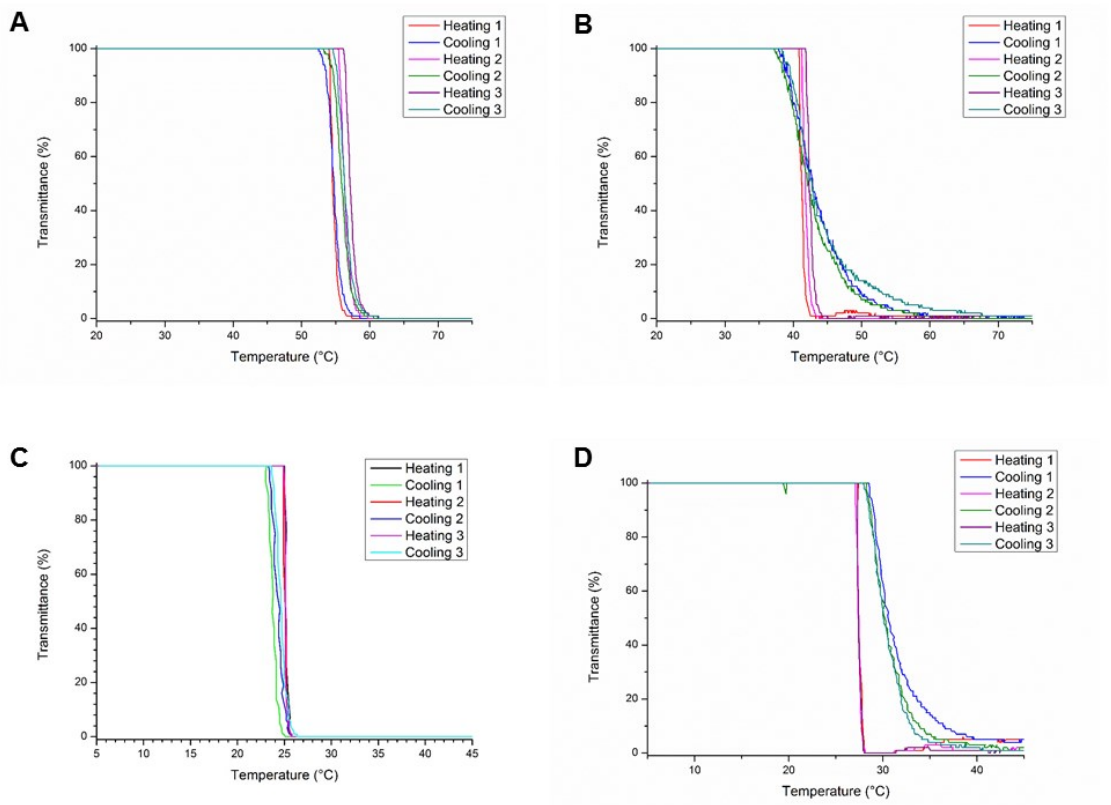

Figure S 9: Turbidity curves during heating and cooling of aqueous solutions (5 mg/mL) with a heating/cooling rate of 1 °C min^{-1} of E) P(EtOx-C3MestOx 50-50), B) P(EtOx-C3MestOx 30-70), C) P(*n*PropOx-MestOx 90-10) and D) P(*n*PropOx-MestOx 80-20).

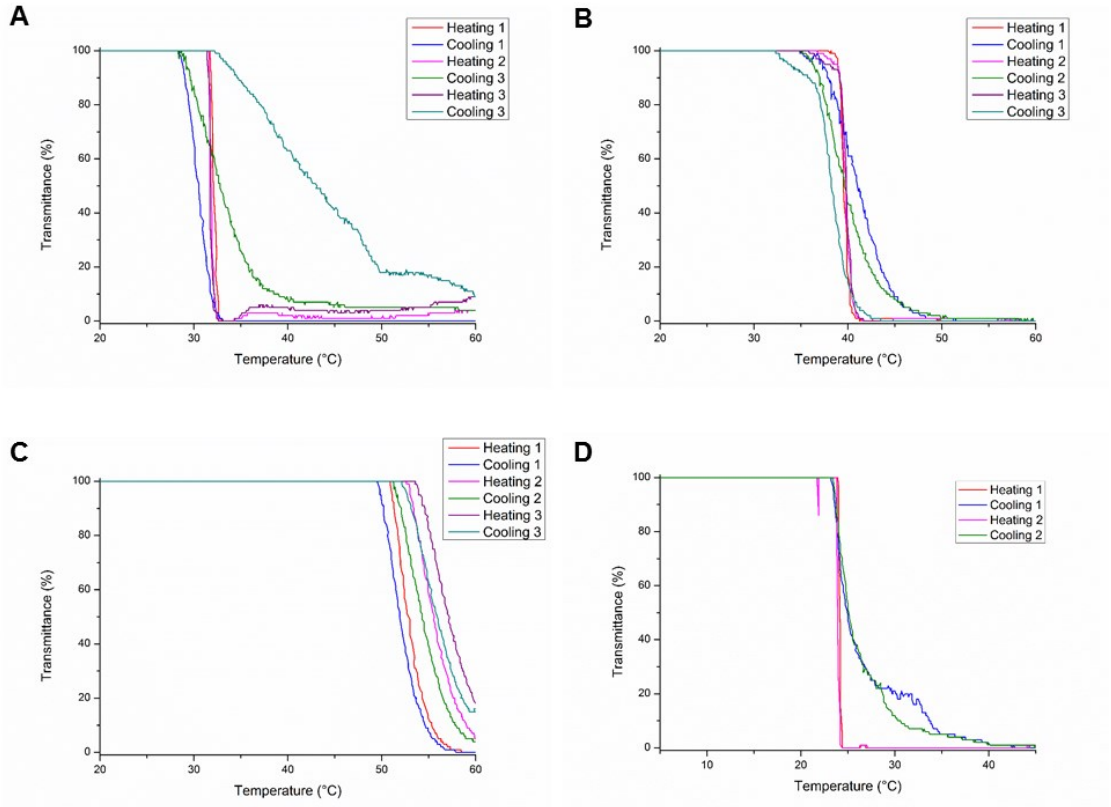

Figure S 10: Turbidity curves during heating and cooling of aqueous solutions (5 mg/mL) with a heating/cooling rate of 1 °C min^{-1} of A) P(*n*PropOx-MestOx 70-30), B) P(*n*PropOx-MestOx 50-50), C) P(*n*PropOx-MestOx 30-70) and D) P(*n*PropOx-C3MestOx 90-10)

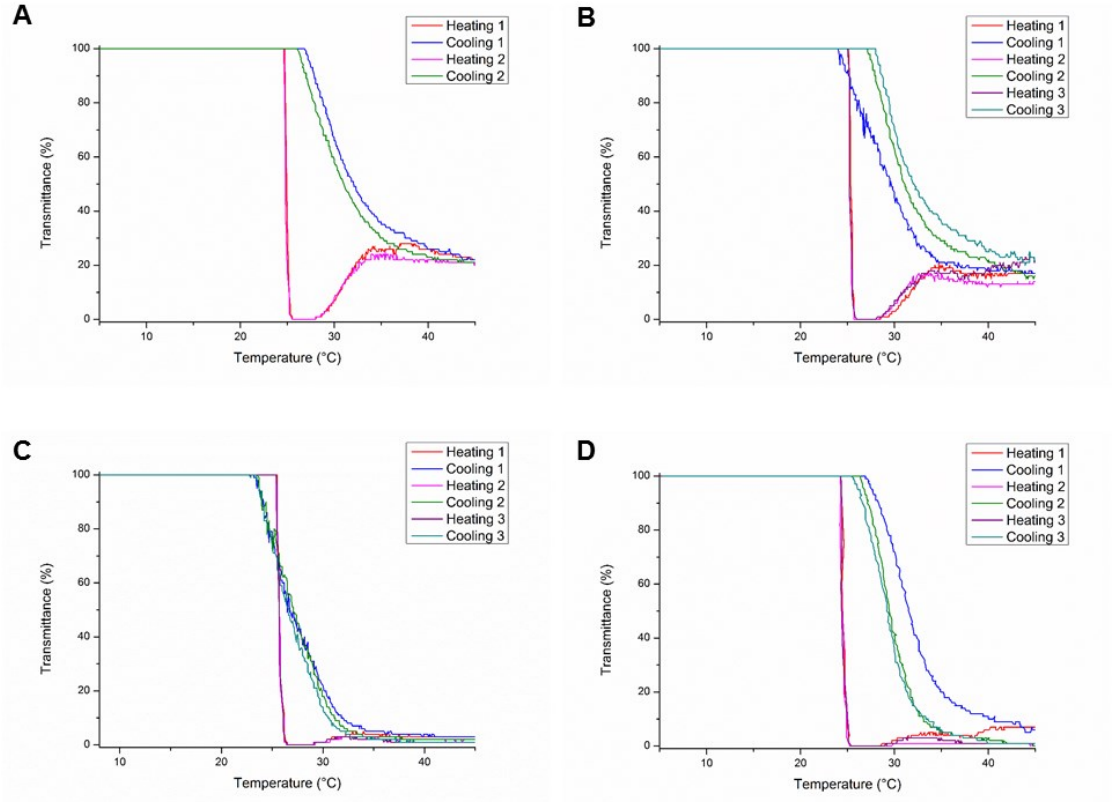

Figure S 11: Turbidity curves during heating and cooling of aqueous solutions (5 mg/mL) with a heating/cooling rate of 1 °C min^{-1} of A) P(*n*PropOx-C3MestOx 80-20), B) P(*n*PropOx-C3MestOx 70-30), C) P(*n*PropOx-C3MestOx 50-50) and D) P(*n*PropOx-C3MestOx 30-70).

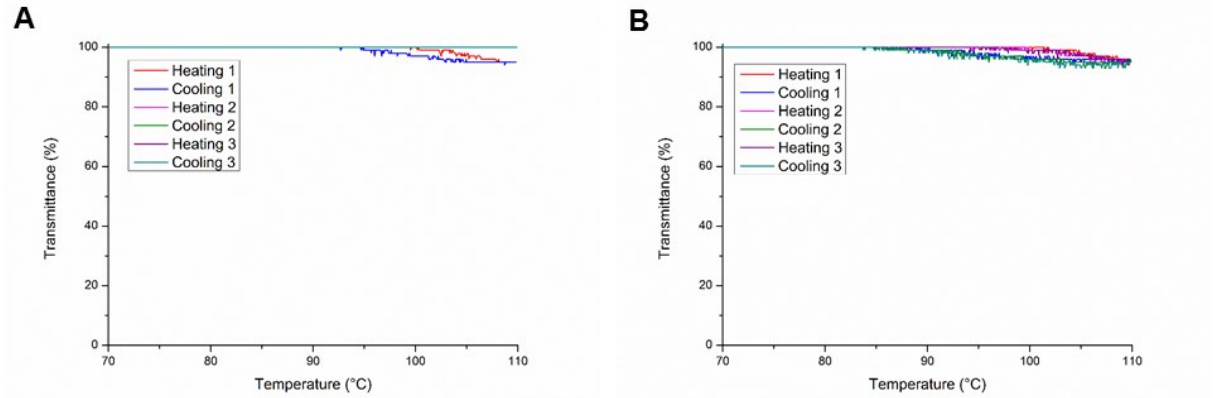

Figure S 12: Turbidity curves during heating and cooling of aqueous solutions (5 mg/mL) with a heating/cooling rate of 1 °C min^{-1} of A) P(MeOx-C3MestOx 49-51) and B) P(MeOx-b-C3MestOx 53-47)

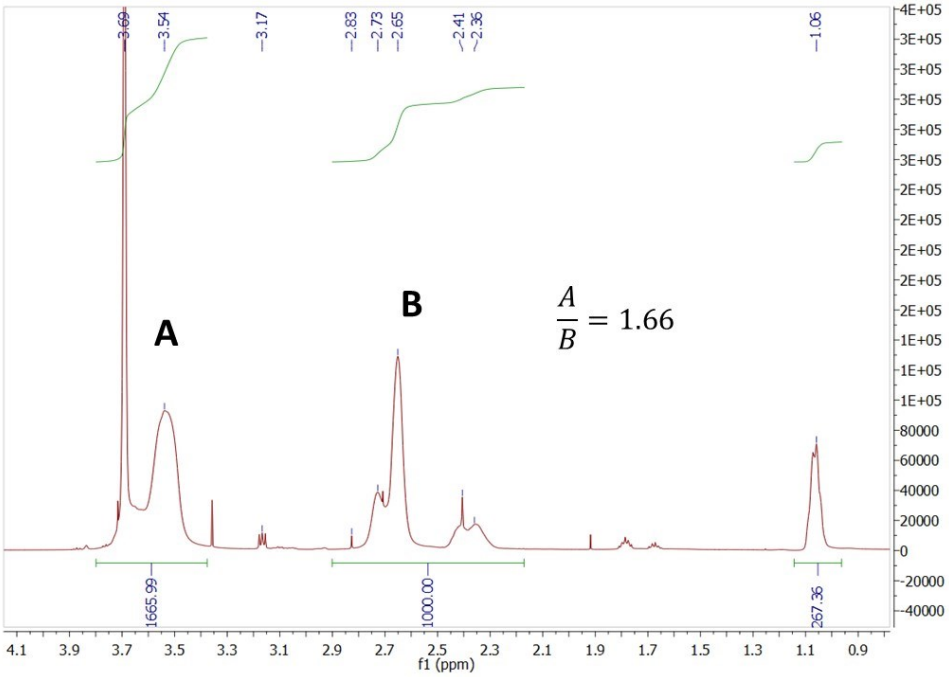

Figure S 13: ^{1}H NMR spectrum of P(EtOx-MestOx 30-70) before T_{CP} measurements in $CDCl_3$

The decrease of the methyl esters is determined by the integration of all side CH_2 protons of the sidechains (peaks of CH_2 next to methyl ester and carboxylic acid are overlapping, δ 2.17 - 2.90 ppm) of which the value is compared to the overlapping peaks of the backbone and the methyl ester (δ 3.37 - 3.80 ppm).

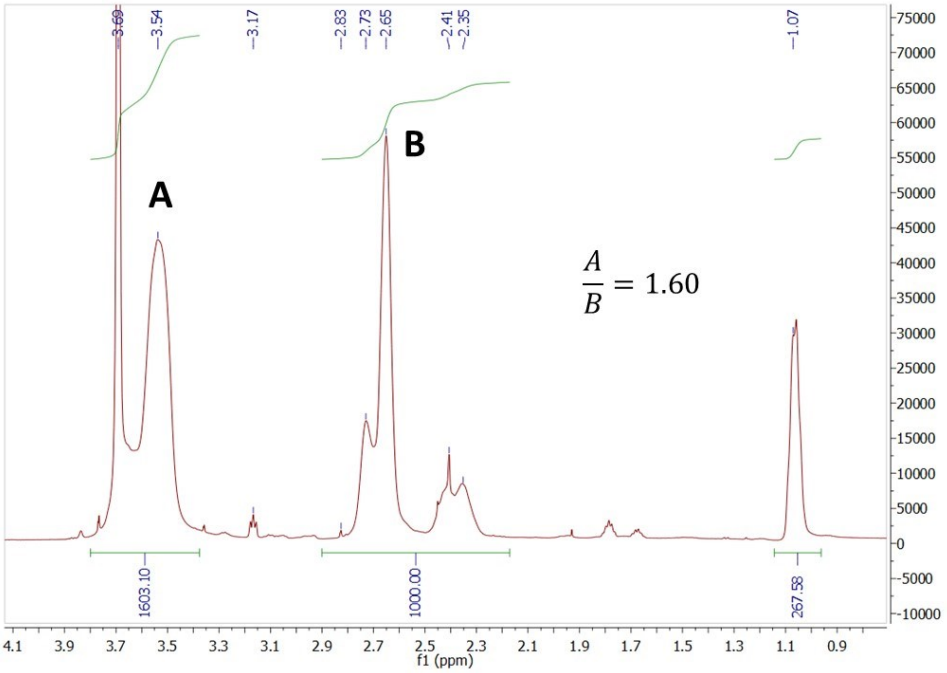

Figure S 14: ^{1}H NMR spectrum of P(EtOx-MestOx 30-70) after T_{CP} measurements

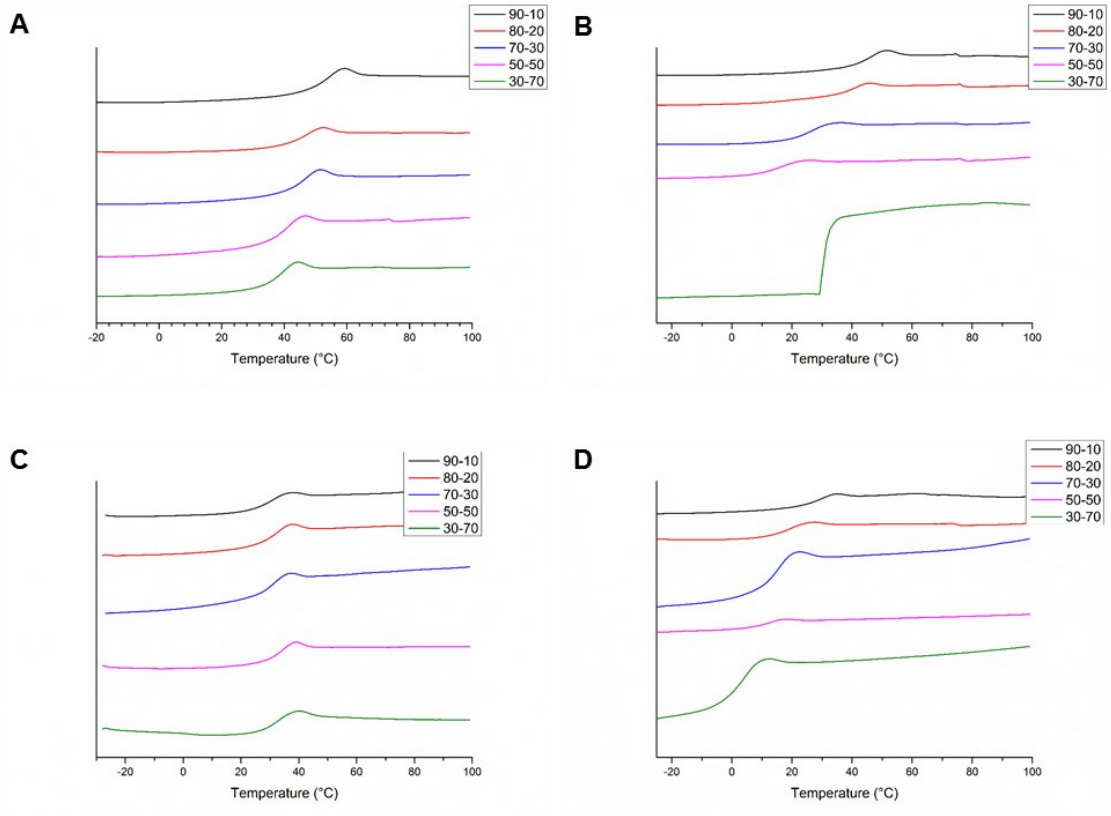

Figure S 15: DSC traces of second heating run (10 K min^{-1}) of A) P(EtOx-MestOx), B) P(EtOx-C3MestOx), C) P(nPropOx-MestOx) and D) P(nPropOx-C3MestOx)

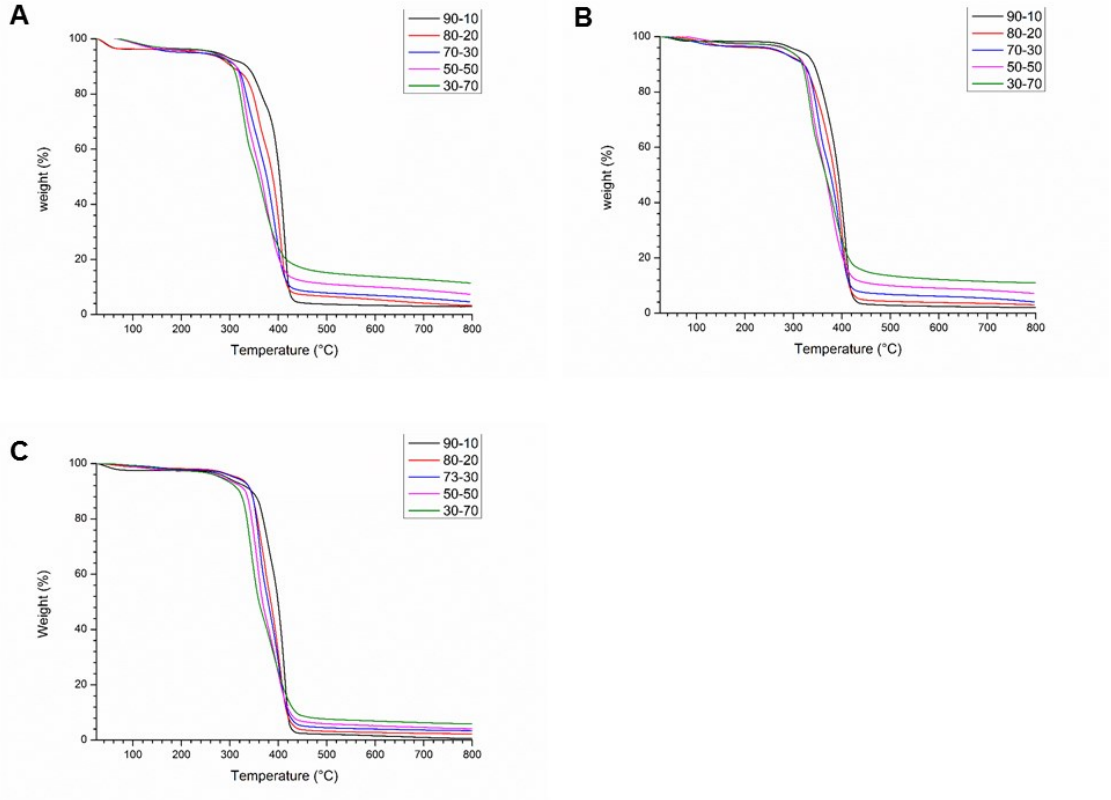

Figure S 16: Thermogravimetric analysis under nitrogen atmosphere at a heating rate of 10 ° C min-1 of A) P(EtOx-MestOx) copolymers, B) P(nPropOx-MestOx) copolymers and C) P(nPropOx-C3MestOx) copolymers

References

1. Ward, M. A.; Georgiou, T. K. *Polymers* **2011,** 3, (3), 1215-1242.
2. Vancoillie, G.; Frank, D.; Hoogenboom, R. *Prog. Polym. Sci.* **2014,** 39, (6), 1074-1095.
3. Roy, D.; Brooks, W. L. A.; Sumerlin, B. S. *Chem. Soc. Rev.* **2013,** 42, (17), 7214-7243.
4. Schild, H. G. *Prog. Polym. Sci.* **1992,** 17, (2), 163-249.
5. Weber, C.; Hoogenboom, R.; Schubert, U. S. *Prog. Polym. Sci.* **2012,** 37, (5), 686-714.
6. Lutz, J.-F. *Adv. Mater.* **2011,** 23, (19), 2237-2243.
7. Kouwer, P. H. J.; Koepf, M.; Le Sage, V. A. A.; Jaspers, M.; van Buul, A. M.; Eksteen-Akeroyd, Z. H.; Woltinge, T.; Schwartz, E.; Kitto, H. J.; Hoogenboom, R.; Picken, S. J.; Nolte, R. J. M.; Mendes, E.; Rowan, A. E. *Nature* **2013,** 493, (7434), 651-655.
8. Koepf, M.; Kitto, H. J.; Schwartz, E.; Kouwer, P. H. J.; Nolte, R. J. M.; Rowan, A. E. *Eur. Polym. J.* **2013,** 49, (6), 1510-1522.
9. Hu, G.; Li, W.; Hu, Y.; Xu, A.; Yan, J.; Liu, L.; Zhang, X.; Liu, K.; Zhang, A. *Macromolecules* **2013,** 46, (3), 1124-1132.
10. Bloksma, M. M.; Paulus, R. M.; van Kuringen, H. P. C.; van der Woerdt, F.; Lambermont-Thijs, H. M. L.; Schubert, U. S.; Hoogenboom, R. *Macromol. Rapid Commun.* **2012,** 33, (1), 92-96.
11. Huber, S.; Jordan, R. *Colloid. Polym. Sci.* **2008,** 286, (4), 395-402.
12. Diehl, C.; Schlaad, H. *Macromol. Biosci.* **2009,** 9, (2), 157-161.
13. Park, J.-S.; Kataoka, K. *Macromolecules* **2006,** 39, (19), 6622-6630.
14. Park, J.-S.; Kataoka, K. *Macromolecules* **2007,** 40, (10), 3599-3609.
15. Hoogenboom, R. *Angew. Chem. Int. Ed.* **2009,** 48, 7978-7994.
16. Zhang, N.; Luxenhofer, R.; Jordan, R. *Macromol. Chem. Phys.* **2012,** 213, (18), 1963-1969.
17. Luxenhofer, R.; Huber, S.; Hytry, J.; Tong, J.; Kabanov, A. V.; Jordan, R. *J. Polym. Sci., Part A: Polym. Chem.* **2013,** 51, (3), 732-738.
18. Sambe, L.; de La Rosa, V. R.; Belal, K.; Stoffelbach, F.; Lyskawa, J.; Delattre, F.; Bria, M.; Cooke, G.; Hoogenboom, R.; Woisel, P. *Angew. Chem. Int. Ed.* **2014,** 53, (20), 5044-5048.
19. Kanazawa, H. *Anal. Bioanal. Chem.* **2004,** 378, (1), 46-48.
20. Luxenhofer, R.; Han, Y.; Schulz, A.; Tong, J.; He, Z.; Kabanov, A. V.; Jordan, R. *Macromol. Rapid Commun.* **2012,** 33, (19), 1613-1631.
21. Sedlacek, O.; Monnery, B. D.; Filippov, S. K.; Hoogenboom, R.; Hruby, M. *Macromol. Rapid Commun.* **2012,** 33, (19), 1648-1662.
22. Zalipsky, S.; Hansen, C. B.; Oaks, J. M.; Allen, T. M. *J Pharm Sci* **1996,** 85, 133-137.
23. Mero, A.; Pasut, G.; Via, L. D.; Fijten, M. W. M.; Schubert, U. S.; Hoogenboom, R.; Veronese, F. M. *J. Controlled Release* **2008,** 125, 87-95.
24. Luxenhofer, R.; Sahay, G.; Schulz, A.; Alakhova, D.; Bronich, T. K.; Jordan, R.; Kabanov, A. V. *J. Controlled Release* **2011,** 153, (1), 73-82.
25. Bloksma, M. M.; Weber, C.; Perevyazko, I. Y.; Kuse, A.; Baumgärtel, A.; Vollrath, A.; Hoogenboom, R.; Schubert, U. S. *Macromolecules* **2011,** 44, (11), 4057-4064.
26. Glassner, M.; Lava, K.; de la Rosa, V. R.; Hoogenboom, R. *J. Polym. Sci., Part A: Polym. Chem.* **2014,** 52, (21), 3118-3122.
27. Hoogenboom, R.; Thijs, H. M. L.; Jochems, M. J. H. C.; van Lankvelt, B. M.; Fijten, M. W. M.; Schubert, U. S. *Chem. Commun.* **2008**, (44), 5758-5760.
28. Guillerm, B.; Monge, S.; Lapinte, V.; Robin, J. J. *Macromol. Rapid Commun.* **2012,** 33, 1600-1612.

29. Volet, G.; Lav, T. X.; Babinot, J.; Amiel, C. *Macromol. Chem. Phys.* **2011,** 212, 118-124.
30. Rossegger, E.; Schenk, V.; Wiesbrock, F. *Polymers* **2013,** 5, (3), 956-1011.
31. Fijten, M. W. M.; Haensch, C.; van Lankvelt, B. M.; Hoogenboom, R.; Schubert, U. S. *Macromol. Chem. Phys.* **2008,** 209, 1887-1895.
32. Levy, A.; Litt, M. *J. Polym. Sci., Part A: Polym. Chem.* **1968,** 6, 1883-1894.
33. Taubmann, C.; Luxenhofer, R.; Cesana, S.; Jordan, R. *Macromol. Biosci.* **2005,** 5, 603-612.
34. Gress, A.; Volkel, A.; Schlaad, H. *Macromolecules* **2007,** 40, 7928-7933.
35. Kelly, A. M.; Hecke, A.; Wirnsberger, B.; Wiesbrock, F. *Macromol. Rapid Commun.* **2011,** 32, 1815-1819.
36. Bouten, P. J. M.; Hertsen, D.; Vergaelen, M.; Monnery, B. D.; Boerman, M. A.; Goossens, H.; Catak, S.; van Hest, J. C. M.; Van Speybroeck, V.; Hoogenboom, R. *Polym. Chem.* **2015,** 6, (4), 514-518.
37. Bouten, P. J. M.; Hertsen, D.; Vergaelen, M.; Monnery, B. M.; Catak, S.; van Hest, J. C. M.; Van Speybroeck, V.; Hoogenboom, R. *J. Polym. Sci., Part A: Polym. Chem.* **2015,** accepted.
38. Hoogenboom, R. Polyoxazoline polymers and methods for their preparation conjugates of these polymers and medical uses thereof. WO 2013/103297 A1, 11 July 2013, 2013.
39. Mees, M.; Hoogenboom, R. *Macromolecules* **2015,** 48, (11), 3531-3538.
40. Grogna, M.; Cloots, R.; Luxen, A.; Jerome, C.; Desreux, J. F.; Detrembleur, C. *J Mater Chem* **2011,** 21, 12917-12926.
41. Steunenberg, P.; Könst, P. M.; Scott, E. L.; Franssen, M. C. R.; Zuilhof, H.; Sanders, J. P. M. *Eur. Polym. J.* **2013,** 49, (7), 1773-1781.
42. Zarka, M. T.; Nuyken, O.; Weberskirch, R. *Chem. Eur. J.* **2003,** 9, 3228-3234.
43. Kotre, T.; Zarka, M. T.; Krause, J. O.; Buchmeiser, M. R.; Weberskirch, R.; Nuyken, O. *Macromol. Symp.* **2004,** 217, 203-214.
44. Rueda, J. C.; Zschoche, S.; Komber, H.; Krahl, F.; Arndt, K. F.; Voit, B. *Macromol. Chem. Phys.* **2010,** 211, 706-716.
45. Zschoche, S.; Rueda, J. C.; Binner, M.; Komber, H.; Janke, A.; Arndt, K. F.; Lehmann, S.; Voit, B. *Macromol. Chem. Phys.* **2012,** 213, 215-226.
46. Rueda, J. C.; Campos, E.; Komber, H.; Zschoche, S.; Haussler, L.; Voit, B. *Des. Monomers Polym.* **2014,** 17, 208-216.
47. Trinh, L. T. T.; Lambermont-Thijs, H. M. L.; Schubert, U. S.; Hoogenboom, R.; Kjøniksen, A.-L. *Macromolecules* **2012,** 45, (10), 4337-4345.
48. Hoogenboom, R.; Fijten, M. W. M.; Thijs, H. M. L.; Van Lankvelt, B. M.; Schubert, U. S. *Des. Monomers Polym.* **2005,** 8, 659-671.

Chapter 4

Poly(2-oxazoline)s with tuneable properties: amidation of methyl ester side chains

Abstract
Methyl ester side chain functionalised poly(2-oxazoline)s are an interesting platform for post polymerisation modification to introduce new properties. Here we present the modification of a homopolymer of 2-methoxycarbonylethyl-2-oxazoline (MestOx) with different primary and secondary amines. Solution and thermal bulk properties are determined with turbidimetry, DSC and TGA measurements. PMestOx has a cloud point temperature of 101 °C, whereas polymers modified with *n*-propylamine, pyrrolidine or piperidine showed cloud point temperatures between 28 and 64 °C, whereas *n*-butylamine modified PMestOx was not watersoluble at all. DSC measurements revealed an increase of glass transition temperature for all eight different modifications ranging from 53-89 °C compared to 39 °C of the starting material.

Introduction
In the 1960s four independent research groups reported the living cationic ring opening polymerisation (CROP) of 2-oxazoline monomers (Scheme 6).[1-4] The resulting poly(2-alkyl/aryl-2-oxazoline)s (PAOx) are a versatile class of polymers with tuneable properties, biocompatibility, stealth and thermoresponsive behaviour.[5-7] Functional groups, often protected, can be introduced during CROP by the use of a functional monomer, initiating or terminating agent, yielding well-defined polymers with control over type and number of functionalities and polymer architecture.[8-17] Poly(2-methyl-2-oxazoline) (PMeOx) and poly(2-ethyl-2-oxazoline) (PEtOx) are interesting candidates for biomedical applications because of their biocompatibility and stealth behaviour similar to poly(ethylene glycol) (PEG).[5-7, 18, 19] PEtOx and PPropOx show thermoresponsive properties. PEtOx has an LCST of ~60 °C, poly(2-*n*-propyl-2-oxazoline) (P*n*PropOx) of ~25 °C, poly(2-cyclopropyl-2-oxazoline) (P*c*PropOx) of ~30 °C and poly(2-isopropyl-2-oxazoline) (P*i*PropOx) of ~38 °C.[5, 20-22] Copolymerisation provides direct access to polymers with tuneable cloud point temperatures (T_{cp}s) from 9 °C to 100 °C.[20-27]

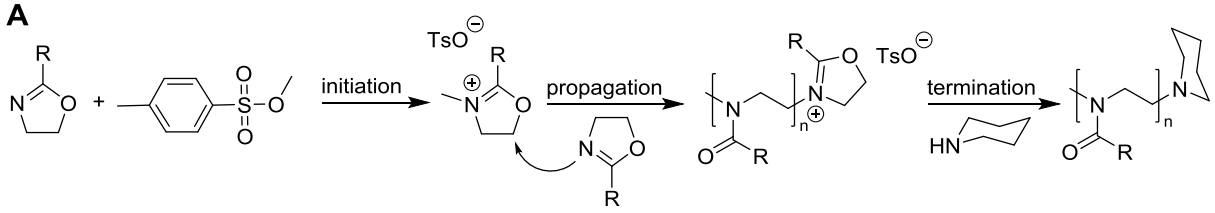

Scheme 6: Cationic ring-opening polymerisation of 2-oxazolines with methyl p-toluenesulfonate as initiator and piperidine as terminating agent.

The incorporation of functional groups into polymer side chains as handles for post-polymerisation modifications, enables the synthesis of a set of polymers with tuneable properties from a single precursor without the need of preparing different monomers. Many different groups and thus types of reactions have been reported for post-polymerisation modifications with a variety of polymers; thiol-ene and thiol-yne reactions, Michael additions (e.g. maleimide coupling), Diels-Alder Cycloaddition, thiol-disulfide exchange, reactions with epoxides, anhydrides, oxazolines and isocyanides, imine formation of aldehydes and ketones with amines, coupling to carboxylic acids and azide-alkyne cycloadditions.[28-32] Substitution reactions, especially of activated esters with amines or alcohols, are the most important class of post-polymerisation modification reactions. The most widely used active ester is *N*-hydroxysuccinimide (NHS) allowing quantitative functionalisation, however polymers modified with NHS are in some cases poorly water soluble.[28, 33] Pentafluorophenyl (PFP)

esters often show a better hydrolytic stability, are soluble in a wide range of solvents and have a higher reactivity than NHS-esters. [28, 32-35]

Poly(2-oxazoline)s can very effectively be functionalized by post-polymerisation modification, for example with thiol-ene[36, 37] and thiol-yne[37] chemistry and copper(I)-catalysed azide-alkyne cycloaddition (CuAAC).[15, 29, 37, 38] CROP does not allow the use of monomers which contain active esters. These reactive groups have to be installed in a post-polymerisation modification synthetic route via the corresponding carboxylic acid, which can be obtained via deprotection of a methyl ester. Carboxylic ester functionalised oxazolines have previously already been used for post-polymerisation functionalisation. The groups of Weberskirch and Weck, for example, used coupling agents to introduce via a carbodiimide amidation reaction a pyrrolidine derivative and a salen ligand respectively.[39, 40]

In chapter 3 we described in detail the synthesis and (thermal) properties of two methyl ester functionalised PAOx polymers, namely PMestOx (**1**) and PC3MestOx (**2**) (Scheme 7). The PMestOx and PC3MestOx homopolymers showed T_{CP}s at 5 mg/mL of 101 °C and 26 °C respectively.[41] Methyl esters are of special interest because they can be easily hydrolysed to their corresponding carboxylic acids providing an easy handle for bioconjugation strategies. Moreover PAOx with methyl ester side chains were recently found to undergo direct, non-catalysed amidation reactions to introduce other functional groups such as alcohols, hydrazide and amines.[42-45] For these amidation reactions no further activation was required, proposedly due to the high concentration of amine reagents employed, and the neighbouring group effect in which the nitrogen groups of the backbone of PAOx participate in the reaction mechanism by stabilisation of the transition state.[43] Although the amidation of MestOx containing polymers with mostly primary amines and one secondary amine (dimethyl amine) was recently described as prior art,[43] this report only proved that amidation reactions are working on homopolymers with one example, PMestOx with 20 repeating units was reacted with 1-aminopropane. The scope of this direct modification reaction and the effect on the polymer properties of PMestOx homopolymers is yet unexplored.

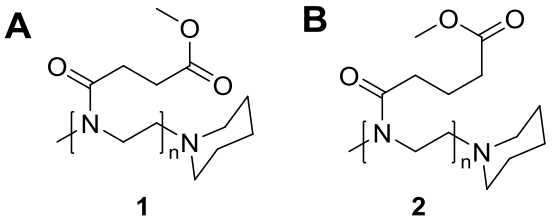

Scheme 7: Structures of A) PMestOx and B) PC3MestOx.

In this chapter the amidation of PMestOx with a series of primary and secondary amines (Scheme 8) was investigated in order to introduce new properties and to exploit the scope of this very straightforward modification reaction. The thermal solution and bulk properties of the resulting polymers were determined by turbidimetry, differential scanning calorimetry (DSC) and thermal gravimetric analysis (TGA), respectively.

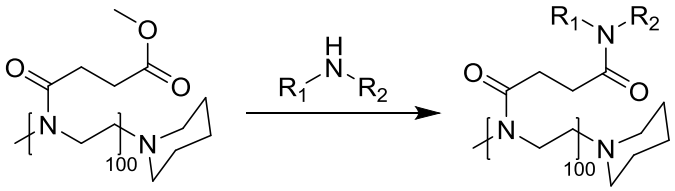

Scheme 8: Amidation of PMestOx with primary and secondary amines yielding PMestOx-amide polymers.

Results and discussion

Homopolymers of MestOx (PMestOx) were prepared as described in chapter 3. Two different batches with a dispersity (Đ) of 1.10 and 1.18 and number average molecular weights (M_n) of 19.4 and 16.1 kDa were used for the amidation reactions.

Amidation reactions with primary amines

The direct amidation reactions were performed according to the method recently reported in literature.[43] PMestOx was dissolved in methylamine (33 wt% solution in absolute ethanol), ethylamine (70% solution in water), *n*-propylamine or *n*-butylamine and stirred overnight at room temperature instead of 70 °C as reported, directly yielding PMestOx-NH-methyl (**3**), PMestOx-NH-ethyl (**4**), PMestOx-NH-propyl (**5**) and PMestOx-NH-butyl (**6**) respectively (Scheme 9). After workup ^{1}H NMR analysis revealed the disappearance of the methyl ester peak at 3.64 ppm and the appearance of peaks corresponding to the amines with the expected integrals indicating near quantitative conversion. Importantly, these amidation reactions were found to be compatible with water which is important for potential future use for bioconjugation. The polymers were also studied with FTIR spectroscopy, also showing the disappearance of the methyl ester band at 1729 cm^{-1} and the appearance of an NH band around 3300 cm^{-1}. SEC analysis showed an increase in molecular weight after amidation, but more importantly Đ remained constant, indicating absence of interchain coupling (Table 7).

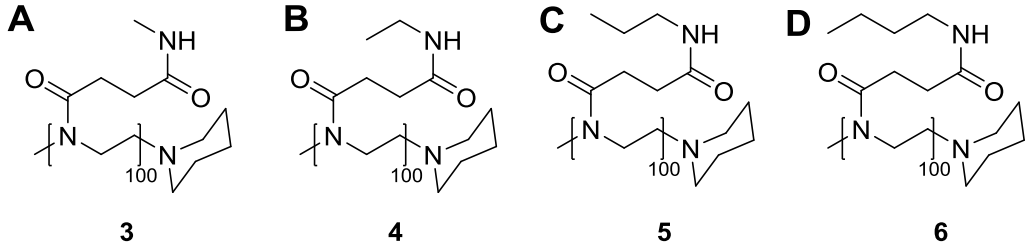

Scheme 9: Polymeric structures after amidation of A) PMestOx-NHmethyl, B) PMestOx-NHethyl, C) PMestOx-NHpropyl and D) PMestOx-NHbutyl.

Amidation with secondary amines

First the amidation reaction was tried with diethyl amine, dipropylamine, diisopropylamine with the same method as described above. Unfortunately, the PMestOx polymer did not dissolve in these amines and the reaction did not proceed. Also the addition of solvent (dichloromethane and methanol were added to dissolve the polymer and/or heat did not yield any product. These secondary amines are probably not reactive enough to perform the amidation without the addition of catalyst.

In literature the air-stable $AlMe_3$ adduct of 1,4-diazobicyclo[2.2.2]octane (DABAL-Me_3), a Lewis acid, (Scheme 10) has been reported for amide formation with secondary amines from low molecular weight methyl esters in THF.[46, 47] Under reflux conditions 18 hours of reaction time were needed for the reaction to go to completion, while under microwave irradiation at 130 °C the reaction was finished in minutes. Therefore the polymer was dissolved in THF and the secondary amines and DABAL-Me_3 were added. After microwave heating to 130 °C, the solution turned into an intractable tar, which was also reported in literature,[47] but no product could be recovered. Two other methods with potassium *tert*-butoxide[48] or sodium methoxide[49] resulted in either no reaction or only hydrolysed methyl esters.

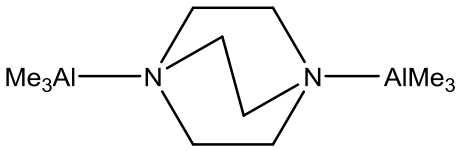

Scheme 10: Structure of $AlMe_3$ adduct of 1,4-diazobicyclo[2.2.2]octane (DABAL-Me_3).

Another paper reported the use of triethylamine as catalyst for such amidation reactions.[50] For the secondary amines reported above this method did also not work with PMestOx. Therefore we switched to the cyclic amines pyrrolidine, piperidine, morpholine and 1-acetylpiperazine to test the effect of the arrangement of the carbon atoms in the amine compound on the amidation reaction. The triethylamine method did work for these amines, yielding PMestOx-pyrrolidine, PMestOx-piperidine, PMestOx-morpholine and PMestOx-1-acetylpiperazine respectively (Scheme 11). The triethylamine route was chosen here because it worked for isopropylamine which did not react in the previously described routes, probably due to steric hindrance. This compound was not tested for its properties, because only a test reaction was performed. The amidations with the cyclic amines without the addition triethylamine should be tried. The reactions with these secondary amines did possibly work because of the higher reactivity of the cyclic amines compared to the linear ones due to steric hindrance. After workup ^{1}H NMR analysis revealed the disappearance of the methyl ester peak at 3.64 ppm and the appearance of peaks corresponding to the amines. The polymers were also studied with FTIR spectroscopy, also showing the disappearance of the methyl ester band at 1729 cm^{-1}. SEC analysis showed an increase in molecular weight after amidation, but more importantly Đ only slightly increased.

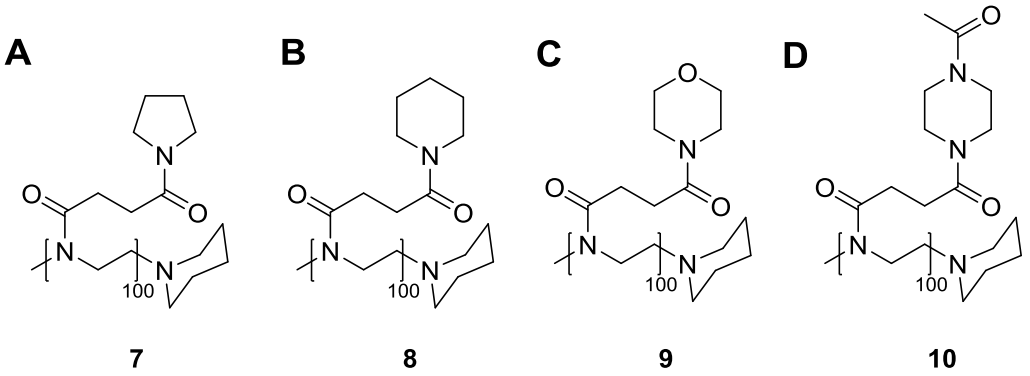

7 8 9 10

Scheme 11: Polymeric structures of PMestOx after amidation with A) pyrrolidine, B) piperidine, C) morpholine and D) 1-acetylpiperazine.

Table 7: Overview of polymer properties after amidation

Amine	SEC[a] before		SEC[a] after		T_{CP} (°C)[b]		T_g (°C)[c]	TGA (°C)[d]
	M_n (kDa)	Đ	M_n (kDa)	Đ	Heating	cooling		
Methylamine	19.4	1.10	25.1	1.13	#	#	82	300
Ethylamine	19.4	1.10	25.6	1.13	#	#	74	305
n-propylamine	19.4	1.10	22.6	1.10	28	*	64	339
n-butylamine	19.4	1.10	22.8	1.09	§	§	53	335
Pyrrolidine	16.1	1.18	13.8	1.25	64	65	70	313
Piperidine	16.1	1.18	¥	¥	23	20	69	293
Morpholine	16.1	1.18	19.1	1.23	#	#	89	343
1-acetylpiperazine	16.1	1.18	18.4	1.32	#	#	70	225

no cloudpoint temperature (T_{CP}) observed up to 100 °C at 5 mg/mL.

* Due to sticking of the precipitated polymers T_{CP} could not be determined.

§ Polymer was not watersoluble
¥ No peak visible in SEC, probably due to low concentration

a. Determined by SEC against PMMA standards
b. Determined by turbidimetry measurements
c. Determined by DSC measurements
d. Onset values of degradation are reported

Solution properties

The modification of PMestOx will change the polymer properties, because of the replacement of the ester moiety by an amide and the introduction of extra carbon atoms into the polymer. T_{CP}s of the modified polymers were determined by turbidimetry of 5 mg mL^{-1} aqueous solutions. All polymers were water-soluble except the *n*-butylamine modified polymer. The polymers PMestOx-NHpropyl, PMestOx-pyrrolidine and PMestOx-piperidine did show reversible LCST behaviour between 23 and 64 °C (Figure 47 and Table 7) while the other four polymers did not show a cloud point up to 100 °C (Figure S 17). The absence of a cloudpoint for the other four polymer was due to a shift in the hydrophilic/hydrophobic balance to the hydrophilic part, because of the ability to form extra hydrogen bonds with the solvent. However the introduction of extra methylene units resulted in a more hydrophobic polymer, leading to a lower T_{CP}. PMestOx was reported a shallow turbidity transition and a T_{CP} of 101 °C,[41] whereas the polymers mentioned above show a sharp transition. PMestOx-NHpropyl had a T_{CP} of 28 °C which is comparable to P*n*PropOx with a T_{CP} for a DP 100 polymer at 5 mg/mL of 27 °C.[41] Although PMestOx-NHpropyl had a longer side chain, the amide that was also introduced restored the hydrophilic/hydrophobic balance. The T_{CP} upon cooling for PMestOx-NHpropyl could not be determined due to coagulation of the precipitated polymer onto the stirring bar and vial, which led to an increased transmittance (Figure 47A). PMestOx-morpholine and PMestOx-1-acetylpiperazine also showed shallow transitions, but they do not reach a transmission of 50%, so no T_{CP} could be determined.

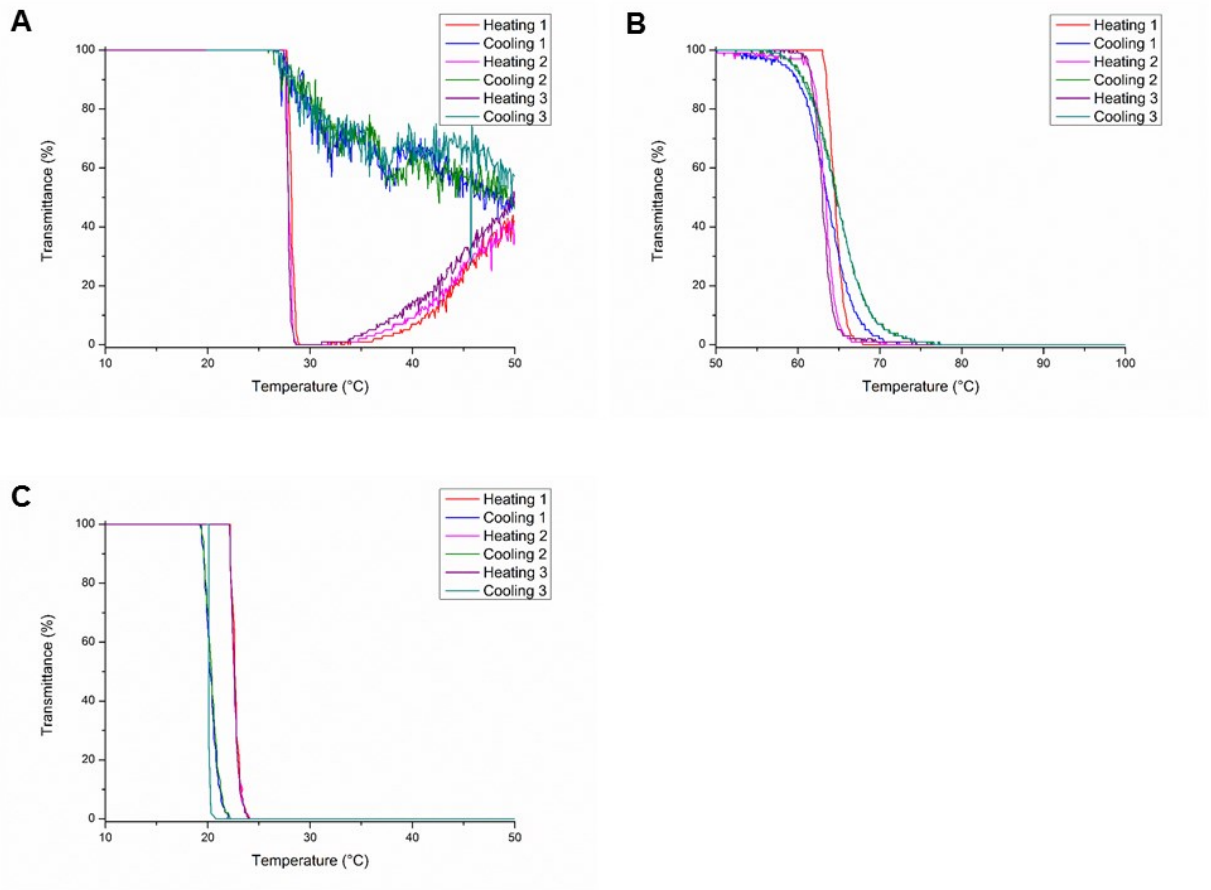

Figure 47: Turbidity measurements for A)PMestOx-NHpropyl, B) PMestOx-pyrrolidine and C) PMestOx-piperidine.

These data show that T_{CP}s can be changed upon post polymerisation modification of the methyl ester groups. The introduction of methylamine or ethylamine lead to the disappearance of LCST behaviour, while propylamine resulted in a T_{CP} of 28 °C and butyl amine resulted in a water-insoluble polymer, clearly showing the influence of the number of carbon atoms in the polymeric chain. Interestingly PMestOx-pyrrolidine contained the same number of carbon atoms as PMestOx-NHbutyl and is highly watersoluble with a T_{CP} of 64 °C. So also the way the carbons are organised is important; cyclic structure are more compact than their linear equivalents and are therefore less exposed to the solvent and have a higher T_{CP}. Increasing the ring with one atom, going from pyrrolidine to piperidine leads to a lower T_{CP}. The introduction of an extra heteroatom in six membered ring leads to the disappearance of T_{CP} and a fully water-soluble polymer up to 100 °C, because more hydrogen bridges can be formed between water and the polymer.

Thermal bulk properties

The thermal bulk properties of the modified PMestOx polymers were further investigated by differential scanning calorimetry (DSC) and thermogravimetric analysis (TGA). All polymers showed a clear glass transition and no melting transition (Figure 48 and Table 7), indicating that they are amorphous. All modifications led to an increase of T_g compared to PMestOx (T_g = 39 °C), indicating reduced chain mobility, i.e. better packing between polymer chains as may be expected by the hydrogen bonding ability of the secondary amide groups. The T_gs of **7**-**10** were plotted against the number of carbon atoms introduced by the amidation reaction (Figure 48C). A linear decrease of T_g was observed with an increasing number of carbon atoms, because polymer packing becomes worse when the side chains are longer. This trend

has also been reported for poly(2-oxazoline)s with alkyl side chains,[51-53] although the decrease of Tg of poly(2-alkyl-2-oxazoline)s is stronger. This can be explained by the better packing of the polymer chains due to the hydrogen bonding ability of the secondary amide groups in the amidated polymers. A second small transition is visible, this is probably an artefact.

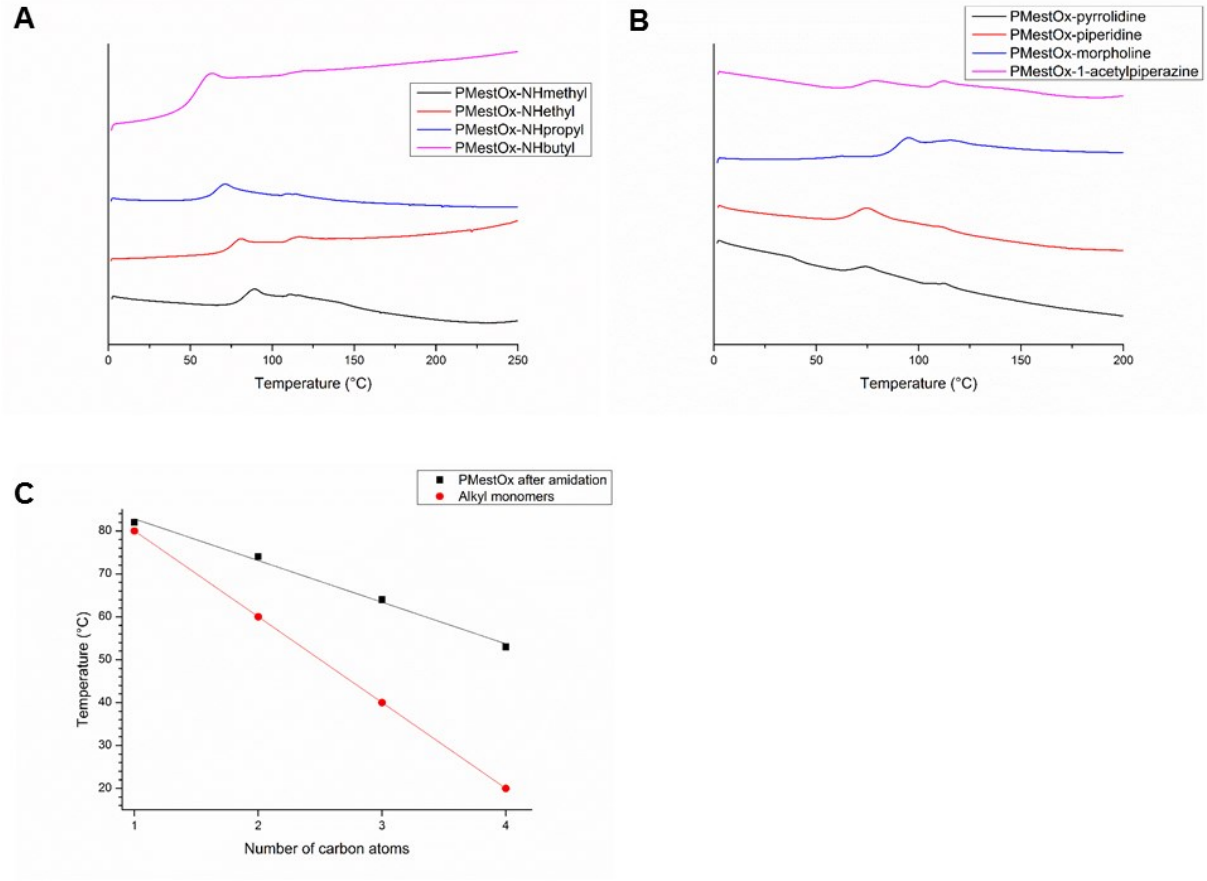

Figure 48: DSC traces of second heating run (10 K min^{-1}) of PMestOx modified with A) primary linear amines yielding polymers **3**-**6** and B) secondary cyclic amines yielding polymers **7**-**10** and C) T_g of polymers **3**-**6** (black) and poly(2-alkyl-2-oxazoline)s (red) versus number of carbon atoms.

TGA analysis revealed that all polymers, except PMestOx-1-acetylpiperazine, are stable up to 300 °C (Figure 49), which is comparable to copolymers of (C3)MestOx with EtOx and nPropOx.[41] The thermal stability increased compared to PMestOx, which was stable up to 250 °C, because the methyl ester was replaced by a more stable amide group. The decreased stability of PMestOx-1-actylpiperazine is mostly likely due to the decomposition of the acetyl group.

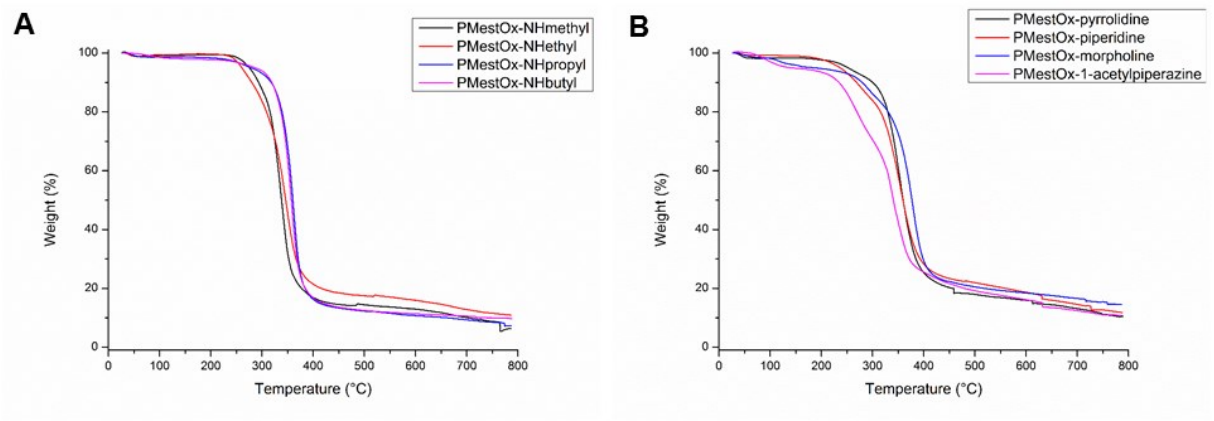

Figure 49: Thermogravimetric analysis of PMestOx modified with A) primary linear amines and B) secondary cyclic amines

Conclusions

We successfully modified PMestOx with different linear primary and cyclic secondary amines. PMestOx has a cloudpoint of 101 °C, the polymers modified with *n*-propylamine, pyrrolidine or piperidine showed a lower T_{CP}, and *n*-butylamine modified PMestOx was not water soluble at all. So the LCST behaviour could be varied over a broad range of temperatures by reaction with different amines. DSC measurements revealed an increase of T_g ranging from 53-89 °C compared to 39 °C of the starting material. When linear primary amines are used, the relation between T_g and number of carbon atoms is linear, similar to the reported trend for poly(2-alkyl-2-oxazoline)s. T_{CP}s and T_gs of PMestOx can be changed by performing an amidation reaction onto the methyl ester, enabling a wide variety of properties from the same PMestOx scaffold. More amidation reactions have to be performed with different amines and also combinations of amines to allow more fine tuning of solution and bulk properties.

Acknowledgements

Samarendra Maji is thanked for performing turbidimetry measurements. Maarten Vergaelen is acknowledged for performing SEC, DSC and TGA measurements.

Experimental section

Materials

2-Chloroethylamine hydrochloride, methyl p-toluenesulfonate (MeOTs), sodium carbonate and ethyl amine (70% solution in water) were purchased from Acros Organics. All other reagents were purchased from Sigma Aldrich and used as received. Methyl *p*-toluenesulfonate (MeOTs) was purified by distillation over barium oxide and stored under argon. Dry solvents were obtained from a solvent purification system from J.C. Meyer, with aluminium oxide drying system and a nitrogen flow. MestOx[9] was prepared according to literature procedures.

Instrumentation

Nuclear magnetic resonance (NMR) spectra were recorded on a Bruker DMC300 (300 MHz for ^{1}H) or a Bruker DMX 500 (500 MHz for ^{1}H).

Polymerisation reaction mixtures were prepared in a VIGOR Sci-Lab SG 1200/750 Glovebox system, with purity levels of less than 1 ppm for O_2 and H_2O.

Polymerisations were carried out in a Biotage Initiator Microwave System with Robot Sixty utilizing capped reaction vials. These vials were heated to 120 °C overnight, allowed to cool

to room temperature and filled with nitrogen prior to use. All microwave polymerisations were performed with temperature control (IR sensor).
Size-exclusion chromatography (SEC) was performed on an Agilent 1260-series HPLC system equipped with a 1260 online degasser, a 1260 ISO-pump, a 1260 automatic liquid sampler (ALS), a thermostatted column compartment (TCC) at 50°C equipped with two PLgel 5 µm mixed-D columns and a guard column in series, a 1260 diode array detector (DAD) and a 1260 refractive index detector (RID). The used eluent was DMA containing 50mM of LiCl at a flow rate of 0.500 ml/min. The spectra were analysed using the Agilent Chemstation software with the GPC add on. Molar mass and PDI values were calculated against PMMA standards from PSS.
Turbidity measurements were performed on an Avantium Crystal 16 platform. Solutions of the polymers were prepared in MilliQ water at 5 mg mL^{-1} and were stirred at room temperature until all polymer was dissolved. Three heating cycles were applied with a heating/cooling rate of 1 °C min^{-1}, temperature ranges of 5-45, 20-60, 20-75, 60-105 or 70-110 °C were used depending on the polymer, and with hold steps of 5 min at the extreme low temperatures, no hold time was applied when the samples were heated above 100 °C; all measurements were performed with a stirring rate of 700 rpm. The cloud points are given as the 50% transmittance point during the first heating run. GC vials with open caps and septa were used for these measurements allowing heating until 110 °C with minor pressure build up as noticed by slight expansion of the septum.
Differential scanning calorimetry (DSC) traces were recorded under nitrogen with a Mettler-Toledo DSC1 module. Glass transition temperatures were obtained from the second heating run with heating/cooling rates of 10 K min^{-1}. Indium was used as a standard for temperature and enthalpy calibrations.
Thermogravimetric analysis (TGA) was performed with a Mettler Toledo TGA/SDTA851e instrument under nitrogen atmosphere at a heating rate of 10 ° C min^{-1} between 25 °C and 800 °C.

Polymer Synthesis
Polymers were prepared as described in chapter 3.

Polymer modifications
Methyl- and ethyl amine modified polymers
100 mg of polymer was dissolved in 0.5 mL of methylamine (33 wt% solution in absolute ethanol) or ethylamine (70% solution in water). The reaction was stirred overnight at room temperature and the solvent was evaporated. The polymer was dissolved in methanol and precipitated in cold diethyl ether twice. The polymers were dissolved in water and freeze dried.

Propyl- and butylamine modified polymers
100 mg of polymer was dissolved in 0.5 mL of propylamine or butylamine. The reaction was stirred overnight at room temperature. 0.5 mL of DCM was added and the polymer was precipitated in cold diethyl ether twice. The precipitate was collected and dried under vacuum.

DABAL-Me_3 catalysed reaction
The DABAL-Me_3 amide reaction was performed as reported in literature.[47] A polymer stock solution with a methyl ester concentration of 0.5 M in THF and a 0.4 M in THF DABAL-Me3 stock solution were prepared. 0.5 mL of both solutions were mixed in a microwave tube and 1 equivalent of the amine was added. The vail was capped and heated for 15 minutes under

microwave irradiation at 130 °C. The solvent was evaporated, the polymer was dissolved in DCM and precipitated in cold diethyl ether.

Potassium *tert*-butoxide (KO*t*-Bu) reaction
This reaction was performed according to literature.[48] 69.7 mg of KO*t*-Bu was dissolved in 2.53 mL THF and stirred for 1 minute in air. 0.52 mL of this solution was added to a 0.255 mL polymer stock solution with a methyl ester concentration of 0.25 M. One equivalent of amine was added and the reaction was stirred for 1 hour at room temperature. The reaction mixture was filtered and the solvent was evaporated. The polymer was dissolved in DCM and precipitated in cold diethyl ether.

Sodium methoxide reaction
This reaction was performed according to literature.[49] PMestOx was dissolved in THF with a methyl ester concentration of 4.0 M. 1.3 equivalents of amine and 5 mol% of sodium methoxide were added. The reaction was stirred for one day at 50 °C. The reaction mixture was filtered and the solvent was evaporated. The polymer was dissolved in DCM and precipitated in cold diethyl ether.

Pyrrolidine, piperidine, morpholine and 1-acetylpiperazine modified polymers
100 mg of polymer was dissolved in 0.5 mL pyrrolidine, morpholine or 0.5 g 1-acetylpiperazine. 100 µL of triethylamine was added and the reaction was stirred at 90 °C for 6 days. 0.5 mL of DCM was added and the pyrrolidine and piperidine modified polymers were precipitated twice in cold diethyl ether. Morpholine and 1-acetylpiperazine polymers were precipitated three times in cold diethyl ether: acetone 3:1. The morpholine modified polymer was subsequently also precipitated in ethyl acetate. The precipitate was collected and dried under vacuum.

^{1}H NMR data of the polymers synthesized

PMestOx 1
^{1}H NMR ($CDCl_3$, 500 MHz): δ 3.64 (br, COOC$\underline{H}_3$, 297 H), 3.46 (br, NC$\underline{H}_2$C$\underline{H}_2$N, 396 H), 3.14 (br, C$\underline{H}_2$NC$\underline{H}_2$ piperidine, 4 H), 2.96 (s, NC$\underline{H}_3$, 3 H), 2.57 (br, COC$\underline{H}_2$C$\underline{H}_2$CO, 396 H), 1.78 (s, C$\underline{H}_2$C$\underline{H}_2$C$\underline{H}_2$ piperidine, 6 H)
FTIR: 2953 cm^{-1} (C-H alkane), 1729 cm^{-1} (C=O of methyl ester), 1637 cm^{-1} (C=O of amide), 1436 cm^{-1} (C-N amide)
SEC: M_n 19.4 kDa, Đ 1.10

PMestOx 2
^{1}H NMR ($CDCl_3$, 500 MHz): δ 3.64 (br, COOC$\underline{H}_3$, 300 H), 3.46 (br, NC$\underline{H}_2$C$\underline{H}_2$N, 400 H), 3.14 (br, C$\underline{H}_2$NC$\underline{H}_2$ piperidine, 4 H), 2.96 (s, NC$\underline{H}_3$, 3 H), 2.57 (br, COC$\underline{H}_2$C$\underline{H}_2$CO, 400 H), 1.78 (s, C$\underline{H}_2$C$\underline{H}_2$C$\underline{H}_2$ piperidine, 6 H)
SEC: M_n 16.1 kDa, Đ 1.18

PMestOx-NH-methyl
^{1}H NMR (MeOD, 500 MHz): δ 3.46 (br, NC$\underline{H}_2$C$\underline{H}_2$N, 396 H), 3.14 (br, C$\underline{H}_2$NC$\underline{H}_2$ piperidine, 4 H), 2.96 (s, NC$\underline{H}_3$, 3 H), 2.70 (br, CH_3, 197 H), 2.57 (br, COC$\underline{H}_2$C$\underline{H}_2$CO, 396 H), 1.78 (s, C$\underline{H}_2$C$\underline{H}_2$C$\underline{H}_2$ piperidine, 6 H)
FTIR: 3313 cm^{-1} (N-H), 2947 cm^{-1} (C-H alkane), 1636 cm^{-1} (C=O of amide), 1418 cm^{-1} (C-N amide)
SEC: M_n 25.1 kDa, Đ 1.13

PMestOx-NH-ethyl
^{1}H NMR ($CDCl_3$, 500 MHz): δ 3.46 (br, NCH_2CH_2N, 396 H), 3.19 (br, CH_2NCH_2 piperidine & $NHCH_2CH_3$, 202 H), 2.96 (s, NCH_3, 3 H), 2.57 (br, $COCH_2CH_2CO$, 396 H), 1.78 (s, $CH_2CH_2CH_2$ piperidine, 6 H), 1.09 (br, CH_3, 197 H)
FTIR: 3306 cm^{-1} (N-H), 2970 cm^{-1} (C-H alkane), 1636 cm^{-1} (C=O of amide), 1457 cm^{-1} (C-N amide)
SEC: M_n 25.6 kDa, Đ 1.13

PMestOx-NH-propyl
^{1}H NMR ($CDCl_3$, 500 MHz): δ 3.46 (br, NCH_2CH_2N, 396 H), 3.19 (br, CH_2NCH_2 piperidine & $NHCH_2CH_2$, 202 H), 2.96 (s, NCH_3, 3 H), 2.57 (br, $COCH_2CH_2CO$, 396 H), 1.78 (s, $CH_2CH_2CH_2$ piperidine, 6 H), 1.49 (br, $NHCH_2CH_2$, 198 H), 0.90 (br, CH_3, 197 H)
FTIR: 3313 cm^{-1} (N-H), 2963 cm^{-1} (C-H alkane), 1628 cm^{-1} (C=O of amide), 1423 cm^{-1} (C-N amide)
SEC: M_n 22.6 kDa, Đ 1.10

PMestOx-NH-butyl
^{1}H NMR ($CDCl_3$, 300 MHz): δ 3.46 (br, NCH_2CH_2N, 396 H), 3.19 (br, CH_2NCH_2 piperidine, 4 H), 2.96 (s, NCH_3, 3 H), 2.57 (br, $COCH_2CH_2CO$, CH_3CHCH_3, 495 H), 1.78 (s, $CH_2CH_2CH_2$ piperidine, 6 H), 1.10 (br, CH_3, 594 H)
FTIR: 3296 cm^{-1} (N-H), 2957 cm^{-1} (C-H alkane), 1629 cm^{-1} (C=O of amide), 1433 cm^{-1} (C-N amide)
SEC: M_n 22.8 kDa, Đ 1.09

PMestOx-NH-isopropyl
^{1}H NMR ($CDCl_3$, 500 MHz): δ 3.46 (br, NCH_2CH_2N, 396 H), 3.19 (br, CH_2NCH_2 piperidine & $NHCH_2CH_2$, 202 H), 2.96 (s, NCH_3, 3 H), 2.57 (br, $COCH_2CH_2CO$, 396 H), 1.78 (s, $CH_2CH_2CH_2$ piperidine, 6 H), 1.49 (br, $NHCH_2CH_2$, 198 H), 0.90 (br, CH_3, 197 H)

PMestOx-pyrrolidine
^{1}H NMR ($CDCl_3$, 500 MHz): δ 3.46 (br, NCH_2CH_2N, 396 H), 3.34 (br, CH_2NCH_2 piperidine & CH_2NCH_2 pyrrolidine, 400 H), 2.96 (s, NCH_3, 3 H), 2.57 (br, $COCH_2CH_2CO$, 396 H), 1.92 (br, CH_2 pyrrolidine, 196 H), 1.78 (s, $CH_2CH_2CH_2$ piperidine & CH2 pyrrolidine, 204 H)
FTIR: 2971 cm^{-1} (C-H alkane), 1630 cm^{-1} (C=O of amide), 1443 cm^{-1} (C-N amide)
SEC: M_n 13.8 kDa, Đ 1.25

PMestOx-piperidine
^{1}H NMR ($CDCl_3$, 500 MHz): δ 3.46 (br, NCH_2CH_2N, 396 H), 3.41 (br, CH_2NCH_2 piperidine, 400 H), 2.96 (s, NCH_3, 3 H), 2.57 (br, $COCH_2CH_2CO$, 396 H), 1.56 (br, $CH_2CH_2CH_2$, 600 H)
FTIR: 2934 cm^{-1} (C-H alkane), 1636 cm^{-1} (C=O of amide), 1443 cm^{-1} (C-N amide)
SEC: no peak visible, probably due to low concentration

PMestOx-morpholine
^{1}H NMR ($CDCl_3$, 500 MHz): δ 3.67(br, CH_2NCH_2, 396H), 3.64 (br, CH_2OCH_2, 396 H), 3.46 (br, NCH_2CH_2N, 396 H), 3.34 (br, CH_2NCH_2 piperidine, 6 H), 2.96 (s, NCH_3, 3 H), 2.57 (br, $COCH_2CH_2CO$, 396 H), 1.78 (s, $CH_2CH_2CH_2$ piperidine, 6 H)
FTIR: 2918 cm^{-1} (C-H alkane), 1634 cm^{-1} (C=O of amide), 1444 cm^{-1} (C-N amide), 1113 cm^{-1} (C-O dialkyl ether)

SEC: M_n 19.1 kDa, Đ 1.23

PMestOx-1-acetylpiperazine
^{1}H NMR ($CDCl_3$, 500 MHz): δ 3.93&3.80 (br, $CONCH_2$, 198 H), 3.46 (br, $NC\underline{H_2}C\underline{H_2}N$, 396 H), 3.19 (br, $C\underline{H_2}NC\underline{H_2}$ piperidine & $CONCH_2$, 202 H), 2.96 (s, $NC\underline{H_3}$, 3 H), 2.57 (br, $COC\underline{H_2}C\underline{H_2}CO$, 396 H), 2012 (br, CH_3, 197 H), 1.78 (s, $C\underline{H_2}C\underline{H_2}C\underline{H_2}$ piperidine, 6 H)
FTIR: 2919 cm^{-1} (C-H alkane), 1634 cm^{-1} (C=O of amide), 1435 cm^{-1} (C-N amide)
SEC: M_n 18.4 kDa, Đ 1.32

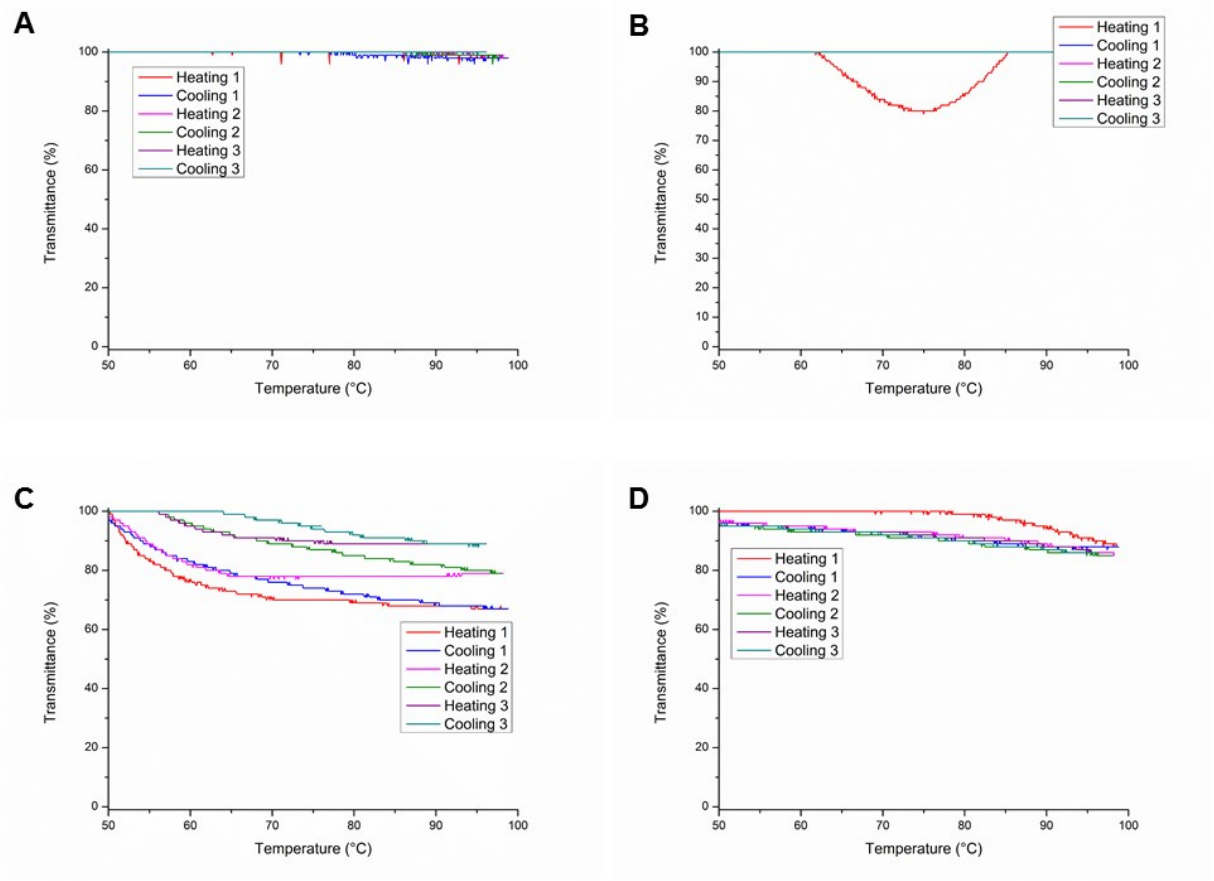

Figure S 17: Turbidity measurements for A) PMestOx-NHmethyl, B) PMestOx-NHethyl, C) PMestOx-morpholine and D) PMestOx-1-acetylpiperazine

References

1. Tomalia, D. A.; Sheetz, D. P. *J. Polym. Sci., Part A: Polym. Chem.* **1966,** 4, 2253-2265.
2. Bassiri, T. G.; Levy, A.; Litt, M. *J. Polym. Sci., Part B: Polym. Lett.* **1967,** 5, 871-879.
3. Seeliger, W.; Aufderhaar, E.; Diepers, W.; Feinauer, R.; Nehring, R.; Thier, W.; Hellmann, H. *Angew. Chem. Int. Ed.* **1966,** 5, 875-888.
4. Kagiya, T.; Narisawa, S.; Maeda, T.; Fukui, K. *J. Polym. Sci. Pol. Lett.* **1966,** 4, 441-445.
5. Hoogenboom, R. *Angew. Chem. Int. Ed.* **2009,** 48, 7978-7994.
6. Luxenhofer, R.; Han, Y.; Schulz, A.; Tong, J.; He, Z.; Kabanov, A. V.; Jordan, R. *Macromol. Rapid Commun.* **2012,** 33, (19), 1613-1631.

7. Sedlacek, O.; Monnery, B. D.; Filippov, S. K.; Hoogenboom, R.; Hruby, M. *Macromol. Rapid Commun.* **2012,** 33, (19), 1648-1662.
8. Guillerm, B.; Monge, S.; Lapinte, V.; Robin, J. J. *Macromol. Rapid Commun.* **2012,** 33, 1600-1612.
9. Bouten, P. J. M.; Hertsen, D.; Vergaelen, M.; Monnery, B. D.; Boerman, M. A.; Goossens, H.; Catak, S.; van Hest, J. C. M.; Van Speybroeck, V.; Hoogenboom, R. *Polym. Chem.* **2015,** 6, (4), 514-518.
10. Bouten, P. J. M.; Hertsen, D.; Vergaelen, M.; Monnery, B. M.; Catak, S.; van Hest, J. C. M.; Van Speybroeck, V.; Hoogenboom, R. *J. Polym. Sci., Part A: Polym. Chem.* **2015,** accepted, DOI: 10.1002/pola.27733.
11. Levy, A.; Litt, M. *J. Polym. Sci., Part A: Polym. Chem.* **1968,** 6, 1883-1894.
12. Kelly, A. M.; Hecke, A.; Wirnsberger, B.; Wiesbrock, F. *Macromol. Rapid Commun.* **2011,** 32, 1815-1819.
13. Gress, A.; Volkel, A.; Schlaad, H. *Macromolecules* **2007,** 40, 7928-7933.
14. Taubmann, C.; Luxenhofer, R.; Cesana, S.; Jordan, R. *Macromol. Biosci.* **2005,** 5, 603-612.
15. Fijten, M. W. M.; Haensch, C.; van Lankvelt, B. M.; Hoogenboom, R.; Schubert, U. S. *Macromol. Chem. Phys.* **2008,** 209, 1887-1895.
16. Verbraeken, B.; Lava, K.; Hoogenboom, R., Poly(2-oxazoline)s. In *Encyclopedia of Polymer Science and Technology*, John Wiley & Sons, Inc.: 2014; pp 1-51.
17. Rossegger, E.; Schenk, V.; Wiesbrock, F. *Polymers* **2013,** 5, (3), 956-1011.
18. de la Rosa, V. R. *Journal of materials science. Materials in medicine* **2014,** 25, (5), 1211-25.
19. Luxenhofer, R.; Sahay, G.; Schulz, A.; Alakhova, D.; Bronich, T. K.; Jordan, R.; Kabanov, A. V. *J. Controlled Release* **2011,** 153, (1), 73-82.
20. Roy, D.; Brooks, W. L. A.; Sumerlin, B. S. *Chem. Soc. Rev.* **2013,** 42, (17), 7214-7243.
21. Weber, C.; Hoogenboom, R.; Schubert, U. S. *Prog. Polym. Sci.* **2012,** 37, (5), 686-714.
22. Bloksma, M. M.; Weber, C.; Perevyazko, I. Y.; Kuse, A.; Baumgärtel, A.; Vollrath, A.; Hoogenboom, R.; Schubert, U. S. *Macromolecules* **2011,** 44, (11), 4057-4064.
23. Huber, S.; Jordan, R. *Colloid. Polym. Sci.* **2008,** 286, (4), 395-402.
24. Diehl, C.; Schlaad, H. *Macromol. Biosci.* **2009,** 9, (2), 157-161.
25. Glassner, M.; Lava, K.; de la Rosa, V. R.; Hoogenboom, R. *J. Polym. Sci., Part A: Polym. Chem.* **2014,** 52, (21), 3118-3122.
26. Park, J.-S.; Kataoka, K. *Macromolecules* **2006,** 39, (19), 6622-6630.
27. Hoogenboom, R.; Thijs, H. M. L.; Jochems, M. J. H. C.; van Lankvelt, B. M.; Fijten, M. W. M.; Schubert, U. S. *Chem. Commun.* **2008,** 44, 5758-5760.
28. Günay, K. A.; Theato, P.; Klok, H.-A. *J. Polym. Sci., Part A: Polym. Chem.* **2013,** 51, (1), 1-28.
29. Lava, K.; Verbraeken, B.; Hoogenboom, R. *Eur. Polym. J.* **2015,** 65, 98-111.
30. Murray, B. S.; Jackson, A. W.; Mahon, C. S.; Fulton, D. A. *Chem Commun* **2010,** 46, (45), 8651-8653.
31. Yang, S. K.; Weck, M. *Macromolecules* **2008,** 41, (2), 346-351.
32. Nilles, K.; Theato, P. *J. Polym. Sci., Part A: Polym. Chem.* **2010,** 48, (16), 3683-3692.
33. Eberhardt, M.; Mruk, R.; Zentel, R.; Théato, P. *European Polymer Journal* **2005,** 41, (7), 1569-1575.
34. Roth, P. J.; Jochum, F. D.; Forst, F. R.; Zentel, R.; Theato, P. *Macromolecules* **2010,** 43, (10), 4638-4645.

35. Zhang, Q. L.; Schattling, P.; Theato, P.; Hoogenboom, R. *Polymer Chemistry* **2012,** 3, (6), 1418-1426.
36. Kempe, K.; Hoogenboom, R.; Jaeger, M.; Schubert, U. S. *Macromolecules* **2011,** 44, (16), 6424-6432.
37. Luxenhofer, R.; Jordan, R. *Macromolecules* **2006,** 39, (10), 3509-3516.
38. Chapman, R.; Bouten, P. J. M.; Hoogenboom, R.; Jolliffe, K. A.; Perrier, S. *Chem. Commun.* **2013,** 49, 6522-6524.
39. Liu, Y.; Wang, Y.; Wang, Y. F.; Lu, J.; Pinon, V.; Weck, M. *J. Am. Chem. Soc.* **2011,** 133, 14260-14263.
40. Zarka, M. T.; Nuyken, O.; Weberskirch, R. *Chem. Eur. J.* **2003,** 9, 3228-3234.
41. Bouten, P. J. M.; Lava, K.; Van Hest, J. C. M.; Hoogenboom, R. *Submitted*.
42. Hoogenboom, R. Polyoxazoline polymers and methods for their preparation conjugates of these polymers and medical uses thereof. WO 2013/103297 A1, 11 July 2013, 2013.
43. Mees, M.; Hoogenboom, R. *Macromolecules* **2015,** 48, (11), 3531-3538.
44. Grogna, M.; Cloots, R.; Luxen, A.; Jerome, C.; Desreux, J. F.; Detrembleur, C. *J Mater Chem* **2011,** 21, 12917-12926.
45. Steunenberg, P.; Könst, P. M.; Scott, E. L.; Franssen, M. C. R.; Zuilhof, H.; Sanders, J. P. M. *Eur. Polym. J.* **2013,** 49, (7), 1773-1781.
46. Novak, A.; Humphreys, L. D.; Walker, M. D.; Woodward, S. *Tetrahedron Letters* **2006,** 47, (32), 5767-5769.
47. Dubois, N.; Glynn, D.; McInally, T.; Rhodes, B.; Woodward, S.; Irvine, D. J.; Dodds, C. *Tetrahedron* **2013,** 69, (46), 9890-9897.
48. Kim, B. R.; Lee, H.-G.; Kang, S.-B.; Sung, G. H.; Kim, J.-J.; Park, J. K.; Lee, S.-G.; Yoon, Y.-J. *Synthesis* **2012,** 44, (01), 42-50.
49. Ohshima, T.; Hayashi, Y.; Agura, K.; Fujii, Y.; Yoshiyama, A.; Mashima, K. *Chem Commun* **2012,** 48, (44), 5434-5436.
50. Fischer, J.; Ritter, H. *Beilstein J. Org. Chem.* **2013,** 9, 2803-2811.
51. Hoogenboom, R. *Eur. J. Lipid Sci. Technol.* **2011,** 113, (1), 59-71.
52. Hoogenboom, R.; Fijten, M. W. M.; Thijs, H. M. L.; Van Lankvelt, B. M.; Schubert, U. S. *Des. Monomers Polym.* **2005,** 8, 659-671.
53. Rettler, E. F. J.; Kranenburg, J. M.; Lambermont-Thijs, H. M. L.; Hoogenboom, R.; Schubert, U. S. *Macromol Chem Phys* **2010,** 211, (22), 2443-2448.

Chapter 5

Cell penetrating polymers

Abstract
Cell penetrating peptides (CPPs) and their synthetic mimics are used to transfer drugs across the biological membrane. Here we report a new polymeric mimic of CPPs based on the biocompatible polymer poly(2-oxazoline). This versatile class of polymers allows the introduction of functional groups in the side chain, such as methyl esters, which can be modified in an efficient three step procedure towards cellular uptake-facilitating guanidinium groups. We prepared a set of guanidine-functionalised polymers of DP 100 to study the effect of monomer distribution and degree of functionalisation on uptake efficiency. It was determined that only the block copolymers with 15 or 20% functionalisation were taken up by cells, clearly showing the influence of polymeric structure and degree of functionalisation. The cell penetrating efficiency was lower compared to the low molecular weight CPP octa-arginine (R8), probably due to the large size of the polymeric construct.

Introduction
Drug molecules need to be balanced in hydrophobic and hydrophilic properties to be therapeutically active; they should be sufficiently water soluble to be transported through the body and be lipophilic enough to cross the lipid bilayer of the cell. Instead of increasing the lipophilicity of a molecule, cell uptake can also be improved by the employment of cell membrane transporter agents. A highly important class of molecular transporters (MoTrs) are the cell-penetrating peptides (CPPs), which often have a viral origin. The first CPP was derived from the HIV-1 protein TAT and consists of amino acids 49-57 of this protein, RKKRRQRRR (R: arginine, K: lysine and Q: glutamine).[1-3] All charged amino acids, both arginine and lysine, were proven to be essential for cellular uptake. Over the years many different CPPs have been identified, of which a considerable number is rich in lysine (**1**) and arginine (**2**) residues, some examples can be found in Table 8. [1, 2]

Table 8: amino acid sequences of cell penetrating peptides

Cell penetrating peptide	**Amino acid sequence**
TAT_{49-57}	RKKRRQRRR (**4**)
Penetratin	RQIKIWFQNRRMKWKK
Pep-1	KETWWETWWTEWSQPKKKRKV
Transportan	GWTLNSAGYLLGKINLKALAALAKKIL
Nuclear localisation sequences	FKKFRKF, SKKKKIKV, GRKRKKRT, VQRKRQKLMP, PKKKRKV, ERKKRRRE, KRPAATKKAGQAKKKL
Oligo-arginines	RRRRRRRR (R_8), RRRRRRRRR (R_9)

Aminoacid abbreviations: A: Alanine, E: Glumatic acid, F: Phenylalanine, G: Glycine, I: Isoleucine, K: lysine, L: Leucine, M: methionine, N: Asparagine, P: Proline, Q: Glutamine, R: arginine, S: Serine, T: Threonine, V: Valine, W: Tryptophan, Y: Tryosine

One of the most effective synthetic CPPs is oligo-arginine (**3**). The number of arginines needed for cell uptake is 5-20, with 7-9 being optimal with regard to performance and ease of synthesis.[3, 4] The activity is furthermore not affected by stereochemistry. Although the exact mechanism of uptake is still not known, it has been demonstrated that the oligo-arginines only function well when these residues are in close proximity of each other, as is the case of course when they are part of a homo-oligopeptide. Another option to construct an active oligo-arginine domain is by combining two peptides with 4 arginines by a disulfide bridge, which leads to similar uptake efficiency as regular octa-arginine. The reversibility of the disulfide bond allows the construction of activatable cell penetrating peptides.[5]

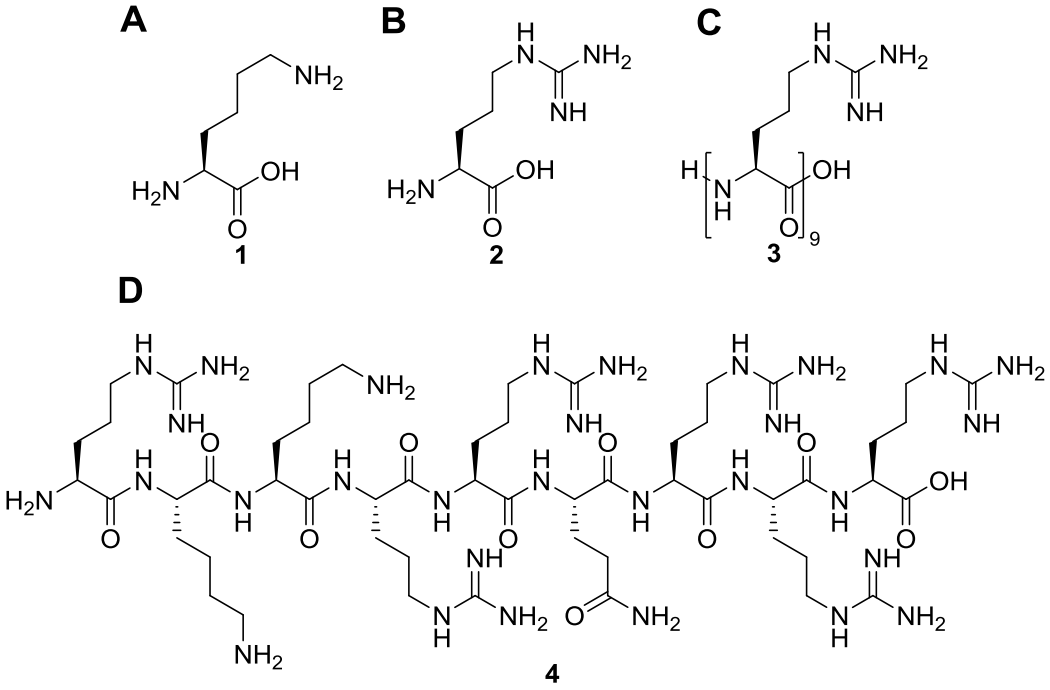

Figure 50: Structures of amino acids and cell penetrating peptides A) lysine and B) arginine, C) nona-arginine and D) TAT peptide

As the guanidine group of the arginine side chain seems to be the dominating functional element, many researchers have investigated the possibility to construct cell penetrating materials by installing this moiety on a wide range of carrier molecules, leading to so-called guanidinium-rich transporters (GRTs).[6, 7] The first example was reported by Wender et al.[4] who prepared polypeptoids with amine groups which were subsequently converted into guanidines via a perguanidinylation reaction. These guanidinium polypeptoids (**5**) showed similar uptake as oligo-arginines. Also the length between the backbone and guanidinium functionality was varied, which showed that longer spacers lead to higher uptake efficiencies, suggesting molecular flexibility is important.[3, 4]

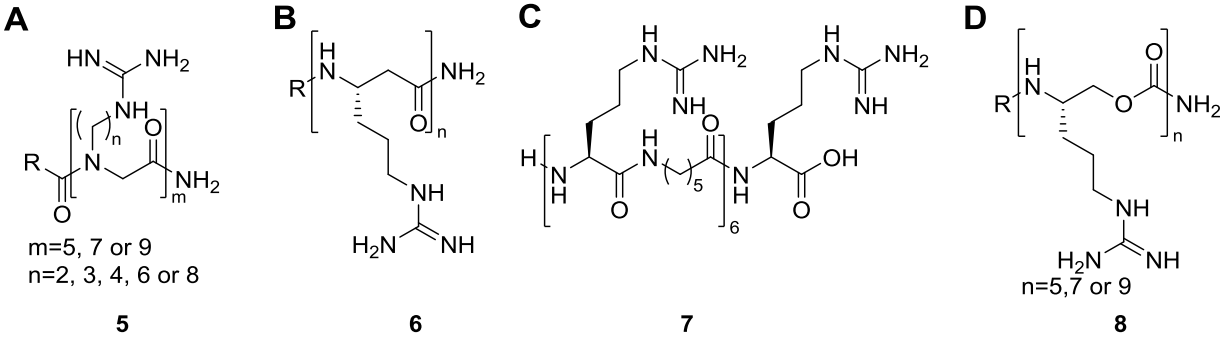

Figure 51: Structure of A) guanidinium polypeptoids, B) β-oligo arginine and C) and D) oligoamides and oligocarbamates with guanidinium side chains, respectively.

The introduction of extra methylene units in the backbone, for example in case of β-peptides (**6**) [8, 9] or an alternating peptide of arginine and aminocaproic acid (**7**) [3, 10] resulted in structures that outperformed or exhibited similar behaviour as the arginine homo-oligomers. In 2002 oligocarbamates bearing guanidinium side chains (**8**) were the first non-amide based MoTrs and the most efficient transporters published at that time.[11]

Nowadays, many examples of GRTs can be found in literature, based on aminoglycosides,[12] dendrimers,[13, 14] sorbitol[15] and inositol.[16] Also a number of oligomeric and polymeric GRTs have been developed. These GRTs are of interest because of their stability, ability to introduce other functionalities, tuneable properties, structural diversity, and ease of production compared to regular CPP synthesis.

Different oligomeric MoTrs have been reported which were either prepared by organocatalytic ring-opening polymerisation to yield biodegradable carbonate oligomers (**9**),[17] or by ring-opening metathesis polymerisation to create oligonorbornenes (**10** and **11**).[18-22] In the former case the 8mer oligocarbonate showed an uptake comparable with R8, whereas the 11mer was twice as effective. Although most polymerisation approaches aim to create oligomers of 7-12 repeating units with guanidine,[17-19] some longer polymers have been reported containing 20-30, 50 or even 100 guanidinium units.[20-22] Oligomers, random[22] and block[20] copolymers have all been shown to enter cells, although no quantification of the MoTrs or structure property relationship studies have been reported. A third class of polymeric MoTrs concerns a polydisulfide polymer (**12**) which can depolymerise in the cell yielding nontoxic degradation products. Uptake in HeLa cells was confirmed using flow cytometry experiments but the efficiency was not compared to existing CPPs.[23, 24] A special oligomeric MoTr was created by positioning the guanidinium group in the main chain of the oligomer. This preorganised and non-hydrolysable chiral bicyclic structure (**13**) showed a two times better uptake than TAT.[25] Uptake could also be improved by the incorporation of aromatic groups in norbonene MoTrs[21] or the conjugation of fatty acids to CPPs.[26]

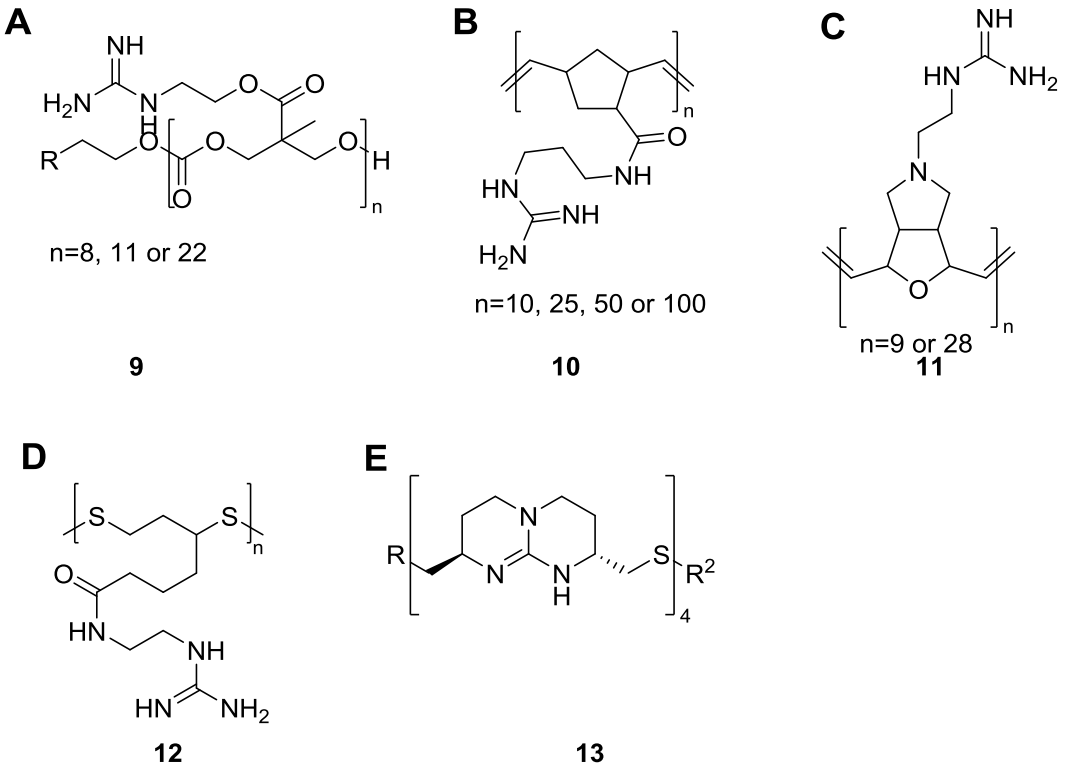

Figure 52: Structures of polymeric MoTrs A) Carbonate oligomers, B)[20] and C)[22] examples of polymers prepared by ring opening metathesis, D) polydisulfide with guanidinium groups and E) oligomer with the guanidinium group in the main chain.

The MoTrs investigated until now all have large backbone structures and in some cases the variation in monomeric units to fine tune the properties is somewhat limited. Furthermore, the

biocompatibility of the non-degradable oligomers is unknown. Poly(2-oxazoline)s might be an interesting alternative option for the synthesis of MoTrs. This class of polymers has a high side chain density, is versatile with respect to its use of monomers, which allows to tune the polymer properties; it is furthermore known to be biocompatible and non-ionic derivatives show stealth behaviour. Although this polymer is not biodegradable, it can be excreted by the kidneys.[27, 28] The versatility of these polymers allows the introduction of reactive groups which can be used for post polymerisation functionalisation. Methyl esters are especially interesting, because they can undergo a direct amidation with a variety of amines to easily introduce other functional groups such as alcohols, hydrazide and amines, as described in chapter 4 and in literature.[29-34]

In this chapter we describe the modification of copolymers consisting of 2-ethyl-2-oxazoline (EtOx) and 2-methoxycarbonylethyl-2-oxazoline (MestOx, **14**) to obtain guanidinium functionalised poly(2-oxazoline)s. Series of random and block copolymers were synthesised to systematically study the effect of functional group distribution along the polymer chain on cellular uptake. Different percentages of MestOx were incorporated to study uptake and toxicity as function of composition. The cell viability was tested for these polymers because cellular uptake and toxicity go hand in hand, before starting uptake studies with confocal microscopy. Flow cytometry experiments were performed to quantify the uptake of the polymers.

Results and discussion

Polymer synthesis and modification

A series of both random and block poly(2-oxazolines) was prepared, with 10, 15 and 20% MestOx. All polymers had low dispersities, Đ < 1.21(Table 9). They were terminated with an azide moiety (Scheme 12) to enable labelling of every polymer chain with a fluorescent dye to allow quantification of cellular uptake. These polymers (P(EtOx-MestOx)N_3) were subsequently reacted with *N*-Boc-ethylene diamine to yield Boc-protected amine functionalised polymer. The Boc group was removed and the corresponding amine was guanidinylated. FITC functionalised with bicyclo[6.1.0]nonyne (BCN) was clicked to the azide to yield a dye-labelled guanidine-functionalised polymer (PAOx(Et-guanidine)FITC). The modifications were performed successfully yielding polymers with an average number of guanidine groups per polymer chain which is comparable to R8 and R9 for the 10% modification, up to the double amount for the 20% degree of guanidinylation. All polymers were purified by precipitation, except for the last two steps. These polymers were purified over Sephadex. All polymers were characterised by ^{1}H NMR and IR spectroscopy.

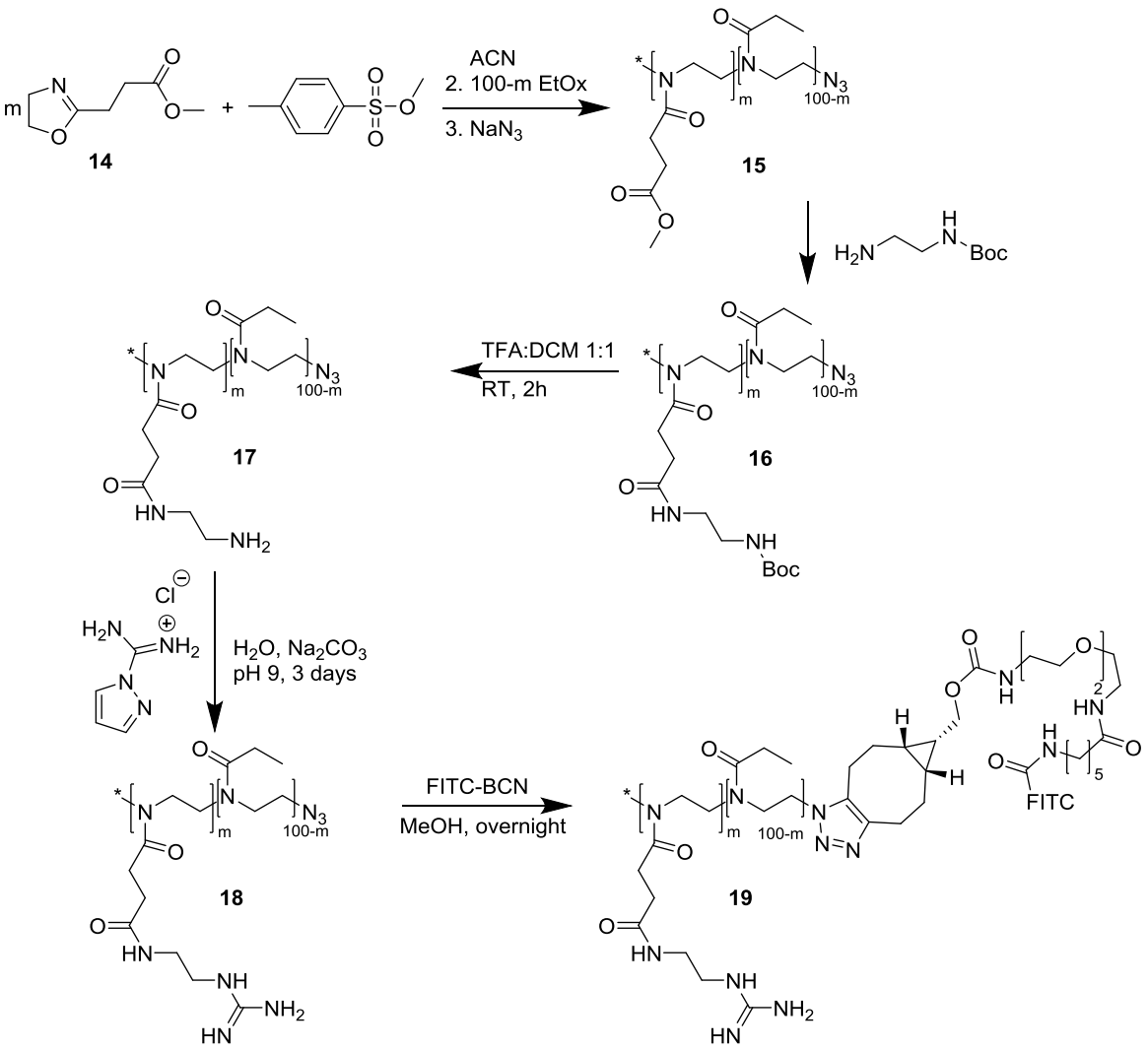

10B: m=10%, block
10G: m=10%, random
15B: m=15%, block
15G: m=15%, random
20B: m=20%, block
20G: m=20%, random

Scheme 12: Synthesis of guanidine-functionalised block copolymers. For the synthesis of the random copolymers EtOx was copolymerized with MestOx in the desired ratio.

Table 9: Overview of polymeric structures and properties

Polymer	**Number of MestOx groups** [a]	**Number of EtOx groups** [a]	**Number of guanidine groups** [a]	**Structure**	**M_n (kDa) MestOx polymer** [b]	**Đ MestOx polymer** [b]
10B	12	94	12	Block	14.5	1.21
10G	12	84	12	Random	16.3	1.16
15B	15	84	15	Block	14.1	1.20
15G	16	84	16	Random	18.0	1.13
20B	23	89	23	Block	14.9	1.16
20G	23	84	23	Random	18.0	1.17

a. determined by ^{1}H NMR spectroscopy
b. determined by SEC against PMMA standards
c. all characterisation was performed on the EtOx-MestOx copolymer (**15**), except for the number of guanidine groups.

Cell viability tests

Cell viability was determined by incubation of HeLa cells with different concentrations (5, 10 and 15 µM) of polymers containing amines **17** and guanidines **19**. Incubations were performed for 90 minutes at 37 °C. After this incubation the cells were washed and incubated with Cell Counting Kit-8. This kit contains a compound that is transformed by living cells to an orange dye which was quantified by UV-Vis spectroscopy.[35] The cell viability was calculated by comparing the absorbance of the treated cells with the absorbance of cells which were not incubated with polymers (Figure 53). The cells were viable with polymer concentrations of 5 and 10 µM, but toxicity slightly increased at 15 µM for the block copolymers whereas the cells were still viable at this concentration for the random copolymers. This lower cell viability in presence of the block copolymers might be due to a higher local concentration of charged groups.

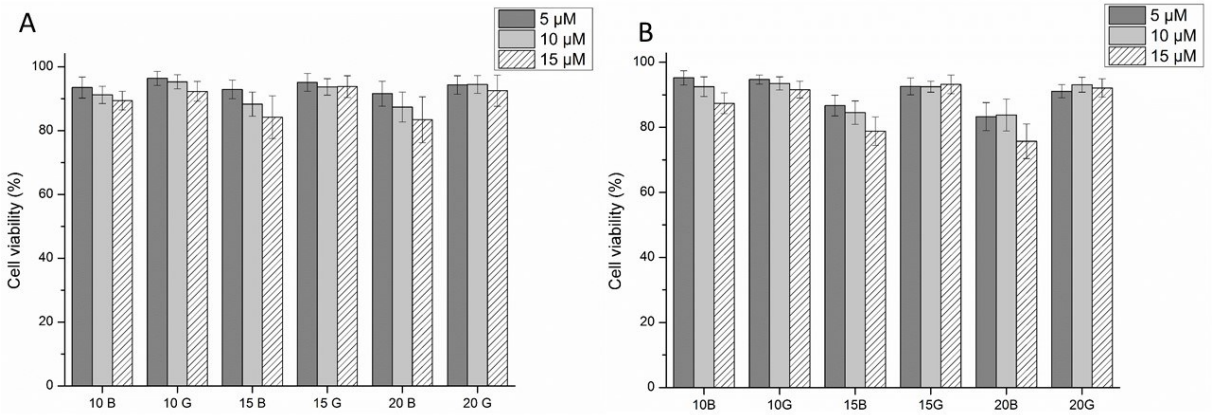

Figure 53: Cell viability of A) amine-functional polymers (**17**) and B) guanidine-functional polymers (**19**) at 5, 10 and 15 µM concentration after 90 minutes incubation, experiments were performed in threefold.

Uptake studies with confocal microscopy

As there were no signs of toxicity at the lower concentrations, HeLa cells were incubated with 5 and 10 µM of polymer for 90 minutes. After washing, the cellular uptake was visualised using confocal fluorescence microscopy. The random copolymers (**19**-10G, **19**-15G and **19**-20G) did not show any uptake at both 5 and 10 µM (Figure S 18 and Figure S 19). In this series only the block copolymers with 15 and 20 % guanidinium groups (**19**-15B and **19**-20B) showed uptake at 10 µM (Figure 55), while at 5 µM (Figure 54) they merely bound to the cell membrane.

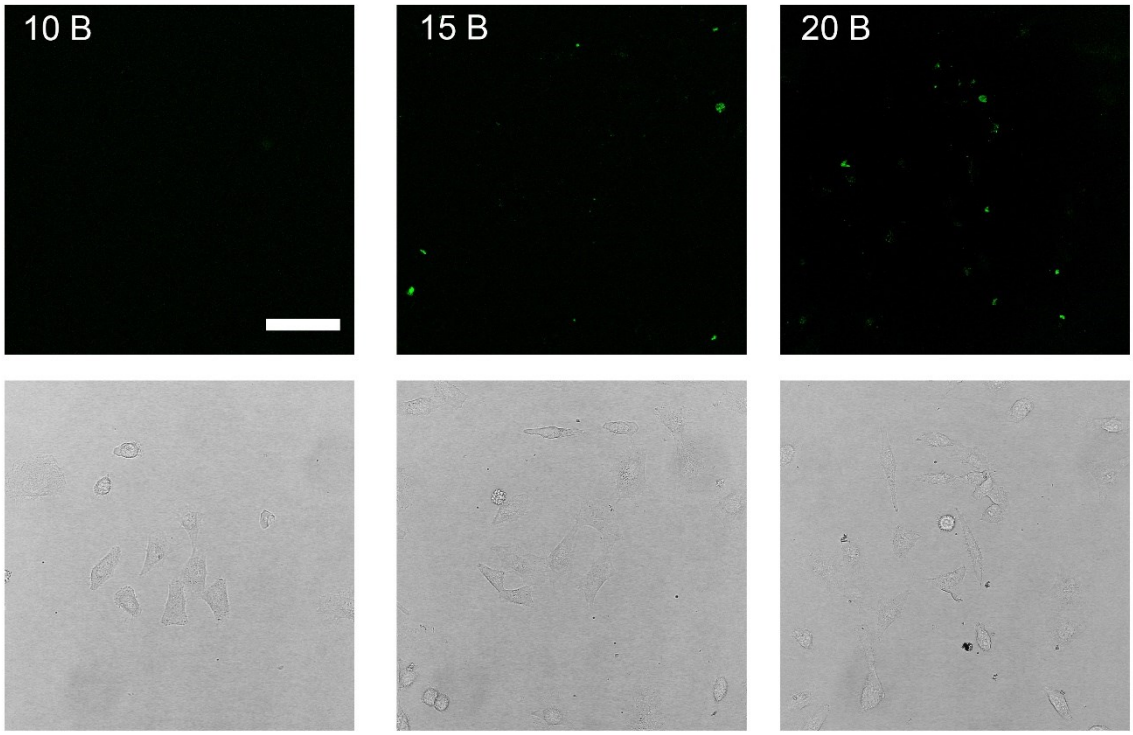

Figure 54: Confocal fluorescence (top) and transmission images (bottom) of a 5 µM uptake experiment of guanidine block copolymers, scale bar is 50 µm.

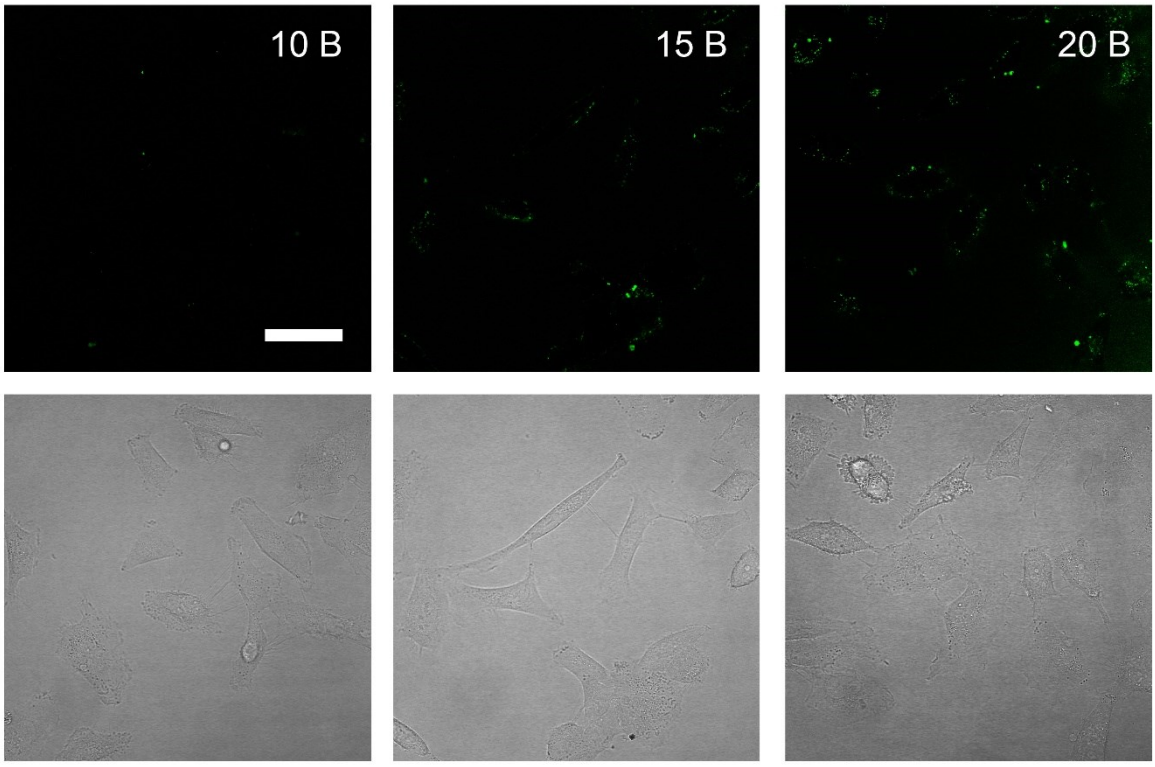

Figure 55: Confocal fluorescence (top) and transmission images (bottom) of a 10 µM uptake experiment of guanidine block copolymers, scale bar is 50 µm.

Uptake studies with flow cytometry

The uptake efficiency of the guanidinium polymers was further quantified by flow cytometry. For comparison R8 was also included in this study. HeLa cells were incubated with 10 µM polymer solutions, untreated cells were used as a negative control and R8 was used a positive control. Cells were treated with trypsin to remove membrane-bound peptides (R8) before measurement. The polymers will resist this treatment and therefore the fluorescence measured in these experiments may be an overestimation (Figure 56). The block copolymers **19**-15B and **19**-20B showed an uptake which was lower than R8; **19**-20B had an uptake efficiency of 50% compared to R8. The random copolymers **19**-15G and **19**-20G carried the same number of guanidinium groups as the block copolymers **19**-15B and **19**-20B but were not taken up, showing that the clustering of these functional groups, as in the block copolymer, is essential for uptake. The chances that a domain of 8 guanidinium groups is formed in the random polymers are really small; $6.0*10^{-6}$ % for **19**-10G, $4.3*10^{-5}$ % for **19**-15G and $4.6*10^{-4}$ % for **19**-20G, so the presence of large enough domains can be excluded. The introduction of more guanidinium groups led to an increase in cellular uptake. So both the monomer distribution as the degree of functionalisation is important for cellular uptake.

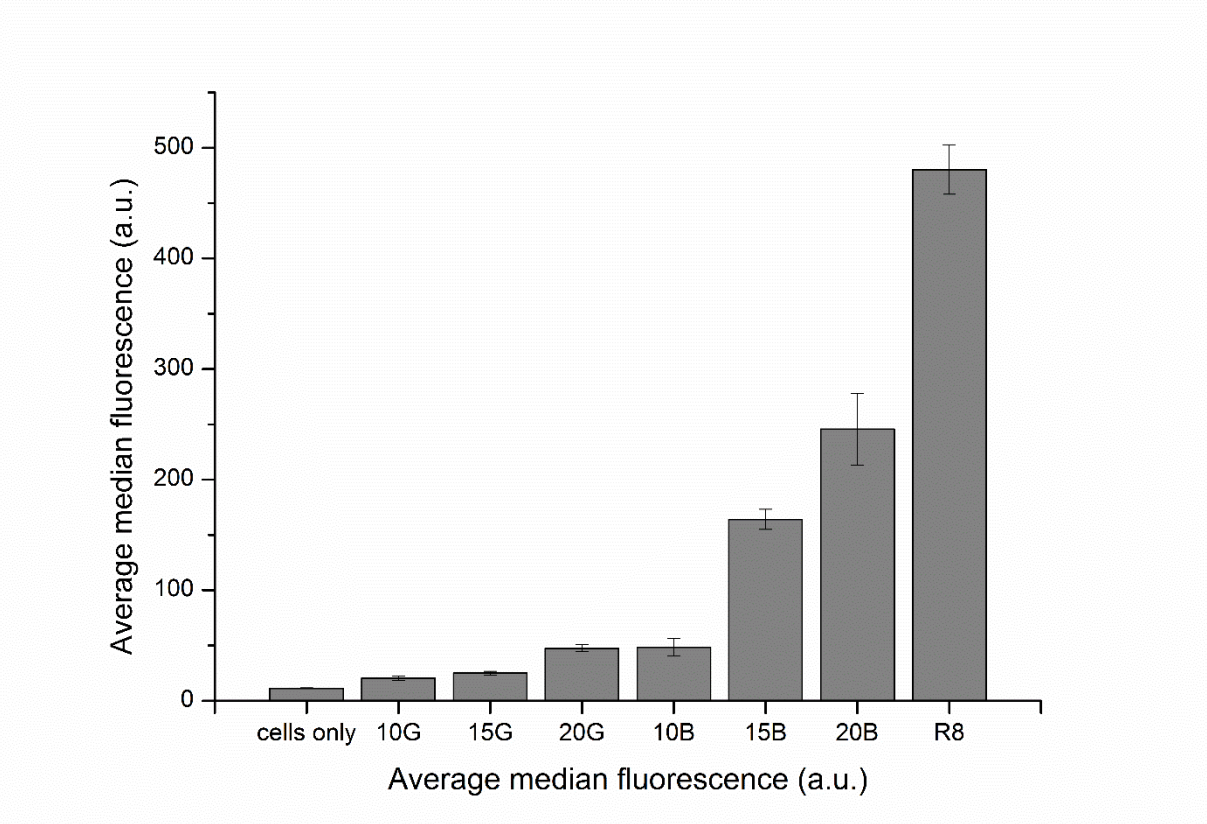

Figure 56: Flow cytometry results of uptake studies of HeLa cells at 10 µM 90 minutes incubation.

The lower uptake efficiency of the polymeric constructs might be due to the size of the polymeric chains, bigger constructs usually need longer incubation times. A similar effect is seen for nanoparticles covered with poly(ethylene glycol) (PEG) chains. The PEGylation suppresses the cellular uptake of these nanoparticles.[36, 37] The MoTrs in literature with higher uptake compared to R8 or TAT are not polymeric but short oligomeric chains. Uptake efficiencies might be increased by testing longer incubation times, because larger objects require more time to cross the cell membrane. Moreover, the length of the spacer between the polymeric backbone and the guanidinium group can be extended by using C3MestOx instead of MestOx to introduce more flexibility which is important for uptake efficiency as reported

in literature.[3, 4] In literature only one polymeric MoTrs has been quantified with flow cytometry, this preorganised non-hydrolysable chiral bicyclic structure (**13**) showed a two times better uptake than TAT.[25] R8s uptake efficiency is also double compared to TAT,[4] so **13** should be comparable to R8 and its uptake is probably higher than **19-**20B.

Conclusions

Poly(2-oxazoline)s with methyl ester groups were post-polymerisation modified to amines and subsequently to guanidinium copolymers. Both random and block methyl ester copolymers were prepared and modified. Both amine and guanidine functionalised polymers from these series did not show toxicity up to 10 μM, however at 15 μM for the block copolymers containing amines or guanidines some minor toxicity was observed. Uptake studies showed that only the block copolymers with 15 or 20% functionalisation were taken up by cells, clearly demonstrating the influence of monomer distribution and degree of functionalisation. The efficiency was lower compared to R8, probably due to the size of the polymeric construct.

Acknowledgement

Saskia Bode is acknowledged for performing the cell studies.

Experimental

Materials

2-Chloroethylamine hydrochloride, methyl p-toluenesulfonate (MeOTs) and sodium carbonate were purchased from Acros Organics. FITC-BCN, officially BCN-POE_3-NH-DY_{495} conjugate (SX-A1030) was purchased from Synaffix BV (Oss, the Netherlands). N-Boc ethylene diamine was purchased from AK scientific. All other reagents were purchased from Sigma Aldrich and used as received, except 2-ethyl-2-oxazoline (EtOx) and methyl p-toluenesulfonate (MeOTs). These were purified by distillation over barium oxide and stored under argon. Dry solvents were obtained from a solvent purification system from MBraun MB SPS800 system under nitrogen atmosphere. Triethylamine was distilled over CaH_2 under argon atmosphere. MilliQ water was obtained from a Labconco Water Pro PS purification system (18.2 MΩ). Fetal calf serum (FCS) was obtained from Integro (Zaandam, The Netherlands), plain Dulbecco's Modified Eagle Medium (DMEM), RPMI-1640 and trypsin/EDTA were from PAA Laboratories (Pasching, Austria). HeLa CCL-2 cells were obtained from American Type Culture Collection (ATCC, Manassas, U.S.A.).

Instrumentation

Nuclear magnetic resonance (NMR) spectra were recorded on a Bruker DMX 500 (500 MHz for ^1H).

Infrared (IR) spectra were obtained using a Bruker Tensor 27 spectrometer in ATR mode.

Electro spray ionisation mass (ESI MS) spectra were recorded on a Thermo Finnigan LCQ Advantage Max.

Polymerisations were carried out in a Biotage Initiator Microwave System with Robot Eight utilizing capped reaction vials. These vials were heated to 140 °C overnight, allowed to cool to room temperature and filled with argon prior to use. All microwave polymerizations were performed with temperature control (IR sensor).

Size-exclusion chromatography (SEC) was performed on an Agilent 1260-series HPLC system equipped with a 1260 online degasser, a 1260 ISO-pump, a 1260 automatic liquid sampler (ALS), a thermostatted column compartment (TCC) at 50°C equipped with two PLgel 5 μm mixed-D columns and a guard column in series, a 1260 diode array detector

(DAD) and a 1260 refractive index detector (RID). The used eluent was DMA containing 50mM of LiCl at a flow rate of 0.500 ml/min. The spectra were analysed using the Agilent Chemstation software with the GPC add on. Molar mass and PDI values were calculated against PMMA standards from PSS.

Monomer synthesis

Monomers were synthesized as described in chapter 2.

Copolymer synthesis with azide terminus (P(EtOx-MestOx)N_3)

MestOx and EtOx were mixed under argon atmosphere in the right monomer ratio with methyl tosylate as initiator, a monomer:initiator ([M]/[I]) ratio of 100 and a final monomer concentration of 4 M in acetonitrile. This solution was heated for 20 minutes at 140 °C in the microwave. After cooling down, an excess sodium azide was added and the reaction was stirred overnight at 80 °C. The remaining solids were removed and the solvent was evaporated. The polymer was dissolved in DCM and precipitated twice in cold diethyl ether yielding a white foam.

P(EtOx-MestOx 84-12)N_3 (10G):

^{1}H NMR ($CDCl_3$. 500 MHz): δ 3.65 (br, OCH_3, 36 H), 3.46 (br, NCH_2CH_2N, 384 H), 2.96 (s, NCH_3, 3 H), 2.56 (br, $COCH_2CH_2CO$, 48 H), 2.35 (b, $COCH_2$, 168 H), 1.12 (br, CH_2CH_3, 252 H)

SEC: M_n 16.3 kDa, Đ 1.16

FTIR: 2100 cm^{-1} (azide), 1735 cm^{-1} (C=O of methyl ester)

P(EtOx-MestOx 84-16)N_3 (15G):

^{1}H NMR ($CDCl_3$. 500 MHz): δ 3.65 (br, OCH_3, 48 H), 3.46 (br, NCH_2CH_2N, 400 H), 2.96 (s, NCH_3, 3 H), 2.56 (br, $COCH_2CH_2CO$, 64 H), 2.35 (b, $COCH_2$, 168 H), 1.12 (br, CH_2CH_3, 252 H)

SEC: M_n 18.0 kDa, Đ 1.13

FTIR: 2100 cm^{-1} (azide), 1735 cm^{-1} (C=O of methyl ester)

P(EtOx-MestOx 84-23)N_3 (20G):

^{1}H NMR ($CDCl_3$. 500 MHz): δ 3.65 (br, OCH_3, 69 H), 3.46 (br, NCH_2CH_2N, 421 H), 2.96 (s, CH_3, 3 H), 2.56 (br, $COCH_2CH_2CO$, 92 H), 2.35 (b, $COCH_2$, 168 H), 1.12 (br, CH_2CH_3, 252 H)

SEC: M_n 18.0 kDa, Đ 1.17

FTIR: 2100 cm^{-1} (azide), 1735 cm^{-1} (C=O of methyl ester)

Block-copolymer synthesis with azide terminus (P(MestOx-b-MestOx)N_3)

MestOx, methyl tosylate and acetonitrile were mixed under argon atmosphere in the right ratios. This solution was heated for 20 minutes at 140 °C in the microwave. After cooling down EtOx was added and the solution was again heated for 20 minutes at 140 °C in the microwave. The final [M]/[I] ratio of 100 and a final monomer concentration (if all monomers would have been added at the same time) of 4 M. Sodium azide was added and the reaction was stirred overnight at 80 °C. The remaining solids were removed and the solvent was evaporated. The polymer was dissolved in DCM and precipitated twice in cold diethyl ether yielding a white foam (95-99%).

P(MestOx-b-EtOx 12-94)N_3 (10B):

^{1}H NMR ($CDCl_3$. 500 MHz): δ 3.65 (br, OCH_3, 36 H), 3.46 (br, NCH_2CH_2N, 424 H), 2.96 (s, NCH_3, 3 H), 2.56 (br, $COCH_2CH_2CO$, 48 H), 2.35 (b, $COCH_2$, 188 H), 1.12 (br, CH_2CH_3, 282 H)
SEC: MestOx block M_n 4.05 kDa, Đ 1.11; block copolymer: M_n 14.5 kDa, Đ 1.21
FTIR: 2100 cm^{-1} (azide), 1735 cm^{-1} (C=O of methyl ester)

P(MestOx-b-EtOx 15-84)N_3 (15B):
^{1}H NMR ($CDCl_3$. 500 MHz): δ 3.65 (br, OCH_3, 45 H), 3.46 (br, NCH_2CH_2N, 396 H), 2.96 (s, NCH_3, 3 H), 2.56 (br, $COCH_2CH_2CO$, 60 H), 2.35 (b, $COCH_2$, 168 H), 1.12 (br, CH_2CH_3, 252 H)
SEC: MestOx block M_n 5.0 kDa, Đ 1.11; block copolymer: M_n 14.1 kDa, Đ 1.20
FTIR: 2100 cm^{-1} (azide), 1735 cm^{-1} (C=O of methyl ester)

P(MestOx-b-EtOx 23-89)N_3 (20B):
^{1}H NMR ($CDCl_3$. 500 MHz): δ 3.65 (br, OCH_3, 69 H), 3.46 (br, NCH_2CH_2N, 408 H), 2.96 (s, NCH_3, 3 H), 2.56 (br, $COCH_2CH_2CO$, 69 H) 2.35 (b, $COCH_2$, 178 H), 1.12 (br, CH_2CH_3, 267 H)
SEC: MestOx block M_n 6.1 kDa, Đ 1.10; block copolymer: M_n 14.9 kDa, Đ 1.16
FTIR: 2100 cm^{-1} (azide), 1735 cm^{-1} (C=O of methyl ester)

Synthesis of PAOx(Et-NHBoc)N_3): amidation of methyl ester
500 mg P(MestOx-b-EtOx)N_3 or P(EtOx-MestOx)N_3 polymer was dissolved in 3 drops of DCM and 5 mL N-Boc ethylene diamine was added. The solution was stirred for 3 days at room temperature. 5 mL DCM was added and the polymer was precipitated in cold diethyl ether twice. The precipitate was collected and dissolved in DCM. The solvent was evaporated yielding a white foam (95-99%).

PAOx(Et-NHBoc 84-12)N_3 (10G):
^{1}H NMR ($CDCl_3$. 500 MHz): δ 3.46 (br, NCH_2CH_2N, 384 H), 3.25 (br, $CONHCH_2CH_2NHBoc$, 24 H) 3.00 (br, $CONHCH_2CH_2NHBoc$ &NCH_3, 27 H), 2.60 (br, $COCH_2CH_2CO$, 48 H) 2.35 (b, $COCH_2$, 168 H), 1.42 (br, $C(CH_3)_3$, 108 H), 1.12 (br, CH_2CH_3, 252 H)
FTIR: 2100 cm^{-1} (azide), 1703 cm^{-1} (C=O of *t*-butyl ester)

PAOx(Et-NHBoc 84-16)N_3 (15G):
^{1}H NMR ($CDCl_3$. 500 MHz): δ 3.46 (br, NCH_2CH_2N, 400 H), 3.25 (br, $CONHCH_2CH_2NHBoc$, 32 H) 3.00 (br, $CONHCH_2CH_2NHBoc$ &NCH_3, 35 H), 2.56 (br, $COCH_2CH_2CO$, 64 H) 2.35 (b, $COCH_2$, 168 H), 1.42 (br, $C(CH_3)_3$, 144 H), 1.12 (br, CH_2CH_3, 252 H)
FTIR: 2100 cm^{-1} (azide), 1703 cm^{-1} (C=O of *t*-butyl ester)

PAOx(Et-NHBoc 84-23)N_3 (20G):
^{1}H NMR ($CDCl_3$. 500 MHz): δ 3.46 (br, NCH_2CH_2N, 421 H), 3.25 (br, $CONHCH_2CH_2NHBoc$, 46 H) 3.00 (br, $CONHCH_2CH_2NHBoc$ &NCH_3, 49 H), 2.56 (br, $COCH_2CH_2CO$, 92 H), 2.35 (b, $COCH_2$, 168 H), 1.42 (br, $C(CH_3)_3$, 207 H),1.12 (br, CH_2CH_3, 252 H)
FTIR: 2100 cm^{-1} (azide), 1703 cm^{-1} (C=O of *t*-butyl ester)

PAOx(NHBoc-b-Et 12-94)N_3 (10B):

^{1}H NMR ($CDCl_3$. 500 MHz): δ 3.46 (br, NCH_2CH_2N, 424 H), 3.25 (br, $CONHCH_2CH_2NHBoc$, 24 H) 3.00 (br, $CONHCH_2CH_2NHBoc$ &NCH_3, 27 H), 2.56 (br, $COCH_2CH_2CO$, 48 H), 2.35 (b, $COCH_2$, 188 H), 1.42 (br, $C(CH_3)_3$, 108 H),1.12 (br, CH_2CH_3, 282 H)
FTIR: 2100 cm^{-1} (azide), 1703 cm^{-1} (C=O of *t*-butyl ester)

PAOx(NHBoc-b-Et 15-84)N_3 (15B):
^{1}H NMR ($CDCl_3$. 500 MHz): δ 3.46 (br, NCH_2CH_2N, 396 H), 3.25 (br, $CONHCH_2CH_2NHBoc$, 30 H) 3.00 (br, $CONHCH_2CH_2NHBoc$ &NCH_3, 33 H), 2.56 (br, $COCH_2CH_2CO$, 60 H), 2.35 (b, $COCH_2$, 168 H), 1.42 (br, $C(CH_3)_3$, 135 H),1.12 (br, CH_2CH_3, 252 H)
FTIR: 2100 cm^{-1} (azide), 1703 cm^{-1} (C=O of *t*-butyl ester)

PAOx(NHBoc-b-Et 23-89)N_3 (20B):
^{1}H NMR ($CDCl_3$. 500 MHz): δ 3.46 (br, NCH_2CH_2N, 408 H), 3.25 (br, $CONHCH_2CH_2NHBoc$, 46 H) 3.00 (br, $CONHCH_2CH_2NHBoc$ &NCH_3, 49 H), 2.56 (br, $COCH_2CH_2CO$, 69 H), 2.35 (b, $COCH_2$, 178 H), 1.42 (br, $C(CH_3)_3$, 207 H), 1.12 (br, CH_2CH_3, 267 H)
FTIR: 2100 cm^{-1} (azide), 1703 cm^{-1} (C=O of *t*-butyl ester)

Synthesis of PAOx(Et-NH_2)N_3: removal of Boc protecting group
500 mg PAOx (NHBoc-b-Et)N_3 or PAOx(Et-NHBoc)N_3 polymer was dissolved in 5 mL DCM and 5 mL TFA was added. The solution was stirred for 2 hours at room temperature and the solvent was evaporated. The polymer was dissolved in MeOH and precipitated twice in cold diethyl ether. The precipitated was collected and dissolved in MeOH. The solvent was evaporated yielding a colourless oil (95-99%).

PAOx(Et-NH_2 84-12)N_3 (10G):
^{1}H NMR (MeOD-d4. 500 MHz): δ 3.46 (br, NCH_2CH_2N, 384 H), 3.32&3.26 (br, $CONHCH_2CH_2NH_2$, 24 H), 3.07 (br, $CONHCH_2CH_2NH_2$ &NCH_3, 27 H), 2.65 (br, $COCH_2CH_2CO$, 48 H), 2.35 (b, $COCH_2$, 168 H), 1.12 (br, CH_2CH_3, 252 H)
FTIR: 3465 cm^{-1} (NH_2), 2100 cm^{-1} (azide)

PAOx(Et-NH_2 84-16)N_3 (15G):
^{1}H NMR (MeOD-d4. 500 MHz): δ 3.46 (br, NCH_2CH_2N, 400 H), 3.32&3.26 (br, $CONHCH_2CH_2NH_2$, 32 H), 3.07 (br, $CONHCH_2CH_2NH_2$ &NCH_3, 35 H), 2.65 (br, $COCH_2CH_2CO$, 64 H), 2.35 (b, $COCH_2$, 168 H), 1.12 (br, CH_2CH_3, 252 H)
FTIR: 3465 cm^{-1} (NH_2), 2100 cm^{-1} (azide)

PAOx(Et-NH_2 84-23)N_3 (20G):
^{1}H NMR (MeOD-d4. 500 MHz): δ 3.46 (br, NCH_2CH_2N, 421 H), 3.32&3.26 (br, $CONHCH_2CH_2NH_2$, 46 H), 3.07 (br, $CONHCH_2CH_2NH_2$ &NCH_3, 49 H), 2.65 (br, $COCH_2CH_2CO$, 92 H), 2.35 (b, $COCH_2$, 168 H), 1.12 (br, CH_2CH_3, 252 H)
FTIR: 3465 cm^{-1} (NH_2), 2100 cm^{-1} (azide)

PAOx(NH_2-b-Et 12-94)N_3 (10B):

^{1}H NMR (MeOD-d4. 500 MHz): δ 3.46 (br, NC$\underline{H_2}$C$\underline{H_2}$N, 424 H), 3.32&3.26 (br, CONHC$\underline{H_2}$CH$_2$NH$_2$, 24 H), 3.07 (br, CONHCH$_2$C$\underline{H_2}$NH$_2$ &NC$\underline{H_3}$, 27 H), 2.65 (br, COC$\underline{H_2}$C$\underline{H_2}$CO, 48 H), 2.35 (b, COC$\underline{H_2}$, 188 H), 1.12 (br, CH$_2$C$\underline{H_3}$, 282 H)
FTIR: 3465 cm^{-1} (NH$_2$), 2100 cm^{-1} (azide)

PAOx(NH$_2$-b-Et 15-84)N$_3$ (15B):
^{1}H NMR (MeOD-d4. 500 MHz): δ 3.46 (br, NC$\underline{H_2}$C$\underline{H_2}$N, 396 H), 3.32&3.26 (br, CONHC$\underline{H_2}$CH$_2$NH$_2$, 30 H), 3.07 (br, CONHCH$_2$C$\underline{H_2}$NH$_2$ &NC$\underline{H_3}$, 33 H), 2.65 (br, COC$\underline{H_2}$C$\underline{H_2}$CO, 60 H), 2.35 (b, COC$\underline{H_2}$, 168 H), 135 H),1.12 (br, CH$_2$C$\underline{H_3}$, 252 H)
FTIR: 3465 cm^{-1} (NH$_2$), 2100 cm^{-1} (azide)

PAOx(NH$_2$-b-Et 23-89)N$_3$ (20B):
^{1}H NMR (MeOD-d4. 500 MHz): δ 3.46 (br, NC$\underline{H_2}$C$\underline{H_2}$N, 408 H), 3.32&3.26 (br, CONHC$\underline{H_2}$CH$_2$NH$_2$, 46 H), 3.07 (br, CONHCH$_2$C$\underline{H_2}$NH$_2$ &NC$\underline{H_3}$, 49 H), 2.6 (br, COC$\underline{H_2}$C$\underline{H_2}$CO, 69 H), 2.35 (b, COC$\underline{H_2}$, 178 H), 1.12 (br, CH$_2$C$\underline{H_3}$, 267 H)
FTIR: 3465 cm^{-1} (NH$_2$), 2100 cm^{-1} (azide)

Synthesis of PAOx(Et-guanidine)N$_3$ or PAOx(Et-guanidine-FITC): Guanidinylation
This reaction was performed according to a literature procedure.[38] PAOx(NH$_2$-b-Et)N$_3$ or PAOx(Et-NH$_2$)N$_3$ polymer was dissolved in 2 mL 65 mM 1*H*-pyrazol-1-carboxaminidine hydrochloride. The pH was adjusted with 5% Na$_2$CO$_3$ solution to pH 9. The solution was stirred for 3 days at room temperature. The polymer was purified over Sephadex 25 and freeze dried, yielding a white fluffy powder (95-99%).

PAOx(Et-guanidine 84-12)N$_3$ (10G):
^{1}H NMR (MeOD-d4. 500 MHz): δ 3.46 (br, NC$\underline{H_2}$C$\underline{H_2}$N, 384 H), 3.28 (br, CONHC$\underline{H_2}$CH$_2$NH, 24 H), 3.07 (br, CONHCH$_2$C$\underline{H_2}$NH &NC$\underline{H_3}$, 27 H), 2.65 (br, COC$\underline{H_2}$C$\underline{H_2}$CO, 48 H), 2.35 (b, COC$\underline{H_2}$, 168 H), 1.12 (br, CH$_2$C$\underline{H_3}$, 252 H)
FTIR: 2100 cm^{-1} (azide)

PAOx(Et-guanidine 84-16)N$_3$ (15G):
^{1}H NMR (MeOD-d4. 500 MHz): δ 3.46 (br, NC$\underline{H_2}$C$\underline{H_2}$N, 400 H), 3.28 (br, CONHC$\underline{H_2}$CH$_2$NH, 32 H), 3.07 (br, CONHCH$_2$C$\underline{H_2}$NH &NC$\underline{H_3}$, 35 H), 2.65 (br, COC$\underline{H_2}$C$\underline{H_2}$CO, 64 H) 2.35 (b, COC$\underline{H_2}$, 168 H), 1.12 (br, CH$_2$C$\underline{H_3}$, 252 H)
FTIR: 2100 cm^{-1} (azide)

PAOx(Et-guanidine 84-23)N$_3$ (20G):
^{1}H NMR (MeOD-d4. 500 MHz): δ 3.46 (br, NC$\underline{H_2}$C$\underline{H_2}$N, 421 H), 3.28 (br, CONHC$\underline{H_2}$CH$_2$NH, 46 H), 3.07 (br, CONHCH$_2$C$\underline{H_2}$NH &NC$\underline{H_3}$, 49 H), 2.65 (br, COC$\underline{H_2}$C$\underline{H_2}$CO, 92 H), 2.35 (b, COC$\underline{H_2}$, 168 H), 1.12 (br, CH$_2$C$\underline{H_3}$, 252 H)
FTIR: 2100 cm^{-1} (azide)

PAOx(guanidine-b-Et 12-94)N$_3$ (10B):
^{1}H NMR (MeOD-d4. 500 MHz): δ 3.46 (br, NC$\underline{H_2}$C$\underline{H_2}$N, 424 H), 3.28 (br, CONHC$\underline{H_2}$CH$_2$NH, 24 H), 3.07 (br, CONHCH$_2$C$\underline{H_2}$NH &NC$\underline{H_3}$, 27 H), 2.65 (br, COC$\underline{H_2}$C$\underline{H_2}$CO, 48 H) 2.35 (b, COC$\underline{H_2}$, 188 H), 1.12 (br, CH$_2$C$\underline{H_3}$, 282 H)
FTIR: 2100 cm^{-1} (azide)

PAOx(guanidine-b-Et 15-84)N$_3$ (15B):

^{1}H NMR (MeOD-d4. 500 MHz): δ 3.46 (br, NC$\underline{H_2}$C$\underline{H_2}$N, 396 H), 3.28 (br, CONHC$\underline{H_2}$CH$_2$NH, 30 H) 3.07 (br, CONHCH$_2$C$\underline{H_2}$NH$_2$ &NC$\underline{H_3}$, 33 H), 2.65 (br, COC$\underline{H_2}$C$\underline{H_2}$CO, 60 H) 2.35 (b, COC$\underline{H_2}$, 168 H), 135 H),1.12 (br, CH$_2$C$\underline{H_3}$, 252 H)
FTIR: 2100 cm^{-1} (azide)

PAOx(guanidine-b-Et 23-89)N_3 (20B):
^{1}H NMR (MeOD-d4. 500 MHz): δ 3.46 (br, NC$\underline{H_2}$C$\underline{H_2}$N, 408 H), 3.28 (br, CONHC$\underline{H_2}$CH$_2$NH, 46 H) 3.07 (br, CONHCH$_2$C$\underline{H_2}$NH &NC$\underline{H_3}$, 49 H), 2.6 (br, COC$\underline{H_2}$C$\underline{H_2}$CO, 69 H) 2.35 (b, COC$\underline{H_2}$, 178 H), 1.12 (br, CH$_2$C$\underline{H_3}$, 267 H)
FTIR: 2100 cm^{-1} (azide)

Synthesis of PAOx(Et-guanidine)FITC: FITC coupling by click chemistry
0.33 g FITC-BCN was dissolved in 0.5 mL MeOH and added to PAOx(Et-guanidine)N_3 or PAOx(guanidine-b-Et)N_3 (0.95 eqv). The solution was stirred overnight. The solvent was evaporated and the polymer was dissolved in MilliQ. The polymer was purified over Sephadex 25 and freeze dried yielding a yellow fluffy powder (95-99%). FTIR measurements did not show a azide stretch anymore.

Cell culture and cell viability assays
Cell culture
HeLa CCL-2 cells were maintained in sterile conditions in Dulbecco's Modified Eagle's medium (DMEM) supplemented with 10% heat-inactivated fetal calf serum (FCS). Cells were maintained on tissue culture plastic and kept at 37 °C in a humidified atmosphere of 7.5% CO_2. Cells were passaged every 2-3 days. Prior to cell viability assays or cellular uptake studies, cells within a confluent layer were detached using trypsin/EDTA. Cells were then resuspended in FCS-supplemented DMEM and the number of cells was counted using a standard inverted microscope and a cell counting chamber (Fuchs-Rosenthal).

Cell viability assay
Cell viability was evaluated using Cell Counting Kit-8 (CCK-8, Dojindo Molecular Technologies). HeLa cells were seeded in 96-well plates to obtain 40,000 cells/well the day of the experiment. On the day of the experiment, cells were incubated with a 100 µL solution of polymer FCS-supplemented DMEM for 90 minutes at 37 °C. The polymer concentration was varied to study the optimal concentration for cellular uptake experiments, concentrations of 5, 10 and 15 µM were used. After incubation, cells were washed 3 times with DMEM + 10% FCS and maintained in this solution after the last washing step. After 4 hours of incubation, the supernatant was removed and a solution of CCK-8 (10 % in DMEM + 10% FCS) was added. After 3 hours of incubation at 37 °C, the absorbance was measured at 490 nm using a microplate reader (Wallac Victor 1420 multilabel counter, Perkin Elmer). The experiments were performed in triplicate and repeated twice independently. Mean values +/- standard deviation are given in Figure 53.

Confocal laser scanning microscopy
HeLa cells were seeded in chambered coverslips (Nunc, Wiesbaden, Germany) at a density of 40,000 cells (one day) or 20,000 cells per well (two days prior) to the experiment. Fluorescein was excited by an Argon laser at 488 nm and emission was collected between 500 and 550 nm. Cells were incubated with the 5 µM or 10 µM polymer solutions for 90 min at 37 ºC. After incubation, cells were washed twice with DMEM + 10 % FCS and the living cells were analyzed immediately by confocal microscopy using a TCS SP5 confocal microscope (Leica

Microsystems, Mannheim, Germany) equipped with an HCX PL APO 63 x N.A. 1.2 water immersion lens. Fluorescein was excited by an argon laser at 488 nm and emission was collected between 500 and 550 nm.

Flow cytometry

HeLa cells were seeded in 24-well plates (Sarstedt, Numbrecht, Germany) one (80,000 cells/well) or two (40,000 cells/well) days prior to the experiment. On the day of the experiment, cells were incubated with the polymer solutions (10 µM) for 90 min at 37 °C in RPMI (Roswell Park Memorial Institute medium) + 10% FCS. After washing the cells with HBS buffer pH 7.4 (10 mM HEPES, 135 mM NaCl, 5 mM KCl, 5 mM $MgCl_2$, 1.8 mM $CaCl_2$), cells were detached by trypsinisation for 5 minutes, spun down and resuspended in 200 µL RPMI + 10% FCS. The fluorescence was measured using a FACS Calibur flow cytometer (BD Biosciences, Erembodegem, Belgium) and subsequently data was analysed with the Summit software (Fort Collins, U.S.A.). Results were based on 10,000 gated cells.

Supplementary information

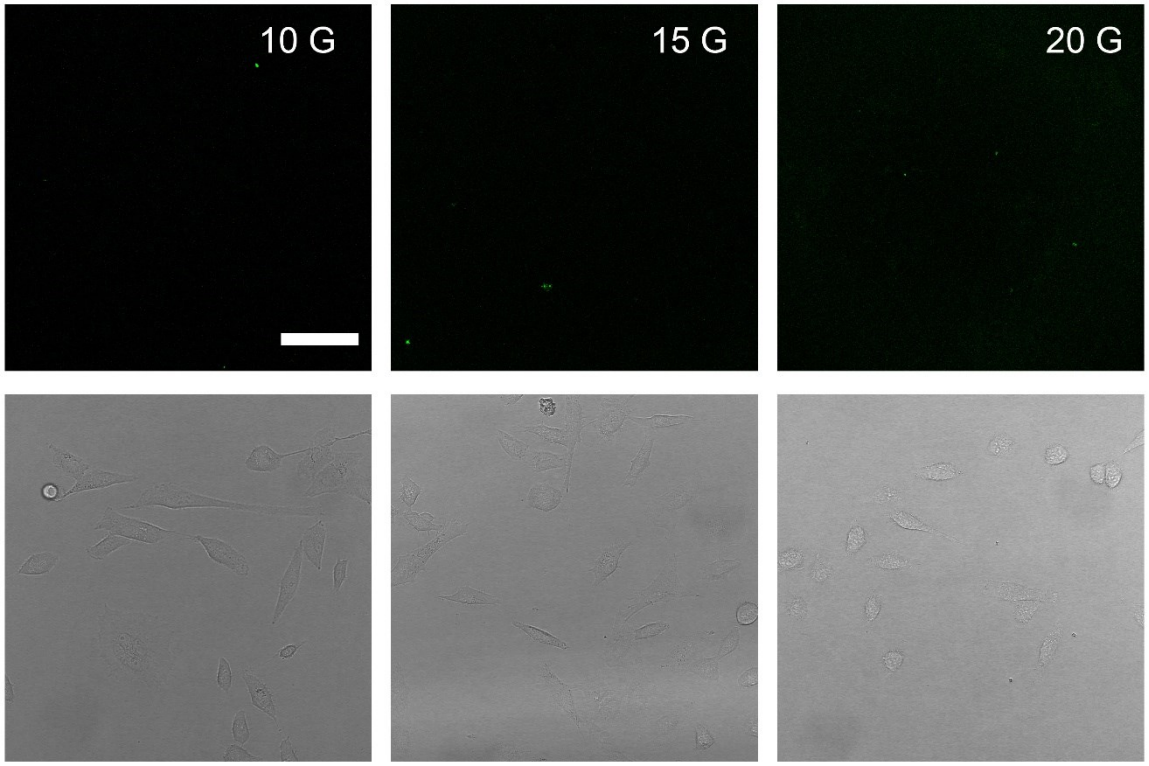

Figure S 18: Confocal fluorescence (top) and transmission (bottom) images of a 5 µM uptake experiment of guanidine random copolymers, scale bar is 50 µm.

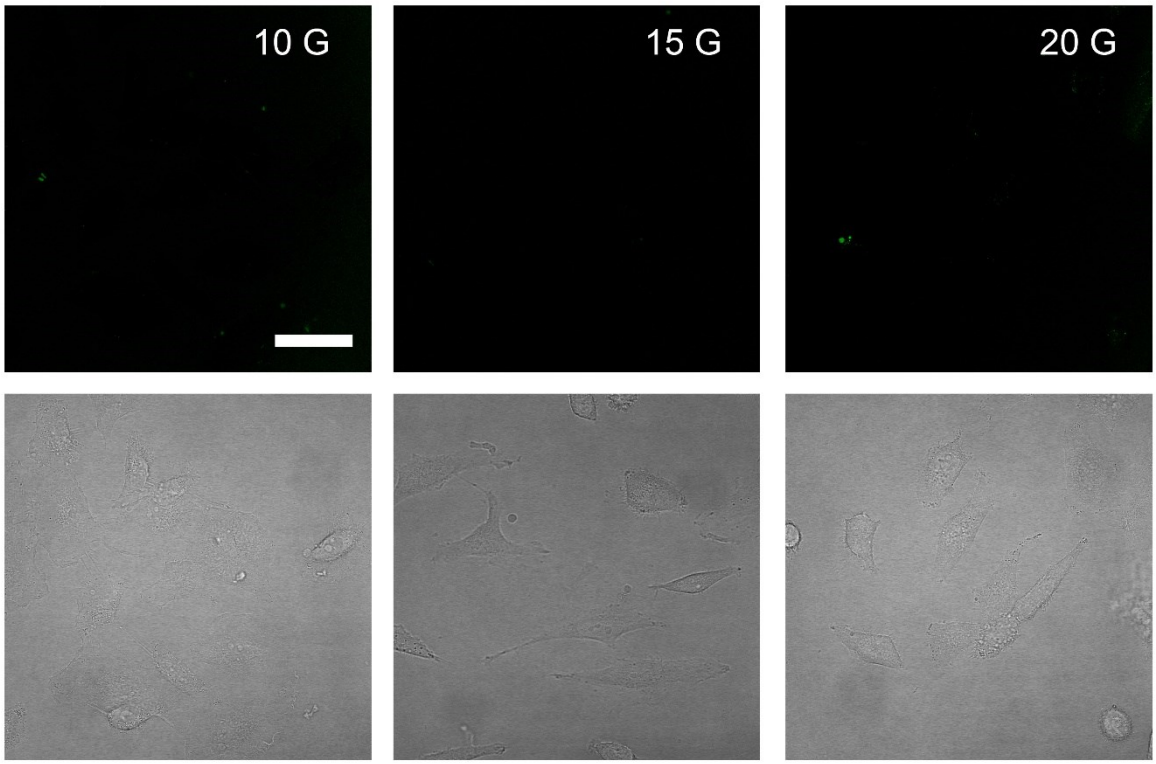

Figure S 19: Confocal fluorescence (top) and transmission images (bottom) of a 10 μM uptake experiment of guanidine random copolymers, scale bar is 50 μm.

References

1. Milletti, F. *Drug Discovery Today* **2012,** 17, (15–16), 850-860.
2. Stewart, K. M.; Horton, K. L.; Kelley, S. O. *Org. Biomol. Chem.* **2008,** 6, (13), 2242-2255.
3. Stanzl, E. G.; Trantow, B. M.; Vargas, J. R.; Wender, P. A. *Acc. Chem. Res.* **2013,** 46, (12), 2944-2954.
4. Wender, P. A.; Mitchell, D. J.; Pattabiraman, K.; Pelkey, E. T.; Steinman, L.; Rothbard, J. B. *Proc. Natl. Acad. Sci. U.S.A.* **2000,** 97, (24), 13003-13008.
5. Bode, S. A.; Wallbrecher, R.; Brock, R.; van Hest, J. C.; Lowik, D. W. *Chem. Commun.* **2014,** 50, (4), 415-7.
6. Wender, P. A.; Galliher, W. C.; Goun, E. A.; Jones, L. R.; Pillow, T. H. *Advanced drug delivery reviews* **2008,** 60, (4–5), 452-472.
7. Wender, P. A.; Cooley, C. B.; Geihe, E. I. *Drug Discovery Today* **2012,** 9, (1), e49-e55.
8. Umezawa, N.; Gelman, M. A.; Haigis, M. C.; Raines, R. T.; Gellman, S. H. *J. Am. Chem. Soc.* **2002,** 124, (3), 368-369.
9. Rueping, M.; Mahajan, Y.; Sauer, M.; Seebach, D. *ChemBioChem* **2002,** 3, (2-3), 257-259.
10. Rothbard, J. B.; Kreider, E.; VanDeusen, C. L.; Wright, L.; Wylie, B. L.; Wender, P. A. *Journal of Medicinal Chemistry* **2002,** 45, (17), 3612-3618.
11. Wender, P. A.; Rothbard, J. B.; Jessop, T. C.; Kreider, E. L.; Wylie, B. L. *J. Am. Chem. Soc.* **2002,** 124, (45), 13382-13383.
12. Luedtke, N. W.; Carmichael, P.; Tor, Y. *J. Am. Chem. Soc.* **2003,** 125, (41), 12374-12375.

13. Chung, H.-H.; Harms, G.; Min Seong, C.; Choi, B. H.; Min, C.; Taulane, J. P.; Goodman, M. *Pept. Sci.* **2004,** 76, (1), 83-96.
14. Nair, J. B.; Mohapatra, S.; Ghosh, S.; Maiti, K. K. *Chem. Commun.* **2015,** 51, (12), 2403-2406.
15. Maiti, K. K.; Lee, W. S.; Takeuchi, T.; Watkins, C.; Fretz, M.; Kim, D.-C.; Futaki, S.; Jones, A.; Kim, K.-T.; Chung, S.-K. *Angew. Chem. Int. Ed.* **2007,** 46, (31), 5880-5884.
16. Maiti, K. K.; Jeon, O.-Y.; Lee, W. S.; Chung, S.-K. *Chem. Eur. J.* **2007,** 13, (3), 732-732.
17. Cooley, C. B.; Trantow, B. M.; Nederberg, F.; Kiesewetter, M. K.; Hedrick, J. L.; Waymouth, R. M.; Wender, P. A. *J. Am. Chem. Soc.* **2009,** 131, (45), 16401-16403.
18. Gabriel, G. J.; Madkour, A. E.; Dabkowski, J. M.; Nelson, C. F.; Nüsslein, K.; Tew, G. N. *Biomacromolecules* **2008,** 9, (11), 2980-2983.
19. Kolonko, E. M.; Kiessling, L. L. *J. Am. Chem. Soc.* **2008,** 130, (17), 5626-5627.
20. Kolonko, E. M.; Pontrello, J. K.; Mangold, S. L.; Kiessling, L. L. *J. Am. Chem. Soc.* **2009,** 131, (21), 7327-7333.
21. Som, A.; Reuter, A.; Tew, G. N. *Angew. Chem. Int. Ed.* **2012,** 51, (4), 980-983.
22. Som, A.; Tezgel, A. O.; Gabriel, G. J.; Tew, G. N. *Angew. Chem. Int. Ed.* **2011,** 50, (27), 6147-6150.
23. Bang, E.-K.; Gasparini, G.; Molinard, G.; Roux, A.; Sakai, N.; Matile, S. *J. Am. Chem. Soc.* **2013,** 135, (6), 2088-2091.
24. Gasparini, G.; Bang, E.-K.; Molinard, G.; Tulumello, D. V.; Ward, S.; Kelley, S. O.; Roux, A.; Sakai, N.; Matile, S. *J. Am. Chem. Soc.* **2014,** 136, (16), 6069-6074.
25. Fernández-Carneado, J.; Van Gool, M.; Martos, V.; Castel, S.; Prados, P.; de Mendoza, J.; Giralt, E. *J. Am. Chem. Soc.* **2005,** 127, (3), 869-874.
26. Herce, H. D.; Garcia, A. E.; Cardoso, M. C. *J. Am. Chem. Soc.* **2014,** 136, (50), 17459-17467.
27. Hoogenboom, R. *Angew. Chem. Int. Ed.* **2009,** 48, 7978-7994.
28. Verbraeken, B.; Lava, K.; Hoogenboom, R., Poly(2-oxazoline)s. In *Encyclopedia of Polymer Science and Technology*, John Wiley & Sons, Inc.: 2014; pp 1-51.
29. Hoogenboom, R. Polyoxazoline polymers and methods for their preparation conjugates of these polymers and medical uses thereof. WO 2013/103297 A1, 11 July 2013, 2013.
30. Mees, M.; Hoogenboom, R. *Macromolecules* **2015,** 48, (11), 3531-3538.
31. Grogna, M.; Cloots, R.; Luxen, A.; Jerome, C.; Desreux, J. F.; Detrembleur, C. *J Mater Chem* **2011,** 21, 12917-12926.
32. Steunenberg, P.; Könst, P. M.; Scott, E. L.; Franssen, M. C. R.; Zuilhof, H.; Sanders, J. P. M. *Eur. Polym. J.* **2013,** 49, (7), 1773-1781.
33. Bouten, P. J. M.; Hertsen, D.; Vergaelen, M.; Monnery, B. D.; Boerman, M. A.; Goossens, H.; Catak, S.; van Hest, J. C. M.; Van Speybroeck, V.; Hoogenboom, R. *Polym. Chem.* **2015,** 6, (4), 514-518.
34. Bouten, P. J. M.; Hertsen, D.; Vergaelen, M.; Monnery, B. M.; Catak, S.; van Hest, J. C. M.; Van Speybroeck, V.; Hoogenboom, R. *J. Polym. Sci., Part A: Polym. Chem.* **2015,** accepted, DOI: 10.1002/pola.27733.
35. Dojindo Measuring Cell Viability/Cytotoxicity: Cell Counting Kit-8. http://www.dojindo.com/Protocol/Cell_Proliferation_Protocol_Colorimetric.pdf (last accessed 2015-04-23),
36. Liu, T.; Thierry, B. *Langmuir* **2012,** 28, (44), 15634-15642.
37. Hama, S.; Itakura, S.; Nakai, M.; Nakayama, K.; Morimoto, S.; Suzuki, S.; Kogure, K. *J Control Release* **2015,** 206, 67-74.

38. Qin, Z.; Liu, W.; Li, L.; Guo, L.; Yao, C.; Li, X. *Bioconjugate Chem.* **2011,** 22, (8), 1503-1512.

Chapter 6

Development of poly(2-oxazoline) based tissue tape

Abstract
One of the main problems in abdominal surgery is the occurrence of leakages and related infections. A number of products are available to seal the wounds, but none of them has an excellent performance on all aspects. Here we present the development of a tissue tape based on poly(2-oxazoline)s, bearing *N*-hydroxysuccinimide (NHS) esters as tissue reactive groups. Two synthetic procedures were established for the preparation of NHS-ester functional poly(2-oxazoline)s. Also an amine functional polymer was made to provide crosslinking between the NHS-ester functionalised poly(2-oxazoline)s allowing to make self-standing crosslinked polymer films. Although these films provided tissue adhesion, a backing material was introduced to provide extra mechanical support and to avoid double-sided adhesion. In this way the strength of the films was significantly improved. Although we successfully demonstrated tissue adhesive properties, the reproducibility of the preliminary results was not optimal and the mechanical properties still need to be improved further.

Introduction
The efficient and reliable closure of internal and external surgical wounds is one of the greatest challenges in surgery. The traditional techniques using sutures and staples have improved in the last decades, but they still have limitations: the most common and serious one is leakage. Gastro-intestinal anastomoses, for example, have a 3-15% risk of leakage which can cause intra-abdominal abscesses, fistula, peritonitis and mortality.[1, 2] A number of innovative materials are available and being developed to provide surgeons an alternative to the current wound closure procedures, although an optimal methodology has not been found yet. Wound-closure materials, which are normally described as haemostatic agents, sealants or adhesives, should meet a significant number of requirements; they must be safe, effective, easily usable, cheap, approved by the Food and Drug Administration (FDA) or labelled with a Conformité Européenne (European Community, CE) mark, biocompatible and biodegradable. From a mechanical point of view they should match the properties of the underlying tissue, they should have an acceptable swelling index and be shelf stable. Most available sealants are lacking in one or more of these requirements.[3-5]

DuraSeal™ Dural Sealant is a poly(ethylene glycol) (PEG)-based sealant used in combination with sutures to close the dural membrane after cranial surgery to prevent leakage of cerebrospinal fluid. This two-component system crosslinks spontaneously when the compounds are mixed. A four-armed star-PEG endcapped with N-hydroxysuccinimide (NHS) esters reacts with trilysine, a tetra-amine crosslinker, yielding a watertight crosslinked network within seconds.[3-9] The NHS ester is an activated ester which can react with the amines present in the crosslinker and amines present in the tissue, allowing covalent binding of the tissue adhesive and the underlying tissue. The adhesion of the DuraSeal product is excellent, but the cohesion is weak. This is due to the poor mechanical properties of PEG, it has a low glass transition temperature (T_g< -40 °C) and a tendency to crystallize into a brittle material.[3, 10] Also important is that the functional groups on the PEG polymer are only present at the termini, so a maximum of 2, 4 or 8 groups for linear, 4-arm star or 8-arm star PEG respectively, can be introduced.

In order to significantly improve on the existing Duraseal™ technology, we aimed to develop a tissue adhesive material with increased crosslink density, based on poly(2-alkyl/aryl-2-oxazoline)s (PAOx), a biocompatible polymer[11-13] containing side chain NHS esters (Figure 57). By crosslinking the PAOx-NHS polymers with trilysine or by a poly(2-oxazoline) with side chain amine functionality, it was expected that a mechanically robust self-standing polymeric tape could be formed. The material properties of this film could furthermore be

adjusted by controlling the content of NHS, the overall monomer composition of the polymers and by adding different ratios of amine-based crosslinker. The adhesion properties of the tape would originate from the remaining activated esters on its surface that can react with amines found on the lysine residues of any protein in tissue, providing covalent conjugation. In this chapter the synthetic procedures toward NHS- functional PAOx are described as well as their application in preliminary tissue tape preparations.

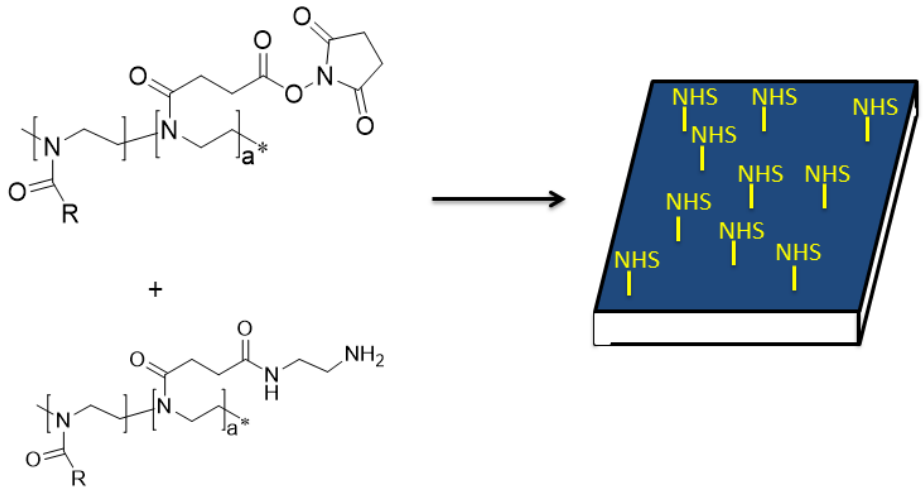

Figure 57: Design of a poly(2-alkyl/aryl-2-oxazoline) based tissue tape consisting of side chain functionalised polymers containing NHS or amine groups.

Results and discussion

In order to prepare a PAOx tissue tape, both an NHS-ester functional and amine-functional PAOx had to be synthesised. Two approaches were followed (Scheme 13). The first route started with commercially available poly(2-ethyl-oxazoline) (PEtOx, Aquazol 50), which was first partially hydrolysed to the corresponding secondary amine backbone,[14-16] and subsequently modified via an amidation reaction to the desired PAOx.[17] In the second approach, the functionalities were directly introduced during the polymerisation of PAOx.[13, 18-23]

Partial hydrolysis route

PEtOx was partially hydrolysed using acidic conditions,[15-17, 24] yielding a copolymer of PEtOx and poly(ethylene imine) (PEtOx-PEI, **1**). The secondary amines of the PEtOx-PEI backbone were used for further functionalisation, by a coupling reaction with methyl succinyl chloride to yield a methyl ester-functionalised polymer, (PEtOx-COOMe, **2**). Subsequently, the methyl esters were removed by hydrolysis with lithium hydroxide, yielding an acid-functionalised polymer, PEtOx-COOH (**3**). These carboxylic acids were finally functionalised with NHS using carbodiimide chemistry, yielding PAOx-NHS (**4**).

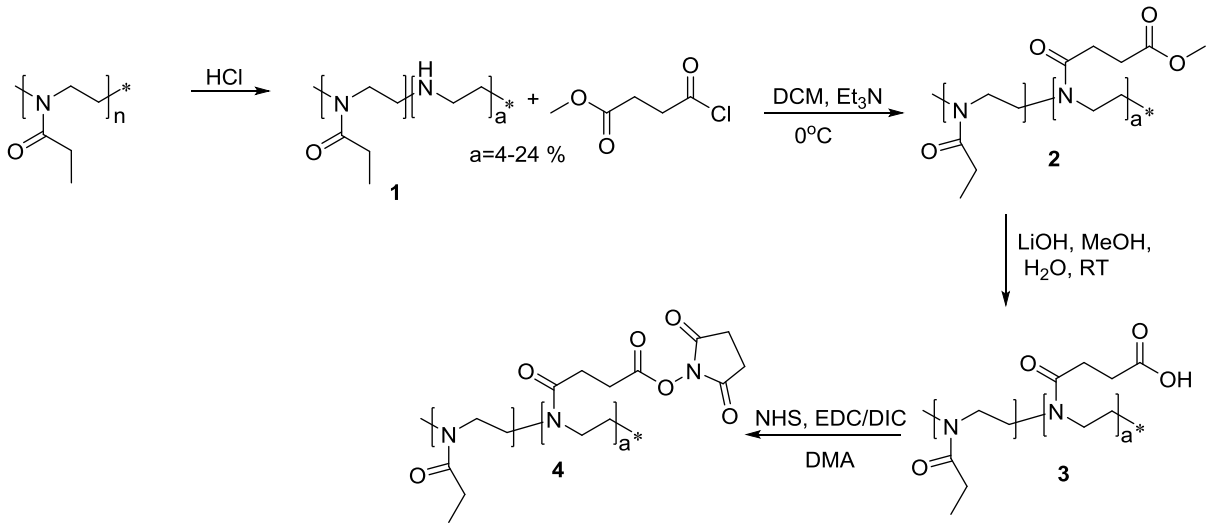

Scheme 13: PAOx-NHS synthesis via partial hydrolysis of poly(2-ethyl-2-oxazoline)

Hydrolysis of PEtOx has been extensively studied,[16, 24] and it was demonstrated that this process is independent of chain length, but highly dependent on temperature. The hydrolysis conversion after 120 minutes is 97% at an internal reaction temperature of 100 °C, 54% at 90 °C, 14% at 73 °C and only 4% at 57 °C.[24] By choosing reaction time and temperature, the degree of hydrolysis can thus be tuned. Because we aimed for a hydrolysis degree of maximum 20% to have a reasonable amount of crosslinkable groups, but avoiding high crosslink densities leading to very stiff materials, we selected 73 °C to have a controlled hydrolysis. We first determined the hydrolysis kinetics of Aquazol® 50, a commercially available PEtOx with a weight average molecular weight of 50 kDa and a dispersity of 3-4. (Figure 58). Kinetics reported in literature[24] were performed with 2.38 g of Aquazol; as we performed the hydrolysis at a large scale using 25 g of Aquazol, more time was needed to heat up the entire reaction mixture to 73 °C, which led to a slower rate of hydrolysis at the start of the reaction.

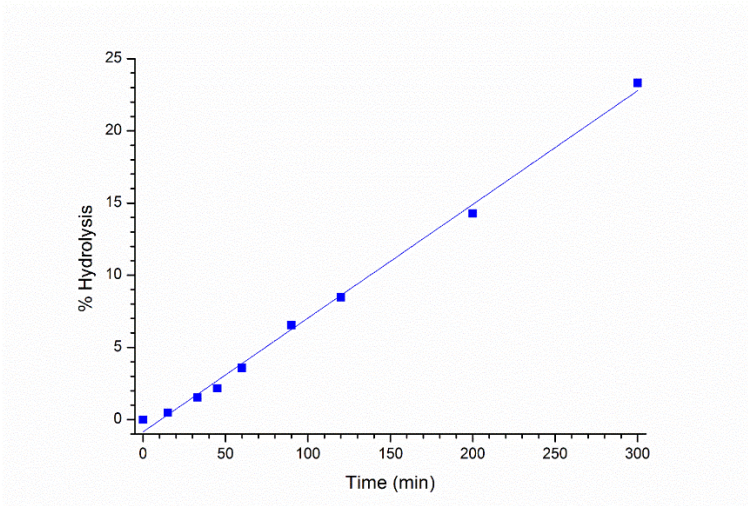

Figure 58: Hydrolysis kinetics of Aquazol® 50 at 73 °C for 25 g of polymer in 526 mL of 5.8 M HCl solution (amide concentration of 0.48 M)

The degree of hydrolysis was not perfectly controllable with this method, and it was also affected by temperature fluctuations of the oil bath. To minimize these fluctuations, the temperature was controlled with a temperature probe in the oil bath and regularly checking the internal temperature and adjusting the probe temperature if necessary. For example, when

aiming at 5% hydrolysis, the final degree of hydrolysis was between 4 and 7.5%, when aiming for 10% hydrolysis, the final degree of hydrolysis was 9-12% and when aiming for 20% hydrolysis 16-24% hydrolysis was observed.

The resulting amine of the PEI was reacted with methyl succinyl chloride in the presence of triethyl amine to obtain the methyl ester functionalised polymer PEtOx-COOMe. Subsequently, the methyl ester was hydrolysed with LiOH to the corresponding carboxylic acid PEtOx-COOH. Both polymers were obtained with quantitative conversions according to ^{1}H NMR spectroscopy.

The NHS ester was first installed using 1-ethyl-3-(3-dimethylaminopropyl)carbodiimide (EDC), which was removed by washing with water. The purification procedure however also resulted in some loss of NHS from the polymer. Therefore, EDC was replaced by diisopropyl carbodiimide (DIC), which could efficiently be removed by precipitation of the polymer in diethyl ether. The NHS-ester content was subsequently determined by ^{1}H NMR and UV-Vis spectroscopy.[25]

In Table 10 an overview is given of the aimed degree of hydrolysis, the obtained degree of hydrolysis (PEI peaks in ^{1}H NMR at δ 2.8 ppm), and the methyl ester (^{1}H NMR peaks at δ 3.65 and 2.6 ppm), carboxylic acid (^{1}H NMR peak at δ 2.6 ppm) and NHS content (^{1}H NMR peaks at δ 2.9 ppm) obtained after purification. All modifications were determined by ^{1}H NMR spectroscopy, except for the NHS content, which was determined both by UV-Vis spectroscopy and ^{1}H NMR spectroscopy. Because the NMR results were more variable, and the UV measurements showed better reproducibility, the UV-values were used for further experiments. The table clearly shows the NHS polymers still contained some free carboxylic acid. Figure 59 depicts the ^{1}H NMR spectra of the different modification stages.

Table 10: Degree of hydrolysis of poly(2-ethyl-2-oxazoline): aimed vs obtained percentages and functionalisation with NHS. PEI: poly(ethylene imine)

Aimed PEI content (%)	PEI content obtained (%)	Methyl ester content (%)	COOH content (%)	NHS content obtained (UV/NMR %)
5	5.6	5.6	5.6	5.3 / 4.2
5	7.2	7.2	7.2	4.4 / 6.1
5	7.4	7.4	7.4	6.6 / 5.7
10	11.0	11	11	8.5 / 7.5
10	12.0	12	12	11.9 / 6.5
20	24.0	24	24	23.0 / 26.5

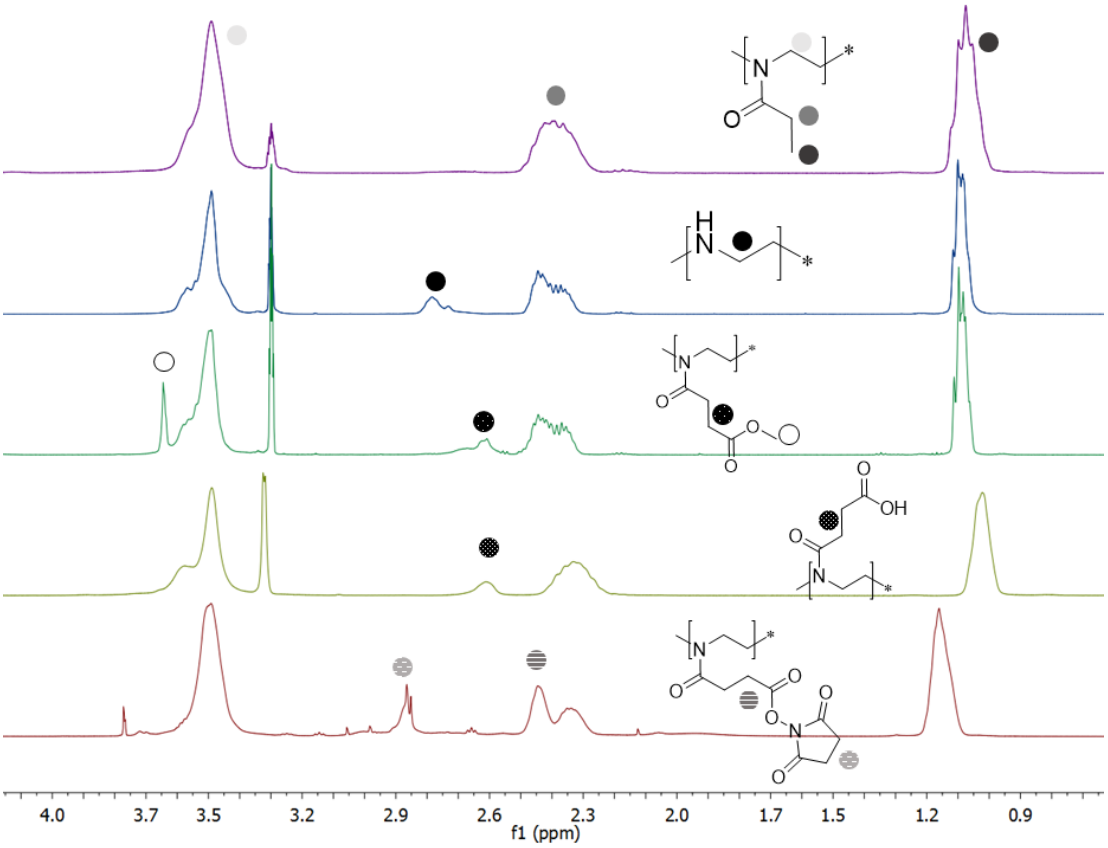

Figure 59: ^{1}H NMR spectra from top to bottom of PEtOx, PEtOx-PEI, PEtOx-COOMe, PEtOx-COOH and PEtOx-NHS

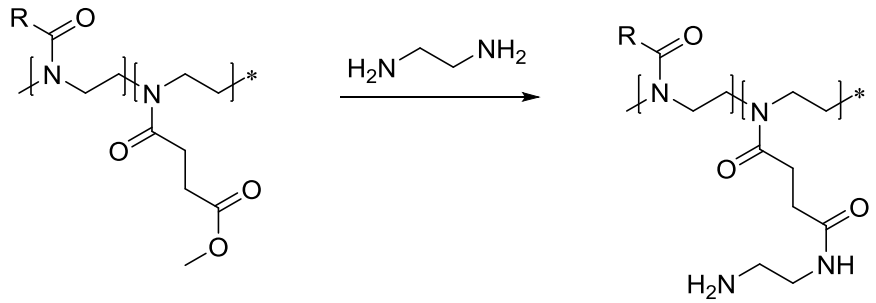

Figure 60: Amidation of PEtOx-COOMe with ethylene diamine to yield PEtOx-NH_2

PEtOx, side chain-functionalised with amines was easily prepared by reacting PEtOx-COOMe with ethylene diamine to yield PAOx-NH_2 (Figure 60). This reaction was performed in bulk, and 30 equivalents of ethylene diamine vs methyl ester were added to avoid coupling of polymer chains. A kinetic study revealed that the methyl ester was not fully converted after 6 hours, but it was after 17 hours, based on the disappearance of the methyl ester resonance in ^{1}H NMR (δ = 3.65 ppm) . This reaction proceeded faster than literature reports indicated.[26] Despite the large excess of ethylene diamine, polymers containing more than 20% methyl esters were partially crosslinked using this procedure, indicated by the presence of gel parts after redissolution of the polymer.

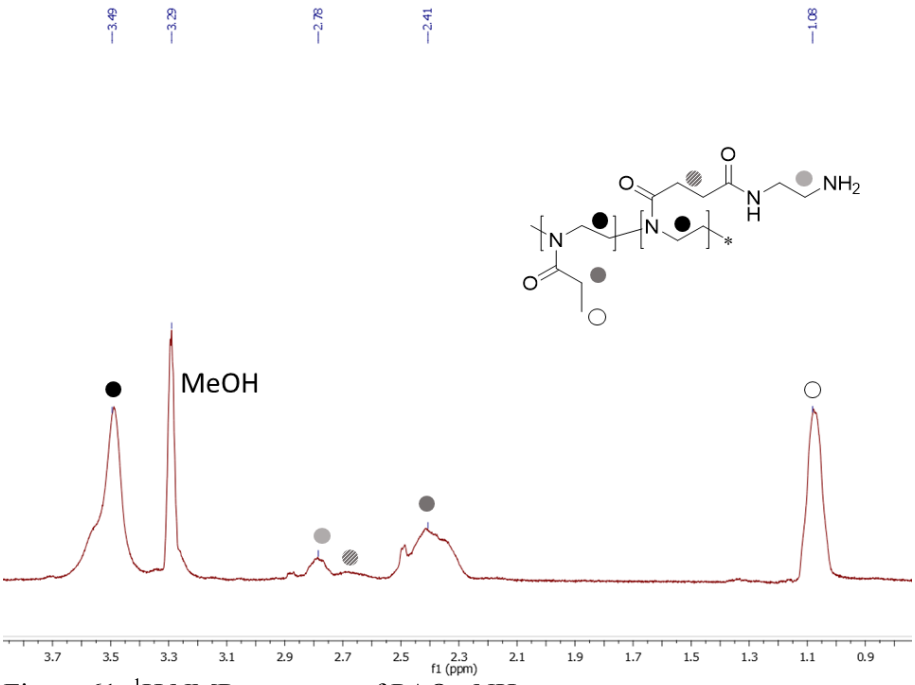

Figure 61: ^{1}H NMR spectrum of PAOx-NH_2

Monomer route

The second developed synthesis route entailed the copolymerisation of a 2-alkyl-2-oxazoline and a methyl ester-functional 2-oxazoline monomer, namely 2-methoxycarbonylethyl-2-oxazoline (MestOx). As both the acid and NHS ester functionalities were incompatible with cationic ring opening polymerisation (CROP) the methyl ester functional polymer was used as starting point for further modification. Although the partial hydrolysis route, described above, is faster, its lack of reproducibility is a big problem for biomedical applications. Furthermore, with the CROP method the ratios of functional and alkyl monomers can be controlled more precisely by addition of the right amounts of those monomers in the polymerisation mixture and the length of the polymer can be controlled by the monomer to initiator [M]/[I] ratio. The polymers obtained by this route are more defined than Aquazol and do not contain a molar mass fraction (M_n>40 kDa) that cannot be excreted by the kidneys. Here we used a MestOx content of 10 mol% for 2-*n*-propyl-2-oxazoline (*n*PropOx) copolymers, and 25, 50 or 75 mol% for 2-methyl-2oxaozline (MeOx) and EtOx copolymers; in all cases an [M]/[I] ratio of 100:1 was used.

MestOx homo- and copolymerisations were performed as described in chapter 3.

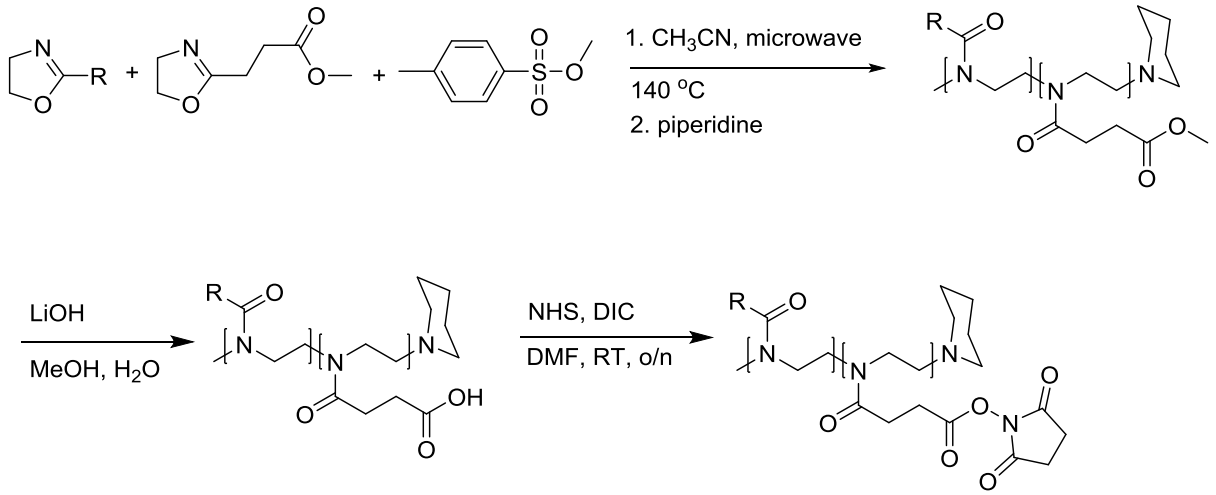

Figure 62: Copolymerisation of MestOx with MeOx (R = CH_3), EtOx ((R = CH_2CH_3) or *n*PropOx (R = $CH_2CH_2CH_3$) and subsequent functionalisation towards PAOx-NHS

Subsequently, the methyl esters of the copolymers were hydrolysed to the corresponding carboxylic acid and NHS was coupled (Figure 62). Unfortunately the NHS coupling to MeOx copolymers did not succeed, probably due to the presence of water in the very hygroscopic polymer; research was therefore continued with the *n*PropOx copolymers of which all MestOx groups were successfully converted into NHS esters (Table 11).

As alternative strategy, the methyl esters of PMestOx homopolymers were partially hydrolysed to the carboxylic acid by the addition of stoichiometric amounts of LiOH to the percentage to be hydrolysed (Figure 63). The degree of hydrolysis was determined by ^{1}H NMR spectroscopy and is listed in Table 11. Subsequently NHS was coupled to these polymers, yielding P(MestOx-NHS) copolymers.
PAOx-NH_2 based on the monomer route was prepared in the same way as described before. The P($EtOx_{77}$-$MestOx_{11}$) copolymer (Đ=1.35) was dissolved in an excess of ethylene diamine and stirred overnight to get PEtOx-NH_2.

Table 11: Methyl ester hydrolysis of PMestOx homo and copolymers, DP 100, to carboxylic acid, followed by NHS modification

Polymer [a]	Đ	Added equivalents of LiOH	Obtained degree of hydrolysis (%)	NHS content obtained (NMR / UV, %)
P($MeOx_{70}$-$MestOx_{23}$)	117	20	24	0
P($MeOx_{50}$-$MestOx_{49}$)	1.16	20	49	0
P($MeOx_{21}$-$MestOx_{57}$)	1.15	20	73	0
P($EtOx_{73}$-$MestOx_{23}$)	1.15	20	25	*
P($EtOx_{42}$-$MestOx_{36}$)	1.16	20	46	*
P($EtOx_{25}$-$MestOx_{76}$)	1.15	20	76	75#
P(*n*$PropOx_{87}$-$MestOx_{10}$)	1.40	2	10	10 / 10
$PMestOx_{95}$	1.15	0.252	23.7	25#
$PMestOx_{95}$	1.15	0.498	48.0	49#
$PMestOx_{95}$	1.15	0.753	74.0	74#

NHS content was only determined by ^{1}H NMR spectroscopy.
* Reaction to NHS was not performed.
a. monomer ratios were determined by ^{1}H NMR spectroscopy

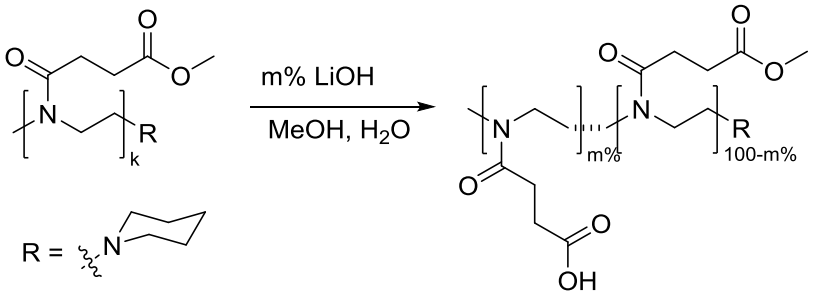

Figure 63: Partial hydrolysis of the methyl esters of PMestOx

After preparing the NHS- and amine-functional poly(2-oxazoline)s the next steps in the procedure toward a tissue tape material were solvent casting of the polymers on a backing material and a crosslinking step between the amine- and NHS-functional polymers. In order to determine the stability of PAOx-NHS polymers under casting conditions from methanol (alcohols are the preferred casting solvents), PAOx (*n*Prop-NHS 11%) was dissolved in deuterated methanol and NHS loss in time was determined by ^{1}H NMR spectroscopy by quantifying the residual bound NHS (Figure 64). After 90 minutes only 2% of the NHS groups was lost, which increased to 55% after 5 days. As film formation is a fast process, this was considered not to be a problem.

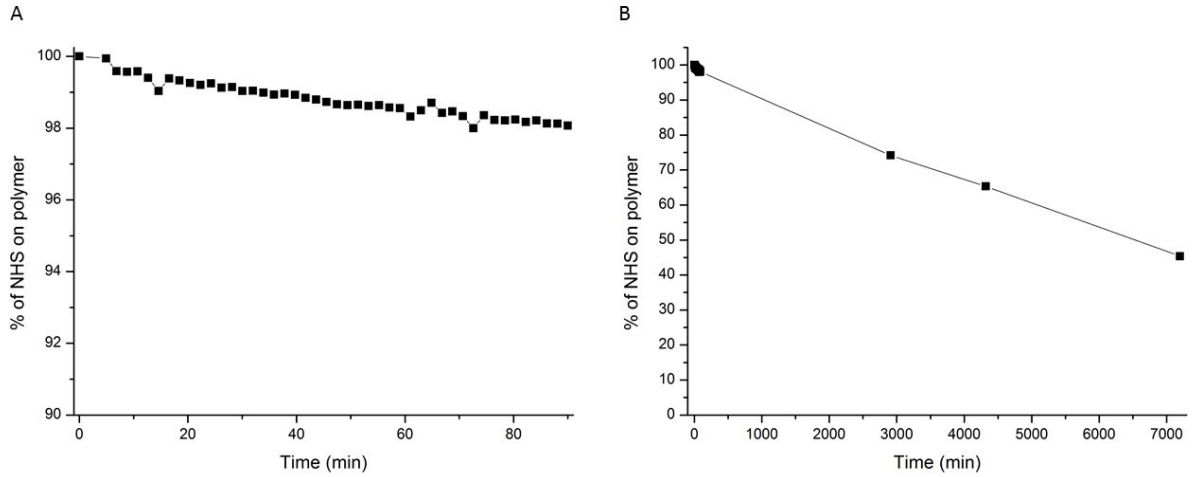

Figure 64: Stability of PAOx (*n*Prop-NHS 11%) in methanol-d4 after 90 minutes (A) and 5 days (B)

The measurement was repeated in deuterated water at 23 °C, in order to avoid precipitation of the polymer as a result of its LCST behavior. In 93 minutes 12.4% of the NHS groups was hydrolysed (Figure 65), indicating water should be avoided during the casting step.

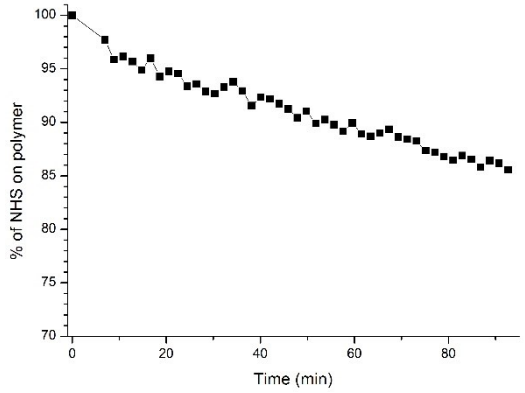

Figure 65: Stability of PAOx (*n*Prop-NHS 11%) in deuterated water

Crosslinking tests

To test the reactivity of the NHS-ester functionalised polymers, PAOx-NHS 12.0% was dissolved in absolute ethanol (EtOH) and mixed with a solution containing PAOx-NH_2 11.9%. Both polymers were prepared by the partial hydrolysis route. The crosslinking reaction was tested using stock solutions of both polymers (28.3 mg/mL for the PAOx-NH_2-polymer and 30.2 mg/mL for the PAOx-NHS polymer) to ensure that every reaction had the same NHS:NH_2 ratio of 1:1. In order to investigate the pH dependence of the reaction different amounts of triethylamine (Et_3N) were added to vary the pH from 7 to 11. The formation of amide bonds only takes place under basic conditions as part of the amines need to be present as free base,[27] on the other hand the NHS esters do not allow high pH values; the half-life of hydrolysis in water is 4-5 hours at pH 7.0 and 0 °C, while at pH 8.6 and 4 °C the half-life drastically decreases to 10 minutes.[28] The crosslink times were determined by a tube inversion test to check when the material formed a gel. Crosslinking proceeded faster when the pH was increased (Figure 66), from pH 9 or higher the crosslink times did not change anymore. As pH values get higher and are coming closer to the pK_a of amines, between 10 and 11, more of the amines become available as free base amines, increasing their reactivity. Although the values tested here are probably still below this pK_a, still more than half of the amines is present as $–NH_2$ group. For higher pH values, the increased percentage of free amines might be counterbalanced by the loss of NHS esters, because these become more unstable at higher pH values; although absolute ethanol was used, the presence of water during processing could not be completely excluded due to the hygroscopic properties of the solvent and the polymers. Solutions within the pH range of 7.5-8.5 proved to be optimal for the crosslinking reactions as the crosslinking was fast and hydrolysis was minimal.

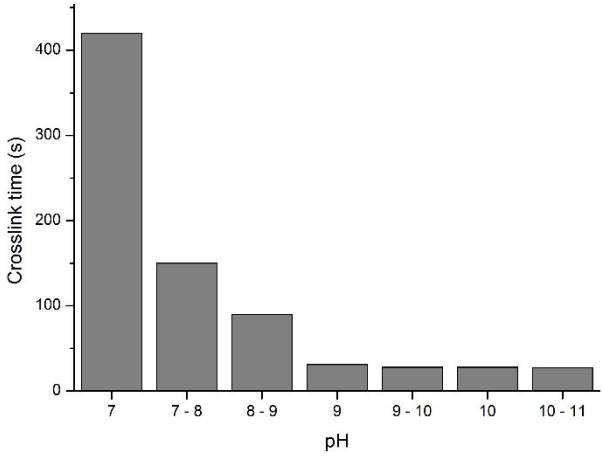

Figure 66: pH dependence of crosslinking of PAOx-NHS 12.0% with PAOx-NH_2 11.9% with an NHS:NH_2 ratio of 1:1 at a polymer concentration of 30 mg/mL.

Tape formation and adhesion tests

Similar to the crosslink tests, PAOx-NHS and PAOx-NH_2 were dissolved separately with a concentration of 100 mg/mL and mixed together. Next, the solution was cast into a mold and the solvent was allowed to evaporate overnight. The NHS:NH_2 ratios were varied to obtain tapes with excess of NHS groups to introduce tissue adhesiveness. The adhesive strength of these tapes was tested on a home-made adhesion test set up (Figure 67). A piece of peritoneum tissue containing a small incision was mounted on top of an Erlenmeyer flask which was connected to a burette. After pressing the tape onto the bovine peritoneum tissue, pressure was increased by the addition of water to the burette until leakage occurred at the tissue, which could be either the result of burst or adhesion failure; the height of the water column at this point was noted as burst pressure.

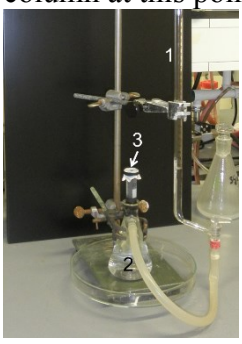

Figure 67: Adhesion test set up with 1) burette, 2) Erlenmeyer flask and 3) tissue or collagen sheet with a 3 mm incision

Tape formation with polymers prepared by the partial hydrolysis route

A range of different tapes was produced, in which the type of crosslinker, the crosslink density and the amount of free NHS groups was varied (Table 12). A number of control experiments were performed and these confirmed that the adhesion was due to the presence of NHS esters and crosslinks in the polymer film. A tape consisting only of PAOx-NHS (entry 2) also adhered well, but dissolved as soon as pressure was built up, while a fully crosslinked tape without any residual NHS groups did not adhere at all (entry 3). Also a tape consisting of only Aquazol 50 (entry 1) dissolved upon the addition of water. All determined burst pressures can be found in Table 12. These results show that the concept of the PAOx based tissue tape works. The use of PAOx-NH_2 resulted in a higher burst pressure than with trilysine

as crosslinker, so therefore the polymeric crosslinker is preferred, which may be expected based on the higher obtainable cross-link density.

Table 12: Burst pressures of PAOx tapes prepared by partial hydrolysis route

Entry	Ratio		PAOx-NHS (%)	PAOx-NH_2 (%)	Height water column (cm)	Leakage by	Adhesion	Remarks
	NHS	NH_2						
1	1	0	0	-	4	Adhesion	Bad	Film dissolved very fast
2	1	0	4.4	-	5	Burst	Good	Film dissolved very fast
3	1	1	4.4	K3*	5	Adhesion	Bad, slippery	
4	5	1	4.4	K3*	15	Adhesion	Good	
5	5	1	4.4	12	31.5#	Burst	Good	
6	2	1	23	6	N.D.	Adhesion	Bad, slippery	
7	5	1	23	6	22.5#	Burst	Good	
8	10	1	23	6	15	Adhesion	Good	
9	3	1	11.9	12	N.D.	Adhesion	Bad, slippery	
10	5	1	11.9	12	24	Adhesion	Good	

Tape contained an air bubble and this caused the burst
- Some burst pressures were not determined because of a lack of adhesion
* K3: trilysine

The disadvantage of all these investigated PAOx tapes was their high degree of swelling upon contact with water and their double sided adhesion which makes them not applicable in the body because of the risk of nerve and blood vessel compression and unwanted adhesions of tissues. To avoid these problems, a backing material was introduced to the design to give both mechanical support and prevent undesired adhesion. As backing material the biodegradable polymer poly(lactic-co-glycolic acid) (PLGA) was chosen.

To cast PLGA films, first PLGA 69:31 and PLGA 50:50 were dissolved in either EtOH or DCM. The polymers did not dissolve well in EtOH, but excellently dissolved in DCM. After casting, the films were dried overnight. Casting PLGA 50:50 resulted in non-flat films, while PLGA 69:31 yielded flat transparent films. The adhesive layer consisting of PAOx-NHS 8.5% and PAOx-NH_2 7.4%was cast directly onto the PLGA films from EtOH. These tapes (5.0x6.3 cm) were cut into four equal pieces for adhesive testing. The thickness of the backing was also varied (entry 1 and 2, Table 13). The tapes with the PLGA backing yielded adhesive tapes with higher burst pressures than the pure PAOx tapes (Table 13), showing the mechanical support of the backing material. The reproducibility of these materials however proved troublesome (entry 3 and 4). When the thickness of the adhesive layer was decreased (entry 5+6), worse results were obtained. When the backing material was made thinner, this increased the strength of the tapes. This can be explained by the fact that this led to less stiff tapes which showed better adhesion. After the burst pressure was reached, a gel was observed on the tissue and the backing, which could be easily removed from this backing, caused by delamination of the adhesive layer and the backing. Although still some work has to be done, the introduction of a backing was found to improve the burst pressure.

Table 13: burst pressures of PLGA backing tapes using PAOx-NHS 8.5% and PAOx-NH_2 7.4% polymers prepared by the partial hydrolysis route, with an NHS:NH_2 ratio of 5:1

Entry	Amount PLGA (g)	Amount PAOx (mg)	Average water column (cm)	Number of experiments
1	0.5	285	45 ± 10	2 #
2	1	285	>39.1 ± 12.4	4 *
3	0.5	285	16.3 ± 8.4	3 §
4	1	285	18.5 ± 10.8	4
5	0.5	143	10.5 ± 2.3	3 §
6	1	143	9.7 ± 1.3	4
7	0.2 ¥	285	24 ± 3	2

Adhesive layer partially delaminated from backing, so only 2 tapes could be tested
* 61.5 cm is the maximum height of the column, reached in one of the measurements
§ One of the four tapes was not used because of the presence of an air bubble
¥ tape of 5.0x5.0 cm

Tape formation with polymers prepared with the copolymerisation route
Because the previously described backing materials are stiff, a more flexible polymer was mixed into the films together with PAOx-NH_2 to provide covalent attachment of the adhesive layer to the backing material, avoiding delamination or detachment during the adhesion test. Therefore commercially available PLGA 75:25 and poly(L-lactide-co-caprolactone) 70:30 (PLC) were mixed, starting with 50:50 mass ratios and to this mixture different amounts of PAOx-NH_2 were added. The films with a low percentage (5 or 10 wt% of PAOx-NH_2 10%) of this latter polymer had good mechanical properties, while the rest appeared brittle. All films were tested for the presence of amines on the surface with nynhydrin and turned blue confirming the presence of amines. Films consisting of only PLGA or PLGA and PLC did not colour by nynhydrin staining.

The adhesive layer can be applied to the backing using different techniques. Solvent casting on top of the backing material is described above. The second method involved the use of coating bars which allowed to spread a thin and even layer over the backing. This method, however, was not successful, because the backing partially dissolved in the used DCM or the coating was uneven due to a not completely flat backing. Another possibility is to spray a polymeric solution onto the backing using a paint brush. When spraying a polymer solution in DCM on the backing, the backing stayed intact, but it was hard to control the amount of polymer which was sprayed onto it. The adhesion strength to collagen sheets of as-such prepared tapes was also not good. A final casting procedure that was investigated was to prepare the backing and the adhesive layer separately, after which they were bonded by hot-pressing both parts together. PAOx(MestOx-NHS 75-25) and PAOx(Et-NH_2 10%) with an NHS:NH_2 ratio of 5:1 were used for the preparation of the adhesive layers. The advantage of this method is that it allows more freedom in the choice of solvents to make the separate parts. Unfortunately, these tapes did not stick onto the collagen sheets used for the adhesion test. So therefore the casting on top of the backing method was used for the further preparation of tapes.

Tapes containing PAOx(*n*Prop-NHS) adhered very well to collagen, so for these the influence of casting solvent and drying time was investigated. Tapes with an NHS:NH_2 ratio of 5:1 were cast from methanol (MeOH), ethanol (EtOH), 1-propanol (1PrOH) or 2-propanol (2PrOH) and ratios of 3:1 and 7:1 were cast from methanol, all onto a backing consisting of

PLGA:PLC 50:50 plus 10 wt% PAOx(Et-NH_2 10%). Each film was made in triplicate, cut into 4 pieces which were tested in the adhesion test after one, two, three and six nights of drying at 40 °C. The burst pressures can be found in Table 14. 2-Propanol and 1-propanol gave the highest burst pressures. Propanol is less hydrophilic than ethanol and methanol, and is therefore better compatible with the slightly hydrophobic NHS groups. When dissolved in propanol the polymer is probably better solvated than in ethanol or methanol and therefore the NHS groups are more available for the amidation reaction by the amines in the tissue. The 7:1 NHS:NH_2 ratio was an improvement compared to 5:1, also here more NHS groups are available for reaction with tissue, but more ratios need to be studied in future work to find the optimum conditions. The drying time also seem to influence the burst pressure, but this effect was not reproducible.

Table 14: burst pressures of tapes prepared of PAOx(*n*Prop-NHS 10%) and PAOx(Et-NH_2 12%) on PLGA:PLC 50:50 + 10 wt% PAOx(Et-NH_2 12%) backings. PAOx polymers prepared by copolymerisation route

NHS:		cm H_2O after x days of drying				Averages					
NH_2	Solvent	1 day	2 days	3 days	6 days	1 day	2 days	3 days	6 days	Per film	Per type
5:1	MeOH	23.5	41.0	59.0	53.0					44.1±11.9	
5:1	MeOH	29.0	24.0	60.0	23.0	21.2	34.5	46.0	36	34.0±13.0	34.4±13.2
5:1	MeOH	11.0	38.5	19.0	32.0	± 6.8	± 7.0	±18.0	± 11.3	25.1±10.1	
5:1	EtOH	25.0	15.0	13.0	23.0					19.0±5.0	
5:1	EtOH	30.0	15.0	23.0	35.0	27.8	23.7	19.3	28.0	25.8±6.8	24.7±6.2
5:1	EtOH	28.5	41.0	22.0	26.0	± 1.9	± 11.6	± 4.2	± 4.7	29.4±5.8	
5:1	1PrOH	60.0	23.0	45.0	23.0					37.8±14.8	
5:1	1PrOH	60.0	45.0	59.0	60.0	60.5	34.0	55.2	46.3	56.0±5.5	49.0±12.5
5:1	1PrOH	61.5	34.0	61.5	56.0	± 0.7	± 7.3	± 6.8	±15.6	53.3±9.6	
5:1	2PrOH	28.0	46.0	41.5	45.0					40.1±6.1	
5:1	2PrOH	40.0	61.5	61.5	61.5	39.3	51.5	54.8	53.7	56.1±8.1	49.8±8.6
5:1	2PrOH	50.0	47.0	61.5	54.5	± 7.6	± 6.7	± 8.9	± 5.8	53.3±4.8	
3:1	MeOH	57.0	56.0	30.0	48.5					47.9±8.9	
3:1	MeOH	15.0#	29.0	27.0	39.0	45.5	47.3	26.0	36.2	31.7±4.9	38.1±12.1
3:1	MeOH	34.0	57.0	21.0	21.0	± 11.5	± 12.2	± 3.3	±10.1	33.3±12.3	
7:1	MeOH	60.0	52.0	40.0	32.0					46.0±10.0	
7:1	MeOH	61.5	55.0	61.5	60.5	50.8	46.0	48.8	40.2	59.6±2.3	46.5±12.0
7:1	MeOH	31.0	31.0	45.0	28.0	± 13.2	± 10.0	± 8.4	±13.6	33.8±5.6	

tape dropped into water before testing, and was excluded from averages

Because an NHS:NH_2 ratio of 7:1 gave high burst pressures, new tapes were prepared with a 7:1 and 5:1 ratio, cast from 2-propanol and dried for 2 days. Again, each film was cut into four pieces and tested (Table 15). This time the 5:1 ratio had a higher burst pressure (41.6 cm H_2O) than the 7:1 (35.2 cm H_2O) and the values were lower than for the previous test, although the variability is large, showing the limited reproducibility of the adhesive strength of these films. A possible explanation can be that the conditions in the lab were a little bit

different, e.g. temperature and humidity. Furthermore, the preparation procedure is not well standardized.

Table 15: Burst pressures of tapes consisting of PAOx(*n*Prop-NHS 10%) and PAOx(Et-NH_2 10%) cast from 2-PrOH with different NHS:NH_2 ratios

Film	NHS:NH_2 ratio	Average burst pressure of 4 film (cm H_2O)
1	7:1	33.9 ± 13.8
2	7:1	31.5 ± 2.5
3	7:1	40.1 ± 12.6
4	5:1	36.0 ± 11.0
5	5:1	46.1 ± 10.6
6	5:1	42.3 ± 6.3

In a final set of experiments tapes were prepared with a polymer with a higher NHS content, namely PAOx(*n*Prop-NHS 30%). Because the solubility of this polymer in 2-propanol was lower, DCM (5 v/v%) was added. The burst pressures can be found in Table 16. In this experiment the 7:1 ratios adhered better (average of 30.6 cm H_2O) than the 5:1 sample (average of 22.0 cm H_2O) of which 3 of the 8 pieces did not stick at all, also here variability is large. This result cannot be explained by the usage of DCM, as an incubation experiment of the backing material with DCM-propanol showed that up to 20% of DCM in the solution was well tolerated. Higher percentages of DCM resulted in the dissolution of the backing material. The variation in burst pressure is due to the hard to reproduce preparation conditions.

Table 16: Burst pressures of films consisting of PAOx(*n*Prop-NHS 30%) and PAOx(Et-NH_2 10%) cast from 2-PrOH:DCM 95:5 with different NHS:NH_2 ratios

Film	NHS:NH_2 ratio	Average Burst pressures (cm H_2O)	Number of experiments
1	5:1	20 ± 8.0	2 #
2	5:1	25.0 ± 8.7	3 #
3	7:1	29.3± 15.4	4
4	7:1	32.0±13.5	4

#: Other films out of four did not stick and were excluded for calculating the average

Conclusions and outlook

Synthetic routes for *N*-hydroxysuccinimide-ester functionalised poly(2-oxazoline)s and amine functionalised poly(2-oxazoline)s were established. The rate of crosslinking of these two polymers is pH dependent with an optimum of pH 7.5-8.5 for fast crosslinking, with a minimum loss of NHS esters due to high pH values. Polymeric tapes required crosslinking to avoid fast dissolution at contact with fluids, however complete crosslinking yielded non-sticking tapes. An NHS:NH_2 ratio of 5:1 to 7:1 seemed to be optimal, but higher contents of NHS need to be tested. Addition of polyester backing materials, containing some PAOx-NH_2 to covalently link it to the adhesive layer, significantly improved the mechanical properties of the adhesive films, although the ratios of PLGA and PLC and NH_2 content have to be optimised. The solvent used for casting the adhesive layer on top of the backing greatly influenced the burst pressure, with 1-propanol and 2-propanol proving the best solvents. Unfortunately, the standard deviation of the adhesion of the films was high, obstructing in depth evaluation of the effect of varying the tape composition. Detailed studies have to be performed to find causes and solutions for this problem.

Acknowledgements
Huub van Kuringen is acknowledged for his help with developing the partial hydrolysis route. Lia Miceli is thanked for her help with pH studies. Marcel Boerman, Harry van der Laan and Bram Keereweer are acknowledged for synthesis and optimization of the polymers. Rosa Félix is thanked for help with the backing materials.

Experimental

Materials
Aquazol® 50 was kindly donated by Polymer Chemistry Innovations. PLGA 69:31 and PLGA 50:50 were kindly donated by Encapson. PLGA 75-25 (PDLG 7507) and PLC 70-30 (7015) were purchased from Purac. 2-Chloroethylamine hydrochloride, methyl p-toluenesulfonate (MeOTs) and sodium tetraborate were purchased from Acros Organics. EDC.HCl was purchased from Fluka. DIC was purchased from Biosolve and sodium carbonate was purchased from Fischer Chemical. All other reagents were purchased from Sigma Aldrich and used as received, except 2-methyl-2-oxazoline (MeOx), 2-ethyl-2-oxazoline (EtOx) and methyl p-toluenesulfonate (MeOTs). These were purified by distillation over barium oxide and stored under argon. Dry solvents were obtained from a solvent purification system from MBraun MB SPS800 system under nitrogen atmosphere. Triethylamine was distilled over CaH_2 under argon atmosphere.

Instrumentation
Nuclear magnetic resonance (NMR) spectra were recorded on a Bruker DMC300 (300 MHz for ^{1}H, 75 MHz for ^{13}C) or a Bruker DMX 500 (500 MHz for ^{1}H, 125 MHz for ^{13}C).

Electro spray ionisation mass (ESI MS) spectra were recorded on a Thermo Finnigan LCQ Advantage Max.

Polymerisations were carried out in a Biotage Initiator Microwave System with Robot Eight utilizing capped reaction vials. These vials were heated to 140 °C overnight, allowed to cool to room temperature and filled with argon prior to use. All microwave polymerizations were performed with temperature control (IR sensor).

Size exclusion chromatography (SEC) was performed on an Agilent 1260 - series HPLC system equipped with a 1260 online degasser, a 1260 ISO-pump, a 1260 automatic liquid sampler, a thermostatted column compartment, a 1260 diode array detector (DAD) and a 1260 refractive index detector (RID). Analyses were performed on a PSS Gram30 column in series with a PSS Gram1000 column at 50 °C. *N,N*-dimethylacetamide (DMA), containing 50 mM of LiCl, was used as an eluent, at a flow rate of 0.593 ml min^{-1}. The SEC traces were analysed using the Agilent Chemstation software with the GPC add on. Number average molecular weights (M_n) and dispersity (Đ) values were calculated against poly(methyl methacrylate) PMMA standards.

Partial hydrolysis route
Hydrolysis kinetics

Aquazol 50 (25 g) was allowed to dissolve in 263 mL water at 60 °C for 1 hour. 263 mL concentrated HCl was added and the oil bath was put at 90 °C and the internal temperature was monitored and kept constant at 73 °C. This temperature was reached in 10 minutes. Samples of the reaction were taken regularly and neutralised to pH 7-9. The solvent was evaporated and the residue was dissolved in deuterated methanol. The degree of hydrolysis was determined by ^{1}H NMR spectroscopy using the signals of the backbone of the polyoxazoline (at δ=3.5 ppm), PEI signals (δ=2.8 ppm) and the remaining CH_2 group in the PEtOx side chain (δ=2.4 ppm); both values were averaged.

PAOx-PEI synthesis

Aquazol 50 (25 g) was allowed to dissolve in 263 mL water at 60 °C for 1 hour. 263 mL concentrated HCl was added and the oil bath was put at 90 °C and the internal temperature was monitored and kept constant at 73 °C. This temperature was reached in 10 minutes. The temperature was kept for the required amount of time. After this, the reaction mixture was concentrated until a viscous solution was obtained. This was neutralised with 4 M NaOH till pH 10-11. Water was evaporated until saturation was almost reached. The work up procedure depends on the degree of hydrolysis. Up to 10%, DCM was added and the polymer was extracted into the organic phase. The aqueous layer was washed a second time with DCM. From 10 to 20% hydrolysis, DCM and 5 % aqueous Na_2CO_3 solution were added and the polymer was extracted. The water layer was washed a second time with DCM. Above 20-25% hydrolysis, the polymer was first collected by freeze drying. DCM was added to dissolve the polymer. The remaining salts were filtered off and the organic phase was washed with 5% Na_2CO_3 solution twice.

The combined organic layers were dried over Na_2SO_4 and the solvent was evaporated, yielding a white foam.

^{1}H NMR (500 MHz, CD_3OD): δ 3.45 ($N(COCH_2)C\underline{H_2}C\underline{H_2}$), 2.80 ($NHC\underline{H_2}C\underline{H_2}$), 2.40 ($COC\underline{H_2}$), 1.11 ($CH_3$).

PAOx-COOMe synthesis

PAOx-PEI was dissolved in DCM (minimum 6.3 mL/ g polymer) and cooled on an ice bath. Triethylamine (2.5 eq) was added and methyl succinyl chloride (2 eq) was added dropwise in 20 minutes. The reaction was stirred overnight. The brown reaction mixture was washed with twice 5% Na_2CO_3 solution and the organic phase was dried over Na_2SO_4. The solution was concentrated and the polymer was precipitated twice in cold diethyl ether, yielding a brown polymer.

^{1}H NMR (500 MHz, $CDCl_3$): δ 3.63 ($COOC\underline{H_3}$), 3.44 ($NC\underline{H_2}C\underline{H_2}$), 2.62 ($COC\underline{H_2}C\underline{H_2}COCH_3$), 2.33 ($COC\underline{H_2}CH_3$), 1.11 ($CH_2C\underline{H_3}$)

PAOx-COOH synthesis

PAOx-COOMe was dissolved in MeOH (10 mL/ g polymer) and water (10 mL/g polymer). 20 equivalents (to methyl ester) of LiOH were added and the reaction mixture was stirred for 3 hours at room temperature. The solution was filtered and acidified with HCl to pH 4. Methanol was evaporated and the water was removed by freeze drying. The polymer was dissolved in MeOH and precipitated in cold acetone twice, yielding a yellow-brown polymer.

^{1}H NMR (500 MHz, CD_3OD): δ 3.45 ($NC\underline{H_2}C\underline{H_2}$), 2.62 ($COC\underline{H_2}C\underline{H_2}COOH$), 2.33 ($COC\underline{H_2}CH_3$), 1.11 ($CH_2C\underline{H_3}$)

PAOx-NHS synthesis

PAOx-COOH was dissolved in DMA (12.5 mL/ g polymer). Two equivalents of NHS and 2 equivalents of EDC.HCl or DIC were added with a syringe. The solution was stirred

overnight at room temperature. The solvent was evaporated and the polymer was dissolved in DCM and washed with water and brine once. The organic phase was dried over Na_2SO_4 and the solvent was reduced. The polymer was precipitated twice in cold diethyl ether yielding a yellow-brown polymer. The NHS content was determined with UV-Vis spectroscopy; the polymer was dissolved in 0.1 M NH_4OH (1 mg/mL) and this was diluted 10 times to measure absorbance at 260 nm. NHS absorbs temporarily (maximum 20 minutes) at 260 nm when deprotonated.[25]
^{1}H NMR (500 MHz, $CDCl_3$): δ 3.45 (NCH_2CH_2), 2.82 (CH_2CH_2. NHS), 2.33 ($COCH_2CH_2CO$ & $COCH_2CH_3$), 1.11 (CH_2CH_3)

PAOx-NH_2 synthesis
Ethylene diamine (30 eqv vs COOMe) was added to PAOx-COOMe. The polymer dissolved in a few minutes and the solution was stirred overnight. The excess of ethylene diamine was evaporated. The polymer was dissolved in MeOH and precipitated in cold diethyl ether twice.
^{1}H NMR (500 MHz, CD_3OD): δ 3.45 (NCH_2CH_2), 2.76 ($NHCH_2CH_2NH_2$), 2.69 ($COCH_2CH_2COOH$), 2.33 ($COCH_2CH_3$), 1.11 (CH_2CH_3)

Monomer synthesis
Monomers were synthesized as described in chapter 2.

Copolymerisation yielding P(MeOx-MestOx). P(EtOx-MestOx) or P(nPropOx-MestOx)
MestOx and MeOx/EtOx/*n*PropOx were mixed under argon atmosphere in the right monomer ratio with methyl tosylate and acetonitrile. This solution was heated for 20 minutes at 140 °C in the microwave. After cooling down, piperidine was added and the reaction was stirred for 1 hour. The solvent was evaporated, the polymer was dissolved in DCM and precipitated twice in cold diethyl ether.

P(EtOx-MestOx)
^{1}H NMR ($CDCl_3$, 300 MHz): δ 3.64 (br, $COOCH_3$), 3.46 (br, NCH_2CH_2N), 3.14 (b, CH_2NCH_2 piperidine), 2.96 (s, NCH_3), 2.63 (b, $COCH_2CH_2CO$), 2.27 (b, $COCH_2$), 1.78 (s, $CH_2CH_2CH_2$ piperidine), 1.12 (br, CH_2CH_3)

P(nPropOx-MestOx)
^{1}H NMR ($CDCl_3$, 300 MHz): δ 3.64 (br, $COOCH_3$), 3.46 (br, NCH_2CH_2N), 3.14 (b, CH_2NCH_2 piperidine), 2.96 (s, NCH_3), 2.63 (b, $COCH_2CH_2CO$), 2.27 (b, $COCH_2$), 1.78 (s, $CH_2CH_2CH_2$ piperidine), 1.63 (b, $COCH_2CH_2$), 0.95 (br, CH_2CH_3)

PAOx-COOH synthesis 2
Copolymer was dissolved in methanol (13 mL/g) and water (1.3 mL/g). 2 equivalents of lithium hydroxide were added and the reaction was stirred overnight. The solvent was evaporated and the polymer was dissolved in MeOH and precipitated in acetone. The precipitate was collected, dissolved in MeOH and acidified to pH 2 with 2 M HCl. The solvent was evaporated, polymer was dissolved in MeOH and precipitated in acetone.

Partial hydrolysis methyl esters
PMestOx (4.5 g) was dissolved in 60 mL MeOH and 6 mL water. This solution was split into three equal portions. To the first 102.84 mg of $LiOH.H_2O$ was added. To the second 203.17 mg and to the third 306.95 mg. The solutions were stirred overnight. The solvent was evaporated and the polymer was dissolved in MeOH and precipitated in acetone. The precipitate was collected, dissolved in MeOH and acidified to pH 2 with 1 M HCl. The

solvent was evaporated, polymer was dissolved in MeOH and precipitated in acetone : diethyl ether 1:1.

Stability measurements with ^{1}H NMR

The NMR signal was locked with only solvent and then the sample was inserted. A continuous experiment was performed where 45 runs of 4 scans were taken with a relaxation time of 2 seconds and waiting time in between runs of 116 seconds. The obtained spectra were integrated for the bound NHS signal and the percentage of the left over bound NHS was calculated and plotted against time.

Crosslink tests

Crosslink tests were performed with a final polymer concentration of 30 mg/mL. 3.40 mg PAOx-NH_2 12% was dissolved in 120 µL EtOH:Et_3N 99:1 and 3.62 mg PAOx-NHS 11.9% was dissolved in 120 µL EtOH. The PAOx-NHS solution was added to the PAOx-NH_2 solution and quickly mixed by vortexing.

pH dependence of crosslinking

42.42 mg of PAOx-NH_2 12% was dissolved in 1.5 mL of absolute EtOH and PAOx-NHS 11.9% was dissolved in 1.5 mL of absolute EtOH. To 100 µL of the PAOx-NH_2 solution 0. 0.5. 0.7. 1.0. 1.5. 1.75 or 2 µL of Et_3N were added and some additional EtOH was added to have equal volumes. To each of the PAOx-NH_2 solutions 100 µL of PAOx-NHS solutions was added and mixed by vortexing. A drop was taken to determine the final pH on pH paper.

Film formation

Cups of anti-adhesive paper of minimal 2.5x2.5 cm were prepared. Sharp fold lines were made and the cups were stapled at the top to avoid leakage and allow easy removal of the staples and thus the tape from the cup. PAOx-NHS and PAOx-NH_2 were dissolved separately in EtOH, at least 10 µL of solvent per mg of polymer, and the dissolution of PAOx-NH_2 could be helped by gently heating or via the addition of 1 v/v% of Et_3N if necessary. Both solutions were mixed and cast into the paper cup and allowed to dry overnight at room temperature or 40 °C.

Adhesion test

The set up as depicted in Figure 67 was prepared and the tissue with a 3 mm circular incision was levelled with the 50 mL mark of the column. All air bubbles were removed from the system and the tissue was secured to the set up. Borate buffer pH 8.5 (prepared by dissolving 38.137 g of disodium tetraborate in 450 mL, and adjusting the pH to pH 8.5 using 1 M HCl solution)was dripped on top of the tissue and removed again with some paper towel. A piece of tape was pushed onto the tissue for 1 minute. The tape was lightly pushed to check if adhesion had occurred. The pressure was increased gradually by the addition of demi water to the column until failure by either adhesion or burst occurred. This value was noted as burst pressure.

PLGA backing

The required amount of PLGA was dissolved in 5 mL DCM and cast in the paper cup. The solvent was allowed to evaporate overnight.

Amine containing backings

The required amounts of PLGA, PLC and PAOx-NH_2 were dissolved in 5 mL DCM and 0.5 mL MeOH and cast in the paper cup. The solvents were allowed to evaporate overnight.

Adhesive layer formation

PAOx-NHS and PAOx(Et-NH_2), total weight polymers 100 mg, were dissolved separately in total 5 mL of DCM. The solutions were mixed and cast in a paper cup and dried overnight at room temperature.

Hotpress

The backing was removed from its paper cup and put on top of the adhesive layer, which stayed in its cup where the staples were removed. A piece of anti-adhesive paper was put on top and this was placed between two Teflon covered metal sheets (cut from a baking tray). This was placed in the hotpress of which the temperature of the bottom plate was manually controlled at 30-40 °C. The films were put on a pressure of 10000 for 5 minutes and allowed to cool down before testing.

References

1. Bruce, J.; Krukowski, Z. H.; Al-Khairy, G.; Russell, E. M.; Park, K. G. *Br. J. Surg.* **2001,** 88, (9), 1157-68.
2. Pickleman, J.; Watson, W.; Cunningham, J.; Fisher, S. G.; Gamelli, R. *Journal of the American College of Surgeons* **1999,** 188, (5), 473-82.
3. Bouten, P. J. M.; Zonjee, M.; Bender, J.; Yauw, S. T. K.; van Goor, H.; van Hest, J. C. M.; Hoogenboom, R. *Prog. Polym. Sci.* **2014,** 39, (7), 1375-1405.
4. Bhatia, S., Traumatic Injuries Chapter 10 Traumatic Injuries. In *Biomaterials for Clinical Applications*, Springer New York: 2010; pp 213-258.
5. Duarte, A. P.; Coelho, J. F.; Bordado, J. C.; Cidade, M. T.; Gil, M. H. *Prog. Polym. Sci.* **2012,** 37, (8), 1031-1050.
6. Confluent Surgical Inc, FDA Executive Summary DuraSeal Dural Sealant System. http://www.fda.gov/ohrms/dockets/ac/04/briefing/2004-4083b1_02_executive%20summary.pdf (last accessed 2015-04-23),
7. Preul, M. C.; Bichard, W. D.; Spetzler, R. F. *Neurosurgery* **2003,** 53, (5), 1189-98; discussion 1198-9.
8. Cosgrove, G. R.; Delashaw, J. B.; Grotenhuis, J. A.; Tew, J. M.; Van Loveren, H.; Spetzler, R. F.; Payner, T.; Rosseau, G.; Shaffrey, M. E.; Hopkins, L. N.; Byrne, R.; Norbash, A. *J. Neurosurg.* **2007,** 106, (1), 52-8.
9. Confluent Surgical Inc, FDA Executive Summary for DuraSeal Xact Sealant System. http://www.fda.gov/ohrms/dockets/ac/09/briefing/2009-4437b1-01%20FDA%20Executive%20Summary.pdf (last accessed 2015-04-23),
10. Harris, J. M., *Poly(Ethylene Glycol) Chemistry. Biotechnical and Biomedical Applications*. Springer US: 1992.
11. Mero, A.; Pasut, G.; Via, L. D.; Fijten, M. W. M.; Schubert, U. S.; Hoogenboom, R.; Veronese, F. M. *J. Controlled Release* **2008,** 125, 87-95.
12. Luxenhofer, R.; Han, Y.; Schulz, A.; Tong, J.; He, Z.; Kabanov, A. V.; Jordan, R. *Macromol. Rapid Commun.* **2012,** 33, (19), 1613-1631.
13. Hoogenboom, R. *Angew. Chem. Int. Ed.* **2009,** 48, 7978-7994.
14. Saegusa, T.; Kobayashi, S.; Yamada, A. *Macromolecules* **1975,** 8, (4), 390-396.
15. Tanaka, R.; Ueoka, I.; Takaki, Y.; Kataoka, K.; Saito, S. *Macromolecules* **1983,** 16, (6), 849-853.
16. Lambermont-Thijs, H. M. L.; van der Woerdt, F. S.; Baumgaertel, A.; Bonami, L.; Du Prez, F. E.; Schubert, U. S.; Hoogenboom, R. *Macromolecules* **2010,** 43, (2), 927-933.

17. Lambermont-Thijs, H. M. L.; Bonami, L.; Du Prez, F. E.; Hoogenboom, R. *Polym. Chem.* **2010,** 1, (5), 747-754.
18. Hoogenboom, R., Polyethers and Polyoxazolines. In *Handbook of Ring-Opening Polymerization*, Wiley-VCH Verlag GmbH & Co. KGaA: 2009; pp 141-164.
19. Verbraeken, B.; Lava, K.; Hoogenboom, R., Poly(2-oxazoline)s. In *Encyclopedia of Polymer Science and Technology*, John Wiley & Sons, Inc.: 2014; pp 1-51.
20. Guillerm, B.; Monge, S.; Lapinte, V.; Robin, J. J. *Macromol. Rapid Commun.* **2012,** 33, 1600-1612.
21. Aoi, K.; Okada, M. *Prog. Polym. Sci.* **1996,** 21, (1), 151-208.
22. Kobayashi, S. *Prog. Polym. Sci.* **1990,** 15, (5), 751-823.
23. Kobayashi, S.; Uyama, H. *J. Polym. Sci., Part A: Polym. Chem.* **2002,** 40, (2), 192-209.
24. Van Kuringen, H. P.; Lenoir, J.; Adriaens, E.; Bender, J.; De Geest, B. G.; Hoogenboom, R. *Macromol. Biosci.* **2012,** 12, (8), 1114-23.
25. Miron, T.; Wilchek, M. *Anal. Biochem.* **1982,** 126, (2), 433-435.
26. Grogna, M.; Cloots, R.; Luxen, A.; Jerome, C.; Desreux, J.-F.; Detrembleur, C. *J. Mater. Chem.* **2011,** 21, (34), 12917-12926.
27. Clayden, J. P.; Greevers, N.; Warren, S.; Wothers, P. D., *Organic Chemistry*. 1st edition ed.; Oxford University Press: 2001.
28. Hayworth, D. http://www.piercenet.com/method/amine-reactive-crosslinker-chemistry. http://www.piercenet.com/method/amine-reactive-crosslinker-chemistry (last accessed 2015-04-23),

Summary

Sutures and staples are widely used for closure of incisions, but it has certain drawbacks, especially for vulnerable and delicate tissues. When wounds have to closed, sutures and staples do not provide a tight seal preventing leakage of gas and fluids. Tissue adhesive materials are developed to provide, in combination with sutures, a watertight seal. Many (polymeric) products are available, but they have several drawbacks. Cyanoacrylates are used for skin closure, but due to their toxic degradation products (formaldehyde) other applications are difficult to realize. Poly(ethylene glycol) gels are biocompatible, but do lack mechanical strength, which limits their applicability. The general challenge regarding synthetic adhesives is to find polymers which are non-toxic and which display good gel strength. The variety of polymers used at the moment is therefore small and most adhesives are based on either PEG, polyurethanes or PLGA. Clearly there is a need for new synthetic polymers which satisfy better the criteria for an optimal tissue adhesive. Biomimetic adhesives are a rapidly expanding research field. Especially the introduction of the dihydroxyphenyl moiety (DOPA), responsible for the adhesive behavior of mussel adhesive proteins, into synthetic polymers, such as polystyrene or PEG, is being explored. This research area shows a lot of perspective in adhesion strength, but long degradation times and the use of toxic oxidizing agents are major concerns. A list of requirements for ideal tissue adhesive materials is included in chapter 1. A class of polymers that is regarded to be potentially very interesting for biomedical applications are the poly(2-oxazoline)s which are described in the second part of chapter 1. Poly(2-alkyl/aryl-2-oxazoline)s (PAOx) are an interesting class of polymers because of their tuneable properties, biocompatibility, stealth behavior and thermosensitivity. The polymers are made by the living cationic ring opening polymerisation (CROP) of 2-oxazoline monomers, allowing easy access to well-defined polymers with controlled end group functionalities. Different strategies for monomer synthesis, the polymerisation mechanism, functional monomers are described. A list of polymer properties is given, consisting of the aqueous solution behaviour, thermal properties and biocompatibility and stealth behaviour.

In chapter 2 the synthesis of the methyl ester functional oxazoline monomers MestOx and C3MestOx is described. Homopolymerisation studies revealed a faster propagation of MestOx and C3MestOx compared to the alkyl monomers, 2-methyl-2-oxazoline (MeOx), 2-ethyl-2-oxazoline (EtOx) and 2-*n*-propyl-2-oxazoline (*n*PropOx). Activation energies for MestOx and C3MestOx were lower than for MeOx and EtOx. The copolymerisation, however, revealed a reversed order of incorporation. The EtOx and *n*PropOx copolymerisations led to a minor deviation from ideal random monomer distribution, whereas the MeOx copolymerisation with MestOx or C3MestOx led to gradient copolymers. Both the polymerisation temperature and the type of monomer influenced the gradient formation, MestOx and 80 °C resulted in a more pronounced gradient than a temperature of 140 °C and with C3MestOx monomer. The large difference in reaction rates between homo- and copolymerisation of MeOx with the ester-containing oxazolines was further corroborated by the determination of the activation energy of MeOx during copolymerisation, which was comparable to homopolymerisation, while the activation energy of MestOx was increased.

The synthesis of series of homo- and copolymers of MestOx and C3MestOx with EtOx and *n*PropOx is described in chapter 3. All polymers, except P($EtOx_{49}$-$MestOx_{51}$), showed cloudpoint temperatures (T_{CP}s) between 24 °C and 108 °C depending on the composition, at a concentration of 5 mg/mL in water. All these polymers were amorphous with glass transition temperatures between -2 °C and 54 °C. The P(EtOx-MestOx), P(EtOx-C3MestOx) and

P(*n*PropOx-C3MestOx) copolymers have glass transition temperatures that can be tuned in between the T_gs of the homopolymers. However, for P(*n*PropOx-MestOx) copolymers, the T_gs of all copolymers are lower than the ones of both homopolymers, indicating suppression of interchain interactions. All homo- and copolymers are thermally stable up to at least 250 °C, whereby copolymers with more (C3)MestOx were found to be less stable. Nonetheless, the stabilities will allow thermal processing, e.g. hot-melt extrusion, at temperatures well above room temperature. Also MeOx-C3MestOx polymers, both gradient and block-copolymers, were prepared with a 25-75 mol% ratio. Both polymers showed thermoresponsive behavior:
the gradient copolymer showed a similar transition as EtOx and *n*PropOx copolymers, while the block copolymer showed a different transmittance curve indicating particle formation.

In chapter 4 the modification of the methyl esters was described. The methyl ester was reacted with a series of primary and secondary amines resulting in their corresponding amides. The linear primary and cyclic secondary amines used are methylamine, ethylamine, *n*-propylamine, *n*-butylamine, pyrrolidine, piperidine, morpholine and 1-acetylpiperazine respectively. The linear primary amines could be used for direct amidations reactions, however the cyclic secondary amines did not react under these conditions. The addition of triethylamine was needed to perform this reaction. The starting polymer PMestOx had a cloudpoint temperature of 101 °C at 5 mg/mL which was modified by these reactions. The introduction of *n*-propylamine, pyrrolidine and piperidine lowered the T_{CP}, while *n*-butylamine resulted in a non watersoluble polymer. The other amines lead to an increase of T_{CP}. So the LCST behaviour of one polymer can be varied over a broad range of temperatures by reacting it with different amines. At the same time glass transition temperatures were raised from 39 °C to a range from 53-89 °C. The relationship between the number of carbons in the primary amines and the resulting T_gs is linear and similar to the reported trend for poly(2-alkyl-2-oxazoline)s. All amidated polymers were found to be thermally stable up to at least 250 °C. The amidation of PMestOx polymers enables a wide variety of properties from the same scaffold. More amines and combinations of amines need to be tested to achieve fine tuning of solution and bulk properties.

Chapter 5 describes the three step post-polymerisation modification of EtOx-MestOx copolymers to yield amine and subsequently guanidinium functionalised poly(2-oxazoline)s. Both random and block methyl ester containing copolymers were prepared and modified. Both amine and guanidinium functionalised copolymers did not show toxicity up to 10 µM, however at 15 µM for the block copolymers containing amines or guanidines some minor toxicity was observed. Uptake studies showed that only the block copolymers with 15 or 20% functionalisation were taken up by HeLa cells, clearly demonstrating the influence of monomer distribution and degree of functionalisation. The efficiency was lower compared to R8, probably due to the size of the polymeric construct, this might be improved by longer incubation times. Also the impact of spacer length between the polymeric backbone and the guanidinium group need to be tested by using C3MestOx instead of MestOx.

One of the main problems in abdominal surgery is the occurrence of leakages and related infections. A number of products are available to seal the wounds, but none of them has an excellent performance on all aspects. In chapter 6 the development of a tissue adhesive material based on poly(2-oxazoline)s, bearing *N*-hydroxysuccinimide (NHS) esters as tissue reactive groups is described. Two synthetic routes were developed for the preparation of NHS-ester functional poly(2-oxazoline)s. The first route started with commercially available poly(2-ethyl-2-oxazoline) (PEtOx) which was partially hydrolysed to yield a copolymer of

poly(ethylene imine) (PEI) and PEtOx. The resulting amine was reacted an acid chloride to yielding a methyl ester functional polymer. Similar methyl ester functionalised polymers were prepared in the second route by the copolymerisation of MeOx, EtOx or *n*PropOx with MestOx. From this point the preparations of NHS functional PAOx were similar. The methyl ester was subsequently hydrolysed to its corresponding carboxylic acid which was reacted with NHS to obtain the NHS functional polymers. Also an amine functional polymer was made to provide crosslinking between the PAOx-NHS polymers allowing to make self-standing crosslinked polymer films. The rate of crosslinking of these two polymers is pH dependent with an optimum of pH 7.5-8.5 for fast crosslinking with a minimum loss of NHS esters due to high pH values. Polymeric tapes required crosslinking to avoid fast dissolution at contact with fluids, however complete crosslinking yielded non-sticking tapes. An NHS:NH_2 ratio of 5:1 to 7:1 seemed to be optimal, but higher contents of NHS need to be tested. Addition of polyester backing materials, containing some PAOx-NH_2 to covalently link it to the adhesive layer, significantly improved the mechanical properties of the adhesive films, although the ratio of PLGA and PLC and NH_2 content have to be optimised. The solvent used for casting the adhesive layer on top of the backing greatly influenced the burst pressure, with 1-propanol and 2-propanol proving the best solvents. Unfortunately, the standard deviation of the adhesion of the films was high, obstructing in depth evaluation of the effect of varying the tape composition. Detailed studies have to be performed to find causes and solutions for this problem.

Samenvatting

Hechtingen en nietjes worden veel gebruikt voor het sluiten van chirurgische snijwonden, maar dit heeft veel nadelen vooral voor kwetsbaar en teer weefsel. Als wonden gesloten worden zorgen hechtingen en nietjes niet voor een water- en luchtdichte afsluiting. Weefselplakkende materialen werden ontwikkelend om, eventueel in combinatie met hechtingen, voor een waterdichte afsluiting te zorgen. Veel (plastic) materialen zijn beschikbaar, maar deze hebben verschillende bezwaren. Cyanoacrylaten (secondelijm) wordt gebruikt voor het sluiten van huidwondjes, maar omdat er bij afbraak giftige degradatieproducten (formaldehyde) ontstaan zijn andere toepassingen moeilijk te realiseren. Poly(ethyleen glycol) (PEG) gelen zijn biocompatibel, maar deze materialen zijn niet sterk, wat de toepasbaarheid beperkt. De algemene uitdaging voor synthetische plakkende materialen is om een polymeer te vinden dat niet giftig is en een goede mechanische eigenschappen heeft. De verscheidenheid van polymeren die op dit moment gebruikt worden is daardoor klein en de meeste plakkende materialen zijn gebaseerd op PEG, polyurethaan of PLGA. Er is duidelijk behoefte aan een nieuw synthetisch polymeer dat de wensen voor een optimaal weefsel plakkend materiaal vervuld. Plakkende materialen die de natuur nabootsen zijn een snel uitbreidende onderzoeksveld, vooral sinds het introduceren van de dihydroxyfenyl eenheid (DOPA), die verantwoordelijk is voor de plakeigenschappen van het mossellijm eiwitten, in synthetische polymeren, zoals polystyreen of PEG, wordt onderzocht. Dit onderzoeksgebied is veel belovend wat betreft plakkracht, maar de lange degradatietijden en het gebruik van giftige oxiderende stoffen zijn verontrustend. Een lijst van eisen voor een ideaal weefsel plakkend materiaal is te vinden in hoofdstuk 1. Een type van polymeren dat potentieel zeer interessant is voor biomedische toepassingen zijn poly(2-oxazoline)s. Deze polymeren worden beschreven in het tweede deel van hoofdstuk 1. Poly(2-alkyl/aryl-2-oxazoline)s (PAOx) zijn interessante materialen vanwege hun afstembare eigenschappen, biocompatibiliteit, stealth gedrag en thermoresponsief gedrag. De polymeren worden gemaakt met behulp van levende kationische ringopening polymerisatie (CROP) van 2-oxazoline monomeren, hiermee kunnen goed gedefinieerde polymeren met gecontroleerde eindgroepen gemaakt worden. Verschillende monomeersynthese routes, het polymerisatiemechanisme en functionele monomeren worden beschreven. Een lijst van polymeereigenschappen, met daarbij gedrag in waterige oplossing, thermische eigenschappen, biocompatibiliteit en stealth gedragen, is gegeven.

In hoofdstuk 2 wordt de synthese van methyl ester gefunctionaliseerde oxazoline monomeren MestOx en C3MestOx beschreven. Homopolymerisatie studies laten zien dat MestOx en C3MestOx een snellere propagatiereactie ondergaan dan de alkyl monomeren, 2-methyl-2-oxazoline (MeOx), 2-ethyl-2-oxazoline (EtOx) en 2-*n*-propyl-2-oxazoline (*n*PropOx). De activeringsenergieën voor MestOx en C3MestOx zijn lager dan die voor MeOx en EtOx. De copolymerisatie laat een omgekeerde volgorde van inbouw van de monomeren zien ten opzichte van de homopolymerisatie. De EtOx en *n*PropOx copolymerisaties leiden tot een kleine afwijking van de ideale willekeurige monomeerverdeling, terwijl MeOx copolymerisatie met MestOx of C3MestOx leidt tot de vorming van gradiënt copolymeren. Zowel het type monomeer als de polymerisatietemperatuur hebben invloed op de vorming van het gradiënt, MestOx en 80 °C leiden tot de vorming van een sterker gradiënt dan C3MestOx en een temperatuur van 140 °C. Het grote verschil in reactiesnelheid tussen MeOx en monomeren met methyl esters werd bevestigd door de bepaling van de activeringsenergie van MeOx en MestOx in de copolymerisatie. De activeringsenergie van MeOx was vergelijkbaar met de homopolymerisatie, terwijl die van MestOx steeg.

De synthese van series homo- en copolymeren van MestOx en C3MestOx met EtOx en *n*PropOx wordt beschreven in hoofdstuk 3. Alle polymeren, behalve P($EtOx_{49}$-$MestOx_{51}$), hebben een troebelingspunt (T_{CP}) tussen de 24 en 108 °C afhankelijk van de samenstelling bij een concentratie van 5 mg/mL in water. Al deze polymeren waren amorf met een glasovergangstemperatuur (T_g) tussen -2 en 54 °C. De P(EtOx-MestOx), P(EtOx-C3MestOx) en P(*n*PropOx-C3MestOx) copolymeren hebben glasovergangstemperaturen die ingesteld kunnen worden tussen de T_gs van de homopolymeren. Echter voor P(*n*PropOx-MestOx) copolymeren, de T_gs van alle copolymeren zijn lager dan die van beide homopolymeren, dit wijst op de onderdrukking van de interacties tussen ketens. Alle homo- en copolymeren zijn stabiel bij verhitting tot 250 °C, waarbij polymeren die meer (C3)MestOx bevatten minder stabiel waren. Niettemin laten deze stabiliteit thermische verwerking boven het smeltpunt toe, zoals bijvoorbeeld extrusie. Ook werden MeOx-C3MestOx polymeren bereid, zowel gradiënt als blok copolymeren met een 25-75 mol% verhouding. Beide polymeren zijn thermoresponsief: het gradiënt copolymeer heeft een vergelijkbare overgang als de EtOx en *n*PropOx polymeren, terwijl het blok copolymeer een andere transmissiecurve laat zien die wijst op de vorming van deeltjes.

In hoofdstuk 4 wordt de modificatie van de methyl esters beschreven. De methyl ester onderging een reactie met primaire en secundaire amines wat resulteerde in de overeenkomstige amides. De lineaire primaire en cyclische secundaire amines die gebruikt werden, zijn respectievelijk methylamine, ethylamine, *n*-propylamine, *n*-butylamine, pyrrolidine, piperidine, morpholine en 1-acetylpiperazine. De lineaire primaire amines werden gebruikt in een direct amidatie reactie, maar de cyclische secundaire amines reageerde niet onder deze omstandigheden, toevoeging van triethylamine was nodig om deze reactie te laten verlopen. Het uitgangsmateriaal, PMestOx, had een troebelingspunt van 101 °C bij een concentratie van 5 mg/mL. Deze troebelingstemperatuur veranderde door de reacties: de introductie van *n*-propylamine, pyrrolidine en piperidine verlaagden de T_{CP}, terwijl de reactie met *n*-butylamine resulteerde in een polymeer dat niet meer wateroplosbaar was. De andere amines resulteerden in een toename van de T_{CP}. Het LCST (onderste kritische oplossingstemperatuur) gedrag van een polymeer kan over een groot temperatuursgebied gevarieerd worden door het te laten reageren met verschillende amines. Tegelijkertijd werden de glasovergangstemperaturen naar van 39 °C naar 53-89 °C verhoogd. Het verband tussen het aantal koolstofatomen in de primaire amines en de bijbehorende T_gs is lineair en vergelijkbaar met trend die waargenomen is voor poly(2-alkyl-2-oxazoline)s. Alle geamideerde polymeren zijn stabiel tot 250 °C. De amidatie van PMestOx geeft toegang tot een grote verscheidenheid aan eigenschappen uitgaande van hetzelfde materiaal. Meer amines en combinaties van amines moeten worden getest om fijne afstemming van de eigenschappen in bulk en oplossing te bereiken.

Hoofdstuk 5 beschrijft de post-polymerisatie modificatie in drie stappen van EtOx-MestOx copolymeren naar amine en vervolgens guanidine gefunctionaliseerde poly(2-oxazoline)s. Statistische als blok copolymeren met methyl esters zijn gemaakt en gemodificeerd. Zowel de amine als de guanidine gefunctionaliseerde copolymeren lieten geen toxiciteit zien tot 10 μM, maar bij 15 μM lieten de blok copolymeren met amines of guanidines een kleine toxiciteit zien. Opnamestudies lieten zien dat alleen de blok copolymeren met 15 of 20% functionalisering werden opgenomen door HeLa cellen. De opname van de polymeren is dus afhankelijk van de monomeer distributie en het aantal functionele groepen. De opname-efficiency is lager dan die van R8, waarschijnlijk komt dit door de grootte van het polymeer. De opname kan mogelijk verbeterd worden door de cellen langer de tijd te geven om het materiaal op te nemen. De invloed van de lengte van de spacer tussen de polymeerhoofdketen

en de guanidine groep moet getest worden door C3MestOx in plaats van MestOx te gebruiken.
Een van de belangrijkste problemen in buikchirurgie is het optreden van lekkages en bijbehorende infecties. Er zijn een aantal producten beschikbaar die wonden waterdicht maken, maar geen een voldoet aan alle eisen. In hoofdstuk 6 wordt de ontwikkeling van weefsel plakkende materialen op basis van poly(2-oxazoline)s beschreven. Deze polymeren hebben *N*-hydroxysuccinimide (NHS) esters als weefselplakkende groep. Twee synthese routes voor de bereiding van NHS-ester functionele poly(2-oxazoline)s worden beschreven. De eerste methode start vanuit een commercieel verkrijgbaar poly(2-ethyl-2-oxazoline) (PEtOx) die gedeeltelijk wordt gehydrolyseerd. Dit resulteert in een copolymeer van poly(ethyleen imine) (PEI) en PEtOx. Het ontstane amine wordt met behulp van methyl succinyl chloride omgezet in een methyl ester functioneel polymeer. Vergelijkbare methyl ester gefunctionaliseerde polymeren worden in de tweede route gemaakt door de copolymerisatie van MeOx, EtOx of *n*PropOx met MestOx. Vanaf de methyl ester is de bereiding van NHS gefunctionaliseerde PAOx hetzelfde. The methyl ester wordt gehydrolyseerd naar het overeenkomstig carbonzuur wat reageert met NHS om NHS gefunctionaliseerde polymeren te verkrijgen. Ook werden er amine gefunctionaliseerde polymeren gemaakt, deze zorgen voor het crosslinken van de PAOx-NHS polymeren zodat een op zichzelf staande gecrosslinkte polymerenfilm gemaakt kan worden. De snelheid van crosslinken tussen de twee polymeren is pH afhankelijk met een optimum tussen pH 7.5 en 8.5. Deze pH waarde zorgt voor snelle crosslinking met een minimum verlies aan NHS esters vanwege hoge pH waarden. De polymeren plakbanden hebben crosslinks nodig om te vermijden dat ze snel oplossen op het moment ze in contact komen met vloeistoffen, echter compleet gecrosslinkte film zorgt voor niet plakkende tapes. Een NHS:NH_2 ratio van 5:1 tot 7:1 lijkt optimaal, maar hogere NHS waarden moeten nog getest worden. Door de toevoeging van een ondersteunende laag, die ook wat PAOx-NH_2 bevat om de lagen covalent aan elkaar te verbinden, verbeterde de mechanische eigenschappen van de films significant. Alhoewel de verhouding van PLGA en PLC en NH_2 hoeveelheid nog geoptimaliseerd moeten worden. Het oplosmiddel wat gebruikt wordt voor het gieten van de plakkende laag boven op de ondersteunende laag heeft grote invloed op de barst-druk; 1-propanol en 2-propanol bleken de beste oplosmiddelen. Helaas is de standaard deviatie van de plakkende films erg hoog, waardoor het effect van variërende samenstelling lastig is te evalueren. Gedetailleerde studies zullen moeten worden uitgevoerd om een oplossing voor dit probleem te vinden.

Dankwoord

Na een heel boekje geschreven te hebben, is het nu tijd voor het laatste en meest gelezen gedeelte van dit boekje. Zonder hulp, advies en gezelligheid van heel veel mensen was het me niet gelukt om dit werk te doen.

Als eerste wil ik mijn promotor **Jan** bedanken voor de goede begeleiding gedurende 4,5 jaar. Je probeerde altijd met oplossingen te komen voor de kleine, op papier simpele stappen in het GATT project die soms tot grote problemen leidden. Ondanks de langzame vooruitgang van dit project wist je me altijd te motiveren om weer verder te gaan. Achteraf ben ik erg blij dat jullie de beslissing hebben genomen om mij naar Gent te sturen om dit proefschrift te vullen en dit heeft goed uitgepakt. Ik kon altijd met vragen bij je terecht, maar vaak werd ik dan doorverwezen naar Gent omdat daar meer kennis aanwezig is.

Met Gent bedoel ik natuurlijk mijn andere promotor **Richard**. Ook jou wil ik bedanken voor de goede begeleiding de afgelopen jaren. Ik heb erg veel geleerd van jouw gigantische ervaring met poly(2-oxazoline)s. Ik vond het erg fijn om op twee plekken te kunnen werken, het labo in Gent was een welkome afwisseling met het lab in Nijmegen. Tijdens de groepsactiviteiten of het nu sport of spel was, was je altijd erg fanatiek. Je spoorde iedereen aan om mee te doen, ook met het vakgroep schaatsen deed je dat erg fanatiek. Helaas eindigde deze voor jou op de spoed, ik hoop dat ik mijn taak als EHBO'er toen goed vervuld heb.

I would also like to thank the members of the committee, **Alan** Rowan, **Roeland** Nolte, **Dennis** Löwik, **Bruno** de Geest, **Sandra** Van Vlierberghe, **Hans** Heuts, **Gisèle** Volet and **Bryn** Monnery for their contribution in the defense and the critical reading of the manuscript. Dennis wil ik ook bedanken voor het meedenken over welke polymeren gemaakt moesten worden voor hoofdstuk 5.

Zonder de vaste medewerkers van de afdeling organische chemie was het niet gelukt om dit boekje te schrijven en deze moeten natuurlijk ook bedankt worden. **Marieke** voor alle administratieve ondersteuning en het gezellige babbeltje iedere keer als ik langs kwam. Het plannen van overleggen was niet het makkelijkste in dit project gezien de vele en drukke agenda's. **Peter** van Dijk voor de bestellingen, ik zal je gezicht niet vergeten toen je kwam zeggen dat er een pakketje voor mij was en dat ik deze zelf maar moest komen halen omdat de 160 gram materiaal geen pakketje was maar een vat verpakkingsmateriaal van minimaal 20 liter. **Paul** voor de hulp bij de NMR metingen op de 500 MHz, de belangstelling voor wat ik nu allemaal aan het meten en natuurlijk de naar jou genoemde Paul Schlebos Vette Hap borrel waar je altijd bamischijven aanbid. **Peter** v G voor de hulp bij de LCQ, **Theo** bij de IR, **Helene** voor GPC, **Ad** voor NMR, **Jan** D, **René** en **Hans** voor hulp op het lab, Desiree, Paula en Jacky voor administratieve ondersteuning. **Astrid** en **Leny** van P&O wil graag bedanken voor de administratie en het geregel van het contract rondom het gezamenlijk doctoraat.

Ook in de vakgroep Organische en Macromoleculaire Chemie heb ik veel ondersteuning gehad van verschillende mensen en ik wil hen graag bedanken daarvoor. **Tom**, voor de vele en geduldige administratie rondom het gezamenlijk doctoraat (al kon u dat woord op den duur niet meer horen), het ritje naar het UFO voor de inschrijving en de computerzaken tijdens mijn eerste twee bezoeken aan Gent. **Jos** voor zijn winkeltje en om mij te voorzien in mijn behoefte in naalden en spuiten, **Tim** voor de NMR, **Pieter** voor de ICT ondersteuning tijdens mijn derde en lange bezoek, **Bernhard** voor GPC en TGA metingen en **Claudia** voor de SEC metingen.

Het grootste gedeelte van mijn promotietijd heb ik besteed aan het GATT project. Dit begon met een heel klein groepje en is uiteindelijk een grote groep van mensen geworden. **Johan**, de man die het project bedacht heeft; je had vaak gekke ideeën en je wist uit allerlei potjes aan te spreken om mensen aan te nemen die het project kwamen versterken. Als eerste kwam **Huub** me helpen. We hadden elkaar een paar maanden eerder in Gent leren kennen waar we de eer van de Nederland, eigenlijk meer Eindhoven, hoog hielden. Je hebt mij toen samen met Victor de kneepjes van de (poly)oxazoline synthese geleerd. Je hulp resulteerde in het op poten zetten van de hydrolyse route voor de synthese van de NHS polymeren. Jij was degene die als eerste een NHS polymeer maakte en per ongeluk een druppel DCM oplossing op je hand liet vallen. Onze, toen nog bruine, polymeren leverde een mooie vlek op je hand op die je er niet af gewassen kreeg. Samen maakte we het eerste gelletje waarmee we lieten zien dat de methode werkte. Na een half jaar verliet je Nijmegen om terug te keren op de TU/e voor een promotieonderzoek daar. Ik weet niet hoe wel het voor elkaar krijgen, maar we hebben dezelfde promotiedatum gepland. Vlak nadat Huub begon, werd ook Encapson bij het project betrokken, bij **Joost**, **Dennis** en **Bram** kon ik altijd aankloppen voor advies. Bram, toen je bij later bij GATT ging werken, werd onze samenwerking intensiever en wisselden we ervaringen met de synthese en materialen uit om zo prototypes te kunnen maken en testen. Toen **Marcel** begon met zijn promotieonderzoek had ik weer een labmaatje die ongeveer hetzelfde werk deed. Ondanks onze krappe start, met zijn drieën in een zuurkast, is de samenwerking goed verlopen. We namen materiaal van elkaar over om de synthese verder te zetten. We irriteerden onze labgenoten met het gezoem van de Turrax en bezetten we met zijn tweeën alle rotorvaps in ons lab. Ook de andere mensen in het GATT team die ik ontmoette tijdens onze grote overleggen. **Harry** het was erg prettig om de medische kant van het verhaal van jou te horen, ik heb erg veel geleerd over de heelkunde, ook heb je bijdrage geleverd aan ons review artikel door hier samen met **Simon** de medische kant van het verhaal correct op papier te zetten. Verder wil ik **Etienne** en **Mark** bedanken. **Maria** and **Alexandra** you made the team quite Spanish.

Rosa, you joint the GATT team shortly after Marcel, although you are not trained in chemistry, I hope I learnt you a lot of chemistry, that must be the case after all the questions you asked me. You learnt me a lot about biomaterials and enjoyed our collaboration. I loved a the chats we had which made the PhD life a lot easier. I really appreciate it that you want to be my paranimf.

Mijn andere paranimf, **Maarten** (aka Big Jim), je hebt een mooie bijdrage geleverd aan mijn doctoraat, terug te lezen in hoofdstuk 2. Het was onderdeel uw masterthesis om de polymerisatiekinetiek van MestOx te onderzoeken, wat uiteindelijk resulteert heeft in twee mooie papers. Ik heb u pas echt leren kennen toen ik voor langere tijd naar Gent kwam en toen was je net begonnen aan uw doctoraat. In die tijd heb ik veel van u geleerd over de praktische kanten van polymerisatiekinetiek.

The first month of my PhD I spent in Nijmegen reading loads of literature. The second month I went to Ghent to learn the labwork of PAOx. I joint, at that time, a very small research group of 8 in total who was having their group meetings in Richards office, hard to understand right now. **Victor**, the Spanish guy, later on responsible for the introduction of the concept ‘Spanish time.’ After my first polymerisation in the microwave you did a little dance together with Huub, to show me how the polymerisation mixture should show waves. I enjoyed our trip to San Diego to visit the ACS national meeting, we had a lot of fun over there. **Lenny**, jij begon tegelijkertijd met mij in Gent, dit bracht het aantal Nederlanders in de

groep op 4. Het was altijd gezellig met jou wat resulteerde in lange praatjes waarbij we soms de tijd uit het oog verloren. Veel succes met je postdoc in Auckland. **Gertjan**, in eerste instantie de enige Belg in de groep, maar je wist je goed staande te houden tegen al dat Nederlandse geweld. Tijdens mijn lange verblijf vond ik de babbels die we, vooral in het bureau, hadden erg prettig.
During my second visit in Ghent, I was working on the methyl ester monomer synthesis. **Bryn**, although I have mentioned you already before, I would like to thank you for the help with this. You taught me a lot about distillations and could not stop talking about high vacuum. Tijdens dit bezoek maakte ik kennis met een aantal nieuwe collega's. **Bart**, het was prettig samenwerken met u, alhoewel het soms lastig was om een trekkast met zijn drieën te delen. Je aanwezigheid op het labo was niet te missen, ik denk dat ik misschien wel een dag slechter gehoord heb nadat je in uw mail las dat je de IWT beurs toegewezen had gekregen. **Kathleen**, onze eerste kennismaking was in Houffalize, toen ik een paar maanden later naar Gent kwam voelde het alsof we elkaar al lang kende. Het was een fijne tijd met u op het labo. Ik heb u wel veel metingen laten doen, wat resulteerde in een publicatie die ook terug te vinden is in hoofdstuk 3. Tijdens de ACS in San Francisco deelde we een kamer met een knus 1.40 m bed en gingen we gezellig samen shoppen. Als een van de eerste collega's wist ik van uw zwangerschap en ik wens je veel geluk met Wouter en Kasper in de toekomst.

I would also like to thank my other labmates and colleagues **Samarendra**, mostly called by your family name Maji, you were always interested in my work and thanks for helping me out with the turbidity measurements. **Bahar**, I met your husband **Martin** (eindelijk een oxazoline poster op de DPD) first, you were the first to stand next to me when I created a fireball in the lab. **Joachim**, eerst student, later collega, altijd in voor een grapje. Een deel van de groep zat uiteindelijk op het vierde: **Maarten M** (Jim), bedankt voor de rit naar de spoed van het UZ. **Glenn**, voor het kijken van een WK wedstrijd op de Oude Markt in Leuven en de overnachting in jullie nieuwe appartement met nauwelijks meubels na Kathleens bruiloft, **Mathias**, giving nice and funny presentations at the group meeting. The Asian corner at the fourth floor, **Qilu**, the first PhD to graduate from the SC group, **Kanykei**, **Dingying** and **Zhanyou**. I also enjoyed talking with the (exchange) students **Silke**, **Jin**, **Özlem**, **Sibel** and **Belgin**.

De relaxroom op het eerste werd gedeeld met de mensen van de Madder groep, ook hen wil graag bedanken voor de hulp en gezelligheid: **Matthias**, **Vicky**, **Duchan**, **Yara**, **Lieselot**, **Nathalie**, **Bram**, **Ellen**, **Kurt**, **Willem**, **Vincent** en **Abhishek**.

Tijdens mijn promotieonderzoek heb ik verschillende studenten mogen begeleiden. **Lia**, you came as an exchange student from the USA and you were the first student I had to supervise. Although the project was not always working along, you worked hard trying to find solutions for the problems we were facing. Only a little part of your work, the pH dependent crosslinking tests, ended up in my thesis. Good luck with finishing Med School and hopefully you or any of your colleagues will be able to use the GATT product. **Harry**, officieel stond je onder begeleiding van Marcel, maar ik vond het erg leuk om je te helpen met je masterstage. Je bent begonnen met het maken van polymeren zodat ik daar weer tapes van kon maken. Het was altijd gezellig met jou op het lab. Ik wens je heel veel succes met je eigen promotieonderzoek in de VS. Tijdens mijn lange verblijf in Gent heb ik samen met Maarten M het bachelorproject mogen begeleiden, de drie bachies waren **Willem**, **Wouter** en **Yentl**. Jullie hebben vier weken hard gewerkt aan het maken van polymerendeeltjes op basis van MeOx en C3MestOx. Alhoewel het einddoel van het project niet gehaald is, zijn jullie kinetiekresultaten terug te vinden in hoofdstuk 2 en een set van de drie copolymeren die jullie

gemaakt hebben in hoofdstuk 3. Het schrijven van mijn review heb ik niet alleen gedaan, **Marleen** was op zoek naar een onderwerp voor haar literatuurscriptie en heeft een mooi stuk werk afgeleverd wat een vermelding op het review opleverde.

Ook in Nijmegen had ik vele collega's die het werken daar leuk maakte. **Britta**, ik kon altijd bij je terecht om mijn hart te luchten en je was bereid om naar me te luisteren en een kop thee te gaan drinken. Chemie bleek een erg kleine wereld toen bleek dat jouw vader en mijn moeder in hun studententijd samen stage hadden gelopen. **Anika**, ik mis de LUNCH! om 12.30 precies en ook het napraten over Wie is de mol of Boer zoekt vrouw. Toen ik begon met mijn promotie was het van Hest-lab nog in vleugel 4, een aantal mensen bedanken om mij wegwijs te maken op het lab. **René**, mijn zuurkastbuurman waar ik altijd met vragen terecht kon met de verhuizing naar vleugel 1 bleef je achter om daarna toch ook de overstap te maken en mijn bureaubuurman te worden. Ik vind het erg leuk dat jij de PAOx heb geïntroduceerd in de projecten bij de HAN en hoop dat dit boekje je nog wat inspiratie bied. **Silvie**, bedankt dat ik gebruik mocht maken van je zuurkast als ik vacuümdestillaties moest doen. **Matthijs**, jij was verantwoordelijk voor mijn eerste labwerk van mijn PhD, ik was nog niet op het lab geweest of jij had het van boven tot onder roze gekleurd. **Saskia**, jij kwam in mijn rijtje bureaus te zitten. Het contact is altijd goed geweest, op een dag was je aan het vloeken op een naam genoot van mij en toen geinde we dat onze projecten zo ver uit elkaar lagen dat we nooit iets samen zouden doen, niet wetende dat het anders zou uitpakken. In de laatste maanden van mijn onderzoek ben ik polymeren CPP mimics gaan maken die we samen hebben getest op cellen, eigenlijk fungeerde is als aangever van de epjes en noemde ik de volumes op dit gepipetteerd moesten worden. Helaas is dit werk nog niet voltooid omdat mijn tijd er opzat. **Nanda**, mijn EHBO-maatje, het was leuk om elkaar in te pakken met verband om te oefenen met zwachtelen, wat verbaasde en geschrokken blikken van de collega's opleverde. I would also like to thank the other member so the van Hest group (**Ruud**, **Morten**, **Sanne**, **Marlies**, **David**, **Joep**, **Annika**, **Fei**, **Ilmar**, **Yingfeng**, **Loai**, **Jan**, **Roger**, **Lise**, **Jorgen**, **Marjoke**, **Emilia**, **Melek**, **Dave**, **Iria**, **Daniela**, **Damei**, **Henk**, **Mariëlle**, **Mark**, **Selma**, **Lianne**, **Zhipeng**, **Anhe** and all students) for their help and making it a nice time.

Ook wil ik graag mijn labgenoten uit vleugel 1 bedanken, ik was een verstekeling van de van Hestgroep op het Rutjes lab. **Thomas**, **Angelique**, **Rinske**, **Thorben**, **Rens** en alle studenten bedankt voor de leuke tijd. **Roel** en **Maike** waren twee andere collega's waarmee Nanda en ik samen de EHBO cursus hebben gevolgd, zeer leerzaam en gezellig. Verder wil de rest van de Rutjes groep ook bedanken voor de gezamenlijke lunches en borrels.

In koffiepauzes bracht in ook veel tijd door met de mensen van de Rowan/Elemans/practicum groep waar ik mijn master gedaan heb, ook na werktijd was het erg gezellig tijdens de Vette hap & Wisky borrels, etentjes en verjaardagsfeestjes. **Hans**, **Femke**, **Onno**, **Niels**, **Zaskia**, **Jialiang**, **Daniël**, **Arjen**, **Dennis**, **Maarten**, **Kathleen**, **Duncan**, **Stijn**, **Johan**, **Luuk**, **Tom**, **Bart** (moeilijke bril), **Tim**, **Roel**, **Maurice**, **Pascale**, **Toine** en **Inès**. **Joris** en zijn familie bedankt voor alle steun en veel succes met het afronden van jouw proefschrift.

Vroeger pakten we bus 2 om naar elkaar toe te gaan, tegenwoordig wonen we iets verder uit elkaar en zien we elkaar minder, maar de gezelligheid is er niet minder om. **Jasper&Aimée** (en Sophie en Isa), **Jurjen&Sabrina**, **Moniek&Michel**, **Renee&Marcel, Koos&Elleke** de etentjes, uitstapjes, verjaardagen, klus- en verhuispartijen hebben voor de broodnodige ontspanning en afleiding gezorgd. Ik hoop dat we deze gezelligheid nog vele jaren kunnen doorzetten. **Bram**, jou zag ik wat minder, dank je wel voor de gezelligheid en het uitwisselen

van promotie-ervaringen. Je begon op dezelfde dag als ik en hebt een half jaar eerder kunnen verdedigen. **Willemijn**, ik ken je al vanuit de tijd dat we beide in Nijmegen studeerden. Toen je naar Utrecht verhuisde zijn we elkaar even uit het oog verloren, maar toen ik de eerste keer in Gent was en foto's postte bleek jij net aangenomen te zijn als doctoraatsstudent in de S8, twee gebouwen verderop op de Sterre. Dit heeft het contact hersteld en ik wil je graag bedanken voor het logeeradres wat je me bood als ik tijdens een kort verblijf een extra nachtje wilde blijven en alle gezellige en eindeloze kletspartijen. Ook delen we een aantal dezelfde hobby's, namelijk handwerken en schaatsen. Je wilde graag gaan schaatsen maar durfde/wilde niet de eerste keer alleen richting Kristallijn fietsen. Ik heb je meegenomen en geïntroduceerd bij **LBSG**, waar ik het erg naar mijn zin heb gehad daarom wil ik mijn oud-clubgenoten voor bedanken. Ik hoop dat we er een jaarlijkse traditie van kunnen maken dat ik jullie coach tijdens het BK afstanden in Eindhoven.

Het familieweekend in Arcen vlak voordat ik voor een aantal maanden naar Gent vertrok was een leuke afwisseling en goed om mijn hoofd leeg te maken en alle promotie-perikelen even te vergeten. Ik wil **oma** hiervoor bedanken en ook alle ooms en tantes, die daarbuiten ook veel belangstelling toonden in mijn onderzoek, neefjes, nichtjes, hun aanhang en achternichtjes en neefje, alle 45 namen opschrijven wordt me iets te gek

In het diepe zuiden van het land vond ik ook vaak afleiding bij **opa** en **oma**. Ook waren de neefjes, die ondertussen niet meer klein zijn, **Felix**, **Wim jr.**, **Henk** en **Sjaak** een goede manier om de stress even te vergeten en natuurlijk de rest van de familie ook.

Thijs en **Simone**, mijn broertje dat vroeger niets met scheikunde te maken wilde hebben en ondertussen de grootste pyromaan van de familie is als verbrandingstechnoloog. Tijdens het over en weer klussen en verhuizen was er, naast het harden werken, ook altijd tijd voor een geintje en goede babbel. Natuurlijk zal ik onze skivakantie naar Serfaus niet vergeten. Ik wens jullie heel veel geluk toe in jullie nieuwe huisje in Amersfoort.

En als laatste wil ik **papa** en **mama** bedanken voor alle steun. Jullie zorgden voor afleiding en ontspanning. Terwijl ik aan het werk was, heeft papa alle binnendeuren van mijn appartement geverfd, iets wat ik enorm waardeer. Jullie bezoekjes aan Gent waren erg leuk, ook al hebben jullie twee keer met veel spullen moeten sjouwen, dit maakte het leven in mijn studioke daar wel een stuk aangenamer.

List of publications

- Petra J.M. Bouten, Kathleen Lava, Jan C.M. van Hest, Richard Hoogenboom, *Thermal Properties of Methyl Ester-Containing Poly(2-oxazoline)s*, **Polymers**, 2016, 7, 10, 1998-2008
- Petra J.M. Bouten, Dietmar Hertsen, Maarten Vergaelen, Bryn D. Monnery, Saron Catak, Jan C.M. van Hest, Veronique Van Speybroeck, Richard Hoogenboom, *Synthesis of poly(2-oxazoline)s with side chain methyl ester functionalities: Detailed understanding of living copolymerisation behavior of methyl ester containing monomers with 2-alkyl-2-oxazolines*, **Journal of Polymer Science Part A: Polymer Chemistry**, 2015, 53, 2649-2661
- Petra J.M. Bouten, Dietmar Hertsen, Maarten Vergaelen, Bryn D. Monnery, Marcel A. Boerman, Hannelore Goossens, Saron Catak, Jan C.M. van Hest, Veronique Van Speybroeck, Richard Hoogenboom, *Accelerated living cationic ring-opening polymerization of a methyl ester functionalized 2-oxazoline monomer*, **Polymer Chemistry**, 2015, 6, 514-518
- Petra J.M. Bouten, Marleen Zonjee, Johan Bender, Simon T.K. Yauw, Harry van Goor, Jan C.M. van Hest, Richard Hoogenboom, *The chemistry of tissue adhesive materials*, **Progress in Polymer Science**, 2014, 39, 7, 1375-1405
- Chapman, Petra J.M. Bouten, Richard Hoogenboom, Katrina A. Jolliffe, Sébastien Perrier, *Thermoresponsive cyclic peptide – poly(2-ethyl-2-oxazoline) conjugate nanotubes*, **Chemical Communications**, 2013, 49, 6522-6524
- Victor R. de la Rosa, Petra J.M. Bouten, Richard Hoogenboom, *First Symposium on Poly(2-oxazoline)s and Related Pseudo-Polypeptide Structures*, **Macromolecular Chemistry and Physics**, 2012, 213, 2669-2673

Curriculum Vitae

Petra Bouten werd geboren op 5 oktober 1986 in Eindhoven. In 2005 behaalde ze haar VWO diploma op Augustinianum in Eindhoven. Hierna verhuisde ze naar Nijmegen om Scheikunde te gaan studeren aan de Radboud Universiteit in deze stad. In 2008 behaalde ze haar bachelordiploma. Ze vervolgde haar studie met een master Chemistry aan dezelfde universiteit. Tijdens de master voerde ze een hoofdvakstage uit in de onderzoeksgroepen van prof. dr. Alan Rowan en prof. dr. Roeland Nolte aan de Radboud Universiteit met als onderwerp Watersoluble Polyisocyanopeptides. Van februari tot en met juli 2010 woonde ze in Montréal, Quebec, Canada om stage te lopen in de groep van dr. Hanadi Sleiman aan de McGill University over DNA Nanotechnology. In februari 2011 behaalde ze haar masterdiploma. In diezelfde maand startte ze onder begeleiding van prof. dr. ir. Jan van Hest en prof. dr. Richard Hoogenboom met een promotietraject aan de Radboud Universiteit en de Universiteit Gent. Dit onderzoek richtte zich in eerste instantie op het ontwikkelen van een General Adhesive Tissue Tape, een plakband voor het interne menselijke lichaam, gebasseerd op poly(2-oxazoline)s. Later verschoof de aandacht naar methyl ester gefunctionaliseerde poly(2-oxazoline)s. Tijdens haar promotietraject verbleef Petra 11 maanden aan de Universiteit Gent. Sinds januari 2015 werkt Petra als chemiedocent en loopbaanbegeleider aan het Summa Laboratorium, onderdeel van Summa College, in Eindhoven. In september 2015 is ze ook gestart als student voor de master Science, Education and Communication aan de Technische Universiteit Eindhoven om haar eerstegraadsbevoegdheid voor docent te halen.

Petra Bouten was born on October 5th, 1986 in Eindhoven. In 2005 she obtained her secondary school diploma at Augustinianum in Eindhoven. Subsequently she moved to Nijmegen to study chemistry at the Radboud University. In 2008 she obtained her bachelor degree. She continued her studies with a master Chemistry at the same university. During her graduation project she worked in the research groups of prof. dr. Alan Rowan and prof. dr. Roeland Nolte on a project called Watersoluble Polyisocyanopeptides. From February until July 2015 she lived in Montréal, Quebec, Canada, during this time she performed an internship on DNA Nanotechnology in the group of dr. Hanadi Sleiman at McGill University. She received her master degree in February 2011. In this same month she started her PhD under supervision of prof. dr. ir. Jan van Hest and prof. dr. Richard Hoogenboom at the Radboud University and Ghent University. This research first focused on the development of General Adhesive Tissue Tape, a tape for the internal human body, based on poly(2-oxazoline)s. Later on the focus shifted to methyl ester functionalized poly(2-oxazoline)s. During her PhD research Petra stayed at Ghent University for 11 months. Since January 2015 Petra is working as chemistry teacher and student mentor at Summa Laboratorium, part of Summa College, in Eindhoven. In September 2015 she started as master student Science, Education and Communication at the Eindhoven University of Technology to obtain her teachers degree.